The Autoxidation of Biodiesel and its Effects on Engine Lubricants

Thomas Iain James Dugmore

A thesis submitted for the degree of Doctor of Philosophy

The University of York
Department of Chemistry
September 2011

Abstract

To investigate the impact of biodiesel on automotive engines during usage, the chemistry of two significant biodiesel components, methyl linoleate and oleate were examined. Both were oxidised in bench top reactors at temperatures between 100 – 170 ^{o}C to represent the different conditions across the engine. Products were identified and quantified by GC-FID and GC-MS to determine the main degradation mechanisms.

Methyl oleate and linoleate were also oxidised with squalane in the reactors to simulate the effects of fuel dilution in the engine lubricant. At lower temperatures methyl linoleate was shown to enhance the rate of squalane oxidation, but as the temperature increased, the pro-oxidant character decreased to become inhibiting by 170 ^{o}C, with the temperature at which this crossover occurred measured at 158 ± 5 ^{o}C – methyl oleate had no effect however.

This temperature dependent behaviour is attributed to the weak C-H bond of the doubly allylic system (the only feature not common to both molecules) and the subsequent reversibility of O_2 addition to the methyl linoleate radical formed via hydrogen abstraction. Studies of a similar molecule, 1,4-pentadiene, revealed ceiling temperatures for this specific reaction as 173 ± 6 ^{o}C which was in good agreement with the experimental value.

The effects of lubricant additives (two antioxidants and a detergent) on the degradation of squalane-methyl linoleate mixtures was also examined. It was shown that at all temperatures the antioxidant could delay the onset of the reactions, but have no effect on them once they started. Similarly, methyl linoleate could reduce the effectiveness of the antioxidants at all measured temperatures showing that the reversible addition of O_2 to allylic radicals was not relevant for these reactions. Two possible mechanisms for this behaviour are discussed along with potential methods for testing them in future experiments. No noticeable effects were observed for the detergent.

Table of Contents

The Autoxidation of Biodiesel and its Effects on Engine Lubricants

List of Figures and Tables

List of Figures

Chapter 1

Chapter 2

Chapter 3

Chapter 4

Chapter 5

List of Tables

Acknowledgements

Firstly, thanks must go to Dr Moray Stark for accepting me onto the project and supervising me throughout for the last three years, not to mention proof reading the entire thesis! Also to Dr Craig Jones and Dr Jola Adamczewka at Lubrizol for funding the project as well as for providing biodiesel and additive samples. Thanks also to Dr Duncan Macquarrie for being my IPM and giving much needed feedback throughout the project. Without you, this project would never even have got started in the first place!

Big thanks to Dr Alfahad Alfadhl for helping me find my feet in those first few weeks, showing me around the lab, how to use equipment and generally helping me get started as well as for his work on additives in lubricants that significantly helped me with my work. Similarly, thanks to Dr Julian Wilkinson for his previous work on lubricant oxidation and to Alexandra Neal, George Parker and Rob Jamieson for their preliminary work on methyl oleate and methyl linoleate which provided an excellent platform for me to get started on. Thanks especially to my fellow group members Peter Hurst, Bernadeta Pochopien and Gareth Moody for help with equipment, contributing ideas and results, pooling intellect together and general support. You've been great company guys and best of luck with your own theses!

On a similar note, thanks to everyone I've been involved with in the Green Chemistry Centre, whether through work, office banter or socialising on nights out you've all helped in one way or another, if nothing else simply by helping make these last three years hugely enjoyable. There are way too many of you to mention here and I'd be sure to forget someone, so I will simply say thank you to you all and the best of luck wherever you end up!

Thanks to Dr Trevor Dransfield and Ben Glennie in the Mass Spectrometry department, but special thanks Dr Karl Heaton for his help, feedback and patience as we were setting up a method for GPC-MS. Likewise thanks must go to glassblowers Brian Smith and Abigail Storey and to Chris Mortimer, Wayne Robinson and Jon Hamstead in mechanical workshops for making and repairing our equipment.

Last and definitely by no means least, big, big thanks to my parents and the rest of my family and close friends for all their support in one way or another over the years.

Author's Declaration

I confirm that the material presented within this thesis is my own work and previously unpresented or unpublished to my knowledge with the exception of the following:

Autoxidation of methyl oleate experiment and GC trace in figure 3.5 carried out by George Parker. Subsequent EI- and CI- MS interpretation carried out by George Parker, Alexandra Neal and Dr Moray Stark.

Denisov cycle in figure 5.5 taken from Mechanism of Regeneration of Hindered Nitroxyl and Aromatic Amines, Polymer Degradation and Stability, by T.E. Denisov, 1989.

Chapter 1. Introduction

1.1 History of Fuels, Crude Oil and Renewables

During the 18th and 19th century, advances in agriculture, mining, manufacture and transport led to a major overhaul in the technology and subsequently culture of the world in what is now known as the Industrial Revolution. As a result, in certain areas, traditional manual labour could no longer produce goods quickly or carry out operations powerful enough to supply the increased demand. Many tasks became mechanised and this process brought with it a new challenge; supplying the machines with sufficient power to keep them running.

The use of fast-flowing rivers to turn water wheels and thus drive machines was one of the first major automated processes, particularly in the textile industry, but this limited industry to places where such rivers could be found. Thomas Savery, then later Thomas Newcomen had used the idea of using a steam driven piston to draw water from a well and drain mines – a jet of steam would be injected into the cylinder to raise the pressure and drive the piston up, then a jet of cold water would cool the cylinder, reducing pressure and pulling the piston back. This design was inefficient, the alternating heating and cooling of the cylinder meant that a lot of energy was lost, resulting in large amounts of fuel usage – however, the idea of using an increase in pressure to drive a piston would ultimately prove to be a significant one for the development of transport.

James Watt's steam engine was the breakthrough model, using a separate cylinder to condense the steam (Spear 2008), followed by several other modifications resulting in a model that used 75% less fuel than Newcomen's engine. Furthermore, in contrast to the water wheels, where the machines had to be taken to the water source, this development meant that an efficient machine now existed that could have its fuel transported to it and hence operate anywhere. The next breakthrough for the transport industry came via William Murdoch, an employee of Watt's and his business partner Matthew Boulton (though it was Watt who patented it). The breakthrough was to attach a beam to the end of the piston which connected via a crank to a cogwheel, which in turn was attached to and rotated around a larger cogwheel meaning the piston could now be used to provide rotational as well as linear motion. This apparatus became known as the 'sun and planet' gear due the nature of the smaller cogwheel orbiting the main wheel. Being able to finally

turn wheels, this system became the engine for the steam train – the first form of transport driven by fuel, rather than natural forces such as the wind or horsepower.

Due to the abundance and cheap cost of coal, the steam engine would go on to be the main form of power in industry for the next century, whilst the steam train became a popular form of transport, particularly in Britain to export the products it was mass producing as the industrial revolution thrived and in the U.S.A. to aid transport across such large areas during colonisation. (Dickinson 2011, Hills 1993)

The next major advance for the transport industry would be the development of the internal combustion engine. This differed from the steam engine in that the fuel was not used to heat water (or any other medium) to power the machine, but rather the combustion of the fuel itself to form carbon dioxide and water vapour provided the increase in pressure necessary to drive the pistons. The earliest internal combustion engines can be traced back to China, Mongolia and Arabic states in the 13th Century, (Gruntman 2004). Similarly, in 16th Century Europe, Da Vinci described a compression-less engine and though this was little more than a toy at the time, it gained fame when Huygens used a model of it working on gunpowder to drive the water pumps at the Versaille palace gardens. The problem with these models was the fuels were all solids and thus the engines had to be stopped after each cycle to be reloaded. In the early 19th century, de Rivaz developed an internal combustion engine that could use hydrogen as a continual fuel supply solving the problem. Unfortunately this design never took off as hydrogen was hard and expensive to obtain in those days, especially in comparison to coal.

Nevertheless the prospect of producing a faster, more powerful engine than the steam engine was still a promising one and the 19th century saw a newfound interest in the internal combustion engine, especially with the advent of the oil industry. Many different designs were proposed or built with varying degrees of success – it is hard to say who made the breakthrough as many inventors failed to patent their designs, or were beaten to it by their rivals, but it is currently accepted that Nikolaus Otto was the first to build and sell the engine (Heywood 1988) – the Otto Cycle Engine (U.S Patent 388,372). Gottlieb Daimler took the design a step further towards what is known today as the gasoline engine and in 1886, Karl Benz received the first patent (DRP No. 37435) for a gasoline-fueled car. The usage of petroleum from crude oil as a source of fuel enabled the internal combustion engine to surpass the steam engine in terms of power output, but could not overtake it in production in areas where coal was more abundant than oil and would require increased costs to import.

In the late 1890's Rudolf Diesel adapted the Otto Cycle Engine in a different manner – by mixing the fuel droplets with the air inside the combustion chamber, rather than drawing it in pre-mixed – to enable it to run on vegetable, rather than mineral oils. The first model was run using peanut oil and Diesel envisaged a large market for the engine as various different plant oils could be produced in all parts of the world (Bryant 1976). Diesel's engine would make him a millionaire and be used throughout industry, particularly where heavy duty, 'dirty' work was required, though due to cheap costs, the fuel that was eventually to be used would be the heavier hydrocarbon fraction from petroleum distillation, as opposed to the vegetable oils Diesel originally intended.

As the oil industry's efficiency increased and the costs decreased, both Daimler and Diesel's engines became the first choice for the transport industry in road (primarily Daimler's engine) and rail (primarily Diesel's, though this was later partially phased out due to electrification of the railway lines) rendering Watt's steam engine obsolete by the end of the 20th century. The burning of fuels for power was, for a long time unregulated as it was believed the atmosphere into which the resulting gases were emitted, was essentially a large, stable, unreactive sink.

In the late 1950's due to the emissions from other industries mainly into the water and land, environmental legislation was introduced. Research from these showed that the atmosphere itself was also a delicate ecosystem, spawning atmospheric chemistry as a new field of research, itself divided into atmospheric regions such as the tropo- and stratosphere and chemistry type such as aerosol and photochemistry (Cadle 1972, Levy II 1972, Nicolet 1972). A particular concern was the absorption of IR-radiation by carbon dioxide and the resulting warming effect it has and will continue to have on the climate of our planet (Johnson 1970, Woodwell 1979, Cox 2000, Wayne 2000) and the subsequent disruption of the ecosystem (Manabe 1975 & 1993, Sarmiento 1998 (Air/ocean system) Attiwill 1970, Cao 1998 (plant and soil carbon sinks)). As a result the Intergovernmental Panel of Climate Change (IPCC) was set up with legislation being gradually introduced to limit CO_2 emissions; most notably the Kyoto Protocol which calls for an average 5.2% reduction in emissions in all areas with respect to 1990 levels during the 2008 – 2012 period. Consequently, EU directives, such as Euro 5 (EC Regulation No. 715/2007) and Euro 6 (EC Regulation No. 595/2009) have set targets on reducing these emissions; the use of biofuels to replace traditional mineral oils is one method thought to have the potential for achieving this. The stated EU directive is that biofuels, including biogas, bioethanol and biodiesel must make up 10% of the fuel share for transport, replacing petrol and diesel

consumption by 2020 (EC Regulation No. 28/2009). Currently, at the time of writing, the European Standard is for diesel fuel to consist of 7% biodiesel (EN590).

Despite environmental concerns demand for crude oil was increasing due to the expansion of the transport industry and other sectors (particularly the chemical synthesis industries) relying on production of crude oil. However new reserves were slow to appear and the rate of replenishment of existing ones was almost negligible compared to their consumption rates (Boult 2003). Demand, coupled with political instability in some oil producing regions, caused the cost of extraction and sale price on the market to begin rising and continued to rise erratically even up until recently. The cost of crude oil rose from $33 per barrel in 2004, to $72 per barrel in 2006, reaching a peak of $147 per barrel by July 2008 and currently averaging $110 per barrel as of April 2011(U.S Department of Energy).

Due to a combination of all these factors, it became clear that crude oil reserves could not continue to sustain the transport industry and unfortunately, the same was true of coal. As such the new challenge for the transport industry has, once again, come down to the choice of fuel. Electrification of the automotive (as with the locomotive) industry has been considered, though this still requires a fuel source elsewhere, as has the use of solar powered cars. The two most popular choices so far have been the return to some of the original ideas for the internal combustion engine – hydrogen (de Rivaz) and vegetable oils (Diesel). Whilst hydrogen is now more easily obtained than in de Rivaz's days, obtaining it on a scale necessary to sustain the transport industry is still problematic, as is the issue of storing it and delivering it to the combustion chamber using the current automobile designs. As Diesel's engine was designed to run on vegetable oils originally, the idea of returning to these oils or modifying them to Biodiesel is currently seen as one of the most feasible methods for replacing diesel from crude oil and hence reducing CO_2 emissions (Hill, J. 2006, Dermibas 2007); the original, non-binding target set for the UK to achieve Kyoto targets was that biofuels should make up 5.75% of fuel usage by 2010 (Department for Transport 2005) – however a legally binding legislation to achieve EU legislation based on the level of success of this target has not been finalised at the current time of writing. Whilst it is true that biofuels release carbon dioxide on combustion, the crop used is planted and harvested each year so, to an extent, the emissions will be absorbed by the following year's crop rather than persist in the atmosphere (Dvorák 2001).

However, both legislative and consumer demands have both changed considerably since Diesel's day and it is impossible to meet these by simply switching back to vegetable

oils. Over the remainder of this chapter, the properties of vegetable oils and their biodiesel derivatives will be discussed as well as the problems associated with their usage. The remaining chapters will be spent trying to identify the causes for some of these problems with the aim that solutions can be found to reduce, or even remove them.

1.2 Biodiesel Manufacture and Properties

Rudolf Diesel's version of the internal combustion engine using peanut oil was designed with the goal of utilising other vegetable oils as a readily available, renewable fuel source. The exact nature of vegetable oils and lipids differ according to the organism they are produced by, but they all follow the same basic structure of up to 3 long chain fatty acids bonded via esterification to glycerol (1,2,3 propantriol) – see figure 1.1

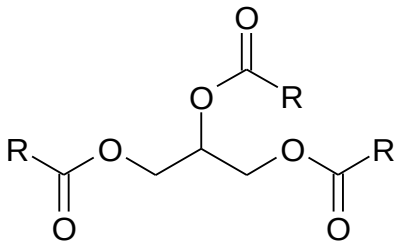

Figure 1.1 – The generic structure of lipids – R = alkyl chain

The alkyl chains are between 8 and 24 carbon atoms long, but typically around 16 and 18 and almost always even numbered due to the enzymatic nature of building free fatty acid chains in blocks of 2 carbon atoms via the continual condensation addition of acetate to the carboxylic acid end of the chain (Hele 1958, Ganguly 1960, Zhang, H 2010).

Whilst Diesel's engine was able to run on peanut oil in the late 19th century, the development of the engine since, coupled with environmental legislation – particularly regards emissions – and consumer demands – such as miles per gallon of fuel, engine speed etc – means that peanut, and other vegetable oils can no longer directly power the diesel engine sufficiently to meet current day criteria. Griffin-Shay had conducted a review of the literature available in 1993 and concluded that vegetable oils would not completely displace petroleum, but that there were a number of beneficial factors to consider when incorporating them in wider usage in this area. In 2000, Srivastava reported the (then) current demands for diesel fuels in India. These included:

- Cetane Number (CN), an index of the time between injection of the fuel into the chamber and subsequent ignition, had to be a minimum 42.00 (Cetane, or hexadecane, the ideal reference compound has a CN of 100).
- Kinematic Viscosity at 38.0 ^{o}C (KV38) of 2.0 – 7.5 cSt.
- Pour point, the lowest temperature at which a liquid will flow, had to be a maximum of 6 ^{o}C (in India, though it was expected to be far lower in colder countries).
- Flash point, the lowest temperature at which there will be sufficient vapour to ignite, had to be a minimum 38 ^{o}C.

It was then further reported that of 14 vegetable oils tested, only 3 (Crambe, Palm and high oleic Safflower oils) met the requirement for cetane number, and none met the criteria for KV38 (the average was between 30 and 40 cSt) – also previously reported by Goering (1982) and Ali (1995). Ultimately, it appeared that projecting for long-term usage in the wider market even with processing, vegetable oils were shown to be unsuitable due to their high freezing points and viscosities during use – presenting particular problems for cold starts and engine wear (Harwood 1984).

A popular solution to the problem of using vegetable oils in Diesel engines is to instead chemically convert them to what is known as biodiesel. Biodiesel is produced via the esterification (normally with methanol) of fatty acids, mainly from arable crops, although the use of non-edible crops, such as Jatropha and Karanjia (Sarin 2007), animal fats, (Nebel 2006) and used cooking oil (Encinar 2005) have also been investigated. The process (for methanol) involves using methanol in its liquid form with a base catalyst such as sodium or potassium hydroxide (Encinar 1999, Dvorák 2001). The sodium/potassium hydroxide mixes with methanol to make sodium/potassium methoxide which then reacts with the fatty acids to cleave them from the glycerine forming glycerol and methyl esters of the fatty acids which can then be skimmed off the top of the mixture as the two phases separate out. The glycerol can then be used for other industrial purposes. Studies have also been done using supercritical methanol (Demirbas 2002), which has the advantage of eliminating the usage of (hazardous) sodium methoxide, with the drawback of being more energy intensive. As methanol is often used to make biodiesel, it is also known as FAME – Fatty Acid Methyl Esters. The crop that is used to produce the biodiesel therefore lends its name to the resulting fuel in the form XME where X is the initial of the crop used. e.g.

RME = Rapeseed Methyl Ester, SME = Soybean Methyl Ester, PME = Palm Methyl Ester etc. As well as lowering the fuel's viscosity and freezing points (Ma 1999) to levels more comparative with mineral diesel, transesterification with methanol also has the added advantage over vegetable oil of being miscible with mineral diesel and hence able to form fuel blends for use in engines (Agarwal 2001).

The usage of other alcohols for transesterification has also been investigated. Du Plessis (1985) compared the stability of methyl and ethyl esters of sunflower oil during storage but found that ethyl esters were less stable at all storage temperatures, leading to increased acidity and viscosity of the fuel over a 3-month period. Knothe (1998) investigated the effect of both the alkyl chain and the alcohol moiety of the ester on the cetane number of the fuel and discovered that whilst a longer chain would increase the cetane of the fuel, branching subsequently decreased it (the highly branched isomer of hexadecane, 2,2,4,4,6,8,8 heptamethyl nonane has a CN of only 15) – leading to problems when using alcohols with more than four carbons for esterification. In addition, as previously noted an increase in carbon number increases the viscosity, creating further problems. Interestingly as well, separate studies by Knothe (1997, 2003, summarised 2005) showed that when the alkyl chain of the ester was unsaturated, the increase in chain length of the alcohol moiety had the potential to decrease the CN.

Similarly, it has been considered not employing any esterification techniques and simply using the free fatty acids (FFA) for biodiesel. However since many studies using FAME with relatively high levels (<20%) of FFA have shown increased problems in acidity, corrosion and overall damage to the fuel injectors and engine (Ghadge 2005, Tiwari 2007, Berchmans 2008, Ranz 2010) it has been concluded that FFA could not meet the current criteria necessary for fuel. Ultimately, due to optimum properties, methyl esters have been generally accepted as the industrial standard for biodiesel.

The choice of which crops to use for biodiesel is still the subject of much debate. Concerning physical properties only, the factors affecting cetane number would suggest that plants favouring the production of longer, saturated chains would be the most suitable, at least during the running of the engine, as the temperatures of combustion would easily overcome the subsequent increase in viscosity; Krisnangkura (2006) provided an empirical method of predicting the temperature dependence of the viscosity of a biodiesel based upon knowing the FAME content. Palm Oil (PME), with a high content of palmitate and stearate, saturated 16 and 18 carbon compounds respectively (Graboski 1998, Ma 1999,

Srivastava 2000, Yuan 2005, Yizhe 2008, Balat 2010), has therefore become a popular choice for biodiesel production.

Outside of normal engine operations, however, the low viscosity, and hence high pour point can cause serious problems for engines running in colder conditions as noted previously. Increasing the amount of unsaturation in the alkyl chain can help lower the viscosity, freezing and pour points at the expense of also lowering the cetane number. Combinations of saturated and unsaturated methyl esters can therefore help balance these properties and crops such as Rapeseed (RME) and Soybean (SME) that produce both palmitate and stearate as well as oleate and linoleate (Ma 1999, Srivastava 2000, Yuan 2005, Yizhe 2008, Balat 2010) (the singly and doubly unsaturated analogues of stearate respectively) have therefore also become popular choices as crops for biodiesel. In addition to their abundance and cheap production the three have now become the leading biodiesel crops in Europe and North America (Bockey 2002) – the three often being used in blends to create commercially available biodiesel.

Another area of concern has been raised on the issue of growing crops for fuel in place of food, particularly in the light of food supplies in 3rd world countries (Srinisavan 2009). It is unfortunate therefore, that the three aforementioned crops are also highly valued in the food industry (Hill, K. 2000, Thoenes 2006). In addition to ethical concern, there is also economical concern that as demand for rapeseed etc increases as a new market opens up for it that prices for these crops will also increase, which is undesirable from the point of view of both the food and fuel markets. Whilst arable crops show good potential for use of biodiesel, they clearly cannot supply the market by themselves.

One solution has been to take the used oil, rather than then virgin material, and put it through the same transesterification processes to produce Used Cooking Oil (UCO) biodiesel (Zhang, Y. 2003). As well as not immediately competing with the food market, due to being used in the fuel industry after usage, UCO biodiesel has another immediate advantage over virgin oil in that it is cheaper due to coming from a waste stream as opposed to a raw material and as such reduces water pollution the need for landfill.

During usage UCO biodiesel has shown very similar physical (pour and flash point) and combustion (CN) properties to virgin oil biodiesel – though the feedstock oil was still a significant determinant in the used oil's properties (Lapuerta 2008). The higher oxygen content of UCO from autoxidation (see section 1.5) during usage led to a reduction in particulate emissions however those that were emitted were smaller in diameter (Lapuerta 2008) which could be a potential barrier depending on how legislation on particulate

matter emissions proceed and may require the need for refinement. At present though FAME from UCO sources complies with current legislation and is a very viable option for fuel that does not compete with food crop production (Enweremadu 2009).

Another proposed option is to use plants that are inedible to humans, yet are also triglyceride, or fatty acid producing. One that has become of considerable interest in Asia is the plant Jatropha (Sarin 2007, Zhang F.L. 2008, Jain 2010). The specific species, *Jatropha curcas* (common name: Ratanjyot), has been identified as a potential biodiesel crop due to its high oil content of between 30-40% (Sarin 2007) and the fact that FAME material produced from it has a desirable cetane number of 51 (Jain 2010) and testing has shown it to have other comparable properties to diesel (Chauan 2006). It is also of interest, not just because it is inedible, but because it can grow in drier, arid conditions that would not be suitable for growing arable crops, hence would not impede upon land used for growing food and as such provides the potential for not only generating fuel, but recapturing wasteland and boosting the economy of local communities that may farm it. Other crops have since been investigated for their potential to achieve similar results, the next most significant being *Pongamia pinnata (*Karanjia), but Jain also identified Kusum, Neem and Mahua as plants to be considered.

In the food vs. fuel debate, these inedible crops, amongst others became the next wave of biodiesels and are sometimes referred to as second generation biodiesels, whilst their predecessors (from rapeseed, soybean etc) are first generation (Naik 2010). But whilst their source material may be different, the biodiesel produced is still a mixture of FAME – Jatropha also contains mainly palmitic, stearic, oleic and linoleic acids – and as such, they can be grouped together when their chemistry is being analysed. 2^{nd} generation biofuels can also differ in production methods, whilst still using the same source materials. There are other areas currently being investigated of producing diesel from other bio-materials such as algae, lignin and cellulose (3^{rd} and 4^{th} generation etc) which at present look like they may depart from the traditional FAME biodiesels. At present, however, FAME is still the predominant form of biodiesel and as such, this chapter and all subsequent ones will (unless otherwise stated) consider biodiesel as FAME mixtures.

1.3 Increasing Usage of Biodiesel

Biodiesel has been in existence in its FAME format since the mid-1930's (Pousa 2007), but never took off as a popular fuel, mainly due to petrol and mineral diesel being considerably cheaper and much more readily available. Instead, vegetable oils and

biodiesels were typically confined to use in times of fuel shortage and other emergency situations (Pousa 2000, Sharma 2009). Usage of biodiesel was otherwise mainly confined to rural, agricultural areas where waste crops could be quickly converted to biodiesel on site to power farming machinery providing an easy fuel source and avoiding the need to import.

Avoiding the need to import was another major factor in biofuel development – crude oil may have been historically preferred due to its high abundance and low cost of production, but there was still the issue of transport. Britain, the U.S.A., Russia and particularly the Middle East all had their own oil reserves to drill, each with their own differing compositions. For instance, one region's oil reserves could be high in aromatics and low in saturates, whilst another may be the reverse (Aske 2001). This meant that Europe, Asia and North America all had plenty of oil to hand and to trade with other to complement each other's strengths and weaknesses. South America's oil reserves were considerably smaller however, meaning importation was necessary – a fact not helped by the fact that the southernmost countries were not amongst the commonly used trade routes, driving the prices up further. Exploiting the region's own natural resources was a much more viable alternative and hence Latin American countries developed an interest in biofuels much earlier than most of the developed world. Brazil's abundance of sugar cane, for instance, made for an easy source of sugars to cheaply ferment to make ethanol. As a result, Brazil's fuel economy is now made up largely of bioethanol which is also one of its major exports – as of 2005 Brazil's production of bioethanol equalled half of the global production (Smeets 2008).

Diesel was still a necessary fuel for heavier machinery though and so, although taking a back seat to bioethanol, research into biodiesel was still a popular area. Globally, interest in biodiesel was revived during the petroleum crisis of the 1970's (Pousa 2000, Radich 2004), triggered by political unrest in Arabian oil producing states, particularly the Iranian Revolution (Campbell 1998) and therefore raising the awareness of the developed world's dependence on cheap petroleum. The Gulf War of 1990-1991 saw another surge in oil prices again sparking interest in renewable fuels which this time around has persisted this far partially due to the noted trend of oil price spikes triggering recession and excessive inflation (Barsky 2004), but also due to increasing interest in environmental issues and climate change during the 2000's as a result of the culmination of research into global warming, sustainability and energy demands leading to stricter legislation on such matters (EU Paper COM (2006) 105).

The 1990's also saw the beginning of commercial production of biodiesel in the U.S.A. with areas such as Europe and India swiftly following (Srivastava 2000) and has been a rapidly expanding market – in the U.S.A. alone production went from 500,000 gallons per annum in 1999 to 6.7 million gallons p.a. in 2000 (Radich 2004) and 114 million gallons p.a. in 2003, with European production at 450 million gallons p.a. in 2003 (Haas 2006). However with arable crops being the most readily available feedstock, they have also become the primary choice for biodiesel production which has led to conflict with food usage due to concern over food prices and third world poverty in what is known as the 'Food vs. Fuel' debate (Srinisavan 2009). Whilst the usage of non-food crops (such as Jatropha), UCO biodiesel or 2nd, 3rd and above generation biodiesel are all being researched, arable crops such as palm, rape and soybean currently make up the bulk of biodiesel feedstocks (Szulczyk 2010), with the food vs. fuel debate currently unresolved at the time of writing.

1.4 Lubrication

Both the steam engine and the internal combustion engine went through several modifications before arriving at the finished models that would become familiar to the world during the industrial revolution. The main aims throughout the developments were to arrive at a design that would make efficient use of the fuel it was using. Watt may have had made the breakthrough that avoided the inefficient alternating of heating and cooling the cylinder, but there was still another major source of heat and energy loss. A tight seal between the piston and cylinder wall was required to prevent escape of the steam as this would prevent the build up and decline of pressure required to drive the piston. This tight fit came with the trade-off of friction between the two surfaces preventing the piston moving as quickly and as smoothly as it would have done otherwise. This required more fuel to drive the piston to overcome the friction and hence resulted in a loss of efficiency. More seriously, the friction between the surfaces also wore them down over time, reducing the tight fit between the walls and allowing steam to escape, once more reducing the efficiency of the engine, but also over time rendering the machinery incapable of carrying out its function properly. Replacing the machinery was undesirable as it was expensive and therefore another challenge was to preserve the working lifetime of the engine for as long as possible.

The same problems arose where the rod met the wheel and on the bearings for the wheels – in fact all areas where moving parts came into contact with either their supports

or each other were, and still are, subject to wear. The solution, fortunately, was therefore universal for all areas and came in the form of lubrication – employing a liquid or grease, a lubricant, between the two surfaces to prevent friction to both allowing two surfaces to slide freely across each other and to prevent wear between them. There is no universal lubricant as different purposes require different properties from their lubricant. Indeed, if there were only a handful of lubricants to choose from, then the most readily available one would generally be the one selected, regardless of the disadvantages which initially, before the advent of crude oil, this was generally the method of selection and early (pre-19th Century) lubricants ranged from goose fat to natural graphite (Lansdown 2004).

However, as the complexity of machinery has evolved, so too has the specificity of the lubricant required and the solution for lubrication of engines came in the same form as the fuel – crude oil. During the fractional distillation process where petrol and diesel are separated out, the unvaporised oil is then put through a second process – vacuum distillation. Through this various types of oils are separated out for different purposes, such as medical, cosmetic and mechanical lubrication (Stachiowak 2005).

The reasons for the necessity of different types of lubricant vary, even amongst the same class, or purpose of lubricant. In mechanical lubrication for instance, a machine designed to operate in cold conditions will need a lubricant that will not freeze at the required operating temperatures. Similarly, machines operating at high temperatures need lubricants which will not evaporate, become too thin, or potentially ignite in the presence of other fuels or sparks. Another factor affecting the lubricant selection can include the type of surface being lubricated. If a surface is chemically active, the lubricant itself must be inert so as not to react with the surface and degrade or destroy it. In fact, the same is true of the lubricant itself – it should ideally be inert and protected in order to prevent its own degradation and contamination. In some situations, the best solution can be to avoid lubrication altogether if it difficult or expensive to administer and its usage can lead to build up of unwanted products.

Automotive engines often experience these problems. Administering the lubricant to the desired areas requires additional pipework and pumps to transport the lubricant around the engine where it subjected to both degradation via oxidation and contamination from the fuel which can lead to unwanted products. Due to the harsh nature of the engine however, avoiding the use of lubricant altogether would damage the engine even further and hence is not a viable option. In order to minimise this problem it is necessary to understand the nature of the fuel contamination as well as the oxidative degradation

mechanisms of the lubricant, also the fuel and more generally the behaviour of the species responsible for oxidation in the first place.

1.5 Oxygen Radicals and Autoxidation

1.5.1 Chemistry of oxygen radicals

Oxygen is rare amongst the elements in the periodic table in that in its common elemental form, O_2, even though it possesses an even number of electrons, rather than fully pairing up, two electrons are left unpaired in the antibonding orbitals (Mulliken 1932). This means the molecule is naturally paramagnetic as opposed to diamagnetic and has led to debates in the scientific community about whether the bonding structure of dioxygen should be properly represented as a double bond (O=O) or as a diradical (·O-O·) (Kearns 1971) – though at present it is conventionally represented as O=O. The molecular orbital diagram of oxygen (figure 1.2) shows the total bond order to be 2 – which is consistent with oxygen forming two bonds in stable molecules, such as peroxides (R-O-O-R) and carbonyls (R-(C=O)-R) (see figure 1.3), yet the radical nature of oxygen reactions is of huge significance in oxidation chemistry, particularly for this subject in the areas of combustion and autoxidation.

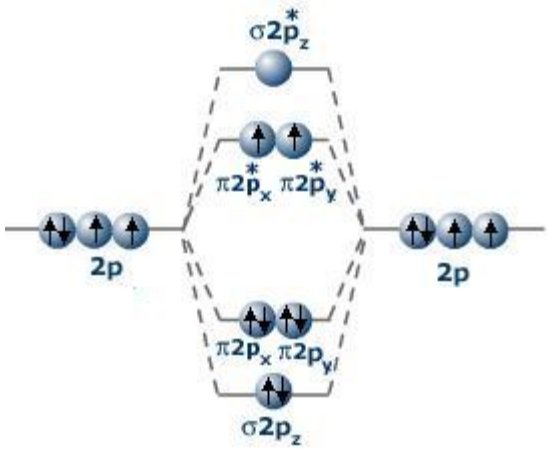

Figure 1.2 – The molecular orbital diagram of O_2 (tutorvista).

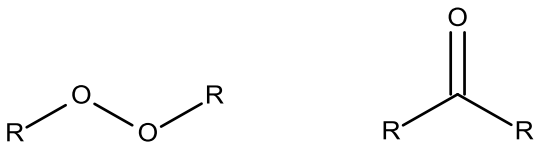

Figure 1.3 – A peroxide and carbonyl compound, typical common examples of oxygen forming two bonds in stable compounds.

Radical reactions due to their nature generate other radicals which typically go on to partake in further radical reactions, triggering a chain reaction. Radicals reactions are therefore rarely single processes but instead a collection generally known as radical chain reactions or radical cycles with the individual reactions falling into three main categories: initiation reactions, (chain) propagation reactions and termination reactions.

Initiation reactions are those that set the cycle in motion by creating one or more unstable, reactive radical species. In controlled radical reactions, such as syntheses, this usually occurs via the homolytic cleaving of a bond to generate two radical species as opposed to the more common heterolytic cleaving which generates two oppositely charged ionic species. In the natural oxidation chemistry of organic molecules however the initiating step comes via oxygen (already a radical species, albeit a relatively far more stable one) and is normally the breaking of a C-H bond (unless there is a more radically reactive functional group present) to give a carbon centred radical and a hydroperoxy radical (Figure 1.2); also known as hydrogen abstraction (Reaction 1.1).

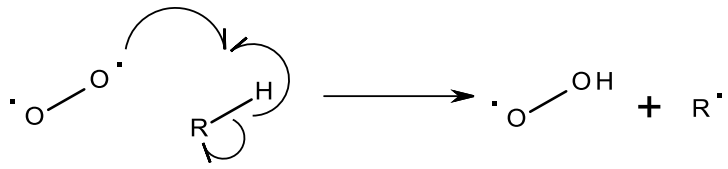

Reaction 1.1

Although homolytic cleaving of a bond is less common in oxidation chemistry, it can still occur naturally if peroxides are formed via cleavage of the O-O bond (Reaction 1.2) to give two alkoxyl radicals (figure 1.2) – or a hydroperoxide if one of the R groups is hydrogen. As oxygen is far more abundant in most systems, this is often a relatively minor reaction as peroxides are typically the product of radical reactions themselves – it has the potential to be highly significant in other fields of chemistry however if peroxides are allowed to build up to high concentrations in unwanted areas e.g. in bottles of flammable solvents and hence cannot be considered insignificant in oxidation chemistry.

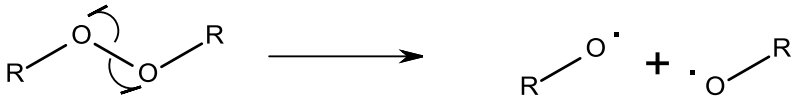

Reaction 1.2

Chain propagation reactions are by far the most common type of reaction in radical cycles and involve the radical species stabilising themselves by reacting with another species to create a more stable molecule, but also producing another radical which itself can participate in a propagation reaction. Propagation reactions are therefore the reactions

that enable the radical cycle to continue by continually providing new species of radicals to react, hence why they are sometimes known as 'chain' propagation reactions. In oxidation chemistry, the species that typically participate the propagation cycle are the oxygen based peroxyl, alkoxyl, hydroxyl and hydroperoxyl radicals – see figure 1.4.

Figure 1.4 – Peroxyl, alkoxyl, hydroxyl and hydroperoxyl radicals respectively, where R ≠ H.

The first types of propagation reaction generally involve the radicals generated in the initiation reactions. One of the most common reactions in oxidation chemistry involves the carbon-centred radical reacting with the abundant and reactive oxygen in the atmosphere to generate a peroxyl radical (figure 1.4, reaction 1.3).

Reaction 1.3

These peroxyl radicals can then stabilise themselves by undergoing hydrogen abstraction again, as in reaction 1.1 to form a hydroperoxide and another carbon centred radical (Reaction 1.4).

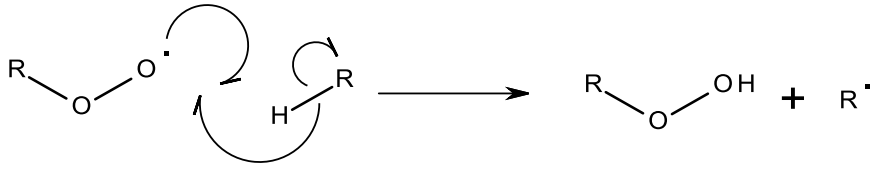

Reaction 1.4

These two reactions are perhaps the most significant of the propagation reactions as the products from one are the reagents for the other and hence allow for the cycle to be formed and to be continued as long as there is oxygen and a hydrocarbon present – see figure 1.5 (Batt 1987, Lightfoot 1992).

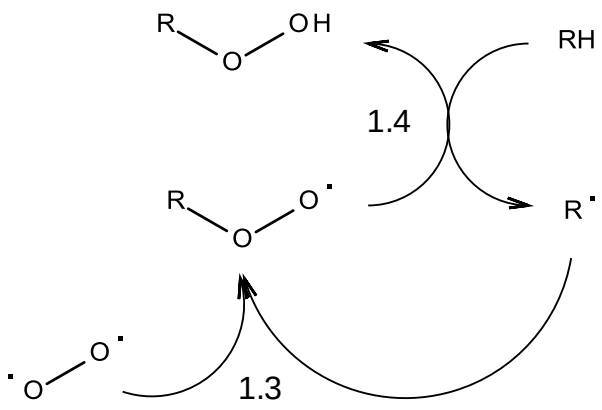

Figure 1.5 – The radical propagation cycle generated by reactions 1.3 and 1.4.

The other type of radicals generated via initiation reactions are the alkoxyl radicals formed from reaction 1.2. These can also participate in hydrogen abstraction reactions as in reactions 1.1 and 1.4, this time creating a carbon centred radical and an alcohol (Reaction 1.5).

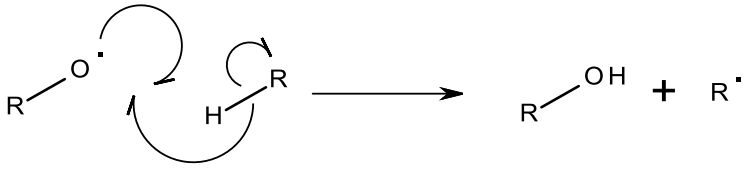

Reaction 1.5

As hydroperoxides from reaction 1.4 can cleave via reaction 1.2, hydroperoxides can also indirectly supply reagents for reaction 1.5, meaning this third propagation reaction can also interact with the radical cycle shown in figure 1.5 as shown below in figure 1.6 (Batt 1987, Lightfoot 1992).

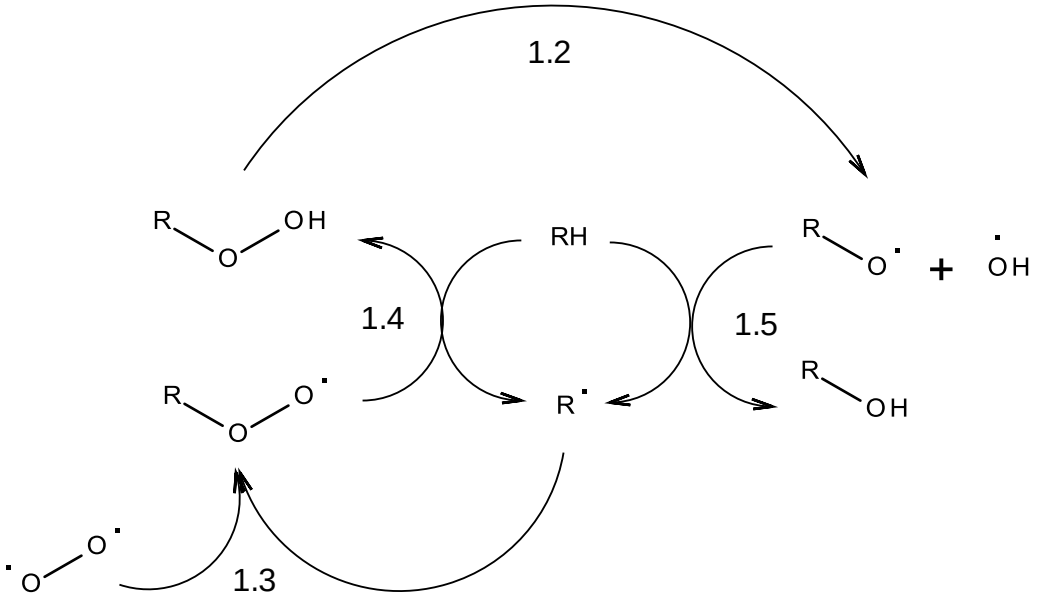

Figure 1.6 – The interaction of the radical propagation cycle with alkoxyl radicals.

The final sets of reactions in radical cycles are termination reactions where two radicals combine to give a stable molecule with no radical species left over. One example is where a carbon centred radical combines with a hydroperoxyl radical rather than oxygen as in reaction 1.3 to form a hydroperoxide (Reaction 1.6).

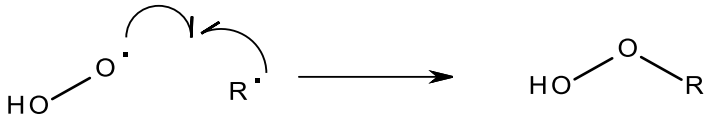

Reaction 1.6

The problem with this reaction is that the hydroperoxide can simply initiate a new cycle by cleaving the O-O bond. The hydroxyl radicals that are formed however can also combine with a carbon centred radical to give an alcohol – a much more stable molecule (Reaction 1.7).

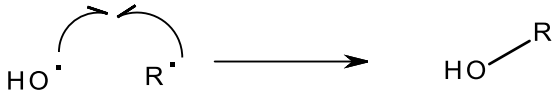

Reaction 1.7

The other main type of termination reaction in the oxidation of organic molecules simply involves two carbon centred radicals combining to create a new carbon-carbon bond (Reaction 1.8).

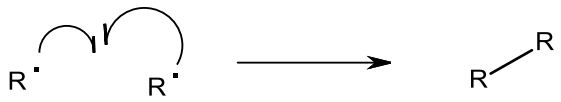

Reaction 1.8

The full set of reactions and how the various species interact in the cycle is summarised below in figure 1.7 (Batt 1987, Lightfoot 1992).

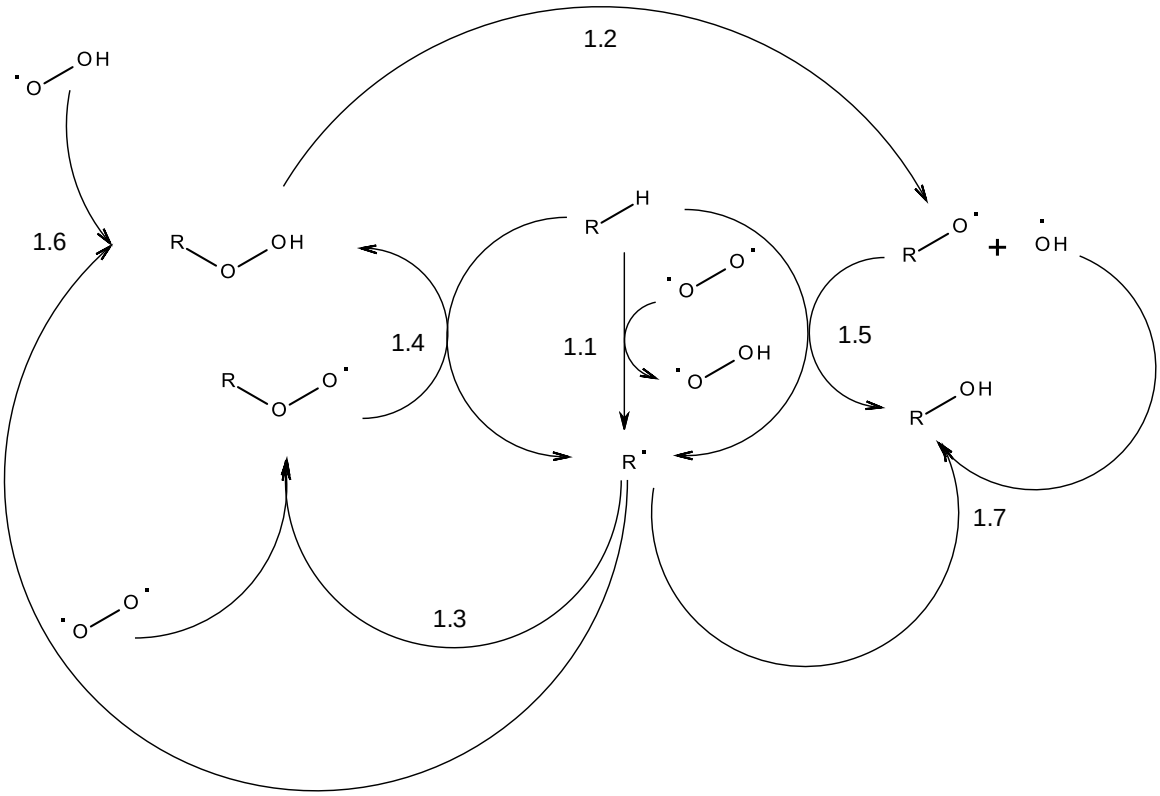

Figure 1.7 – The overall summarised radical cycle.

The R-H bond that is broken in the initiation reaction depends on the bond strength. A uniform molecule, such as methane or cyclohexane, will have no hydrogen atom preferentially abstracted, but most molecules will have structural (such as branching) or electronic (from heteroatoms) properties that can comparatively weaken the R-H bond. The strength of the R-H bond is directly related to the stability of the resulting R· radical; the more stable the lower the R-H Bond Dissociation Energy (B.D.E.). This can be shown by examining the everyday consequences of oxidation reactions. The oxidation of some of the simplest organic molecules also happens via one of the most common natural oxidation reactions – combustion.

1.5.2 Combustion of VOCs and light-fuels.

The chemical definition of combustion is given in the Oxford English Dictionary as 'the development of light and heat from the chemical combination of a substance with oxygen'. The substance in question can be a variety of materials, both inorganic and organic, as oxygen, being a powerful oxidising agent, will react with most materials. Lighting, fireworks and even some lasers are built around knowing the emission spectra of various metals upon reaction with oxygen, for example, yet for the purpose of fuel it is the emission of energy in the form of heat that is of importance and this is almost always obtained – certainly in the internal combustion engine – from organic materials. As the backbone for all organic materials is carbon, it naturally follows that the complete combination of any organic compound will yield carbon dioxide – leading to emissions problems as outlined at the beginning of this chapter. If there are no other heteroatoms present in the molecule, the other product of the reaction will come from the combination of hydrogen with oxygen to form water vapour. Complete combustion of hydrocarbon fuels is therefore given by the overall reaction in Equation 1.1:

$$C_nH_m + \left(n + \frac{m}{4}\right)O_2 \rightarrow nCO_2 + \frac{m}{2}H_2O \qquad \text{Equation 1.1}$$

In reality, the process of combustion is a combination of the sub-reactions in the previous section. Cool-flame studies on 2-methyl pentane by Affleck back in 1967 identified several intermediates during the process suggested a multi-step process for combustion as a whole (Lignola 1987), beginning with initiation via reaction 1.1. Using the simplest organic molecule, methane, as an example, this initial step can be shown in figure 1.8.

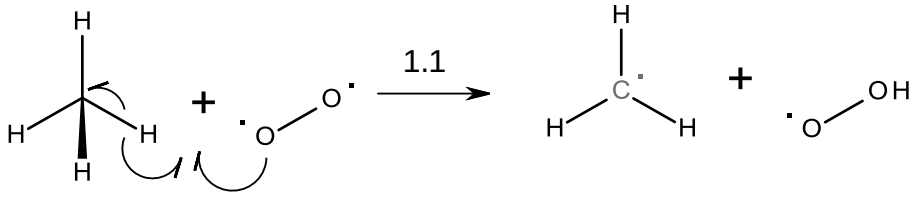

Figure 1.8 – The hydrogen abstraction of methane by oxygen as the opening stage of combustion.

The methyl ($CH_3\cdot$) radical, is however, very unstable as indicated by the relatively high Bond Dissociation Energy (B.D.E.) of the C-H bond estimated at 435-440 kJ mol^{-1} (McMillen, 1982, Siegbahn 1985, Blanksby 2003) and hence this initiating reaction will not occur spontaneously under standard conditions, but instead will require an input to kick-start the reaction, such as the high temperatures found in a spark. As the carbon-centred radicals are highly-reactive though, they will then react very rapidly with other radicals in chain propagation reactions (as shown in reactions 1.1-1.7 and outlined in figure 1.5) or with the other carbon centred radicals to terminate the chain reaction – in the case of the methyl radicals to form ethane. Hence, despite the simplicity of equation 1.1, the process of combustion, being a summary of reactions 1.1-1.7, is in fact much more complex.

As the reactions are exothermic the energy released is sufficient to allow further reactions between methane and oxygen, setting up a chain reaction which will persist as long as there is enough fuel (methane or another combustible material) and oxygen present to receive that energy.

The next molecule in the chain, ethane, combusts in a very similar manner to methane, except with the additional reaction of the alkoxy radical breaking the C-C bond, rather than a C-H bond (see figure 1.9), and stoichiometrically requiring another oxygen atom.

Figure 1.9 – The cleaving of a C-C bond via an alkoxy radical.

The initial hydrogen abstraction is easier than for methane however due to the C-H bonds in ethane having a lower B.D.E of 423.0±1.7 kJ mol^{-1} (Blanksby 2003). This lower B.D.E. comes from the resulting alkyl radical being stabilised via the positive inductive effect of the CH_3 group stabilising the carbon bearing the unpaired electron. This effect is small however and the relatively lower B.D.E. is still very high by comparison to other organic molecules and as a result, spontaneous combustion of ethane will not occur under standard conditions but will still require an initial input of energy to start the process off.

As the carbon chain gets progressively longer, the inductive effect gets progressively more significant in stabilising the alkyl radical with the result that the initial energy required to start the oxidation (combustion) process gets gradually smaller. However, as the carbon chain increases in length, it gets heavier and hence its boiling point decreases; meaning it is less likely to enter the vapour phase to mix with oxygen. In addition more oxygen molecules are required to consume the entire molecule. The net result being for straight chain, saturated hydrocarbons the initial oxidation step becomes easier as the chain length increases, but this comes at the expense of combustibility. Ultimately, there comes a point where the hydrocarbon in question becomes too heavy to enter the gas phase easily at which point it can no longer be considered a viable option as a fuel.

1.5.3 Heavier Hydrocarbons and Lubricants

Obviously combustibility in many cases is not a desirable property; neither is the ability to react spontaneously with oxygen or the atmosphere in general. In fact, a wide range of materials are selected for their physical properties and complete chemical inertness is a valued property – lubricants are a typical example of these. Virtually all machinery utilizing moving parts – from engines to computer hard disks (Hsu 2004, Stachiowak 2005) – that come into contact with each other employ a lubricant of some description in order to maintain smooth working order by reducing friction between the surfaces and hence subsequent wear. Saturated hydrocarbons are therefore good candidates as they typically have no functionality and are only known for their ability to react with oxygen. As stated in the previous section, in light, volatile hydrocarbons, this property manifests itself in the form of combustion – a process that requires an initial energy input to get started. Heavier hydrocarbons are therefore not subject to this problem at room temperature. However as the fuel combusts energy is released to drive the motor; no process is completely energy efficient and the wasted energy from combustion is released as heat, meaning the temperature inside the engine is vastly increased and can achieve an average of over 250 ^{o}C inside the combustion chamber on the cylinder walls (Hayes 1993). The areas where the lubricant is required to operate generally do not reach such high temperatures, but the lubricant can still be expected to operate at temperatures ranging from -10 ^{o}C (depending on local temperature) upon start-up to 180 ^{o}C (Moritani 2003, Taylor 2004) during full operation. Straight chain alkanes cannot meet this criteria – alkanes that are liquid at room temperature and at -10 ^{o}C will boil by 180 ^{o}C (Owczarek

2003), similarly, alkanes that would be liquid at these higher temperatures will be solid by -10 ^{o}C.

Branching of the chain can help resolve this problem and enable the molecule to remain liquid over a larger range of temperatures as well as retaining a working viscosity (Jabbarzadeh 2002) – if the viscosity of the lubricant is too high it will not lubricate the moving parts properly leading to increased friction and overall inefficiency. If it is too low it will not form a proper film between the moving parts and hence not prevent wear. The most common oils used for lubricating engines are mineral oils and are obtained through fractional distillation of crude oil – specifically the unvapourised oil from the first column, which is then passed through a second vacuum column (Stachiowak 2005). The fraction is often filtered and purified yet can still contain over 100 different compounds (Kimura 1982, Stachiowak 2005) which are generally large carbon-number branched hydrocarbons. This makes up what is known as the 'base-fluid' or 'base-stock' of the lubricant and generally accounts for 95% of the lubricant – the remaining 5% are chemicals known as additives which are introduced to improve various properties of the lubricant (Stachiowak 2005) – these will be covered in greater detail in Chapter 6. As the compounds in the base-fluid are similar in carbon number, boiling point and other physical properties they can be hard to separate to determine an accurate picture of the composition in most cases. In lubricant modelling however, Gupta (1997) noted that 24 carbon chain molecules with various levels of branching appeared to show good correlation with the physical and chemical properties of mineral oil lubricants. Squalane ($C_{30}H_{62}$, 2,6,10,15,19,23 hexamethylcosane) has been used in many other studies to model lubricant behaviour in various systems (Adamczyk 1984, Kumagai 1995, Deegan 1999) and Gupta suggested that $C_{30}H_{62}$ was a reasonable average chemical formula for the components of a lubricating oil base fluid. Squalane has been used in this study as well – its properties will be discussed in greater detail in Chapter 4 – but it is important to note that the introduction of branching, whilst improving the physical properties of the base-fluid also alters its chemical properties with respect to resisting oxidation.

Whilst discussing the initial stages of combustion for linear alkanes, it was mentioned that a longer alkyl chain could help stabilise an alkyl radical through the inductive effect. This is most effective when the carbon atom bearing the unpaired electron sits in the middle of the chain so that it can receive stabilisation from two directions; i.e. for propane, a hydrogen atom on the central carbon atom will be more easily abstracted than a hydrogen atom on the terminal carbon atom; this is the same for butane and so on

through increasing chain lengths (Batt, 1987). Branching therefore provides a third alkyl chain around the central carbon atom to stabilise the radical further reducing the C-H B.D.E. For comparison the B.D.E's of the C-H bond required to make the n-butyl, i-butyl and t-butyl radicals (see figure 1.10) are 423.0±1.7, 413.4±2.1 and 403.8±1.7 kJ mol^{-1} respectively (McMillen 1982, Seetula 1997, Blanksby 2003).

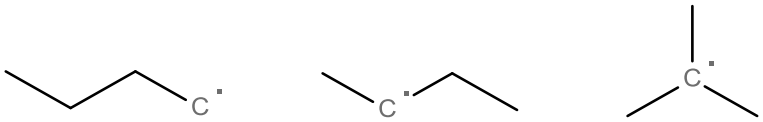

Figure 1.10 – From left to right, the n-butyl, i-butyl and t-butyl radicals.

The branching of the hydrocarbon chain therefore enables easier initiation of the oxidation sequence due to lowering the B.D.E. – still not low enough though to undergo hydrogen abstraction (reaction 1.1) at room temperature. As discussed earlier, however, the temperatures a lubricant experiences during engine usage far exceed room temperatures with the result that the lubricants can start undergoing noticeable autoxidation. The fact that it will still not vaporise means that it will not combust as lighter hydrocarbons do, but are capable of forming stable compounds, either through cleaving the carbon chain (fragmentation) or adding to it (addition) (Stark et al 2011). In figure 1.6, the fourth reaction showed the formation of methanal (formaldehyde) which would be instantly consumed itself to complete the combustion process. The process by which this is formed is similar to longer chain oxidation products. These take the form of aldehydes or ketones, and are formed depending upon where the initial hydrocarbon is abstracted from; the end or middle of the chain. Aldehydes can also be formed if the alkoxyl radical is formed in the middle of the carbon chain by breaking the C-C bond as shown in figure 1.7. If the hydrocarbon is branched, the cleaving of the carbon chain is almost inevitable as the tertiary hydrogens are the ones that preferentially undergo abstraction, meaning in order to form the carbonyl group, the only adjacent bonds available to break are the C-C bonds. Normally, the C-C bond that is cleaved is the one that will yield the most stable alkyl radical – for instance in squalane, the main chain is typically broken so as not to form the methyl radical (Stark 2011).

Whilst not deteriorating completely to CO_2 and H_2O, this process of autoxidation of the lubricant base fluid is still undesirable as the length of the carbon is the main factor determining the viscosity (Krisnangkura 2006) and the fragmentation of the chain will

lower it. Of more concern is the ability of two alkyl radicals to combine with each other to terminate the radical chain reaction (see figure 1.11) – for instance the ability of two methyl radicals to combine to form ethane – this in turn will thicken the base fluid.

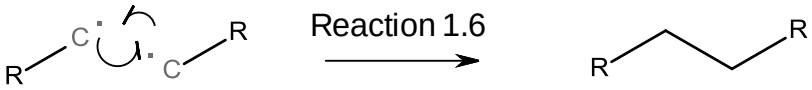

Figure 1.11 – The combination of two alkyl radicals to terminate a radical reaction.

The oxidation of a lubricant base fluid is therefore a significant problem as its oxidation resistance properties will determine its effective working lifetime and as such the bulk of lubricant chemistry research is focused on prolonging this lifetime. A large part of the research goes towards developing additives that will prevent oxidation or remove unwanted oxidation products – this will be covered in greater detail in chapter 6. Another large area of research is to investigate what affects the oxidation processes in the first place and this has been the main focus for this project – specifically how biodiesel affects these properties.

1.5.4 Lipids and Biodiesels

It was previously mentioned in section 2 that double bonds within biodiesel systems could improve the physical properties, such as lowering the pour point and freezing point of the fuel at the expense of also lowering the cetane number, but the introduction of unsaturated sites also fundamentally alters the oxidation properties of the fuel. In the previous two sections hydrogen abstraction as the initiation step for oxidation was discussed, establishing that the more stable the alkyl radical, the weaker the C-H bond and hence the easier oxidation could occur. Tertiary hydrogens were shown to be relatively labile compared to primary and secondary ones. Introduction of a double bond into the system introduces two different types of C-H bond, the vinyl and allylic bonds. Vinyl bonds are the C-H bonds where the carbon is part of the double bond, whereas allylic bonds are those adjacent to the double bond (see figure 1.12).

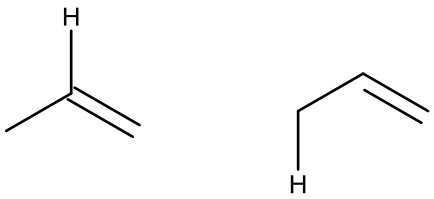

Figure 1.12 – A vinyl and allylic C-H bond, respectively.

Due to being electron deficient already, the vinyl bond is very strong at 460.2 ± 8.4 kJ mol^{-1} (McMillen 1982, Blanksby 2003) however the allylic hydrogen atoms are extremely relatively labile compared to those on saturated chains due to the fact that the resulting radical can undergo resonance stabilisation around the double bond (Figure 1.13). This gives an allylic C-H B.D.E. of 361.9 ± 8.8 kJ mol^{-1}; when a second, non-conjugated, double bond is introduced so that the allylic C-H is adjacent to two double bonds (Figure 1.14), the extra resonance stabilisation lower the B.D.E even further to 318±3 kJ mol^{-1} (McMillen 1982, Trenwith 1983, Clark 1991, Pratt 2003, Blanksby 2003).

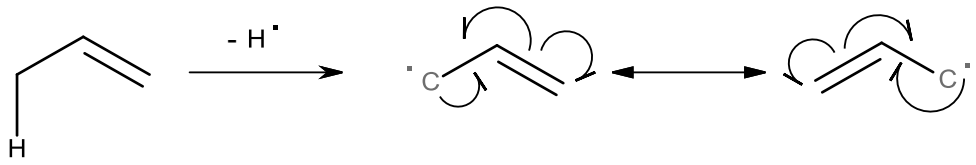

Figure 1.13 – The abstraction of an allylic hydrogen atom and subsequent resonance stabilisation mechanism.

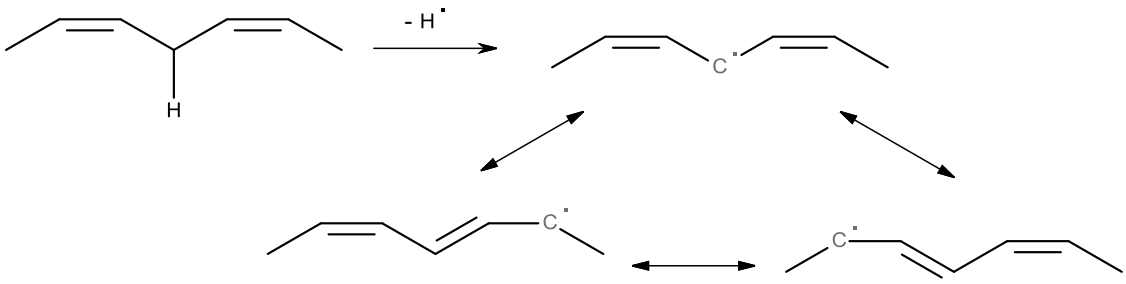

Figure 1.14 – The abstraction of a doubly allylic hydrogen atom and subsequent resonance stabilisation structures.

With the C-H B.D.E. so low no extra energy input is required to initiate hydrogen abstraction and hence it can occur in the atmosphere under standard conditions. This

process of oxygen initiated radical attack, without the aid of other reagents or catalysts is known as autoxidation (Ross, 1949) and is a well known phenomenon in the chemistry of fatty acids (Gardner 1989) from which biodiesel is derived. Most of the initial studies of autoxidation have been carried out on fatty acids and triglycerides with the area of interest being lipid chemistry and the effects on human health, but more recent studies at ambient conditions have been concerned with the potential for long-term storage of biodiesel and the subsequent change in properties over time (Bondioli 2003, Bouaid 2007). However, as previously discussed, the temperatures, pressures and chemical conditions achieved during engine use far exceed standard atmospheric ones and the subsequent change in physical and chemical properties under these conditions is a relatively new one, but one of increasing interest in the automotive industry and the basis for the research undertaken in this project.

1.6 Effect of Biodiesel on Automotive Engines

Methyl esters of fatty acid chains have become the popular choice of biodiesel due to their favourable performances in automotive engines compared to, for example, their ethyl ester counterparts, but as previously mentioned, the knowledge of their chemistry at present is largely based on lipid chemistry and autoxidation at ambient conditions (e.g. Ross 1949, Gardner 1989, Bondioli 2003) which current diesel engines greatly exceed (Hayes 1993, Moritani 2003, Taylor 2004). Neither are conditions across the engine uniform. A simplified model of the four stroke diesel engine can be broken down into three main areas, the combustion chamber, the piston assembly or ring pack and the sump (figure 1.15).

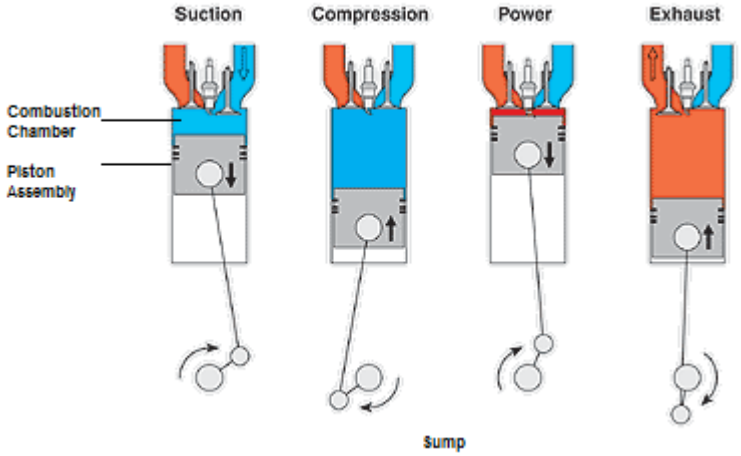

Figure 1.15 – Schematic diagram of the four phases of the four stroke diesel engine (Borg Warner 2011).

As its name implies, there are four main stages to the engine cycle. Firstly, the air is drawn in as the intake valve opens and the piston is drawn down (intake). Secondly, the valve closes so the fuel air mixture is compressed as the piston pushes back up through the cylinder (compression). Thirdly, the fuel/air mixture ignites under the extreme heat and pressure it is subjected to under the compression stage, the resulting pressure increase from gas production driving the piston back down the cylinder (power). Finally, the exhaust valve opens allowing the reagent gases to leave the chamber, the drop in pressure helping to draw the piston back up the cylinder (exhaust) (Ferguson 1986).

1.6.1 Combustion Chamber

From a chemistry perspective, the reason the engine can be simplified into three areas is that these are the areas the main different types of chemistry occur in. In the combustion chamber, the main chemistry that occurs is the combustion of hydrocarbons according to the general Equation 1.1 (section 1.5.2). This is a simplified equation for the combination of reactions that occur during the combustion a saturated hydrocarbon and hence the real chemistry becomes more complex due to the presence of other atmospheric molecules – most notably NOx causing unwanted side reactions (Bowman 1975, Lazaroiu 2007); FAME also adds the extra complication of double bonds and oxygen into the fuel molecule. Whilst clean combustion is the main and intended chemistry in the combustion chamber, it is the side reactions that are of significance to the performance of the engine. Although they are very minor – the combustion process is very efficient both with mineral and biodiesel (Tormos 2010) the unwanted chemical products tend to manifest in the form of thick, soot-like particles (Hiroyasu 1976) that can clog up the fuel injectors.

1.6.2 Piston Assembly

The issue of the unburned fuel is then of importance as it migrates down the wall of the cylinder past the piston assembly. This area is lubricated to ensure smooth operation of the piston, due to the fact that friction in this area is the main contributor to overall mechanical power loss (Wakuri 1992, Priest 1999, Tan 2010). Due to the continuous reciprocal motion of the piston, the lubricant is exposed to heavy wearing from the friction surfaces as well as contamination from exhaust gases and other combustion products – any unburnt fuel that migrates down the wall is also subject to these conditions – which, when combined with the heat generated through friction contributes significantly to the degradation of the lubricant (Gamble 2003). Investigating the nature of lubricant

degradation has proved problematic due to the fact that the temperatures and pressures the piston rings (which form the seal between the piston and cylinder wall) vary as the piston itself moves up and down the cylinder, meaning the lubricant itself is subjected to a wide range of conditions (Hamrock 1994, Tan 2010). The resulting products here are carbonaceous deposits on the piston rings (Kim 1998) which then increase the amount of friction between the piston and the cylinder walls reducing the efficiency of the piston, and hence the engine over time. Whilst the chemistry behind these deposits is unclear, the use of both vegetable oil and biodiesel has been seen to increase their formation (Shahid 2008), which poses a significant problem as the piston assembly is currently considered in the studies mentioned to be one of the major areas of lubricant degradation.

1.6.3 Sump

The final area of chemistry occurs in the sump underneath the piston. This is where lubricant and unburned fuel accumulate as they migrate down the cylinder walls. Being further away from the combustion chamber and moving parts it is also the lowest temperature part of the engine. The sump is also the reservoir from which accumulated oil is pumped out to re-lubricate the piston assembly and other moving parts of the engine. Any chemical changes that occur to the lubricant here, whether from addition of other chemicals (a process known as fuel dilution), or reactions of the existing ones, and the change in physical properties that result will therefore fundamentally affect the performance of the entire engine – there is still some debate about whether the gums and sediments found in the combustion chamber and piston assembly are really formed there, or whether they are transported and deposited there from the sump. Bush (1991) compared oil samples from the top ring zone and the sump against fresh oil and noted that the piston assembly oil showed greater levels of degradation compared to the sump, but that the sump also showed degradation characteristics such as a reduction in concentration of the base fluid. From this, it was proposed that the sump and the piston assembly should be considered as two separate reaction areas. The main unwanted products seen in the sump are sludge-like materials that can gum up the lubricant and make it less efficient. The use of biodiesel in some engines has seen an increase in the formation of these sludges, especially with the use of unsaturated ones. A study on palm oil (Sapaun 1996), which is composed mainly of saturated or singly unsaturated fatty acid chains (Sumathi 2008), revealed on short term test to show very comparable levels of combustion chamber wear, carbon deposits and lubricant oil contamination compared to mineral diesel. By

comparison, studies on soybean and tallow biodiesel containing larger amounts of unsaturated material (Ali 1995) showed both to increase the carbon residue by up to 10 times the amount left by a standard No.2 Diesel fuel; although this was reduced to comparable levels by blending the fuels in ratios as high as 60:40 Diesel:FAME levels.

In addition, due the introduction of diesel particulate filters (DPFs – detailed in the next section) and post-injection cycles to burn off excess soot has seen increased levels of fuel migrating down the walls of the cylinder to end up in the lubricant sump (Rakopoulos 2006). As biodiesel is less volatile than mineral diesel (Goodrum 2002, Reboucas 2001) it has a greater tendency to accumulate in the sump leading to high levels (typically around 5 – 10% higher than mineral diesel; Thornton 2009) of fuel dilution of the lubricant which is subsequently pumped throughout the engine (Rakopoulos 2006). In addition to reduced volatility, vegetable oil derived methyl ester biodiesel is more prone to oxidation than mineral diesel hence as it accumulates it is believed that it continues to oxidise to form sludges and varnishes which, when pumped through the engine can cause the increased ring-sticking noted by Labeckas (2006). As a result of this, increased oxidation and viscosity of the engine lubricant were also observed in this study, though at this stage there is no clear consensus amongst the literature as to whether biodiesel is causing increased oxidation of the lubricant, or simply contaminating it with its own breakdown products.

1.6.4 Legislative Demands and Restrictions

The engines that biodiesel seems to exacerbate sludge formation most prominently are the ones that utilise a technique known as Direct Injection (DI). Legislative demands are one of the reasons why a straight switch back to vegetable oils is not possible due to the call for reduction of emissions of various exhaust products, but the one crucial to direct injection engines is the legislation relating to Particulate Matter (PM) emissions. Particulate Matter is the name given to any solid particle product such as soot, ash or sand which when airborne can coat buildings, help form smog and, when inhaled, cause respiratory problems (El-Fadel 2000). It is therefore of interest to keep their emission into the atmosphere as low as possible – this is currently achieved in engines by having a filter, known as a Diesel Particulate Filter (DPF) in the exhaust which will trap any particulate emissions as they pass through. In order to prevent the filter being clogged up, DI engine inject an excess of fuel through the engine to burn the particulate aggregate off the filter – as a result excess fuel leads to excess unburned fuel which ends up in the sump leading to greater fuel dilution of the lubricant (Rakopoulos 2006). As PM emissions are required to

be as low as possible, DPFs and the DI engines that necessitate them are becoming more commonplace – in Europe, the Euro 5 and Euro 6 legislation, particularly EC Regulation No. 595/2009 has called for them to be a mandatory feature of diesel engines.

As a result this has impeded the progress of biodiesel into the market as DI engines are unable to cope with the large amounts of fuel dilution as a result. Current European legislation states that biodiesel can form a maximum of 7% of the fuel blend in a diesel engine; the blend being known as B07 for common, commercial distribution. If the blend is any higher than 7%, then it must be labelled as such (i.e. a blend of 10% biodiesel would be B10, 25% B25 etc) at the pump so that people who still choose to buy it do so at their own discretion. The upper limit is currently set at 7% as when deposits and sludge start to form in the engine it reduces its efficiency meaning more fuel is consumed per unit distance and hence emissions increase, including CO_2 which is counter-productive to using biodiesel as a means of CO_2 reduction. From the consumer perspective the reduction in efficiency is also undesirable as it also reduces the lifetime of the engine making it less value for money. A product that is less appealing is therefore also unattractive for engine manufacturers.

1.6.5 Emissions

Biodiesel still shows great promise for supplying the automotive industry because despite these issues, biodiesel still provides a large potential for carbon emission reductions as theoretically, all the carbon that is released as CO_2 will be taken up the following year in the next crop; assuming 100% crop yield. The full life-cycle assessment must also take into account carbon emissions from the farm processes – tractors, ploughs, etc and so biodiesel is not completely carbon-neutral, but can still reduce CO_2 emissions by 3.2kg compared to mineral diesel for every 1kg of fuel. Also as FAME contains no sulphur, biodiesel combustion emits no SO_2 (Körbitz 1999). and can also provide a 39% reduction in particulate matter (PM), 50% soot reduction and 20% CO as well as reductions in hydrocarbon and polyaromatic emissions; the latter two being strongly influenced by the biodiesel source material (Lapuerta 2008, Xue 2011). Due to the higher oxygen content of FAME, biodiesel has been noted to increase NO_x emissions which is less desirable, however Lapuerta noted that the injection process was slightly advanced with biodiesel and several studies (Walker 1994, Marshall 1995, Graboski 1998) proposed that to delay the injection process could reduce NOx emissions at the expense of increasing PM and soot; though these levels would still be lower than for mineral diesel. Leung

(2006) proposed that other injection parameters could be changed to reduce NO_x levels without the tradeoff of increasing PM and soot emissions and whilst at the time of writing there is no finalised or patented method, there does appear to be good scope to combat NO_x increases, thus eliminating the only negative emissions characteristic of biodiesel when compared to mineral diesel.

1.7 Project Aims

Whilst biodiesel shows significant promise as a potential renewable automotive fuel, it can still never be fully integrated as a stand-alone fuel as long as some of the associated problems remain unresolved and must continue to be used in conjunction with mineral diesel. In particular, with respect to being used independently of mineral diesel, the problem of increased engine fouling must be overcome.

In order to combat the formation of deposits and sludges, the chemical mechanisms behind their formation need to be understood and hence this forms the base upon which this project shall be focused. Whilst there has been significant work in the automotive industry in researching the practical problems associated with biodiesel usage, much of the work in understanding the chemical mechanisms of the breakdown of fatty acid methyl esters has been the study of biodiesels in their commercial form as a mixture of several different FAME compounds. Others have been generic studies of how biodiesel behaves or how they are related to the general autoxidation mechanisms, especially with respect to fatty acid and lipid autoxidation at room temperature, as previously discussed in sections 1.2 – 1.4. This project aims to further this understanding by breaking down biodiesel into its individual FAME components so as to analyse their chemistry individually. They will be broken down into two categories: mono-unsaturated and poly-unsaturated which are represented by methyl oleate and methyl linoleate respectively. As the poly-unsaturated FAME are so far understood to be the most chemically important, methyl linoleate will be the main focus for this project. However, it was reported that (at the time of writing) it was unknown whether these engine problems were caused by biodiesel actively altering the chemistry of the other components of the engine lubricant, or simply causing adverse effects by contaminating either them directly or via their breakdown products. As a result, it was concluded that to determine this, it was necessary to investigate the chemistry both of biodiesel and of biodiesel/lubricant systems.

By using the knowledge gained through this study, it will then be applied to seeing how these mechanisms impacts on other engine components; crucially the lubricant base

fluid, but also general antioxidants employed to inhibit oxidative degradation in mineral diesel/lubricant systems.

1.8 References

Adamczyk, A.A. Kach, R.A. A Combustion Bomb Study of Fuel-Oil Solubility and HC Emissions From Oil Layers, *Twentieth Symposium (International) on Combustion/The Combustion Institute*, 1984, 37-43.

Affleck, W.S. Fish, A. Two-stage Ignition under Engine Conditions Parallels that at Low Pressures, *Eleventh Symposium (International) on Combustion/The Combustion Institute*, 1967, 1003-1013.

Agarwal, A.K. Das, L.M. Biodiesel Development and Characterization for Use as a Fuel in Compression Ignition Engines. *J. of Eng. For Gas Turbines and Power*, 2001, **123,** 440-447.

Alexiadas, A. Global Warming and Human Activity: A Model for Studying the Potential Instability of the Carbon Dioxide/Temperature Feedback Mechanism, *Ecological Modelling*, 2007, **203(3-4),** 243-256.

Ali, Y. Hanna, M.A. Cuppett, S.L. Fuel Properties of Tallow and Soybean Oil Esters. *J. Am. Oil Chem. Soc.* 1995, **72(12)**, 1557-1564.

Aske, N. Kallevik, H. Sjöblom, J. Determination of Saturate, Aromatic, Resin and Asphaltenic (SARA) Components in Crude Oils by Means of Infrared and Near-Infrared Spectroscopy, *Energy and Fuels*, 2001, **15,** 1304-1312.

Attiwill, P.M. Atmospheric Carbon Dioxide and the Biosphere, *Environmental Pollution*, 1971, **(1),** 249-261.

Balat, M. Balat, H. Progress in Biodiesel Processing, *Applied Energy*, 2010, **87(6),** 1815-1835.

Barsky, R. Kilian, L. Oil and the Macroeconomy since the 1970's, *National Bureau of Economic Research*, Working Paper 10855, October 2004.

Batt L, Reactions of Alkoxy and Alkyl Peroxy Radicals, *International Reviews in Physical Chemistry*, 1987, **6(1),** 53-90.

Benson, S.W. Combustion, A Chemical and Kinetic View, *Twenty-First Symposium (International) on Combustion/The Combustion Institute*, 1986, 703-711.

Berchmans, H.J. Hirata, S. Biodiesel Production from Crude *Jatropha Curcas* L. Seed Oil with a High Content of Free Fatty Acids, *Bioresource Technology*, 2008, **99(6),** 1716-1721.

Blanksby, S.J. Ellison, G.B. Bond Dissociation Energies of Organic Molecules, *Acc. Chem. Res.* 2003, **36,** 255-263.

Bockey, D. Situation and Development Potential for the Production of Biodiesel – An International Report, 2002.

Bondioli, P. Gasparoli, A. Della Bella, L. Tagliabue, S. Toso, G. Biodiesel Stability under Comercial Storage Conditions over One Year, *Eur. J. Lipid Sci. Technol.* 2003, **105,** 735-741.

Borg-Warner Turbo and Emission Systems - http://www.3k-warner.de/products/turbochargerPrinciples.aspx - accessed 12/08/11

Bouaid, A. Martinez, M. Aracil, J. Long Storage Stability of Biodiesel from Vegetable and Used Frying Oils, *Fuel*, 2007, **86,** 2596-2602.

Boult, P.J. Fisher, Q.J. Clinch, S.R. Lovibond, J R. Cockshell, C.C. Geomechanical, microstructural, and petrophysical evolution in experimentally reactivated cataclasites: Discussion, *AAPG Bulletin*. 2003, **87**, 1681-1683.

Bowman, C.T. Kinetics of Pollutant Formation and Destruction in Combustion, *Prog. Energy Combust. Sci.* 1975, **1,** 33-45.

Bush, G.P. Fox, M.F. Picken, D.J. Butcher, L.F. Composition of Lubricating Oil in the Upper Ring Zone of an Internal Combustion Engine, *Tribology International*, 1991, **24(4),** 231-233.

Bryant, L. The Development of the Diesel Engine, *Technology and Culture*, 1976, **17(3),** 432-446.

Cadle, R.D. Formation and Chemical Reactions of Atmospheric Particles, *Journal of Colloid and Interface Science*, 1972, **39(1),** 25-31.

Campbell, C.J. The End of Cheap Oil, *Scientific American*, March 1998.

Cao, M. Woodward, F. I. Dynamic Responses of Terrestrial Ecosystem Carbon Cycling to Global Climate Change, *Nature*, 1998, **393,** 249-252.

Carlton, A.C. James Watt (1736 – 1819), *Journal of the Franklin Institute*, 1953, **256(4),** 375-376.

Chauhan, R.D. Sharma, M.P. Saini, R.P. Singal, S.K. Biodiesel from *Jatropha* as Transport Fuel – A Case Study of UP State, India, *Journal of Scientific and Industrial Research*, 2006, **66(5),** 394-398.

Cox, P.M, Betts, R.A. Jones, C.D. Spall, S.A. Totterdell, I.J. Acceleration of Global Warming due to Carbon-Cycle Feedbacks in a Coupled Climate Model, *Nature*,2000, **408,** 184-187.

Clark, K.B. Culshaw, P.N. Griller, D. Lossing, F.P. Martinho Simões, J.A. Walton, J.C. Studies of the Formation and Stability of Pentadienyl and 3-Substituted Pentadienyl Radicals, *J. Org. Chem.* 1991, **56,** 5535-5539.

Deegan, R.D. Leheny, R.L. Menon, N. Nagel, S.R. Dynamic Shear Modulus of Tricresyl Phosphate and Squalane, *J. Phys. Chem. B,* 1999, **103,** 4066-4070.

Demirbas, A. Biodiesel from Vegetable Oils via Transesterification in Supercritical Methanol, *Energy Conversion and Management,* 2002, **43,** 2349-2356.

Dermibas, A. The Importance of Biodiesel as Transportation Fuel, *Energy Policy,* 2007, **35,** 4661-4670.

Dickinson, H.W. A Short History of the Steam Engine, *Cambridge University Press,* 1939 (Online 2010).

Du Plessis, L.M. De Villiers, J.B.M. Van Der Walt, W.H. Stability Studies on Methyl and Ethyl Fatty Acid Esters of Sunflowerseed Oil, *J. Am. Oil Chem. Soc.* 1985, **62(4),** 748-752.

Dvorák, A. Skopal, F. Komers, K. Transesterification of Rapeseed Oil in a Feedback Reactor, *Eur. J. Lipid Sci. Technol.* 2001, **103,** 742-745.

EN590:2004. Automotive Fuels. Diesel. Requirements and Test Methods. 27/08/2004. ISBN: 058044119 9

European Commission Paper COM(2006) 105 – A European Strategy for Sustainable, Competitive and Secure Energy, 8/3/2006.

European Commission Regulation No. 715/2007 – Euro 5

European Commission Regulation No. 28/2009

European Commission Regulation No. 595/2009 – Euro 6

El-Fadel, M. Massoud, M. Particulate Matter in Urban Areas: Health-based Economic Assessment, *Science of the Total Environment,* 2000, **257(2-3),** 133-146.

Encinar, J.M. González, J.F. Sabio, E. Ramiro, M.J. Preparation and Properties of Biodiesel from *Cynara cardunculus* L. Oil, *Ind. Eng. Chem. Res.* 1999, **38,** 2927-2931

Encinar, J.M. González, J.F.Rodríguez-Reinares. Biodiesel from Used Frying Oil. Variables Affecting the Yields and Characteristics of the Biodiesel, *Ind. Eng. Chem. Res.* 2005, **44,** 5491-5499.

Enweremadu, C.C. Mbarawa, M.M. Technical Aspects of Production and Analysis of Biodiesel from Used Cooking Oil – A Review, *Renewable and Sustainable Energy Reviews,* 2009, **13(9),** 2205-2224.

Ferguson, C.R. Internal Combustion Engines, *John Wiley, New York,* 1986.

Florides, G.A. Christodoulides, P. Global Warming and Carbon Dioxide Through Sciences, *Environment International,* 2009, **35**, 390-401.

Gamble, R.J. Priest, M. Taylor, C.M. Detailed Analysis of Oil Transport in the Piston Assembly of a Gasoline Engine, *Tribology Letters,* 2003, **14(2),** 147-156.

Ganguly, J. Studies on the Mechanism of Fatty Acid Synthesis: VII. Biosynthesis of Fatty Acids from Malonyl CoA, *Biochim. Biophys. Acta,* 1960, **40,** 110-118.

Gardner, H.W. Oxygen Radical Chemistry of Polyunsaturated Fatty Acids, *Free Radical Biology & Medicine,* 1989, **7,** 65-86.

German Patent (DRP) No. 37435 – Karl Benz, gasoline fuelled car

Ghadge, S.V. Raheman, H. Biodiesel Production from Mahua (*Madhuca Indica*) Oil having Free Fatty Acids, *Biomass and Bioenergy,* 2005, **28(6),** 601-605.

Goering, C.E. Schwab, A.W. Dangherty, M.J. Pryde, E.H. Heakin, A.J. Fuel Properties of Eleven Vegetable Oils. *ASAE* 1982, **25(6)**, 1472-1477.

Goodrum, J.W. Volatility and Boiling Points of Biodiesel from Vegetable Oils and Tallow, *Biomass and Bioenergy*, 2002, **22**, 205–211.

Graboski, M.S. McCormick, R.L. Combustion of Fat and Vegetable Oil Derived Fuels in Diesel Engines, *Prog. Energy Combust. Sci.* 1998, **24,** 125-164.

Griffin Shay, E. Diesel Fuel from Vegetable Oils: Status and Oppurtunities, *Biomass and Bioenergy,* 1993, **4(4),** 247-242.

Gruntman, M. Blazing the Trail: The Early History of Spacecraft and Rocketry, *American Institute of Aeronautics and Astronautics,* 2004.

Gupta, S.A. Cochran, H.D. Cummings, P.T. Shear Behaviour of Squalane and Tetracosane under Extreme Confinement. I. Model, Simulation Method and Interfacial Slip. *J. Chem. Phys*, 1997, **107(23),** 10316-10326.

Haas, M.J. McAloon, A.J. Yee, W.C. Foglia, T.A. A Process Model to Estimate Biodiesel Production Costs, *Bioresource Technology,* 2006, **97(4),** 671-678.

Hamrock, B.J. Fundamentals of Fluid Film Lubrication, 1994, *McGraw-Hill Publishing*.

Harwood, H.J. Oleochemicals as a Fuel: Mechanical and Economic Feasability, *J. Am. Oil Chem. Soc.,* 1984, **61(2)**, 315-324.

Hayes, T.K. White, R.A. Peters, J.E. Combustion Chamber Temperature and Instantaneous Local Heat Flux Measurements in a Spark Ignition Engine, *SAE Technical Paper 930217*, 1993.

Hele, P. Biosynthesis of Fatty Acids, *Brit. Med. Bull.* 1958, **14(3),** 201-206

Heywood, J.B. – Internal Combustion Engine Fundamentals, International Edition, *McGraw-Hill Book Company,* 1988.

Hill, J. Nelson, E. Tilman, D. Polasky, S. Tiffany, D. Environmental, Economic and Energetic Costs and Benefits of Biodiesel and Ethanol Biofuels, *PNAS,* 2006, **103(30),** 11206-11210.

Hill, K. Fats and Oils as Oleochemical Raw Materials, *Pure Appl. Chem.* 2000, **72(7),** 1255-1264.

Hills, R.L. Power from Steam: A History of the Stationary Steam Engine, *Cambridge University Press,* 1993.

Hiroyasu, H. Kadota, T. Models for Combustion and Formation of Nitric Oxide and Soot in Direct Injection Diesel Engines, *Soc. Automotive Eng. Paper No. 760129,* 1976.

Hsu, S.M. Nano-lubrication: Concept and Design, *Tribology International,* 2004, **37(7),** 537-545.

Jabbarzadeh, A. Atkinson, J.D. Tanner, R.I. The effect of Branching on Slip and Rheological Properties of Lubricants in Molecular Dynamics Simulation of Couette Shear Flow, *Tribology International,* 2002, **35(1),** 35-46.

Jain, S. Sharma, M.P. *Prospects* of Biodiesel from Jatropha in India: A Review, *Renewable and Sustainable Energy Reviews,* 2010, **14,** 763-771.

Johnson, F.S. The Balance of Atmospheric Oxygen and Carbon Dioxide, *Biological Conservation,* 1970, **2(2),** 83-89.

Jones, E. Combustion of Methane, *Nature,* 1956, **178,** 1112.

Kearns, D.R. Physical and Chemical Properties of Singlet Molecular Oxygen, *Chemical Reviews,* 1971, **71(4),** 395-427.

Kim, J.S. Min, B.S. Lee, D.S. Oh, D.Y. Choi, J.K. Characteristics of Carbon Deposit Formation in Piston Top Ring Groove of Gasoline and Diesel Engine, *1998 SAE International Congress & Exposition; Detroit, MI, USA,* 1998, 147-154.

Kimura, Y. Okabe, H. An Introduction to Tribology, *Youkandou Press,* 1982, 69-82

Knothe, G. Bagby, M.O. Ryan, T.W. *Soc. Automotive Eng. Technical Paper No. 971681* 1997.

Knothe, G. Bagby, M.O. Ryan, T.W. III. Precombustion of Fatty Acid and Esters of Biodiesel. A Possibile Explanation for Differing Cetane Numbers. *J.Am. Oil Chem. Soc.* 1998, **75(8),** 1007-1013.

Knothe, G. Dependence of Biodiesel Fuel Properties on the Structure of Fatty Acid Alkyl Esters, *Fuel Processing Technology,* 2005, **86,** 1059-1070.

Körbitz, W. Biodiesel Production in Europe and North America, an Encouraging Prospect, *Renewable Energy,* 1999, **16,** 1078-1083.

Krisnangkura, K. Yimsuwan, T. Pairintra, R. An Empircal Approach in Predicting Biodiesel Viscosity at Various Temperatures, *Fuel,* 2006, **85,** 107-113.

Kumagi, A. Takahashi, S. Viscosity and Density of Liquid Mixtures of n-Alkanes with Squalane, *International Journal of Thermophysics,* 1995, **16(3),** 773-779.

Kyoto Protocol, http://kyotoprotocol.com.

Labeckas, G. Slavinskas, S. Performance of direct-injection off-road diesel engine on rapeseed oil, *Renewable Energy,* 2006, **31**, 849-863.

Lansdown, A.R. Lubrication and Lubricant Selection, A Practical Guide, 3rd Edition, *Tribology in Practice Series, Professional Engineering Publishing,* 2004.

Lapuerta, M. Rodríguez-Fernández, J. Agudelo, J.R. Diesel Particulate Emissions from Used Cooking Oil Biodiesel, *Bioresource Technology,* 2008, **99,** 731-740.

Lapuerta, M. Armos, A. Rodríguez-Fernández, J. Effect of Biodiesel Fuels on Diesel Engine Emissions, *Progress in Energy and Combustion Science,* 2008, **34(2),** 198-223.

Lazaroiu, G. Modeling and Simulation Combustion and Generation of NO_x, *Fuel Processing Technology,* 2007, **88,** 771-777.

Leung, D.Y.C. Luo, Y. Chan, T.L. Optimization of Exhaust Emissions of a Diesel Engine Fuelled with Biodiesel, *Energy & Fuels,* 2006, **20(3),** 1015-1023.

Levy II, H. Photochemistry of the Lower Troposphere, *Planetary and Space Science,* 1972, **20,** 919-935.

Lightfoot, P.D. Cox, R.A. Crowley, J.N. Destriau, M.Hayman, G.D. Jenkin, M.E. Moortgat, G.K. Zabel, F. Organic Peroxy Radicals: Kinetics, Spectroscopy and Tropospheric Chemistry, *Atmospheric Environment,* 1992, **26A(10),** 1805-961.

Lignola, P.G. Reverchon, E. Cool Flames, *Prog. Energy Combust. Sci.* 1987, **13,** 75-96.

Ma, F. Hanna, M.A. Biodiesel Production: A Review, *Bioresource Technology,* 1999, **70,** 1-15.

Manabe, S. Wetherald, R.T. The Effects of Doubling CO_2 Concentration on the Climate of a General Circulation Model, *J. of the Atmos. Sci.* 1975, **32(1),** 3-15.

Manabe, S. Stouffer, R.J. Century-scale Effects of Increased Atmospheric CO2 on the Ocean-atmosphere System, *Nature,* 1993, **364,** 215-218.

Mantashyan, A.A. Khachatryan, L.A. Niazyan, O.M. Arsentyev, S.D. On the Reactions of Peroxy Radicals in the Slow Combustion of Methane and Ethylene, *Combustion and Flame,* 1981, **43,** 221-227.

Marshall, W. Schumacher, L.G. Howell, S. Engine Exhaust Emissions: Evaluation of a Cummins L10E when Fuelled with a Biodiesel Blend. *SAE paper 952363*, 1995.

McMillen, D.F. Golden, D.M. Hydrocarbon Bond Dissociation Energies, *Ann. Rev. Phys. Chem,* 1982, **33,** 493-532.

Monyem, A. Canakci, M. Van Gerpen, J.H. Investigation of Biodiesel Thermal Stability Under Simulated In-Use Conditions, *Applied Engineering in Agriculture*, 2000, **16(4)**, 373-378.

Moritani, H. Nozawa, Y. Oil Degradation in Second-Land Region of Gasoline Engine Pistons, *R&D Rev. Toyota CRDL*, 2003, **38,** 36-43.

Mulliken, R.S. The Interpretation of Band Spectra Part III. Electron Quantum Numbers and States of Molecules and Their Atoms, *Rev. Mod. Phys.* 1932, **4(1),** 1-86.

Naik, S.N. Goud, V.V. Rout, P.K. Dalai, A.K. Production of First and Second Generation Biofuels: A Comprehensive Review, *Renewable and Sustainable Energy Reviews,* 2010, **14(2),** 578-597.

Nebel, B.A. Mittelbach, M. Biodiesel from Extracted Fat out of Meat and Bone Meal, *Eur. J. Lipid Sc. Technol.* 2006, **108,** 398-403.

Nicolet, M. Aeronomic Chemistry of the Stratosphere, *Planetary and Space Science,* 1972, **20,** 1671-1702.

Nitschke, W.R. Wilson, C.M. Rudolph Diesel, Pioneer of the Age of Power, *The University of Oklahoma Press*, Norman, OK 1965.

Owczarek, I. Blazej, K. Recommended Critical Temperatures. Part I. Aliphatic Hydrocarbons. *J. Phys. Chem. Ref. Data* 2003, **32(4)**, 1411-1428.

Oxford English Dictionary, *Oxford University Press,* 1996.

Pousa, G.P.A.G. Santos, A.L.F. Suarez, P.A.Z. History and Policy of Biodiesel in Brazil, *Energy Policy,* 2007, **35(11),** 5393-5398.

Pratt, D.A. Mills, J.H. Porter, N.A. Theoretical Calculations of Carbon-Oxygen Bond Dissociation Enthalpies of Peroxyl Radicals Formed in the Autoxidation of Lipids, *J. Am. Chem. Soc.* 2003, **124**, 5801-5810.

Priest, M. Dowson, D. Taylor, C.M. Predictive Wear Modelling of Lubricated Piston Rings in a Diesel Engine, *Wear,* 1999, **231,** 89-101.

Radich, A. Biodiesel Performance, Costs and Use, *Energy Information Administration,* 2004.

Rakopoulos, C.D. Antonopoulos, K.A. Rakopoulos, D.C. Hountalas, D.T. Giakoumis, E.G. Comparative Performance and Emissions Study of a Direct-injection Diesel Engine Using Blends of Diesel fuel with Vegetable Oils or Bio-diesels of Various Origins, *Energy Conversion and Management,* 2006, **47**, 3272-2387.

Ranz, A. Maier, E. Lankwayr, E. Determination of Fatty Acid Derivatives in Fuel and Diesel Oil, *Fuel*, 2010, **89(8),** 2133-2139.

Ross, J.R. Gebhart, A.I. Gerecht, J.F. The Autoxidation of Methyl Oleate. *J. Am. Chem. Soc.* 1949, **71**, 282-286.

Ryan, T. W. III. Dodge, L.G., Callahan, T.J. The Effects of Vegetable Oil Properties on Injection and Combustion in Two Different Diesel Engines, *J.Am.Oil Chem.Soc*, 1984, **61**, 1610–1619.

Sapaun, S.M. Masjuki, H.H. Azlan, A. The Use of Palm Oil as Diesel Fuel Substitute. *J. Power Energy A.* 1996, **210**, 47–53.

Sarin, R. Sharma, M. Sinharay, S. Malhorta, R.K. Jatropha – Palm Biodiesel Blends: An Optimum Mix for Asia. *Fuel*, 2007, **86,** 1365-1371.

Sarmiento, J.L. Hughes, T.M.C. Stouffer, R.J. Manabe, S. Simulated Response of the Ocean Carbon Cycle to Anthropogenic Climate Warning, *Nature*¸1998, **393,** 245-249.

Seetula J.A. Slagle I.R. Kinetics and thermochemistry of the R+ HBr $\leftrightarrow$ H+ Br (R= *n*-C_3H_7, *iso*-C_3H_7 , *n*-C_4H_9 , *iso*-C_4H_9 , *sec*-C_4H_9 or *tert*-C_4H_9) equilibrium, *J. Chem. Soc. Faraday Trans.* 1997, **93,** 1709-1719.

Shahid, E.M. Jamal, Y. A Review of Biodiesel as a Vehicular Fuel, *Renewable and Sustainable Energy Review*, 2008, **12(9),** 2484-2494.

Sharma, Y.C. Singh, B. Development of Biodiesel: Current Scenario, *Renewable and Sustainable Energy Reviews*, 2009, **13(6-7),** 1646-1651.

Siegbahn, P.E.M. Multireference CCI Calculations on the Bond Dissociation Energies of Methane, *Chemical Physics Letters,* 1985, **119(6),** 515-522.

Smeets, E. Junginger, M. Faaij, A. Walter, A. Dolzan, P. Turkenburg, W. The Sustainability of Brazilian Ethanol—An Assessment of the Possibilities of Certified Production, *Biomass and Bioenergy*, 2008, **32(8),** 781-813.

Spear, B. James Watt: The Steam Engine and Commercialization of Patents, *World Patent Information*, 2008, **30,** 53-58.

Srinisavan, S. The Food v Fuel Debate: A Nuanced View of Incentive Structures, *Renewable Energy*, 2009, **34(4),** 950-954.

Srivastava, A. Prasad, R. Triglycerides-based Diesel Fuels, *Renewable and Sustainable Energy Reviews,* 2000, **4,** 111-133.

Stachowiak, G.W. Batchelor, A.W. Lubricants and their Composition, *Engineering Tribology,* 2005, **Ch. 3**, 51-101.

Stark, M.S. Wilkinson, J.J. Lindsay Smith, J.R. Alfadhl, A. Pochopien, B.A. Autoxidation of Branched Alkanes in the Liquid Phase, *Ind, Eng. Chem. Res.* 2011, **50,** 817-823

Sumathi, S. Chai, S.P. Mohamed, A.R. Utilization of Palm Oil as a Source of Renewable Energy in Malaysia, *Renewable and Sustainable Energy Reviews,* 2008, **12**, 2404–2421.

Szulcyk, K.R. McCarl, B.A. Market Penetration of Biodiesel, *Renewable and Sustainable Energy Reviews,* 2010, **14(8),** 2426-2433.

Tan, Y.C. Ripin, Z.M. Frictional Behaviour of Piston Rings of Small Utility Two-Stroke Engine Under Secondary Motion of Piston, *Tribology International*, 2010, **44,** 592-602.

Taylor, R.I. Evans, P.G. *In-situ* Piston Measurements, *Proc. Instn. Mech. Engrs.* 2004, **218**(J: J. Engineering Tribology), 185-200.

Thoenes, P. Biofuels and Commodities Market – Palm Oil Focus, FAO, Commodities and Trades Division.

Thornton, M.J. Alleman, T.L. Luecke, J. McCormick, R.L. Impacts of Biodiesel Fuel Blends, Oil Dilution on Light-Duty Diesel Engine Operation, *National Renewable Energy Laboratory*, Conference Paper NREL/CP-549-44833, August 2009.

Tiwari, A.K. Kumar, A. Raheman, H. Biodiesel Production from Jatropha Oil *(Jatropha Curcas*) with High Free Fatty Acids: An Optimised Process, *Bioresource Technology*, 2007, **31(8),** 569-575.

Tormos, B. Novella, R. García, A. Gargar, K. Comprehensive Study of Biodiesel Fuel for HSDI Engines in Convencional and Low Temperature Combustion Conditions, *Renweable Energy*, 2010, **35,** 368-378.

Trenwith, A.B. Dissociation of 3-methyl-1,4-pentadiene and the Resonance Energy of the Pentadienyl Radical *J. Chem. Soc. Faraday Trans. 1*, Physical Chemistry in Condensed Phases, 1982, **78(10),** 3131-3136.

Tutorvista.com http://www.tutorvista.com/content/chemistry/chemistry-iv/atomic-structure/oxygen-molecule.php Accessed 04/08/2011

U.S Department of Energy report **2011** http://tonto.eia.doe.gov/oog/info/twip/twip.asp 27/04/2011

U.S. Patent 388,372, 08/1888 – Nikolaus Otto, Otto Cycle Engine.

Wakuri, Y. Hamatake, T. Soejima, M. Kitahara, T. Piston Ring Friction in Internal Combustion Engines, *Tribology International*, 1992, **25(5),** 299-308.

Walker, K. Biodiesel from Rapeseed, *J. R. Agric. Soc. Engl.* 1994, **155,** 43–47.

Wayne, R.P. Chemistry of Atmospheres, 3rd Edition, *Oxford University Press*, 2000, 50-60.

Woodwell, G.M, MacDonald, G.J. Revelle, R, Kelling, C.D. The Carbon Dioxide Problem: Implications for Policy in the Management of Energy and Other Resources, *Report to the Council on Environmental Quality*, 1979, Reprinted 2008.

Yizhe, L. Guirong, B. Hua, W. Determination of 11 fatty acids and fatty acid methyl esters in biodiesel using ultra performance liquid chromatography, *Chinese Journal of Chromatography*, 2008, **26(4)**, 494-498.

Xue, J. Grift, T.E. Hansen, A.C. Effect of Biodiesel on Engine Performances and Emissions, *Renewable and Sustainable Energy Reviews*, 2011, **15(2),** 1098-1116.

Yuan, W. Hansen, A.C. Zhang, Q. Vapour Pressure and Normal Boiling Point Predictions for Pure Methyl Esters and Biodiesel Fuels, *Fuel*, 2005, **84,** 943-950.

Zhang, F.L. Niu, B. Wang, Y.C. Chen, F. Wang, S.H. Xu, Y. Jiang, L.D. Gao, S. Wu, J. Tang, L. Jia, Y.J. A Novel Betain Aldehyde dehydrogenase gene from *Jatropha Curcas*, encoding an enzyme implicated in adaptation to environmental stress, *Plant Science*, 2008, **174,** 510-518.

Zhang, H. Machutta, C.A. Tonge, P.J. Fatty Acid Biosynthesis and Oxidation, *Comprehensive Natural Products II*, 2010, **8.07**, 231-275.

Zhang, Y. Dubé, M.A. McLean, D.D. Kates, M. Biodiesel Production from Waste Cooking Oil: 1. Process Design and Technological Assessment, *Bioresource Technology*, 2003, **89(1),** 1-16.

Chapter 2. Experimental

2.1 Materials

All gases, oxygen, nitrogen, helium and hydrogen were purchased at 99.9% purity from BOC. Biodiesel model chemicals methyl oleate (methyl octadec -9-*cis*-enoate) and methyl linoleate (methyl octadec-9,11-*cis*,*cis*-dienoate) were all purchased at 99% purity from Sigma-Aldrich. The lubricant model chemical squalane (2, 6, 10, 15, 19, 23 hexamethyl tetracosanoate), were also purchased at 99% from Sigma Aldrich. See figure 2.1 for all chemical structures. Dodecane and hexadecane, for calibration purposes, were also purchased at 99% purity from Sigma-Aldrich.

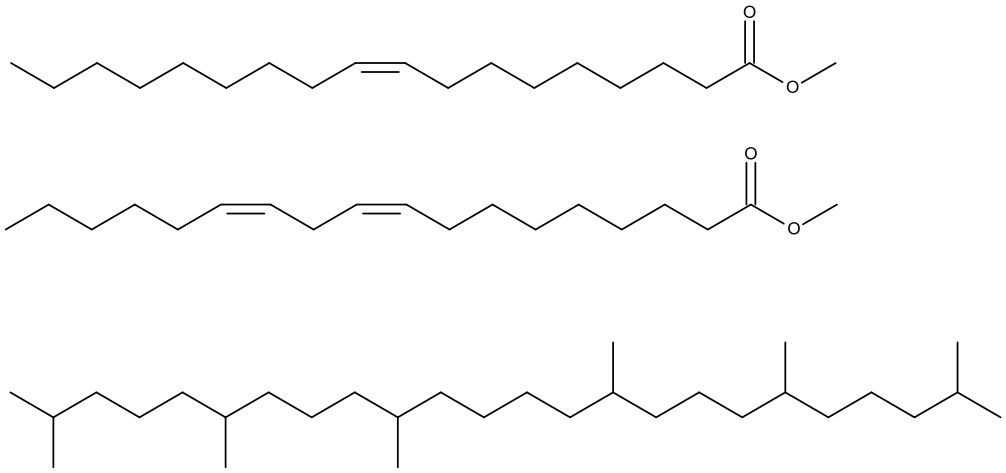

Figure 2.1 – From top to bottom, the chemical structures of methyl oleate, methyl linoleate and squalane.

Rapeseed (RME), Soybean (SME), Palmseed (PME), Coconut (CME) and 3 Karanjia (KME) methyl ester biodiesels were supplied by Lubrizol Ltd. Used cooking oil biodiesel (UCO) was also supplied by Double Green Ltd. The phenolic antioxidant Irganox L107 (octadecyl 3-(3,5 di-tertbutyl, 4-hydroxy phenyl) propanoate – see figure 2.2) was supplied by BASF.

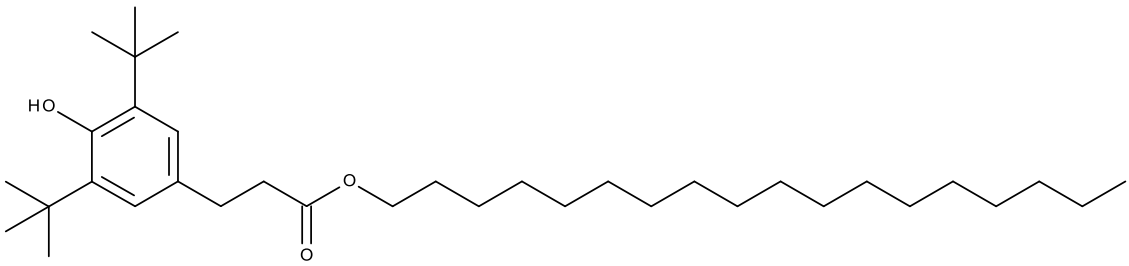

Figure 2.2 – The chemical structure of octadecyl 3-(3,5 di-tertbutyl, 4-hydroxy phenyl) propanoate (Irganox L107).

An aminic antioxidant (Lubrizol code, OS146100) and an overbased sodium sulphonate detergent (Lubrizol code, OS102880) were also supplied by Lubrizol Ltd. Their generic chemical structures are given in figure 2.3, but the R groups are not specified.

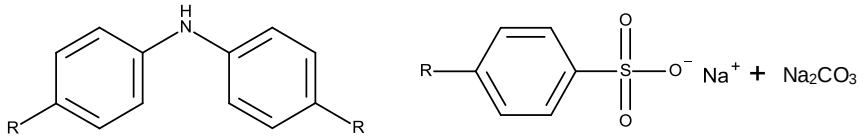

Figure 2.3 – The generic chemical structures of the aminic antioxidant (OS146100) and sodium sulphonate detergent (OS102880).

2.2 Oxidation Reactions

The main reactions were carried out were autoxidation reactions in bench top reactors, previously described by Wilkinson (2006), Alfahdl (2008) and Stark et al (2010). They fell into two categories: static oxidation, where the reactor was supplied by a single shot of oxygen and then sealed, and flow oxidation, where oxygen and the exhaust gases were free to flow through the reactor. Both methods have been modified slightly since Wilkinson described them and so the full details are given below.

2.2.1 Static Oxidation

1 cm^3 of substrate was sealed inside a stainless steel microreactor with an internal volume of 10.53 cm^3 or a larger reactor with an internal volume of 65.19 cm^3 (see figure 2.4 and Table 2.1).

Small Reactor Large Reactor

Figure 2.4 – External and internal views of the small and large reactors

Table 2.1 – Reactor Properties

	Large	Small
Internal Radius (cm)	5.35	2.15
Depth (cm)	2.9	2.9
Reactor Volume (cm^3)	65.19	10.53

When the small reactor was used, the air was pumped out of the reactor head space and the system was then briefly stirred, via a magnetic PTFE stirrer bar, to remove any dissolved gases, which were vacuum pumped out of the system to ensure no oxidation occurred whilst the substrate was below the desired temperature.

Once all gases were removed, the system was sealed and then heated to the desired temperature via a contact hotplate designed to fit around the reactor. The temperature was monitored with a K-Type thermocouple which was inserted into the lid of the reactor with pressure constantly monitored with a pressure gauge linked to a chart recorder.

When the larger reactor was used, rather than vacuum pumping the air out, the system was purged with nitrogen to remove all the oxygen - measured with an oxygen sensor (Teledyne Analytical ClassR-17MED) which was recorded on a PC using an

analogue to digital converter (Picotec ADC-20). Once all oxygen was removed from the system, the exhaust pipe was closed to prevent escape of any gas and nitrogen was allowed to enter the system to increase the pressure above atmospheric pressure. The input pipe was then also closed to completely seal the system, which was tested to see if the pressure remained constant and therefore free from leaks. After that, both taps were reopened to allow a constant flow of nitrogen again, and the system was heated as before.

Once the system was at the desired temperature, 1000 mbar of oxygen (99.9% purity) was introduced to the system, and then resealed to ensure no additional oxygen entered the system, and that no volatile products escaped. The system was then stirred to mix the oxygen into the substrate. As oxygen was used up by the substrate, the pressure began to drop. Once the pressure reached the minima on the graph (see figure 2.2) and began increasing again, it was evidence of water vapour being produced, at which point the oxidation reaction was presumed to have finished and the system was then quenched by immersing in ice or cold water.

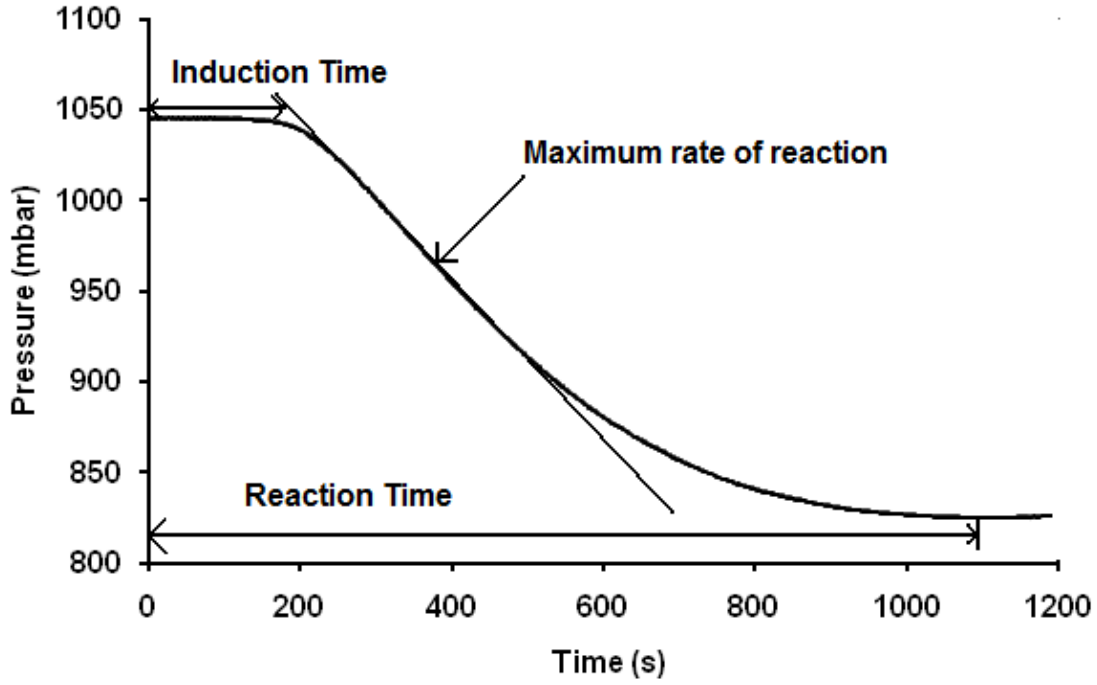

Figure 2.5 – Example of a pressure trace with the Induction Time and Reaction Time marked.

The time taken between the introduction of oxygen to the system, and the rate of reaction to reach its maximum is known as the Induction Time; the time at which the pressure minimum is reached, is the Reaction Time (see Figure 2.5).

2.2.2 Flow Oxidation

A volume of 5 cm^3 of substrate was introduced into the large stainless steel reactor, with internal volume 65.19 cm^3 (see figure 2.4 and table 2.1) and heated to the desired temperature under a flow of nitrogen to ensure no oxidation occurred before the desired temperature was reached, with the temperature of the liquid measured directly with a pre-calibrated K-Type thermocouple, accurate to ± 0.1 ^oC. Once the required temperature was reached, a flow of oxygen was introduced at a pressure of 1.05 bar and a flow rate of 0.08 dm^3 min^{-1}. The gas output from the reactor was passed through a cold trap to condense any volatile oxidation products and the oxygen content of the exhaust gas was measured with an oxygen sensor (Teledyne Analytical ClassR-17MED). The reaction was initiated by stirring, using a magnetic PTFE stirrer bar to ensure thorough oxygenation of the liquid. The temperature and pressure inside the reactor, as well as the oxygen content of the output gas flow, were recorded on a PC using the same analogue to digital converter (Picotec ADC-20) as for the static oxidation reaction. Liquid samples were also withdrawn at regular intervals and stored at –10 ^oC prior to analysis. To stop the reaction, stirring was ceased and the reactor was purged with nitrogen to prevent any further oxidation.

2.3 Viscosity measurements

Kinematic Viscosity (KV), as mentioned in the introduction, is an important measurement in industry for assessing the quality and suitability of a lubricant. Normally, KV is measured at either 40 or 100 ^oC (KV40 and KV100 respectively). All KV measurements for this work were at 40 ^oC carried out in a thermostatically controlled water bath.

A viscometer, consisting of a U-shaped capillary tube (of various grades – depending on substrate) was used to contain the substrate. Pressure is applied via a pipette filler to tube A to force 0.3 ml of substrate into tube B up to mark E (see figure 2.6). The tube was left in a water bath for 10 minutes to allow the temperature to stabilise. The temperature was 40.000 ^oC ± 0.001 ^oC, as determined by an ASTM compliant thermometer with a range of 38.6 – 41.4 ^oC. The liquid was then forced back through the tubing until the meniscus was above mark C. The time taken for the meniscus to fall from mark C down to mark D was recorded. This was repeated 3 times for reproducibility and the viscosity was calculated via Equation 2.1:

$$\eta = t_e C_0 \qquad \text{Equation 2.1}$$

Where:

η = Viscosity in cSt ($mm^2\ s^{-1}$)

t_e = Efflux time in s

C_0 = Viscometer constant (given with each different grade of viscometer) in $cSts^{-1}$

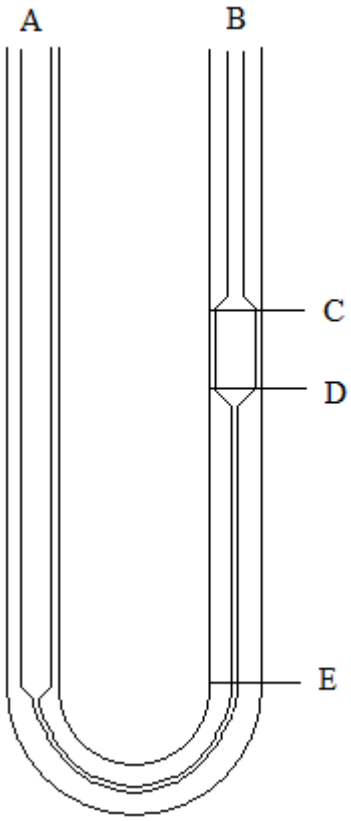

Figure 2.6 – A schematic diagram of the viscometer tubes used.

2.4 Chemical analysis

2.4.1 Gas Chromatography

An injection volume of 0.3 μl of all samples were analysed via a Varian 3380 gas chromatagraph equipped with a 1079 injector, flame ionization detector and a 5 % phenyl, 95 % dimethylpolysiloxane capillary column (Phenomenex Zebron ZB-5HT), of 30 m length 0.25 mm internal diameter and 0.25 μm film thickness and a split ratio of 50:1.

The injector and detector were set to 350 ^oC, the column started at 50 ^oC and was ramped up to 340 ^oC at a rate of 5 $^oC\ min^{-1}$, then held for 22 mins giving a total run time of 80 minutes

The data was collected using JCL6000 integration with the sample rate of 2 per second

The instrument was calibrated at various points during the project by injecting authentic samples of dodecane, hexadecane, methyl oleate and squalane of several known concentrations to measure peak area versus concentration and also how the effective carbon number (the amount of carbon numbers capable of being oxidised to CO_2 – Wainwright 1983, Scanlon 1985) of a compound affected the peak area signal. From the individual calibration plots, the calibration factor was calculated from the gradient (peak area v concentration) for each compound and then plotted against the effective carbon number (see figure 2.7 – the error bars are calculated from the standard error of the linear regression for the lines of best fit for each calibration plot) to give the overall calibration factor for the GC.

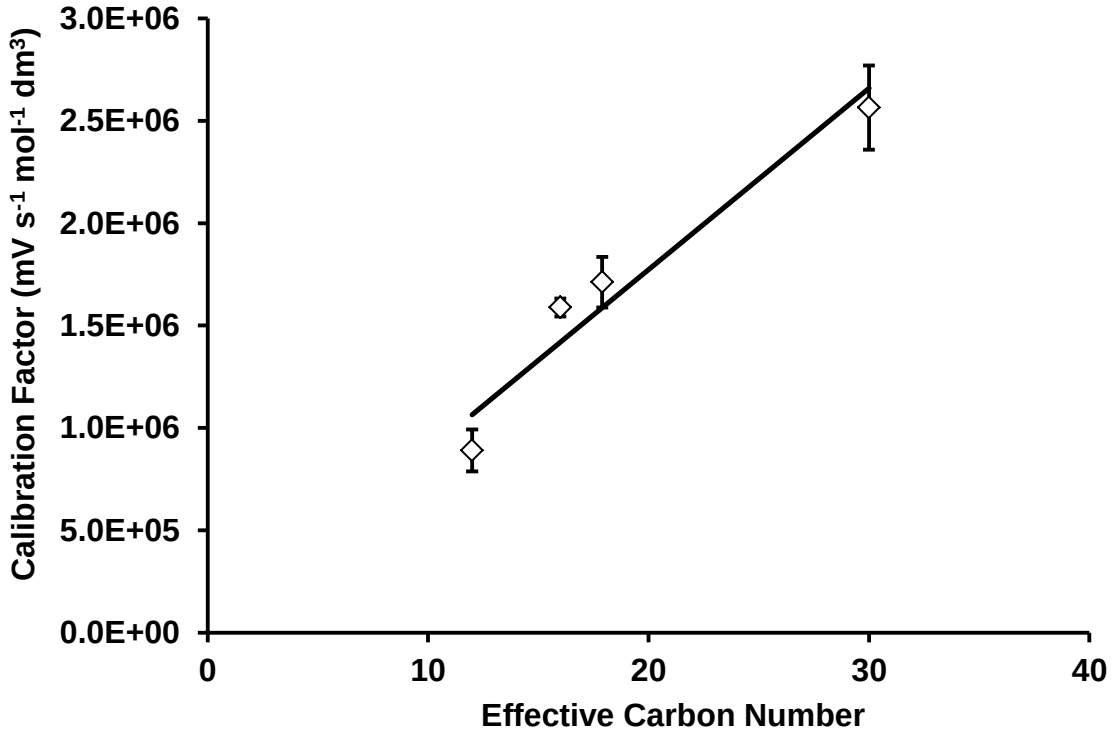

Figure 2.7 – The calibration plot for the response factor according to effective carbon number of the GC.

From the linear regression of the line of best fit of this graph, an overall mean standard error for concentrations measured by GC was calculated as 5.7%.

2.4.2 Mass Spectrometry

Product identity from the oxidation reactions was analysed by GC-mass spectrometry using electron impact (EI) and field ionisation (FI) (Williams and Fleming 1989) using NIST database matches and verified, where possible, by comparing with the mass ion given by GC-MS/FI. Where available, these were also confirmed by injecting authentic samples to compare retention time. GPC mass spectrometry was also carried out on the separated samples using electron spray ionisation (ESI).

All EI-MS, FI-MS and ESI-MS were carried out using a WATERS GCT Premier Mass Spectrometer coupled to an Agilent 7890A GC. For EI, the electron energy was set at 70.0 eV with an emission current of 691.1 μA for the GC-MS methods. For ESI the capillary voltage was set 4500V at 45nA using acetonitrile as a solvent. The heater was set to 180 ^{o}C in all cases.

2.5 References

Alfadhl, A. The Behaviour of Antioxidants in Lubricant Base Fluids at High Gasoline Engine Temperatures. *PhD Thesis, University of York*, **2008**.

Scanlon, J.T. Willis, D.E. Calculation of Flame Ionization Detector Relative Response Factors Using the Effective Carbon Number Concept, *Journal of Chromatographic Science*, 1985, **23(8),** 333-340

Stark, M.S. Wilkinson, J.J. Lindsay Smith, J.R. Alfadhl, A. Pochopien, B.A. Autoxidation of Branched Alkanes in the Liquid Phase, *Ind, Eng. Chem. Res.* 2011, **50,** 817-823

Wainwright, M.S. Haken, J.K. Effective Carbon Number of Methane in Gas Chromatography, *Journal of Chromatography*, 1983, **256,** 193-199

Wilkinson, J.J. The Autoxidation of Branched Hydrocarbons in the Liquid Phase as Models for Understanding Lubricant Degradation. *PhD Thesis, University of York*, **2006**. 231-233

Williams, D.H. Fleming, I. Spectroscopic Methods in Organic Chemistry, 1989, 4th Edition

NIST database, www.nist.gov, 21/2/2011

Chapter 3. The Liquid Phase Autoxidation of Methyl Linoleate and Methyl Oleate at Elevated Temperatures

3.1 Introduction

In the Introduction chapter environmental and political factors driving forward the production of biodiesel were investigated, as well as the chemical, mechanical and economic factors inhibiting them; the latter being heavily influenced by the first two. Also investigated was the evolution of biodiesels from traditional vegetable oils to the fatty acid methyl esters (FAME) currently used for biodiesel as well as the factors that drove this development.

The main reason was that vegetable oils themselves have been shown to have relatively poor fuel properties due to relatively high freezing points and high viscosities (Goering 1982) , hence must be chemically altered to make them suitable for use in engines designed for conventional diesel. Transesterification with methanol to produce FAME mixtures was shown to produce a sufficient improvement in properties necessary for automotive use with regards to freezing points, combustion, viscosity and oxidative stability (Knothe 2008, Zhang 1988, Du Plessis 1985). The problem with this method is that whilst these methyl esters displayed better oxidative stability and physical properties compared to their equivalent monoesters and triglycerides respectively, the fatty acid chains that contribute to these esters can still have multiple highly reactive unsaturated carbon-carbon double bonds (Dermibas 2009). By comparison, the traditional mineral oils used in engines are generally saturated hydrocarbons and aromatics (Gómez-Carracedo 2003), with little to no additional functionality and are typically unreactive towards chemical breakdown, except during the high temperature of combustion, which is what has made them effective fuels.

These unsaturated sites in FAME biodiesel typically have singly or doubly allylic C-H bonds which are weaker (369.0 ± 8.8 and 318 ± 3 kJ mol^{-1} respectively) than saturated sites (424 ± 4.2 kJ mol^{-1} Golden 1969, McMillen 1982, Trenwith 1982, Clark 1991, Pratt 2003, Blanksby 2003 – see figure 3.1) and are hence capable of reacting rapidly with oxygen-centred radicals in a process known as autoxidation (Ross 1949) to form oxidation products such as ketones and epoxides (Hamberg 1973), especially at the harsh temperatures found in combustion engines via the radical cycle summarised below and explained in greater detail in the introduction (Lightfoot 1992).

$RH + O_2 \rightarrow R\bullet + HO_2\bullet$ Reaction 3.1

$RO_2H \rightarrow RO\bullet + \bullet OH$ Reaction 3.2

$R\bullet + O_2 \rightarrow RO_2\bullet$ Reaction 3.3

$RO_2\bullet + RH \rightarrow RO_2H + R\bullet$ Reaction 3.4

$RO\bullet + RH \rightarrow ROH + R\bullet$ Reaction 3.5

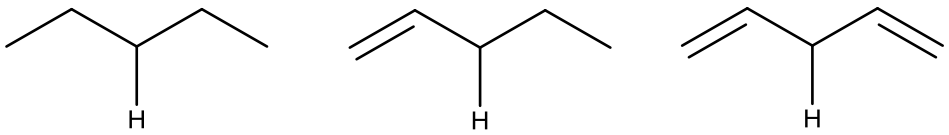

424.0 ± 4.2 369.0 ± 8.8 318 ± 3

Figure 3.1 – The saturate, monounsaturated and doubly unsaturated C-H bonds and their respective B.D.Es.

This subsequent increase in use of biodiesel has resulted in noted detrimental problems with regards to the engine performance. Listed amongst the problems caused by this included (but was not limited) to ring sticking (Kim 1998, Labeckas 2006, Shahid 2008), injector fouling (Hiroyasu 1976, Tormos 2010) and degradation of the lubricant (Bush 1991, Sapaun 1996, Gamble 2003), which in turn resulted in reduced efficiency and therefore increased costs and emissions.

In this Chapter, the chemistry of biodiesel oxidation will be considered. To achieve this, two different monoesters, methyl oleate (methyl *cis*-octadec-9-enoate) and methyl linoleate (methyl *cis*-*cis*-octadec-9,12-dienoate) were used to represent the chemical degradation of polyunsaturated biodiesels, in particular, identifying the products of oxidation and the rate at which they are formed at temperatures ranging from 100 ^{o}C to 170 ^{o}C, representative of various temperatures found in different areas of a diesel engine from the sump (lowest) to the piston ring assembly and piston assembly (highest) (Taylor 2004, Moritani 2004). Methyl linoleate was chosen as a biodiesel analogue due to the fact that

linoleic acid is a commonly occurring fatty acid in many crops used for biodiesel (Ma 1999, Srivastava 2000, Yuan 2005, Balat 2010). Consequently after transesterification, the corresponding methyl ester, methyl linoleate, is a significant component of biodiesel (Monyem 2000), especially in rapeseed and soybean methyl ester biodiesel blends (Yizhe 2008). Also, as polyunsaturated compounds are more reactive than monounsaturated and saturated ones (Bors 1987, Monyem 2000), the hypothesis that methyl linoleate is one of the primary chemicals responsible for the enhanced formation of engine deposits and accelerated rate of lubricant oxidation will be further investigated in Chapter 4.

Meanwhile, methyl oleate has been a molecule of interest for a long time as a model to try and mimic fatty acid and lipid chemistry. Ross investigated the autoxidation of it in 1949 at 35 ^{o}C and identified the migration of the double bond by noting the formation of hydroperoxides only at the 8, 9, 10 and 11 positions on the chain which, combined with Farmer's (1943) previous work on double bond migration led to Frankel (1984 and 1985) identifying this process to be the main cause of fat and lipid degradation which, at present, is widely accepted. These models, coupled with both the previous knowledge and current research of methyl oleate chemistry can therefore lend themselves to the study of methyl linoleate and biodiesel autoxidation. Methyl oleate is of course also worthy of study in its own right in this field as it is also a common biodiesel component (Monyem 2000, Srivastava 2000, Yuan 2005, Yizhe 2008) and hence can contribute to this study by helping understand the role of singly unsaturated FAME components in biodiesel degradation and fuel dilution.

3.2 Results

3.2.1 Gas Chromatography

Figures 3.1 and 3.2 show the GC traces for methyl linoleate oxidised in the static oxidation reaction method at 170 ^{o}C. Figure 3.2 shows the peaks that eluted up to and including methyl linoleate, whereas figure 3.3 shows those that eluted after and including methyl linoleate. The reason for this is that the peaks that eluted before methyl linoleate were spread out over a 30 minute period. Those that eluted afterwards however were mainly in a 4 minute window from 33.5 to 37.5 minutes (shown in figure 3.4 for clarity) (with the exception of the minor peak at around 61 minutes) hence the chromatogram are being presented separately for clarity. Figure 3.5 shows the GC trace for methyl oleate under the same conditions.

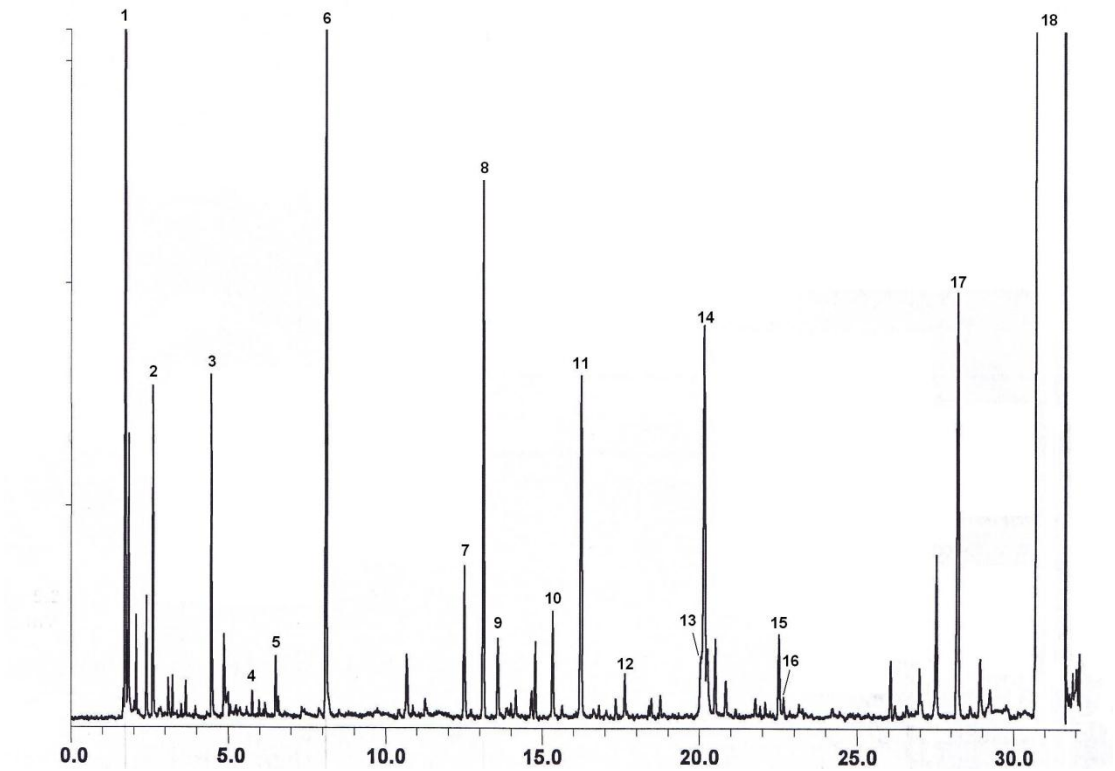

Figure 3.2 – The Gas Chromatogram of the oxidation products of methyl linoleate at 170 ^{o}C before and including methyl linoleate elution.

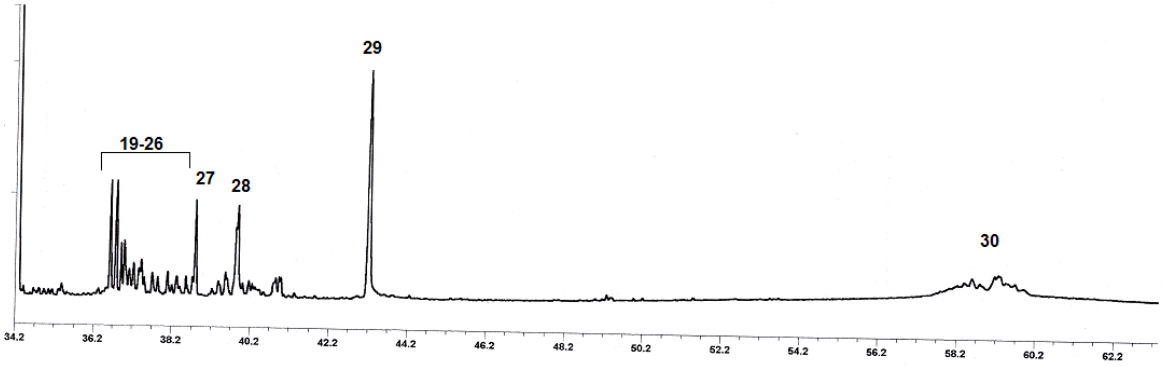

Figure 3.3 – The Gas Chromatogram of the oxidation products of methyl linoleate at 170 ^{o}C after methyl linoleate elution.

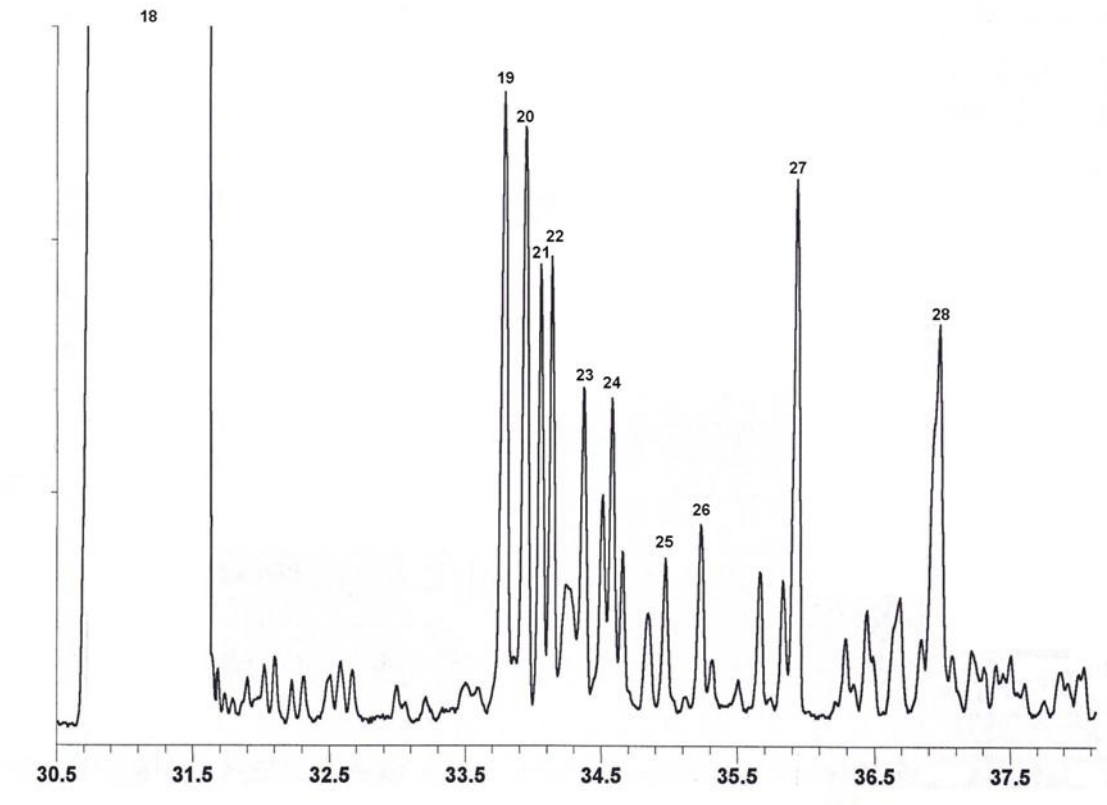

Figure 3.4 – The close up of peaks 19-28 for clarity.

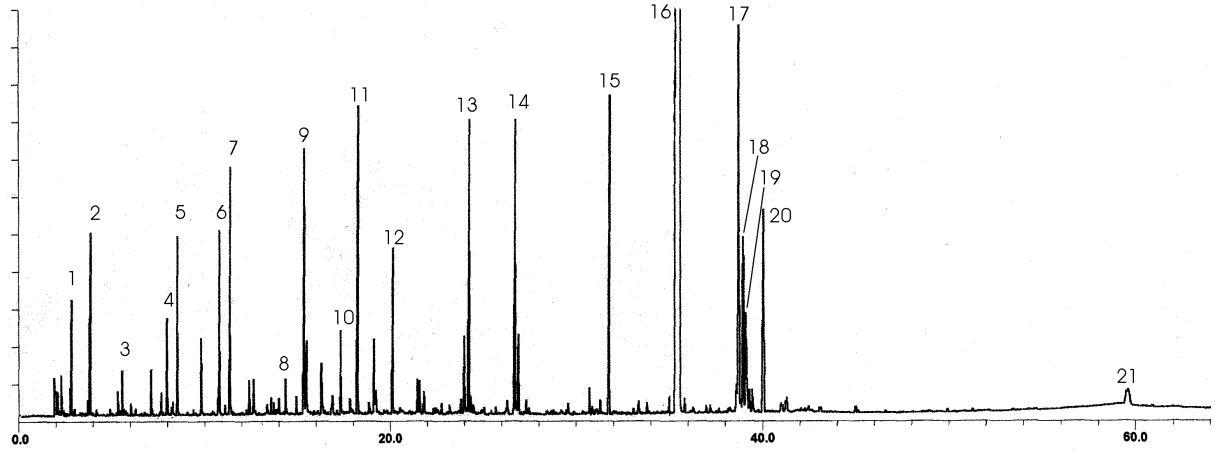

Figure 3.5 – The Gas Chromatogram of the oxidation products of methyl oleate at 170 ^{o}C. Peaks 1 – 15 have been intensified 6-fold for clarity.

3.2.2 Mass Spectrometry

EI- and FI-MS were carried out for each of the peaks in figures 3.2-3.4. Full MS data is given in tables A.1 and A.2 in Appendix A for EI- and FI- respectively. Some peaks gave no signal in EI-MS, whilst other gave none in FI-MS, however for clarity the product identification is given in both tables.

In addition to the spectra analysis, peaks 1, 6 and 18 (see figure 3.2 and table A.1) were also confirmed by comparing retention times against authentic samples. The two isomers of 2,4 decadienal are most likely to be Z,Z (peak 7) followed by E,Z (peak 8) as the double bond rearranges itself upon addition of the oxygen radical and subsequent cleavage of the 8-9 C-C bond. As the E double bond is formed preferentially due to the reduced steric hindrance, the E,Z isomer would be expected to be the major product. Peaks 19-22 were identified as epoxide products from previous work done on methyl oleate oxidation (Lercker 2003), with the peaks coming out in the same order with the same relative retention times, confirmed by the mass ion of m/z=294. The positional isomers have initially been identified by the fragmentation pattern in the GC-MS/EI mass spectra obtained. Peaks 20 and 22 had a peak of m/z=185, matching the fragment of a carbon centred carbonyl radical at the 9 position and subsequent cleavage, indicating the epoxide formation between the 9 and 10 positions on the carbon chain (see figure 3.6). Peaks 19 and 21 did not possess this fragment peak and hence the epoxide could not have been formed here and must subsequently have been between the 12 and 13 positions.

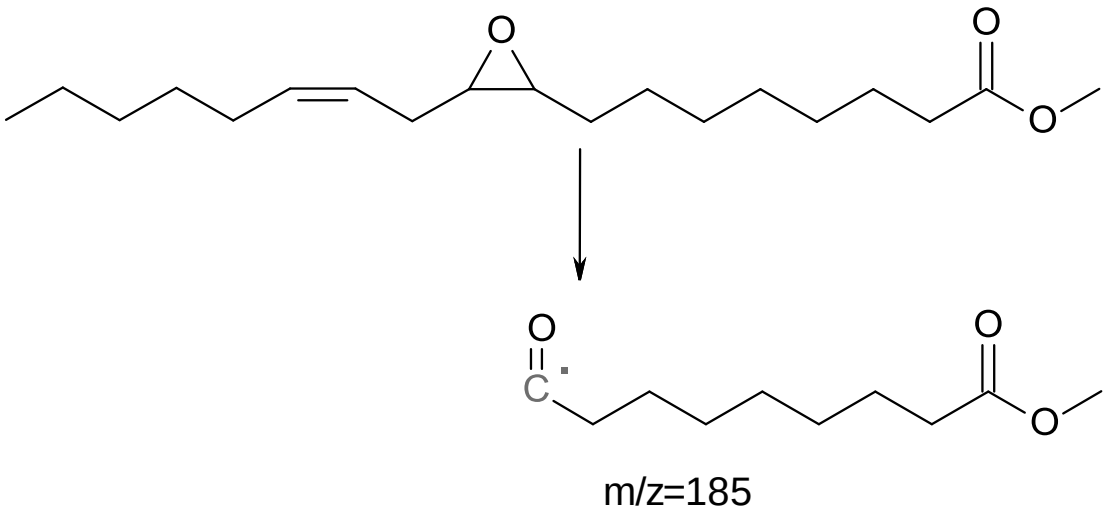

Figure 3.6 – The fragmentation of an epoxide to give the m/z = 185 fragment in EI-MS

From the m/z = 310 mass ion and the retention times being similar to the previous work done on methyl oleate oxidation, peaks 23-26 are believed to be alcohol products, but from the spectra, it has not yet been possible to identify the alcohol position on the chain.

Similarly, from the m/z = 308 mass ion and the retention times being similar to the previous work done on methyl oleate oxidation (Frankel 1984), peaks 27 and 28 have been identified as ketones, most likely with the carbonyl group being at the 9 and 13 positions

(respectively), as they are the most stable (see Discussion section). As with identifying the positional isomers on the epoxides, peak 27 possessed the m/z = 185 ion, with a relative intensity of 11%, indicating it is most likely at the 9- position. If it was at the 13- position, there would be a significant fragment at m/z = 237. Whilst this fragment was observed, it was very minor at only 1% relative intensity grouped with a more prominent peak at m/z = 235 (4% relative intensity) suggesting the m/z = 237 is merely an isotope peak. Peak 28 did possess the m/z = 237 peak with a relative intensity of 66% (compared to peak 27 at only 5%), suggesting that it could correspond to having the carbonyl group at the 13-position, especially with the m/z = 308 mass ion. However, whilst this peak showed up with a relative intensity of 27% in the EI-MS, an FI-MS for this peak was not obtained in the spectra, so it is unable to be confirmed whether or not this is definitely the mass ion.

Peak 29 was not observed in either EI- or FI-MS from this sample, but showed up on all GC traces and is therefore suspected to be an impurity (due to the matching retention time, most likely squalane from other experiments) or a ghost peak from the GC.

Finally, from the mass ion of m/z = 586, peak 30 has been assigned as the dehydrodimer. The FI-MS spectra did not detect this peak, but an automated mass ion calculation was performed on this cluster of peak giving a probable mass ion of m/z = 586. An accurate mass analysis was also performed on this peak which was given as m/z = 586.496 ± 1 which exactly matches a molecular formula of $C_{38}H_{66}O_4$, which in turn corresponds to two methyl linoleate molecules each minus a hydrogen atom. This product would be expected to be formed from termination reactions of methyl linoleate radicals to form a new C-C bond with the two missing hydrogen atoms coming from hydrogen abstraction. As with the alcohols, from the spectra, the exact position of the C-C bridge between the two molecules is unknown. The peak itself appears as a double cluster with near identical MS profiles, suggesting the presence of several different dimer isomers.

As with methyl linoleate, the mass spectra for the GC-MS analysis of methyl oleate autoxidation products (from figure 3.5) are presented in Tables A.3 and A.4 in Appendix A. The fragmentation products are mainly aldehydes and their corresponding alkanes, as described with methyl linoleate previously. Similarly, the addition products are the epoxides as well as alcohol and ketone products, as well as the dehydrodimer.

In addition to mass spectra, peaks 2,6,7 and 16 were verified by comparing the retention time with pure samples. The epoxides were also verified from Lercker's (2003) work on methyl oleate oxidation. The remaining addition products, alcohols, ketones and

the dimer were verified from Frankel's (1984) work on methyl oleate hydroperoxides, although the exact structure of the dimer isomer (or more likely isomers) could not be exactly determined.

3.2.3 Methyl Linoleate Decay

Following the identification of the autoxidation products of methyl linoleate it was then necessary to determine which were the dominant ones, but also which would react further and decay over time and which ones would be persistent. To determine this, the flow oxidation reactions were then carried out on methyl linoleate to measure the change in concentration of ML and its products over time. Figure 3.7 shows the change in concentration of ML over time, within the ±5.7% error associated with the GC at 170 ^{o}C as an example.

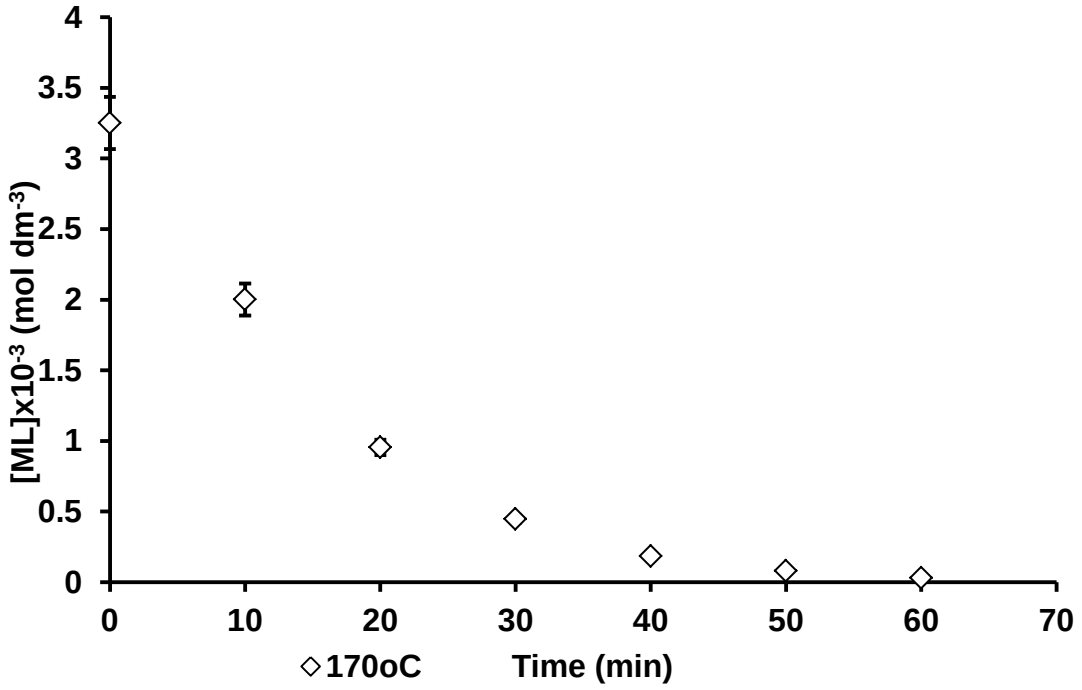

Figure 3.7 – The change in concentration of ML over time at 170 ^{o}C with a 0.08 dm^3 min^{-1} flow of oxygen.

Taking the natural logarithms of the concentration of squalane over time in this oxidation reaction yielded a straight-line plot indicating that the autoxidation of methyl linoleate is approximately first order with respect to ML – see figure 3.8. The decay of ML was also found to yield straight-line graphs at 100, 130 and 150 ^{o}C, the other 3 temperatures used in this study – see figure 3.9.

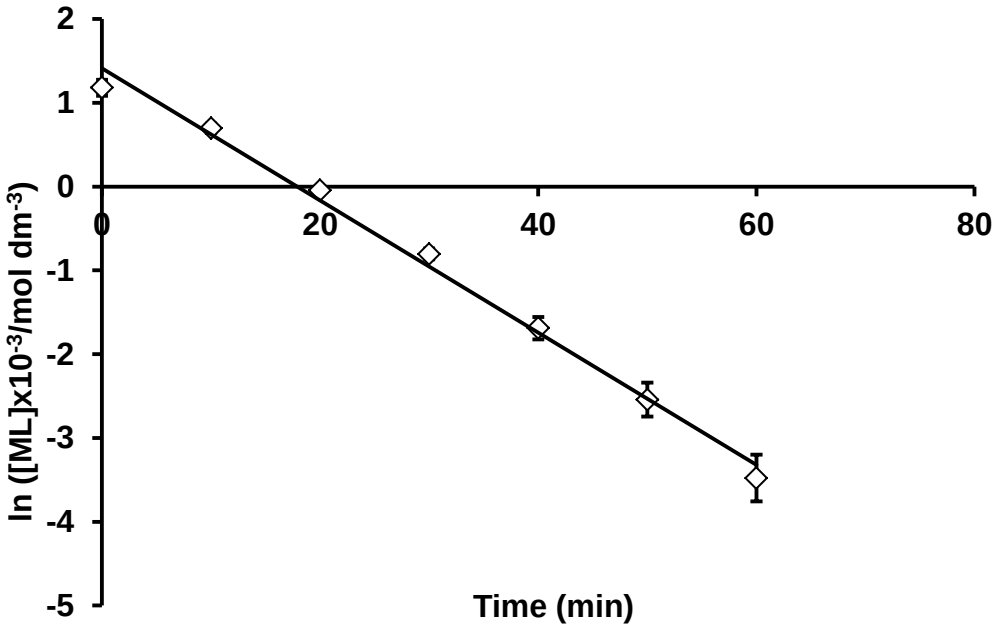

Figure 3.8 – The logarithmic decay of ML over time at 170 ^{o}C with a 0.08 dm^{3} min^{-1} flow of oxygen.

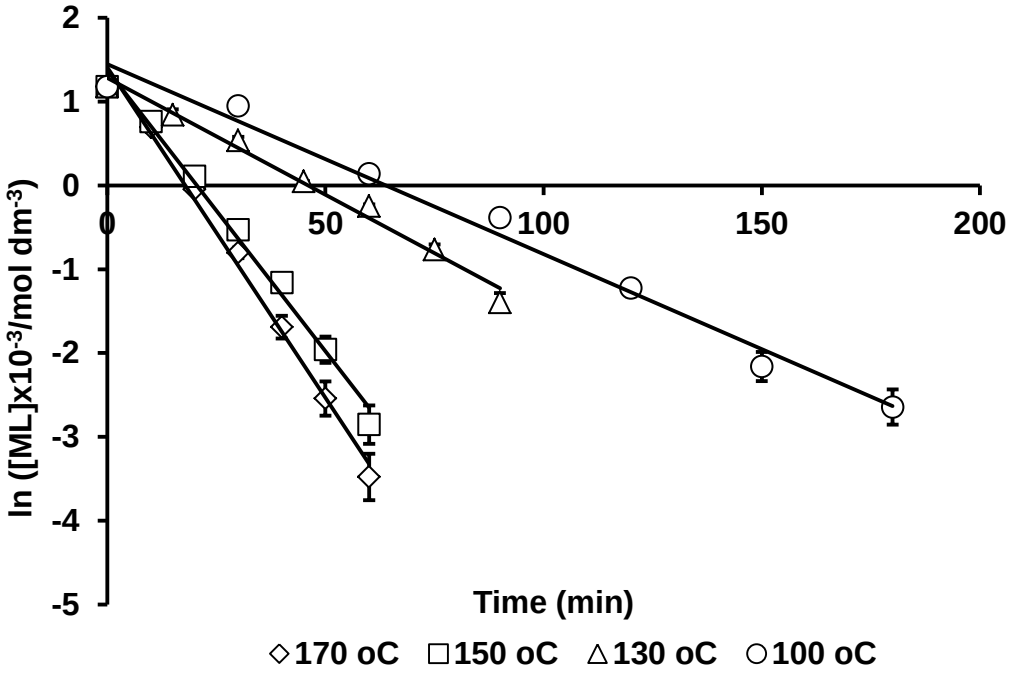

Figure 3.9 – The logarithmic decay of ML over time between 100 – 170 ^{o}C with a 0.08 dm^{3} min^{-1} flow of oxygen.

As the reaction is approximately psuedo first-order with respect to methyl linoleate the autoxidation of methyl linoleate can be represented by Equation 3.1, with the observed rate constant derived from the gradient of the line of best fit being given as k_{ML}.

$$\frac{d[ML]}{dt} \simeq k_{ML}[ML] \qquad \text{Equation 3.1}$$

From the k_{ML} values calculated, an Arrhenius plot was carried out to calculate an apparrent activation energy for methyl linoleate autoxidation. Figure 3.10 shows the k_{ML} values calculated at the different temperatures, whilst figure 3.11 shows the Arrhenius plot for the activation energy calculation. However, whilst the data points in figure 3.9 all correlate well with first-order decay, the data points in figure 3.11 do not neatly fit a straight line as would be expected for an Arrhenius diagram plotted in this way with only 1 point sitting on the line of best fit despite the fact that the errors associated with the k_{ML} values are obtained from the linear regression of the best-fit lines of the logarithmic decay graphs and represent the calculated standard error – ca. a 65% chance the true value lies within the quoted error limits. This plot would give an apparent activation energy for the autoxidation methyl linoleate of 26.6 ±7.2 kJ mol^{-1}, instead however there is indication that there are perhaps Arrhenius plots for two different reactions on the graph – one between 100 – 130 ^{o}C and the other from 150 – 170 ^{o}C with apparent activation energies of 8.6 and 12.50 kJ mol^{-1} respectively (no errors shown as each calculation is made from only two data points).

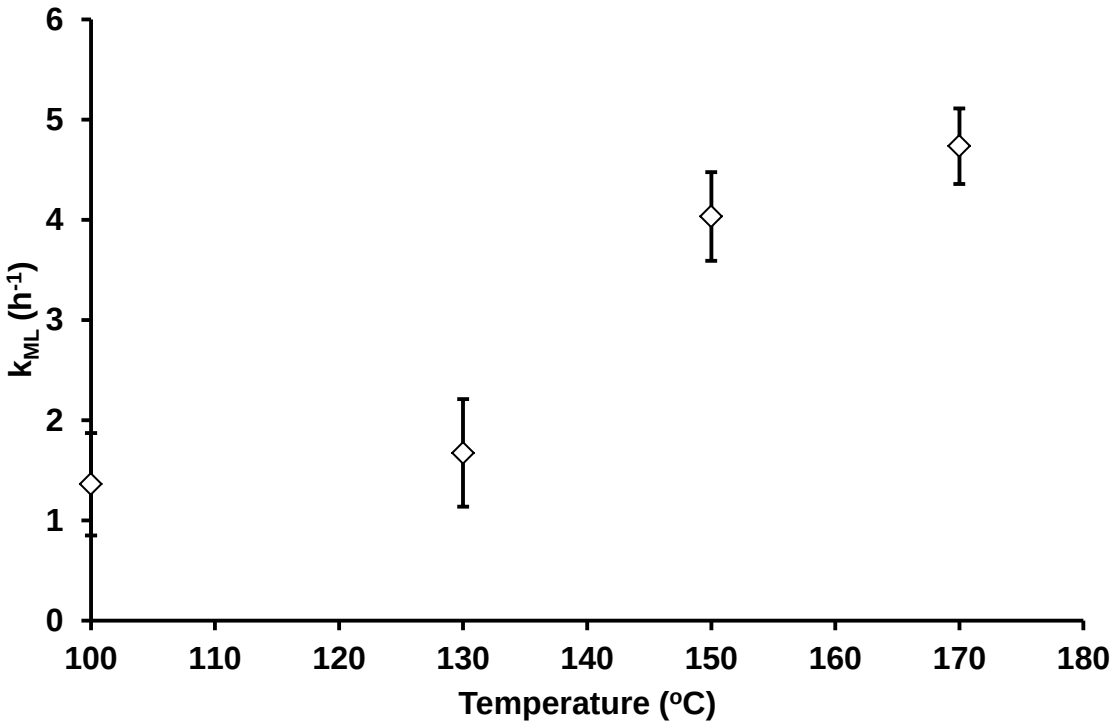

Figure 3.10 – The k_{ML} values for methyl linoleate oxidation reaction versus temperature

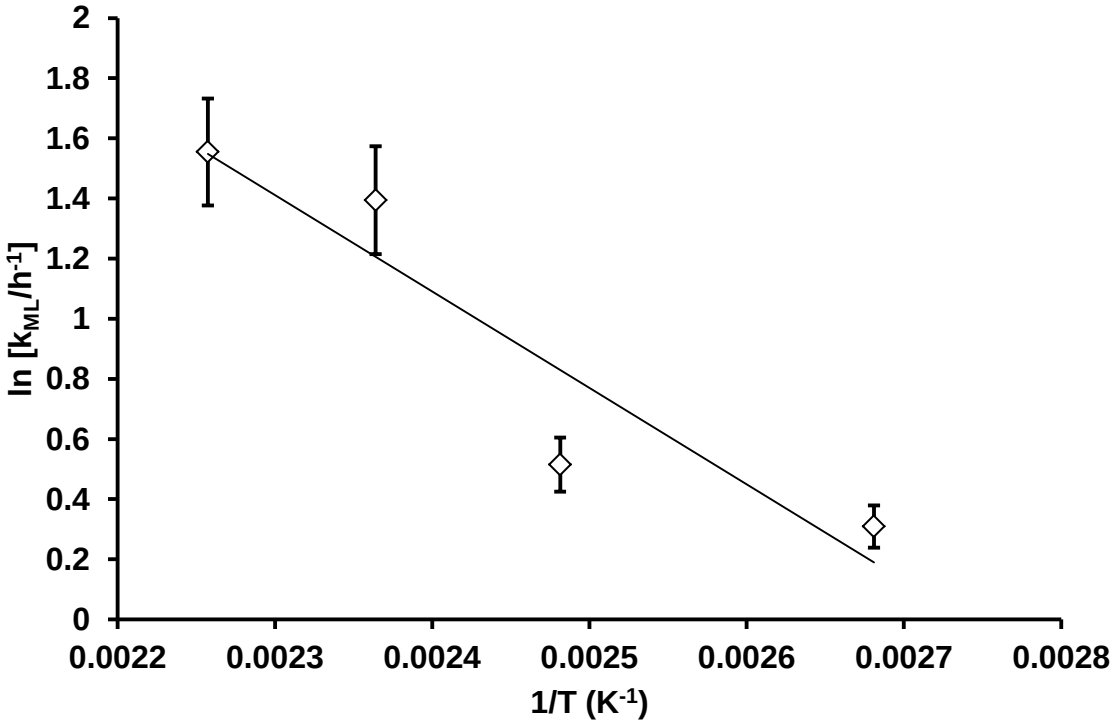

Figure 3.11 – Arrhenius plot for methyl linoleate autoxidation between 100 – 170 °C.

3.2.4 Autoxidation Product Formation and Decay

For the scission products – where the carbon chain of methyl linoleate has fragmented into two to give two smaller products – the most significant ones on the spectra (figure 3.2) are from the cleavage of the 8-9 C-C bond to give methyl octanoate (peak 6) and the corresponding aldehydes 2,4-decadienal (peaks 7 and 8) (figure 3.12 – see Discussion for detailed mechanism) shown in figure 3.13.

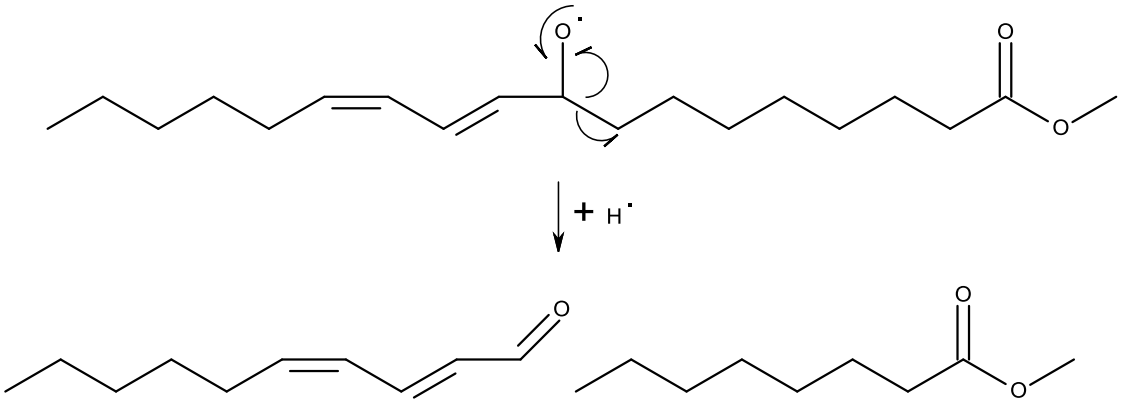

Figure 3.12 – The cleavage of the 8-9 C-C bond to give methyl octanoate and 2,4 decadienal.

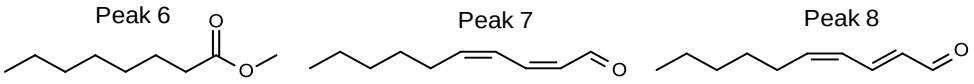

Figure 3.13 – From left to right, the chemical structures of methyl octanoate, 2,4 decadienal (Z,Z) and 2,4 decadienal (E,Z).

The change in concentration of methyl octanoate over time in the flow oxidation reactions is shown figure 3.14 (top). The middle and bottom plots show the same data for the Z,Z and E,Z isomers of 2,4 decadienal respectively. For all 3 graphs the concentrations appeared to increase, reaching a concentration maximum before decaying away again at 100 – 150 ^{o}C. At 170 ^{o}C, only decay was noted, suggesting the concentration maximum was reached before the first sample was withdrawn. In all 3 cases though, the concentration appeared to reach a higher maximum point as the temperature decreased, e.g. 0.040 mol dm^{-3} at 170 ^{o}C and 0.099 mol dm^{-3} at 100 ^{o}C for methyl octanoate.

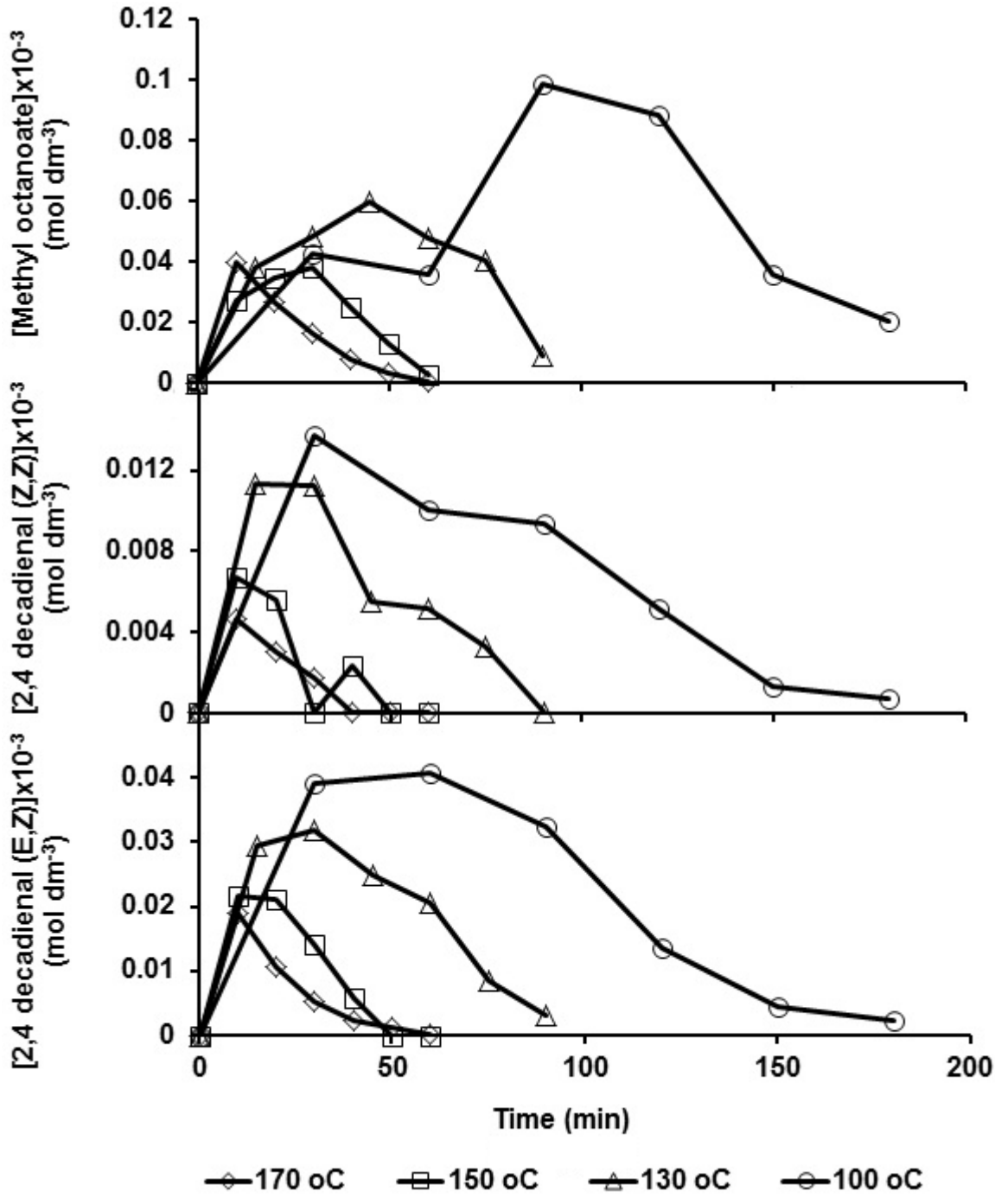

Figure 3.14 – From top to bottom, the formation and decay of methyl octanoate, 2,4 decadienal (Z,Z) and 2,4 decadienal (E,Z) over time.

The next two major peaks were 1 and 17 which were identified as pentane and the corresponding aldehyde 13-oxo methyl tridec-9,11-dienoate from cleavage of the 13-14 C-C bond – see figures 3.15 and 3.16.

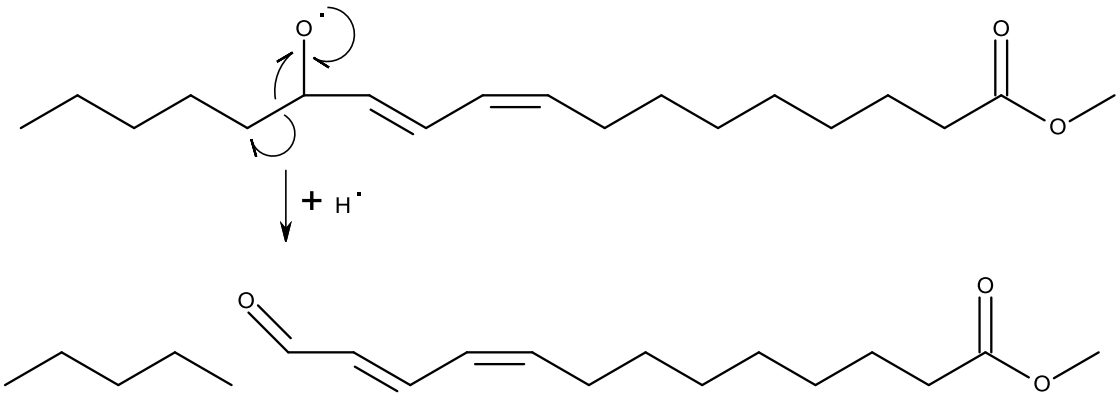

Figure 3.15 – The cleavage of the 13-14 C-C bond to give pentane and 13-oxo methyl tridec-9, 11-dienoate.

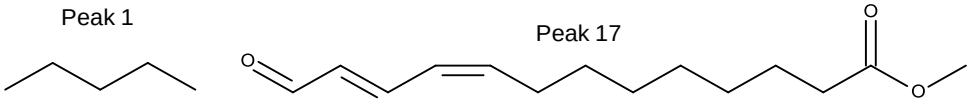

Figure 3.16 – The chemical structures of pentane and 13-oxo methyl tridec-9,11-dienoate.

Figure 3.17 shows the formation and decay graphs for them at the top and bottom respectively. Trends were harder to spot for these as both products appeared to be in decay from when the first sample was withdrawn. As with the previous 3 graphs, however, the concentration maxima for both increased as the temperature decreased.

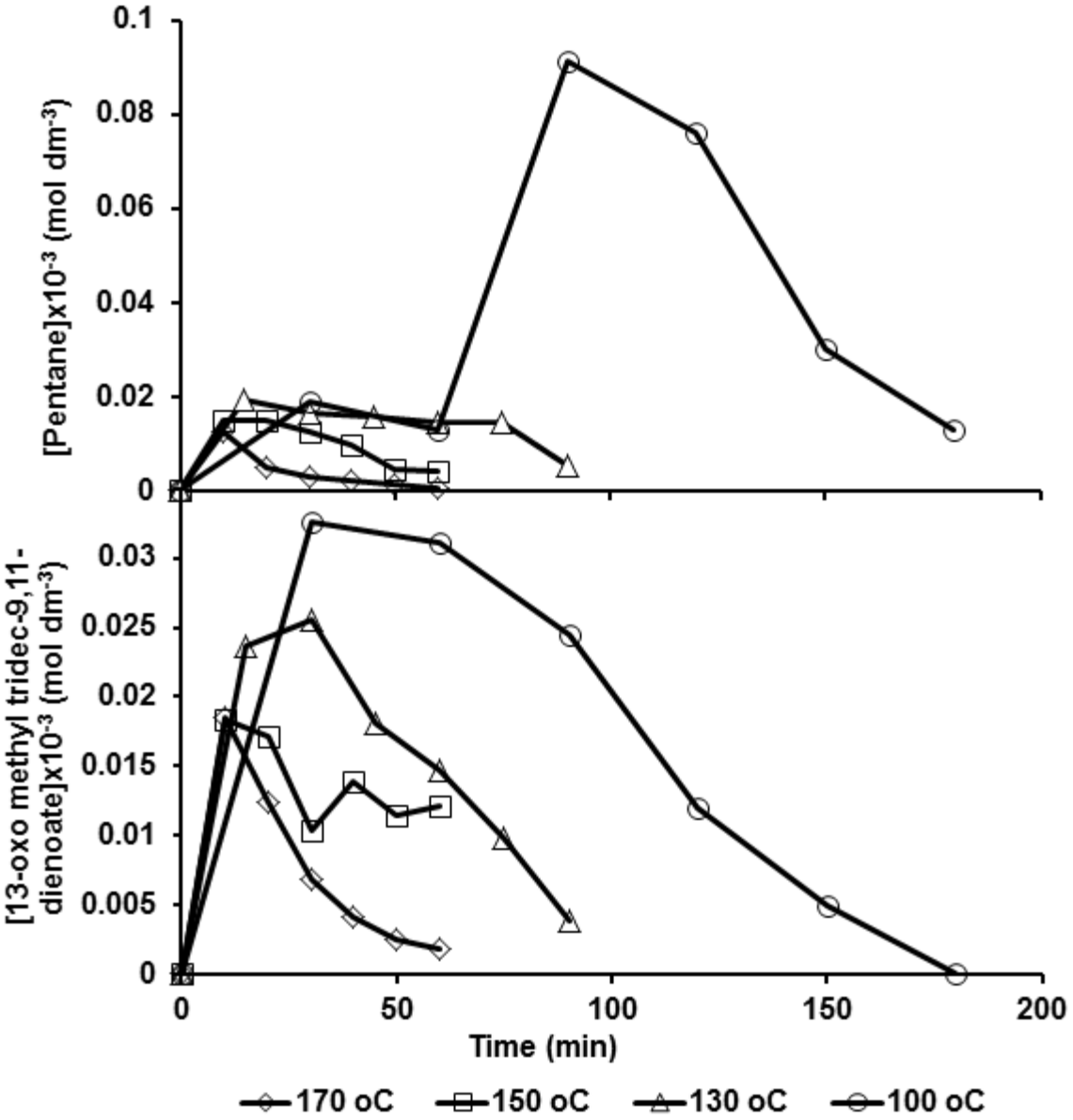

Figure 3.17 – From top to bottom, the formation and decay of pentane and 13-oxo methyl tridec-9,11-enoate over time.

The other major peaks observed were for hexanal (peak 2), 2-heptenal (peak 3), 9-oxo methyl nonanoate (peak 11) and 10-oxo methyl dec-8-enoate (peak 14) – see figure 3.18. The formation and decay graphs for them are displayed in figure 3.19 from top to bottom respectively. The same trend was observed for these as for the previous products – formation followed by decay, with the concentration maximum being higher at the lowest temperatures. Hexanal and 2-heptenal were, once again, only observed in decay at 170 ^{o}C, but the concentration maxima were noted for 9-oxo methyl nonanoate and 10-oxo methyl

dec-8-enoate at 170 ^{o}C this time, perhaps suggesting they formed slower than the other products.

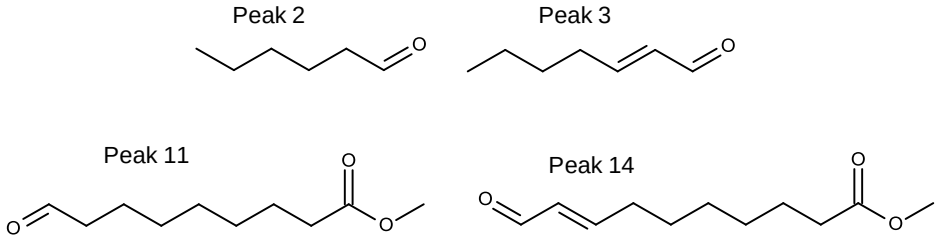

Figure 3.18 – Left to right, top to bottom, the chemical structures of hexanal, 2-octenal, 9-oxo methyl nonanoate and 10-oxo methyl dec-8-enoate.

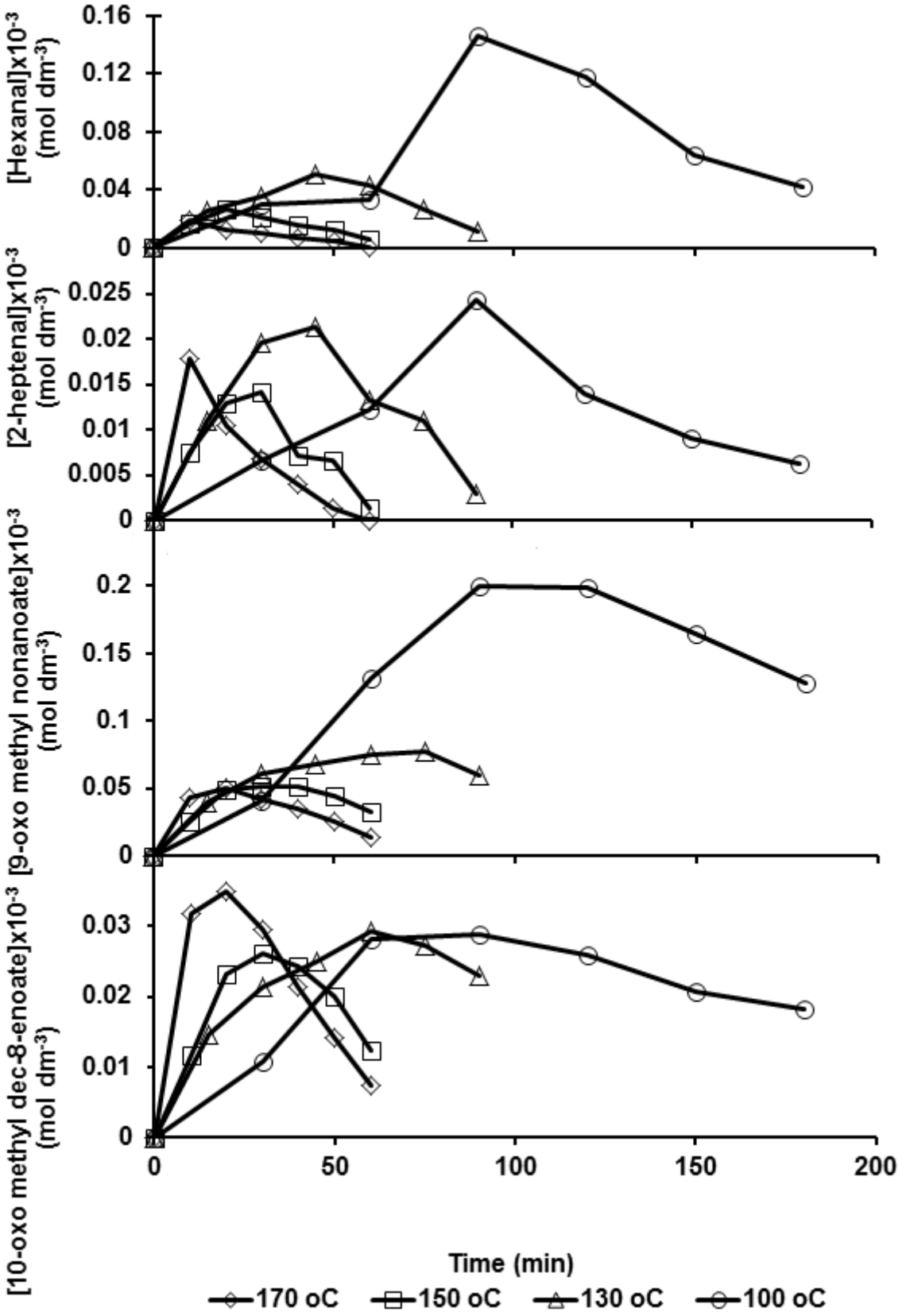

Figure 3.19 – From top to bottom, the formation and decay of hexanal, 2-heptenal, 9-oxo methyl nonanoate and 10-oxo methyl dec-8-enoate over time.

After the major fragmentation products, the minor peaks that were detected and that gave signal in either EI- of FI-MS (or both) were methyl heptanoate (peak 4), 2-octenal (peak 5), 8-oxo methyl octanoate (peak 9), 8-hydroxy methyl octanoate (peak 10) (all shown in figure 3.20), 10-oxo methyl decanoate, (peak 12) methyl nonandioic acid (peak 13), 11-oxo methyl undec-9-enoate (peak 15) and 12-oxo methyl dodec-9-enoate (peak 16) (figure 3.21).

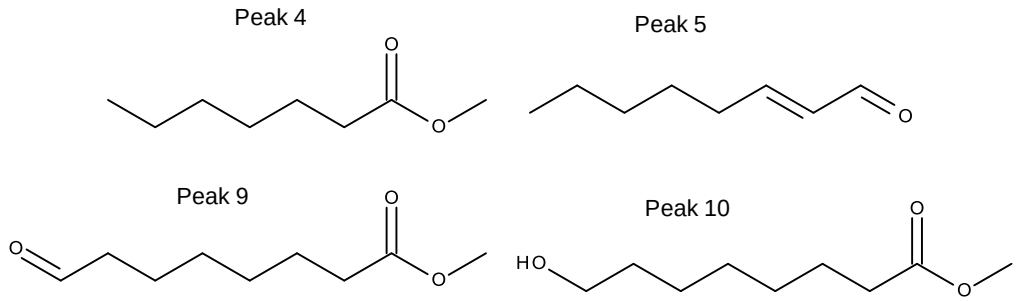

Figure 3.20 – Left to right, top to bottom, the chemical structures of methyl heptanoate, 2-octenal, 8-oxo methyl octanoate and 8-hydroxy methyl octanoate.

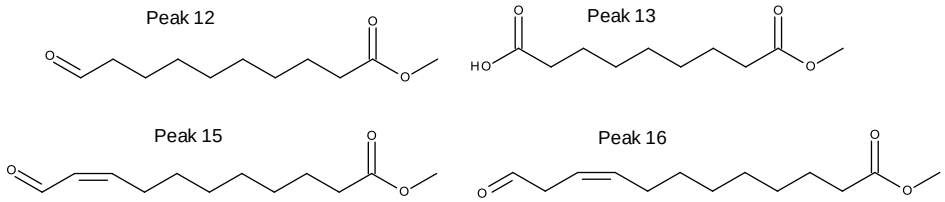

Figure 3.21 – Left to right, top to bottom, the chemical structures of 10-oxo methyl decanoate, methyl nonandioic acid, 11-oxo methyl undec-9-enoate and 12-oxo methyl dodec-9-enoate.

Because these were minor products, patterns could be harder to determine due to the associated error of the GC sometimes taking the peak area below the limit of detection – with peaks sometimes barely distinguishable above the noise of the baseline. Figure 3.22, for example, shows the formation and decay of methyl heptanoate over time. At 130 ^{o}C, no peak areas were detected above the noise until 60 minutes into the reaction. At 100 ^{o}C, the variation due to GC error took the peaks below the limit of detection midway through the reaction. Even when a peak was detected in each sample at 150 ^{o}C, the concentration seemed to shoot up mid-way through – the only temperature where any notable trend was noted was 170 ^{o}C which showed methyl heptanoate in decay over time.

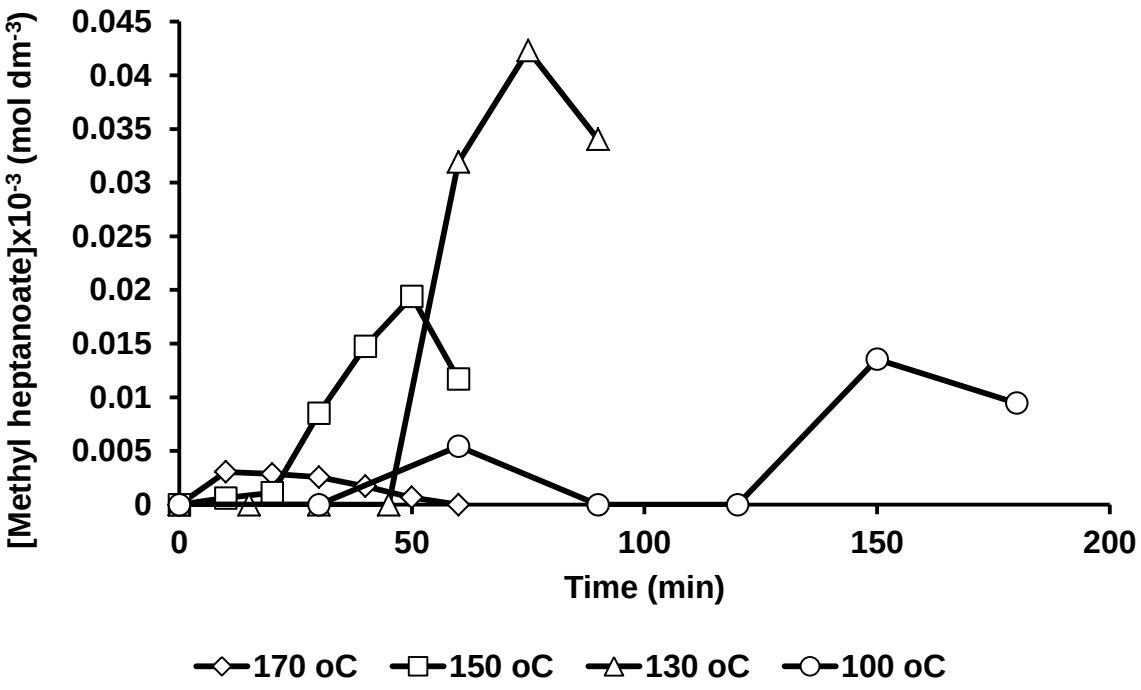

Figure 3.22 – The formation and decay of methyl heptanoate over time.

Figure 3.23 shows the same graph for 2-octenal which showed comparable trends to the major products identified. Figure 3.24 shows the graphs for 8-oxo methyl octanoate (top) and 8-hydroxy methyl octanoate (bottom). The former showed similar trends, except that at 130 and 100 ^{o}C the product had not started decaying, hence concentration maxima this time could not be determined at the lowest temperatures, compared to previous examples where it was the higher temperatures that the maximum could not be determined for. It did seem likely from following the trend of the curvature that, like the others, the concentration maxima was higher at the lower temperatures. The latter, by comparison, showed concentration maxima for all temperatures except 130 ^{o}C, however, unlike the previous examples, the maxima appeared to be roughly the same for all temperatures, resembling more of a 'threshold' concentration.

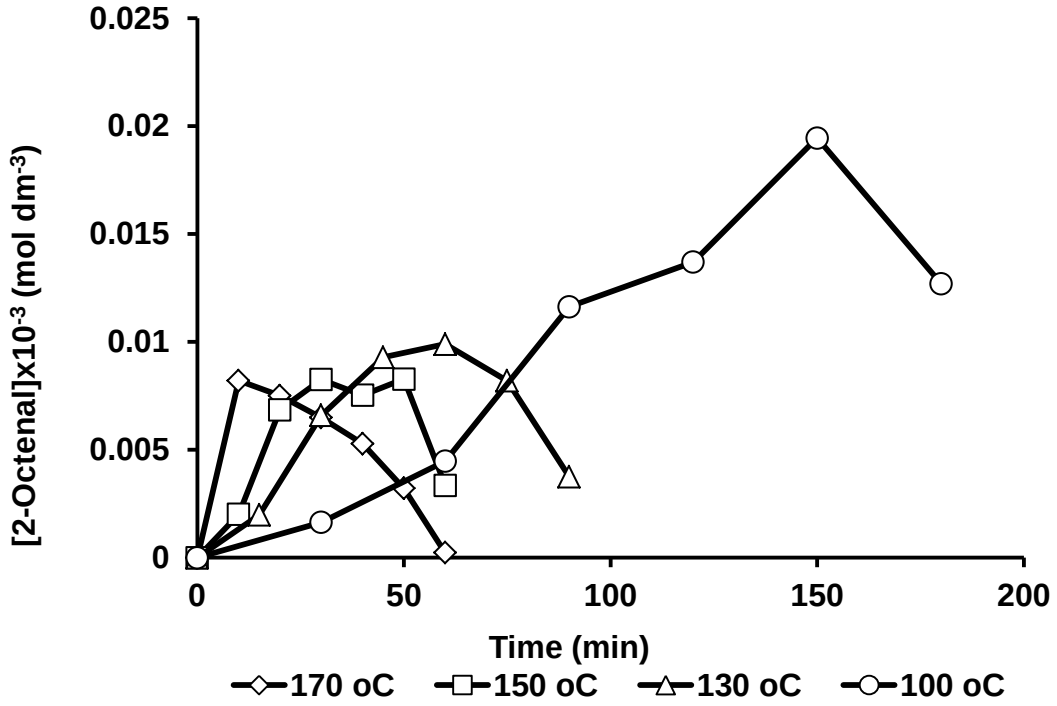

Figure 3.23 – The formation and decay of 2-octenal over time.

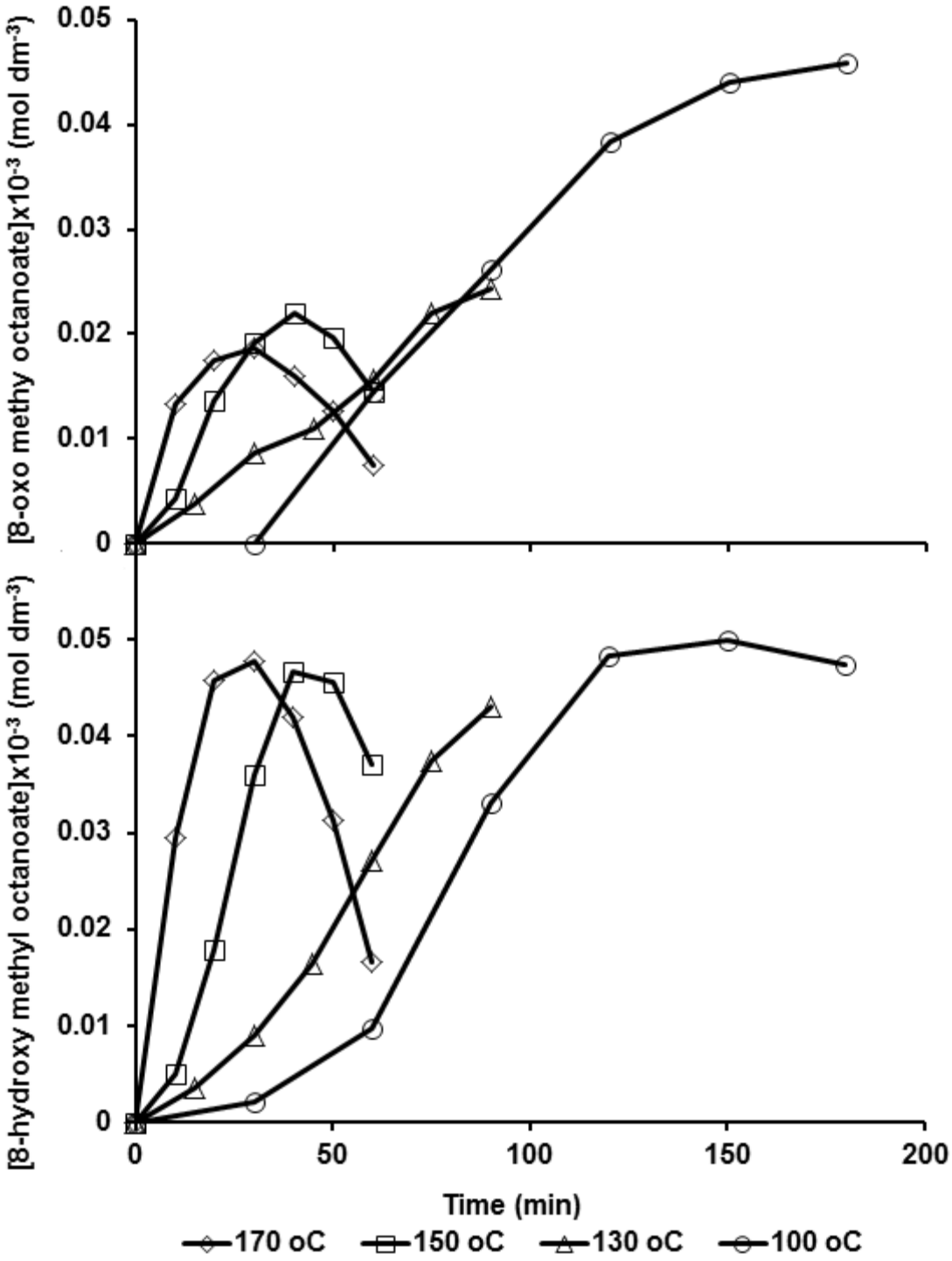

Figure 3.24 – From top to bottom, the formation and decay of 8-oxo methyl octanoate and 8-hydroxy methyl octanoate over time.

Following the initial identification from the static oxidation reaction, 10-oxo methyl decanoate and methyl nonandioic acid were not identified again in the flow oxidation reactions, hence there is no concentration versus time data reported for them in this section.

Figure 3.25 shows the data for 11-oxo methyl undec-8-enoate (top) and 12-oxo dodec-8-enoate (bottom) over time however. Both exhibited similar behaviour to the majority of the other scission products, except the concentration maximum was not observed for 12-oxo methyl dodec-8-enoate at 130 ^{o}C.

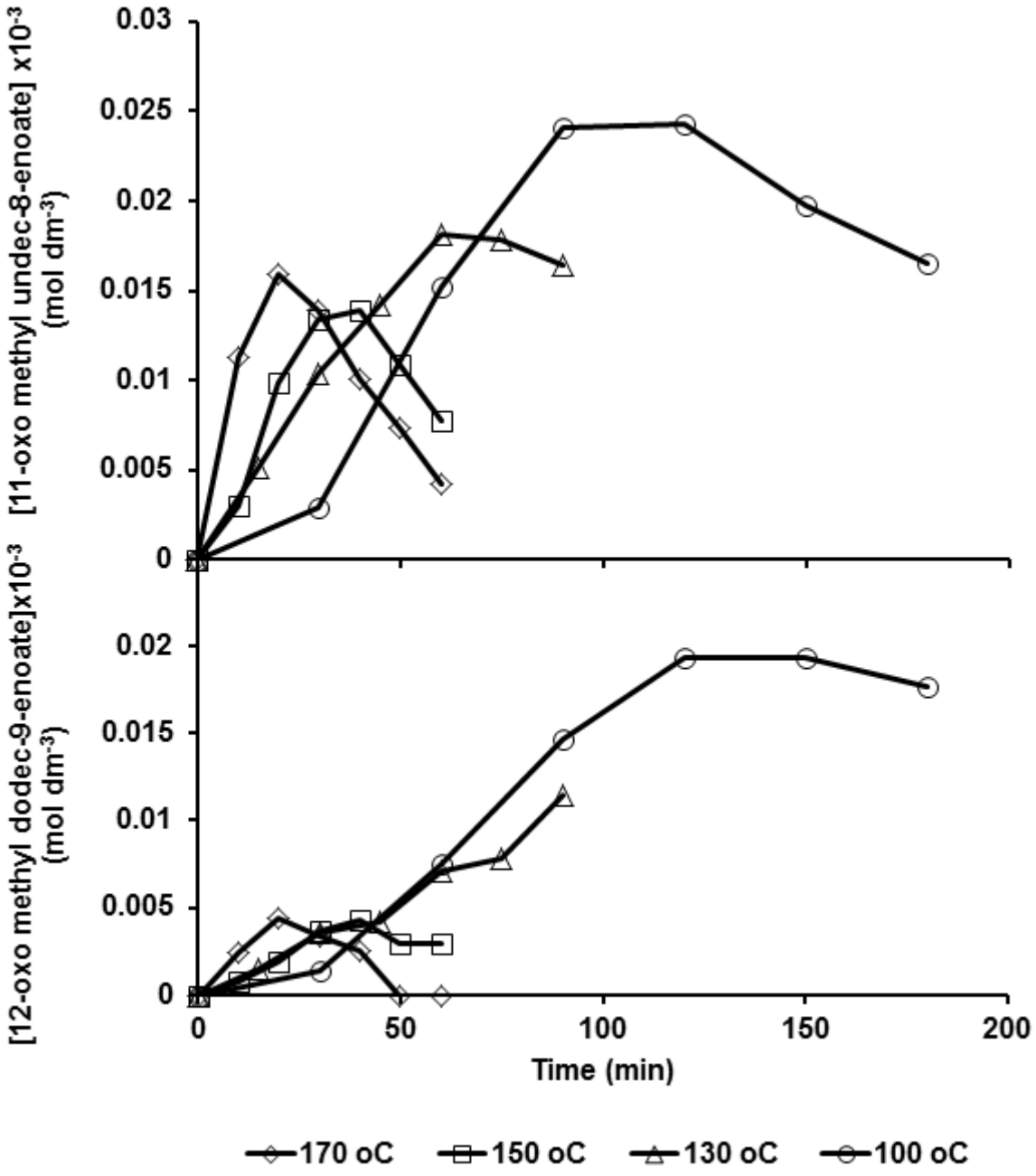

Figure 3.25 – From top to bottom, the formation and decay of 11-oxo methyl undec-8-enoate and 12-oxo methyl dodec-9-enoate over time.

After methyl linoleate eluted, the main products observed in the GC spectra were the addition products – where ML reacted with oxygen without subsequent cleavage of the carbon chain. Whilst being identified as a collection of epoxides, alcohols and ketones, only the epoxides (peaks 19 – 22) had all four of their positional isomers identified. Their formation and decay are presented in figure 3.26 (the main carbon chain being represented as ML for brevity). Whilst they followed the same product build-up followed by decay, the most noticeable difference between the epoxides and the scission products was that the highest concentration maxima were now found at the highest temperatures and got lower as the temperature decreased in direct opposition to the trends shown by the scission products.

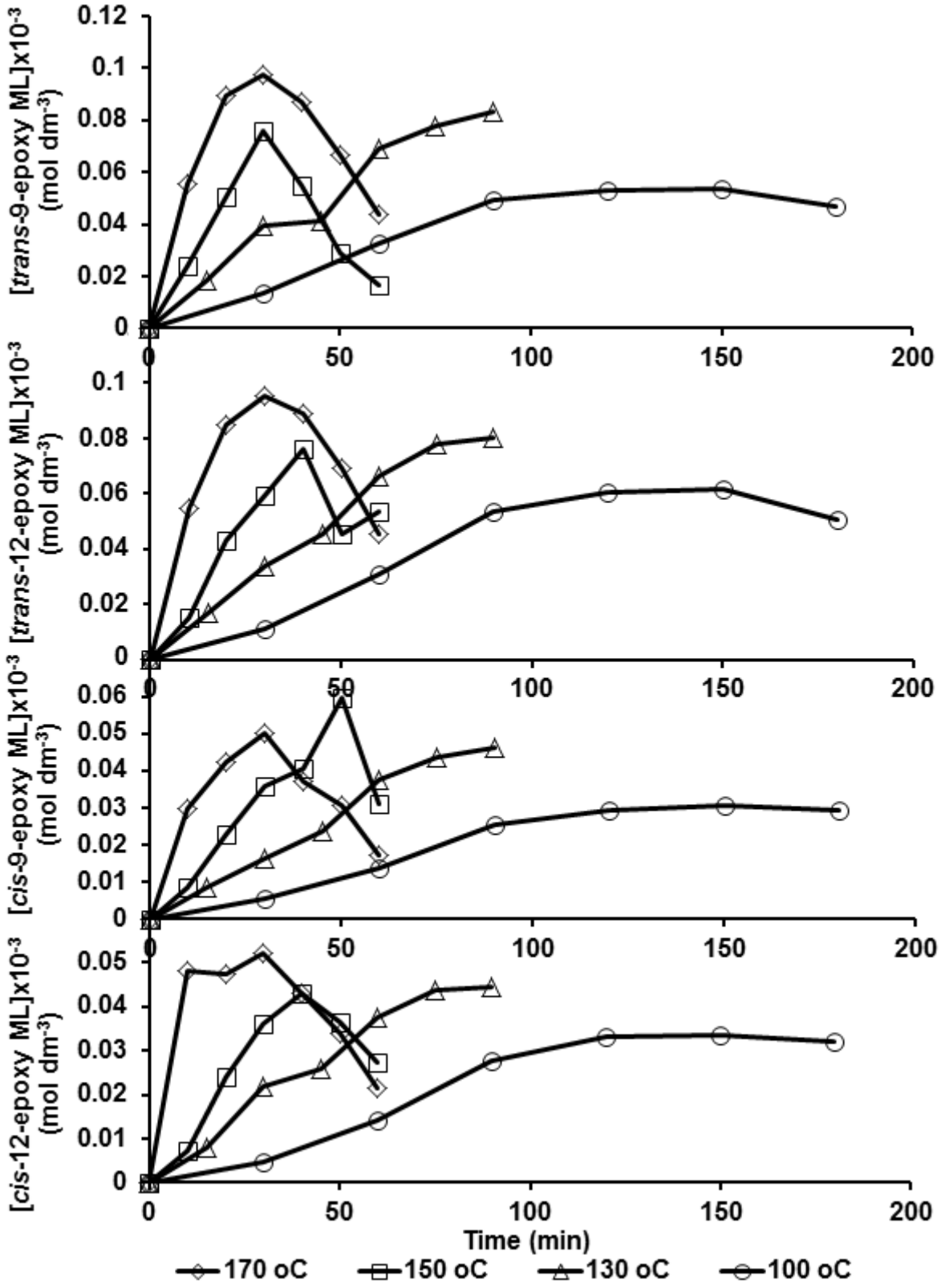

Figure 3.26 – From top to bottom, the formation and decay of methyl *trans*-9-epoxy octadec-12-enoate, methyl *trans*-12-epoxy octadec-9-enoate, methyl *cis*-9-epoxy octadec-12-enoate and methyl *cis*-12-epoxy octadec-9-enoate over time over time.

Of the 4 peaks identified as alcohols from the static oxidation reaction, only the first one was consistently identifiable by its retention time in the flow oxidation reactions; after this several other peaks (possibly minor ketones) started appearing overlapping the remaining 3 alcohol peaks leading to increasingly poor resolution to obtain concentrations and in some cases making identifying the original peak nearly impossible. For this reason only one graph for the methyl linoleate alcohols is shown in figure 3.27. Concentration maxima were only obtained at 130 and 150 ^{o}C (though the one for 150 ^{o}C appears to be anomalously high), at 100 and 170 ^{o}C only decay of the alcohol was noted, though as with the scission products it did appear the higher concentrations were found as the temperature decreased.

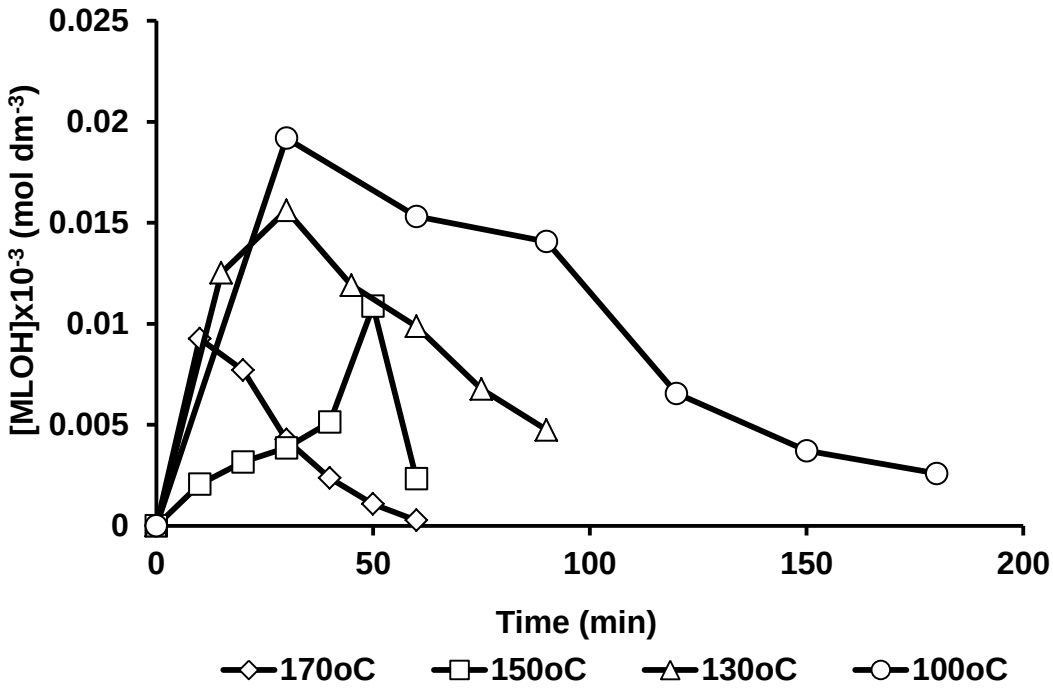

Figure 3.27 – The formation and decay of the first methyl linoleate alcohol (exact positional isomer unknown) over time.

The graphs for the two ketones are shown in figure 3.28 (methyl 9-oxo octadec-10,12-dieanote, top and methyl 13-oxo octadec-9,11-dienoate, bottom). The 9-oxo isomer shows the rise and fall in concentration with the highest maxima being shown at lowest temperatures, though the graph patterns for 100 and 130 ^{o}C are very similar, as are those for 150 and 170 ^{o}C. Due to some anomalously high values for the 11-oxo isomer noticeable trends are very hard to identify however. Finally, in the flow oxidation reactions

the dimer was not observed in the GC traces hence no data on its formation and decay is presented here.

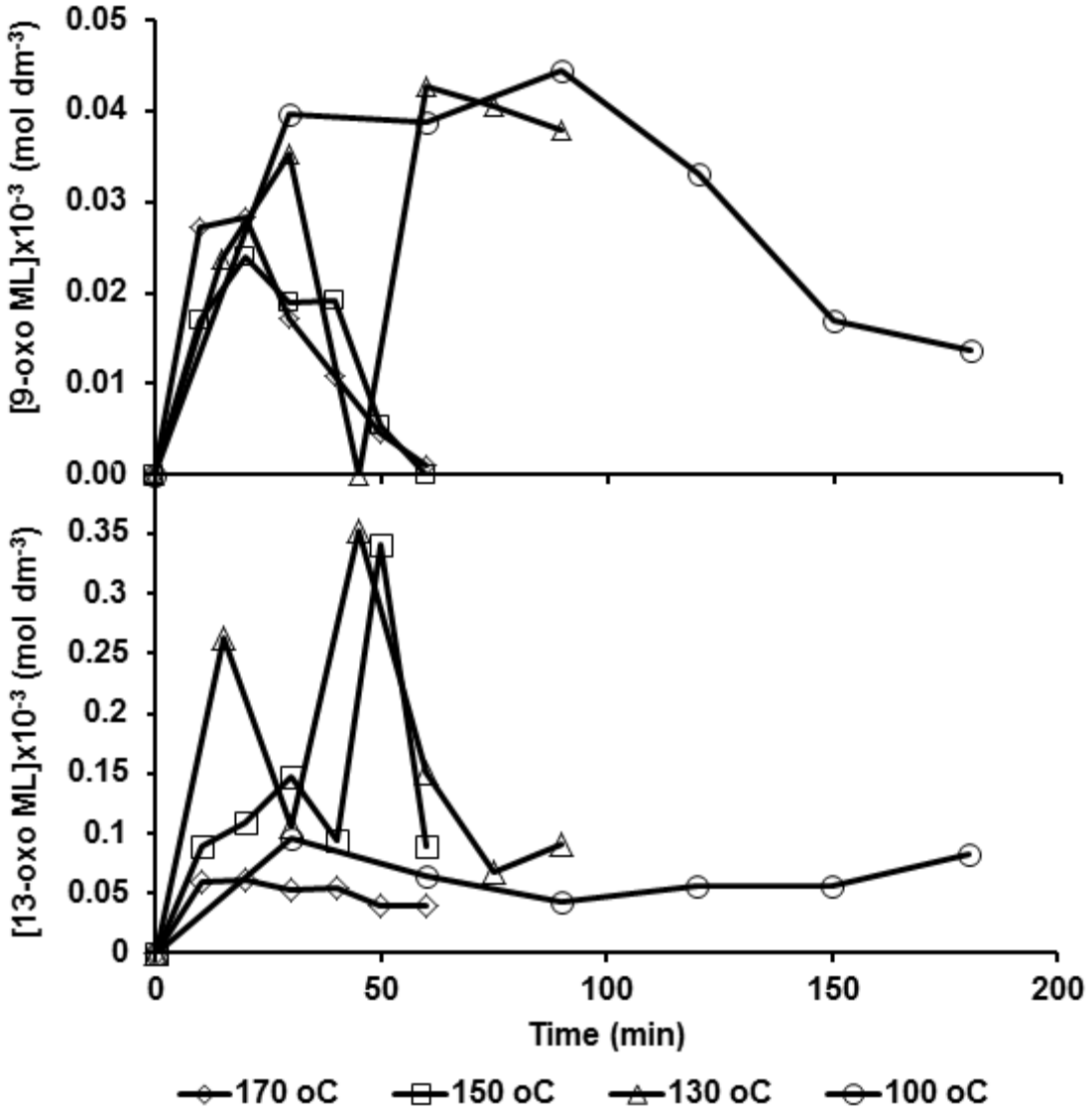

Figure 3.28 – From top to bottom, the formation and decay of methyl 9-oxo octadec-10,12-dienoate and methyl 13-oxo octadec-9,11-dienoateover time.

3.3 Discussion

3.3.1 Mechanisms of Autoxidation

The formation of fragmentation products can be explained by the radical abstraction mechanism proposed and identified in previous work involving autoxidation of unsaturated hydrocarbons (Ross 1949, Frankel 1985). The autoxidation of methyl linoleate begins with an oxygen-based radical (normally an alkoxyl radical in the propagation cycle) abstracting an allylic hydrogen atom from the carbon chain to form a doubly allylic carbon centred radical (from reaction 3.4 in the Introduction). The doubly allylic hydrogen is

preferred due to the resonance structures the adjacent double bonds can provide – see figure 3.29 (Chan 1979). Alkoxyl radicals can therefore form on the 9, 11 and 13 positions on the carbon chain (Structures A-C in figure 3.30) by cleaving the hydroperoxide bond formed in reaction 3.4 (when $RO_2\bullet$ = $MLO_2\bullet$) to give a hydroxyl radical and an oxygen centred alkoxy radical on the carbon chain (Reaction 3.2) through the radical propagation cycle initially described in the introduction.

Structures A and C would be expected to be favoured due to the conjugation formed by migration of the double bonds. Fragmentation can then occur as the oxygen radical cleaves the carbon chain to give an aldehyde and carbon centred radical (Reaction 3.6). The carbon centred radical can then either abstract another hydrogen atom from a hydrocarbon (Reaction 3.7) to propagate the cycle or undergo reactions 3.3, 3.2 and 3.6 to give the subsequent aldehyde. In addition, the oxygen centred radical can also abstract a hydrogen atom to form the corresponding alcohol (Reaction 3.8).

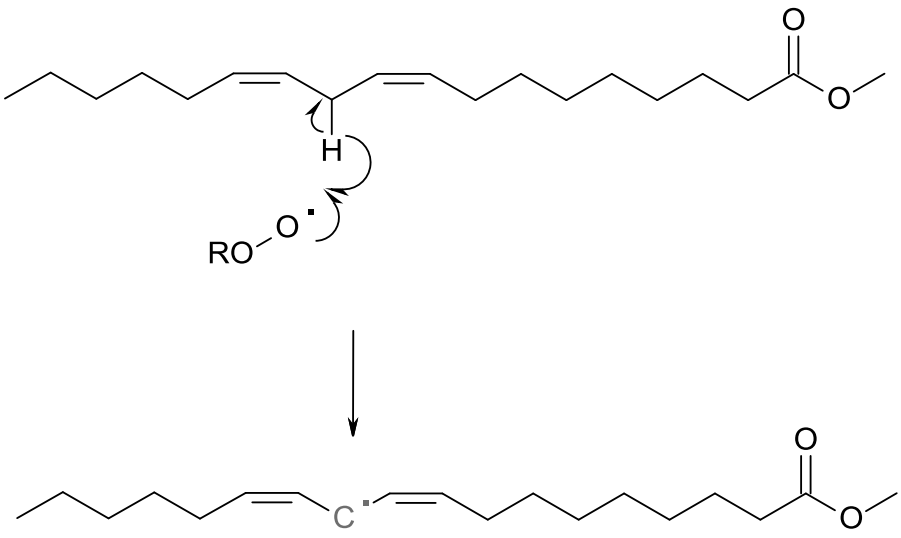

Reaction 3.4

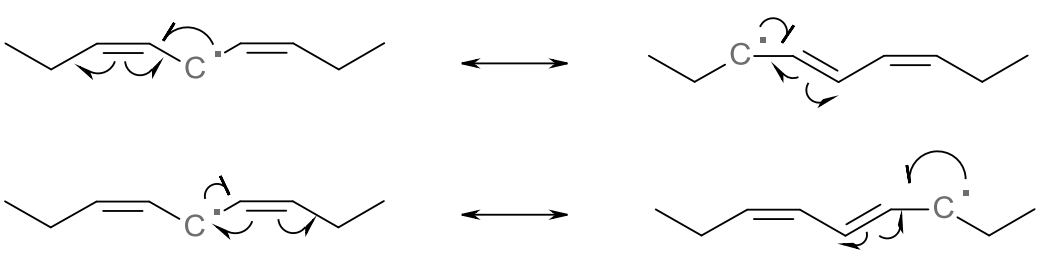

Figure 3.29 – The resonance stabilisation of a doubly allylic radical.

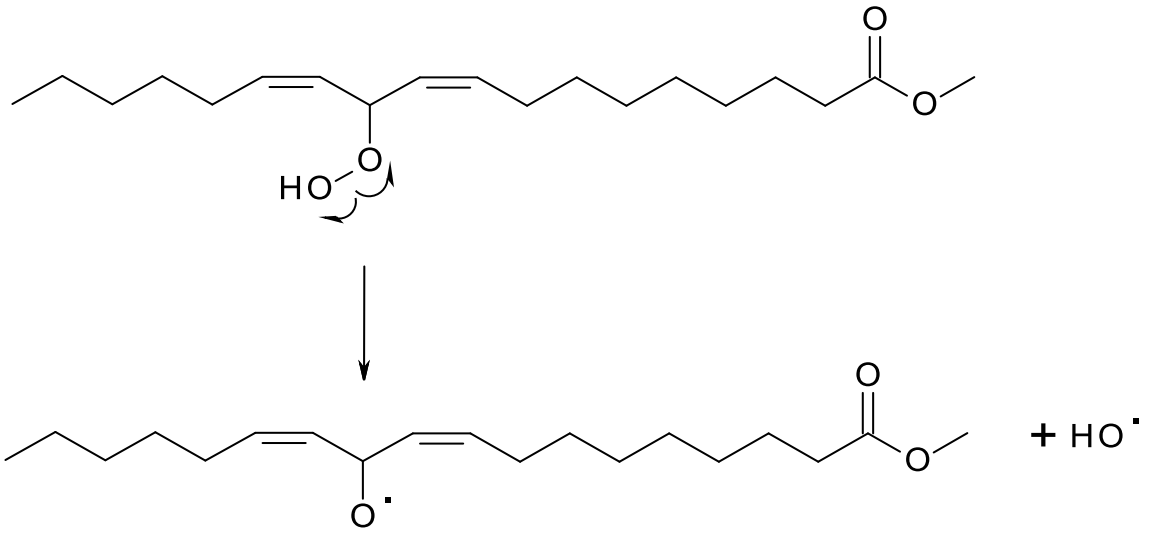

Reaction 3.2

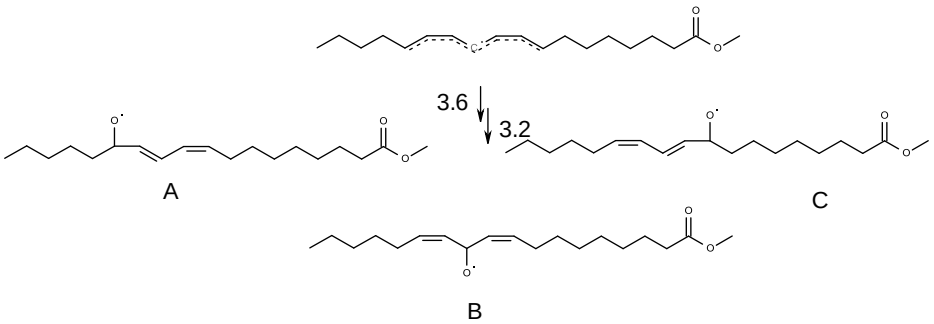

Figure 3.30 – The three main alkoxyl radical isomers of methyl linoeate autoxidation.

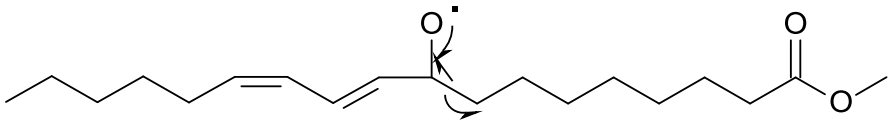

Reaction 3.6

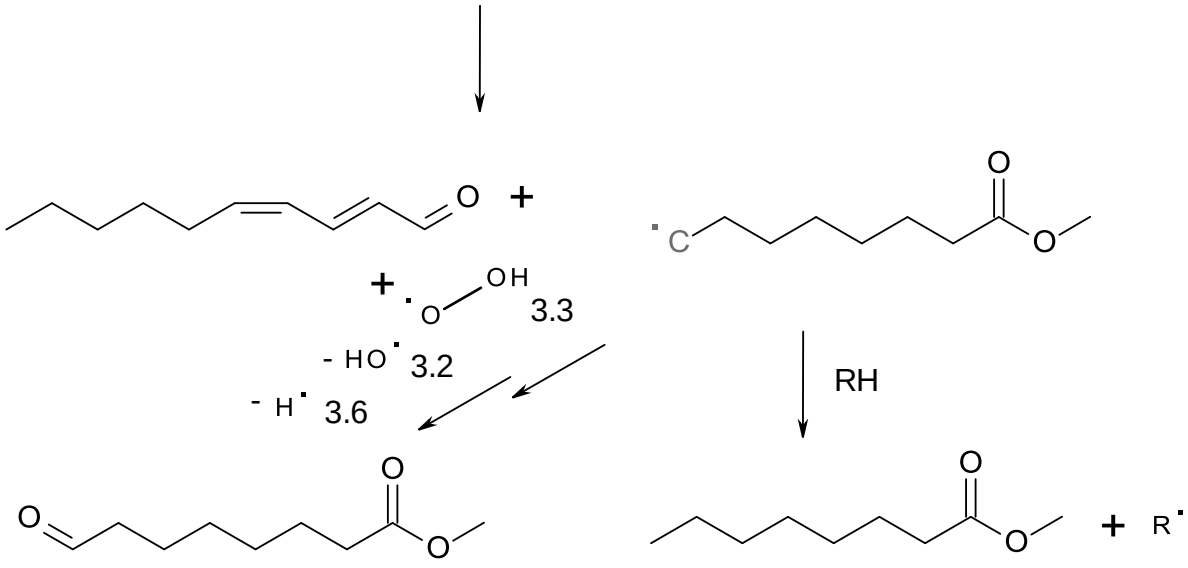

Reaction 3.7

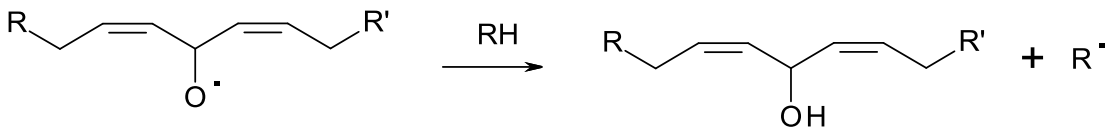

Reaction 3.8

The singly allylic hydrogen atoms can also be abstracted to give the oxygen radicals at the 8, 10, 12 and 14 positions (Reaction 3.7, Structures D-G), but this would not be expected to be favourable due to only 2 resonance structures per hydrogen (see figure 3.31) – only three minor products (methyl heptanoate, 10-oxo methyl decanoate and 10-oxo methyl dec-8-enoate) were detected from these radicals – see below.

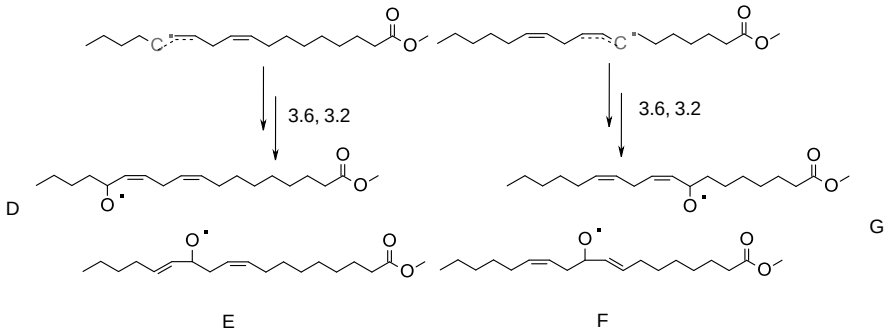

Figure 3.31 – The positional isomers of the alkoxyl radicals of methyl linoleate after singly allylic hydrogen abstraction.

Peroxyl radicals can also add to carbon-carbon double bonds initially forming a peroxyl adduct which is sufficiently unstable to rapidly cleave to form an alkoxyl radical and an epoxide (Reaction 3.9), however there is no stereoselectivity to this reaction hence both the *cis*- and *trans*- isomers are formed (Filipova 1982, Lercker 2003, Giuffreida 2004).

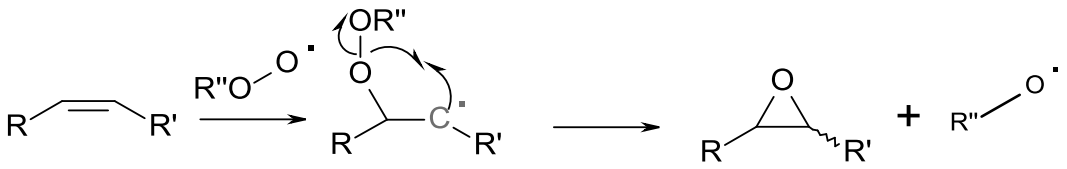

Reaction 3.9

Hydroxyl radicals can also add to carbon-carbon double bonds to form hydroxyl and alkyl adducts (Lightfoot 1992). The resulting carbon-centred radical can add an oxygen molecule to form a peroxide, which subsequently cleaves to give an alkoxyl radical as seen before in reactions 3.4 and 3.2. The C-C bond can then undergo cleavage (Reaction 3.6) to give an aldehyde and a hydroxyl- alkyl radical, which will then react with oxygen to form another aldehyde and hydroperoxyl radical (Reaction 3.10) (Sonawane 1986).

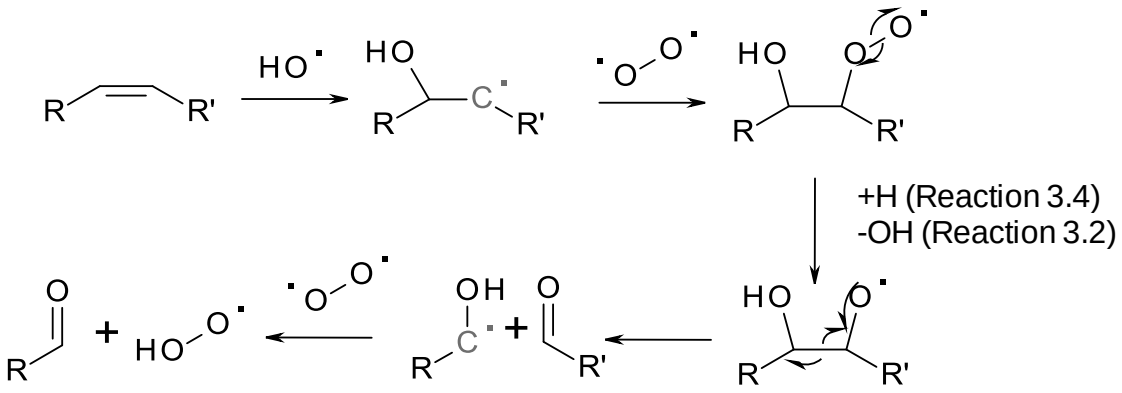

Reaction 3.10

From each of the 7 resonance structures and the reaction mechanisms, the reaction pathways for the identified products have been proposed from the seven different alkoxyl structures given and the subsequent radical reactions, shown in Table 3.5. In addition to the radical pathways, 8-oxo methyl octanoate can also, theoretically, be formed from the detected 8-hydroxy methyl octanoate by oxidation of the primary alcohol to the corresponding aldehyde. Two of the minor products, methyl nonandioic acid and 10-oxo methyl decanoate are slightly anomalous in that they do not entirely fit the radical mechanisms listed and therefore must have undergone additional reactions making them likely secondary decay products. Methyl nonandioic acid could theoretically be formed via oxidation of the aldehyde 9-oxo methyl nonanoate to the corresponding carboxylic acid. Similarly 10-oxo methyl decanoate could theoretically be formed from 10-oxo methyl dec-8-enoate via hydrogenation of the double bond. Further work would be required to confirm these however.

Table 3.1 – The proposed reaction pathways for the epoxides and fragmentation products from the different methyl linoleate alkoxyl radicals.

Peak No.	Product	Structure	Reaction 3.x
1	Pentane	A (Fig 3.41)	6, then 7
2	Hexanal	A (Fig 3.41)	6 10 on 12-13 bond
3	2-Heptenal	E (Fig 3.42) B (Fig 3.41)	6 6,3,2,6
4	Methyl Heptanoate	G (Fig 3.42)	7, then 7

5	2-Octenal	B (Fig 3.41)	6
6	Methyl Octanoate	C (Fig 3.41)	6, then 7
7	2,4 decadienal (Z,Z)	C (Fig 3.41) C (Fig 3.41)	6 6,3,2,6
8	2,4 decadienal (E,Z)	C (Fig 3.41) C (Fig 3.41)	6 6,3,2,6
9	8-oxo Methyl Octanoate	G (Fig 3.42) C (Fig 3.41)	6 6,3,2,6 Alcohol oxidation of 8-hydroxy methyl octanoate
10	8-hydroxy Methyl Octanoate	C (Fig 3.41)	6, 3,2,6
11	9-oxo Methyl Nonanoate	C (Fig 3.41)	6
12	10-oxo Methyl decanoate	F (Fig 3.42)	6, then 7 plus hydrogenation of double bond
13	Methyl Nonandioic acid	C (Fig 3.41)	6, then oxidation
14	10-oxo Methyl dec-8-enoate	F (Fig 3.42) B (Fig 3.41)	6 6,3,2,6
15	11-oxo Methyl undec-9-enoate	B (Fig 3.41)	6
16	12-oxo Methyl dodec-9-enoate	A (Fig 3.41) E (Fig 3.42)	10 on 12-13 bond 6
17	13-oxo Methyl tridec-9,11-dienoate	A (Fig 3.41)	6
19	Methyl *trans*-9-epoxy octadec-12-enoate		9 on 9-10 bond
20	Methyl *trans*-12-epoxy octadec-9-enoate		9 on 12-13 bond
21	Methyl *cis*-9-epoxy octadec-12-enoate		9 on 9-10 bond
22	Methyl *cis*-12-epoxy octadec-9-enoate		9 on 12-13 bond

The products being formed via resonance structures A and C is consistent with these being the most prominent peaks in the GC spectra. As well as knowing how methyl linoleate degrades and what it breaks down into, the next main steps in investigating the chemistry of methyl linoleate as a biodiesel component are to understand which are

favoured products and how fast they form (as well as decay) and hence identify the dominant mechanisms responsible for degradation.

3.3.2 Formation and Decay of Products

Pentane and 13-oxo methyl tridec-9,11-dienoate are the two products from the scission of the 13-14 C-C bond on Structure A (see figure 3.15). For each of the resulting hydrocarbons, there is also the possibility of the corresponding aldehyde being formed, though pentanal was not directly observed. However, there are a cluster of unidentified peaks at the start of the spectra, only two of which (pentane and hexanal) gave major signals in EI-MS. In FI-MS there is a peak which has the mass ion of m/z = 86, which is the mass ion of pentanal, however because of the loss of other peaks on the FI-MS trace, at present it is not possible to match this to a specific peak on the GC trace, nor to confirm it via EI-MS.

Hexanal can be formed by scission of the 12-13 C-C bond; the other product would be expected to be methyl dodec-9,11-dienoate (figure 3.32), but the m/z = 210, which would be the mass ion, has failed to be identified by either EI or FI-MS, suggesting it either rearranges and/or reacts to form an, as yet unknown, more stable product, most likely by reacting with oxygen, or that hexanal is formed via Reaction 3.10 (figure 3.33) giving 12-oxo methyl dodec-9-enoate as the other scission product which was observed, but as a relatively minor product.

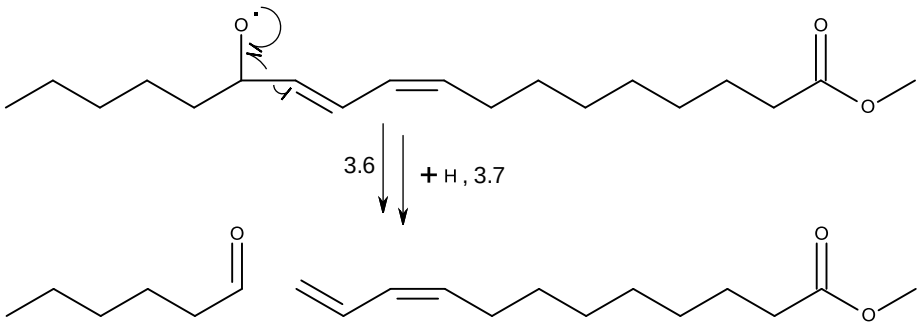

Figure 3.32 – The theoretical cleaving of the 12-13 C-C bond via reactions 3.6 and 3.7 to give hexanal and methyl dodec-9,11-dienoate.

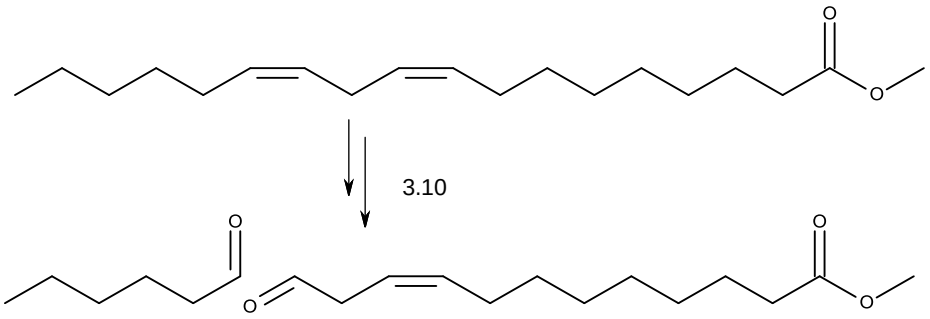

Figure 3.33 – The theoretical cleaving of the 12-13 C-C bond via reaction 3.10 to give hexanal and 12-oxo methyl dodec-9-enoate.

Whilst these three are all major products initially, they are all, for different reasons, prone to subsequent rapid decay, especially as the temperature increases. 13-oxo methyl tridec-9,11-dienoate is also a polyunsaturated molecule, and hence capable of undergoing autoxidation itself. Being an aldehyde, hexanal is subject to further oxidation to hexanoic acid. Pentane, being a volatile alkane with no functionality, most likely evaporates from the reactor to collect in the gas trap. All three exhibit the same trend of reaching a larger maximum concentration, after a longer period of time as the temperature decreases.

2-Octenal and 11-oxo methyl undec-9-enoate are the two aldehyde fragmentation products from structure B. As with hexanal, the theoretical corresponding alkene (methyl dec-9-enoate and 1-heptene respectively – see figure 3.34) products are not observed.

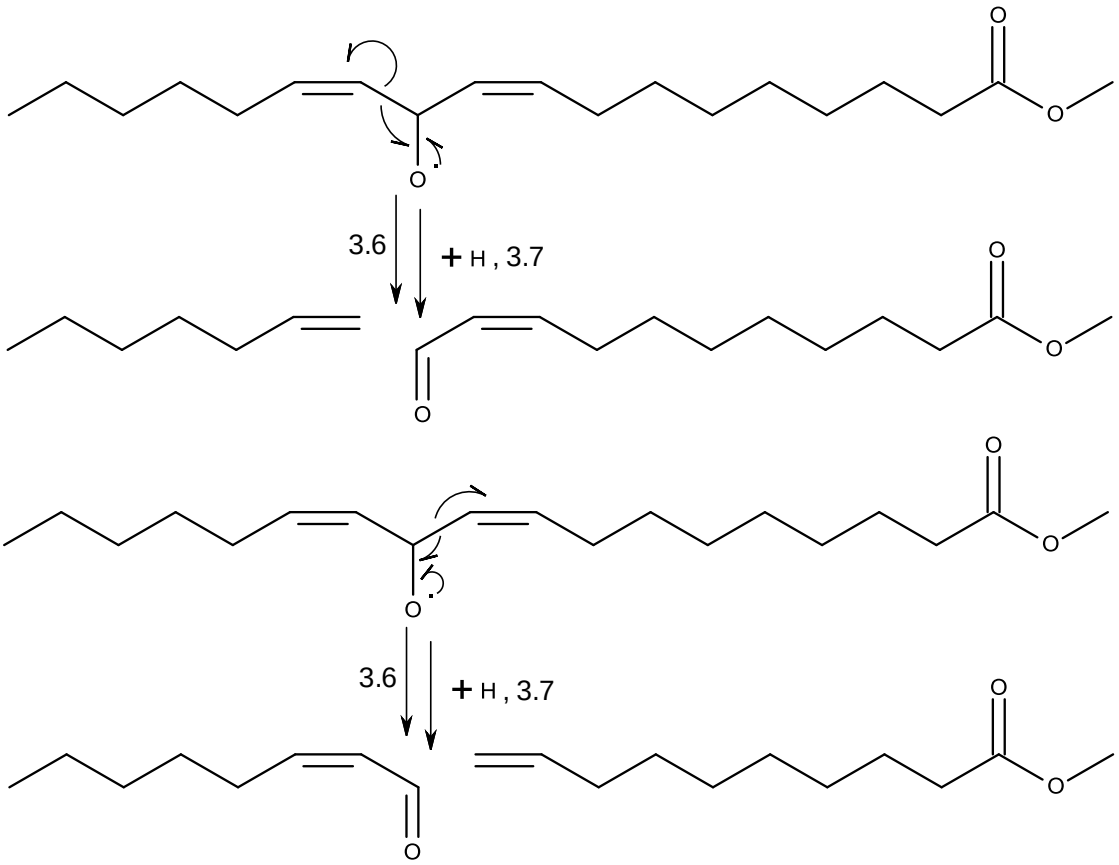

Figure 3.34 – The cleaving of the 11-12 C-C bond to give 1-heptene and 11-oxo methyl undec-9-enoate (top) and the 10-11 C-C bond to give methyl dec-9-enoate and 2-ocetenal (bottom) from structure B.

However, in this instance, as the carbonyl is conjugated with the double bond, these aldehydes could not have been formed via reaction 3.10, again suggesting that the carbon centred radicals will not proceed via reaction 3.7 if the resulting product will be a terminal alkene, instead most likely rearranging the double bonds to form a thermodynamically favoured conjugated aldehyde via reactions 3.6, 3.2, 3.3 and 3.6 to give 2-heptenal alongside 11-oxo methyl undec-9-enoate and 10-oxo methyl dec-8-enoate alongside 2-octenal (see figure 3.35) both of which were detected but as major products in comparison to 2-octenal and 11-oxo methyl undec-9-enoate. These two products can also be formed from structures E and F respectively however (Table 3.5) suggesting both routes to formation are taken. As with the products from structure A, they follow the pattern of building up to a higher maximum concentration, followed by a decay in concentration; most likely to their corresponding carboxylic acids, over a slower period of time as the temperature decreases.

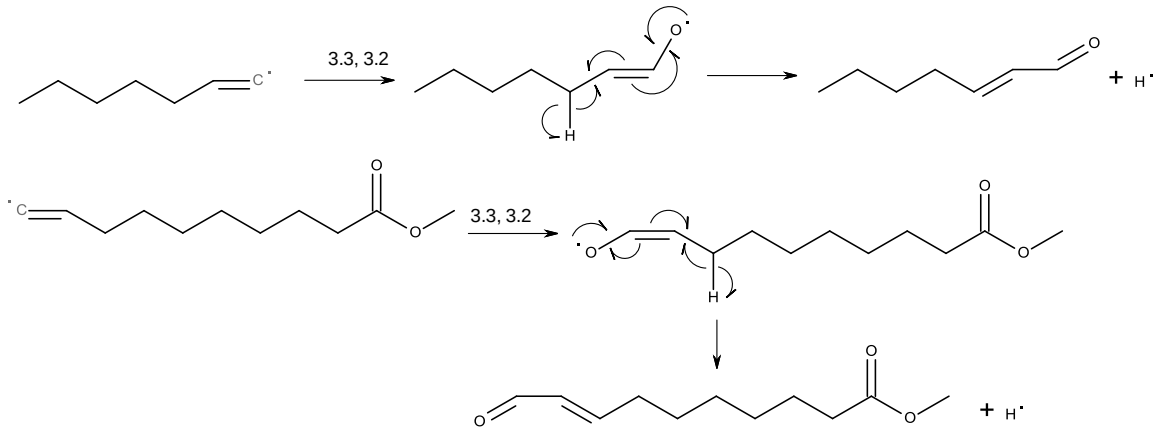

Figure 3.35 – The theoretical rearrangement of the terminal alkene radicals to form 2-heptenal and 10-oxo methyl dec-8-enoate.

Methyl octanoate and 2,4-decadienal are the two products formed from the scission of the 8-9 C-C bond (figure 3.12) on Structure C. 9-oxo methyl nonanoate can be formed from the scission of the 9-10 C-C bond, but as before, the corresponding molecule of 1,3-nonadiene is not observed. If 9-oxo methyl nonanoate is formed via Reaction 3.10, then non-3-enal would be the corresponding molecule (see figure 3.36), but this was not observed either, so it is impossible to be sure at this point what the path for its formation is.

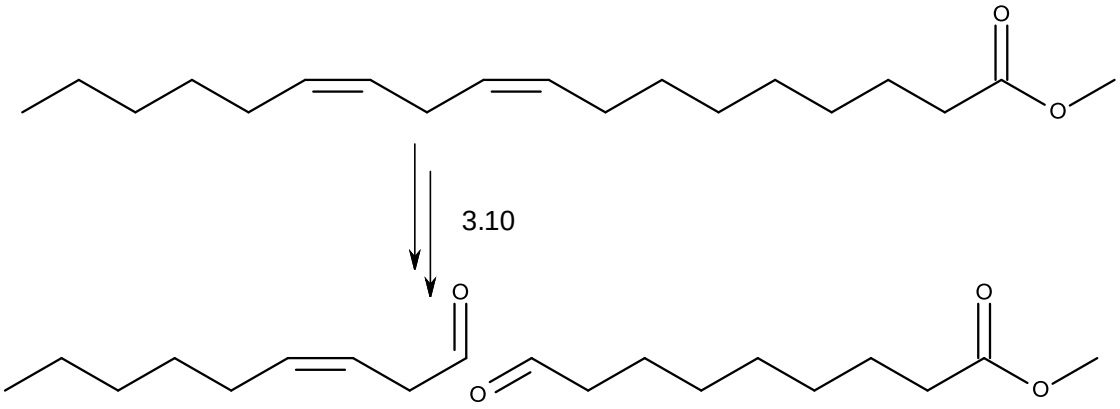

Figure 3.36 – The theoretical cleaving of the 9-10 C-C bond via reaction 3.10 to give non-3-enal and 9-oxo methyl nonanoate.

As with the products from structures A and B, all 3 follow the pattern of building up to a higher maximum concentration, followed by a decay over a slower period of time as the temperature decreases. The two aldehyde methyl esters are most likely oxidised to their corresponding acids (methyl nonandioic acid being the only acid product directly

observed) whilst 2,4-decadienal can be oxidised to 2,4-decadienoic acid, or can undergo autoxidation on either of its double bonds, hence its rapid decay rate despite it being a major initial product.

8-hydroxy methyl octanoate can be formed via the scission of the 8-9 C-C bond as well, but instead of forming the alkane, the carboxyl radical can either react with a hydroxyl radical in a termination step or react with oxygen via Reactions 3.3, 3.2 and 3.7. Its decay route is most likely oxidation to 8-oxo methyl octanoate and unlike the other observed products, whilst the temperature affects the formation and decay rates, it seems to have no effect on concentration maxima, suggesting instead that there is a threshold concentration it can reach before it gets used up; at least within the temperature ranges studied. For each of the aldehydes observed, the corresponding alcohol should theoretically be formed as well, but 8-hydroxy methyl octanoate was the only one directly observed, albeit as a relatively minor product suggesting the scission alcohol products are either produced in minor quantities or rapidly oxidised to aldehydes.

8-oxo methyl octanoate has the most formation routes of all the observed products; scission of the 8-9 C-C bond from structure G, scission of the 8-9 C-C bond from structure C, and then undergoing Reaction 3.6 or direct oxidation of 8-hydroxy methyl octanoate. Its formation and decay trends follow the same pattern of reaching a higher concentration maxima over a longer period of time at lower temperatures.

For the addition products, the alcohols and ketones are all also formed from their respective alkoxyl radicals and follow the same trends for formation and decay as the scission products with the ketones being formed when a C-H bond is cleaved rather than a C-C bond in reaction 3.6 (see figure 3.37). The alcohols can be oxidised further to the corresponding ketones, whilst both species maintain the double bonds and can therefore continue to undergo autoxidation by hydrogen abstraction of the allylic C-H bond.

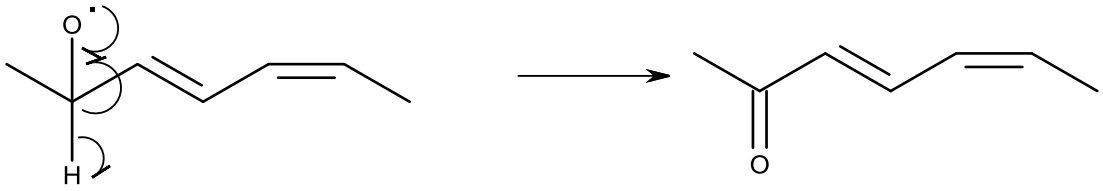

Figure 3.37 – The formation of ketones via reaction 3.6.

The dehydrodimer, unlike the other species, is not derived from an alkoxyl radical, but is instead formed via a termination reaction between two ML radicals. Nevertheless, the first step to their formation is still hydrogen abstraction. As the dimer was undetected in the flow oxidation reactions, it is impossible to examine its formation or decay patterns, though it does suggest it is short-lived which would be expected as the species would theoretically now possess a C-H bond that is not only allylic but tertiary as well (see figure 3.38).

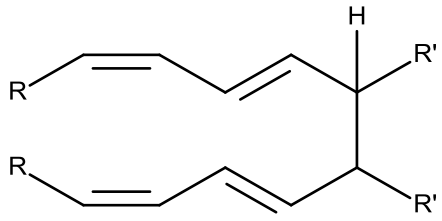

Figure 3.38 – The theoretical allylic and tertiary C-H bond of the methyl linoleate dehydrodimer; positional isomer arbitrarily assigned.

The epoxides are all formed via Reaction 3.10 over the double bonds. As there is no control over the stereochemistry of the epoxides, each double bond will form two isomers, *cis*- and *trans*-. Whilst formation and decay still happens more slowly at lower temperatures, the key difference between the epoxides and the scission products, alcohols and ketones is that the concentration maxima is higher at higher temperatures.

3.3.3 Dominant Mechanisms of Degradation

Whilst there are a variety of different products from methyl linoleate (and methyl oleate) degradation, they all come from just two main pathways. The scission products, alcohols and ketones are all formed by the initial reaction of hydrogen abstraction from an allylic, or doubly allylic C-H bond, whereas epoxides are formed over the C=C bonds. At all temperatures the epoxides were noted to be the major products, yet products from the hydroperoxide route were more numerous hence at first glance it is not straightforward to identify the dominant autoxidation mechanisms. Figure 3.39 shows the combined concentrations of all products formed by both epoxidation (C=C reaction) and hydroperoxide (C-H scission) at all temperatures. This reflects the trends seen in the graphs for the individual products; product build up followed by decay, with the hydroperoxide products increasing in maximum concentration with temperature, whilst the epoxides decrease in concentration as the temperature rises.

Figure 3.40 shows the ratio of hydroperoxide to epoxide products at all temperatures. From this graph there is a much more noticeable trend of hydroperoxide products outnumbering epoxide products as the temperature decreases suggesting a shift in preferred autoxidation mechanism with temperature, which is also consistent with the observations in the Arrhenius plot in figures 3.10 and 3.11 where there was an indication of two different reactions being represented with temperature change. From these graphs it is unclear at which point these mechanisms switch over but a rough calculation can be made by taking a line of best fit from figure 3.40 to get the intercept for at time = 0 for each temperature and plotting it against temperature, shown in figure 3.41. By performing a linear regression on the line of best fit through the data points in this graph, a rough cross-over temperature of 176.5 ± 10.2 ^{o}C can be calculated.

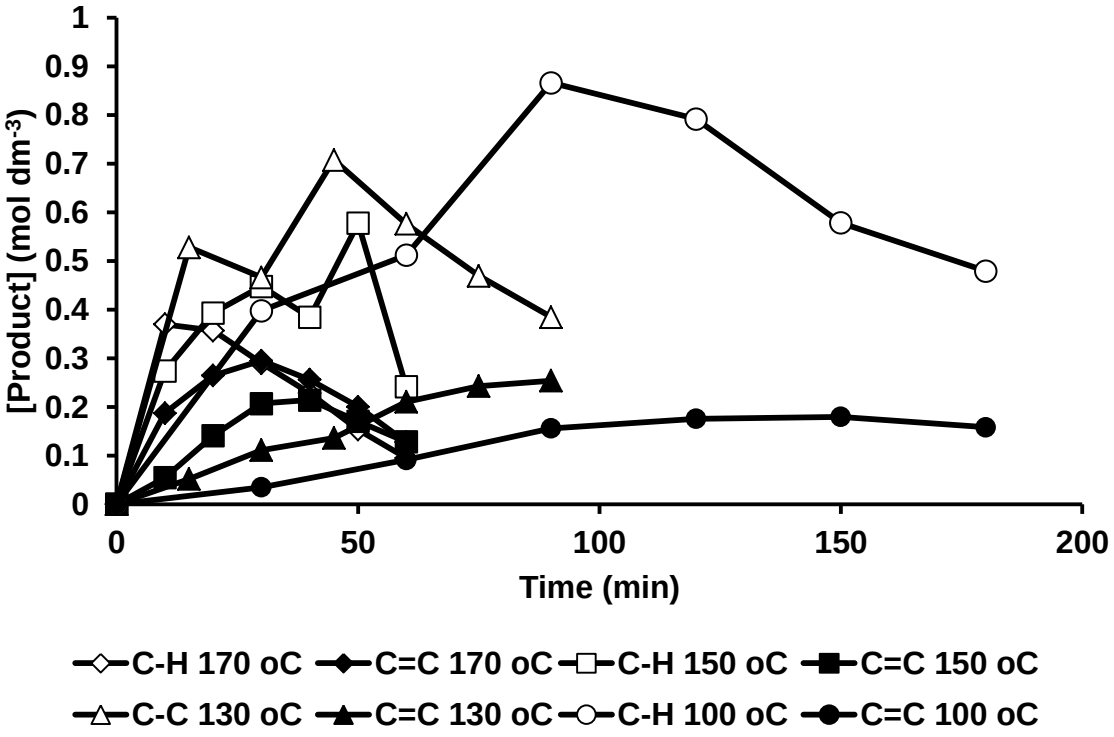

Figure 3.39 – The total concentrations of products formed by C-H and C=C bond addition at all temperatures.

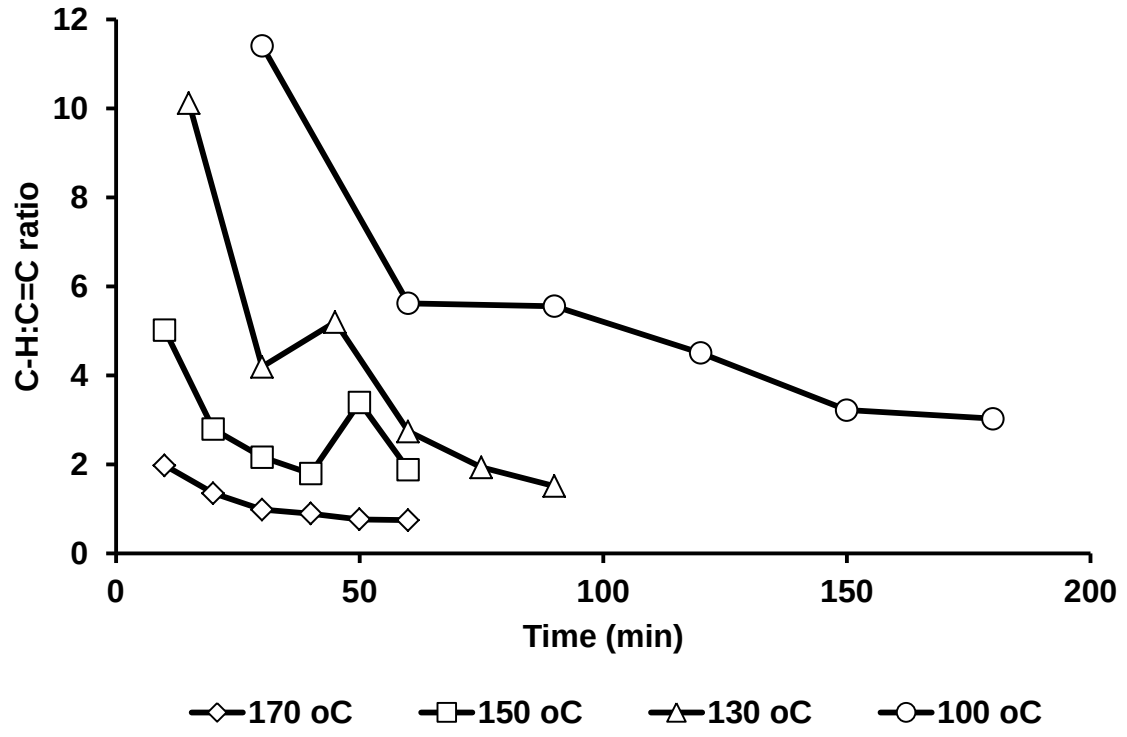

Figure 3.40 – The ratio of products formed by C-H bond scission to C=C bond addition at all temperatures.

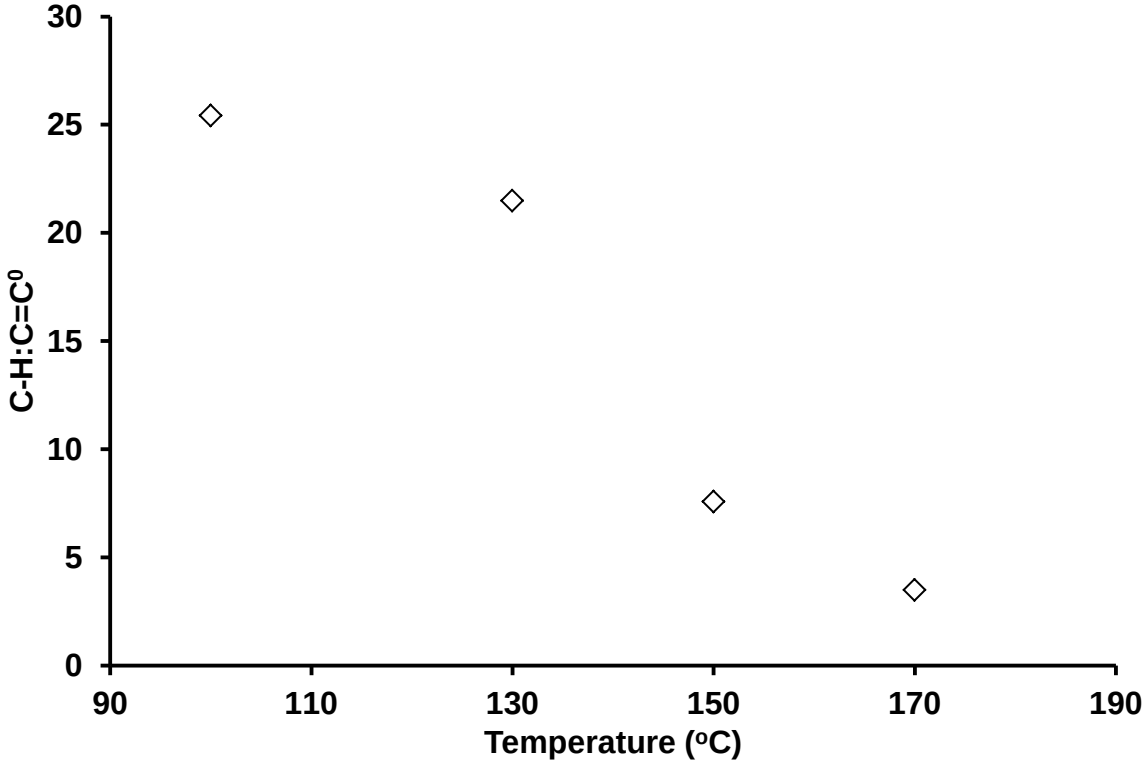

Figure 3.41 – The maximum ratio of hydroperoxide to epoxide products versus temperature.

Mechanistically, this crossover temperature represents the temperature at which the rate of RO_2• radicals reacting via hydrogen abstraction, $k_{3.4}$, (from reaction 3.4, RO_2• + RH $\rightarrow$ RO_2H + R•) is equal to the rate of those reacting by addition to the double bond, $k_{3.10}$ (from reaction 3.10, RO_2• + RC=CR $\rightarrow$ RC(O)CR + RO•) – see equation 3.1.

$$T = T_c \; when \; \frac{k_{3.4}}{k_{3.10}} = 1 \qquad \text{Equation 3.1}$$

This crossover temperature is not entirely accurate as a couple of assumptions have to be made. The main one is from the extrapolation of the lines of best fit in figure 3.40 to the start point and assuming that this represents the rate of formation of products only, i.e. no decay reactions are taking place. However even though only an approximate temperature can be calculated for the crossover of mechanism dominance, the very fact such a crossover exists is highly significant for modelling biodiesel behaviour in the engine. All the major literature on autoxidation cited in this study, from lipid degradation in the body to long term biodiesel storage, have identified hydroperoxides as the main route of degradation. However all these studies were carried out at ambient, body, or cool temperatures which are greatly exceeded in the combustion engine. At these temperatures this study shows oxygen-based radicals starting to break down unsaturated compounds via epoxidation rather than hydrogen abstraction suggesting that either $k_{3.4}$ is slowing as temperature increases, or that $k_{3.10}$ is increasing rapidly with temperature to the point where radical addition has superseded hydrogen abstraction as the main reaction route of RO_2• radicals. Either way this suggests a need to adapt the current autoxidation model of unsaturated compounds at higher temperatures to more accurately represent biodiesel behaviour in the engine.

There is a third potential mechanism for degradation of the carbon chain – addition of hydroperoxyl radicals to the C=C bond to form two aldehydes (reaction 3.10). This one is harder to quantify however as all the products identified in this study that could have been formed via this route also had the hydroperoxide route as a mechanism for formation. In addition to this many of the mirror fragmentation products observed for these products corresponded to the hydroperoxide mechanism rather than HO• addition (e.g. methyl octanoate and 2,4-decadienal from structure C); in fact, with the exception of 12-oxo methyl dodec-9-enoate for hexanal (both of which can be formed via the hydroperoxide route) none of the theoretical mirror products for HO• addition were observed. This

suggests that hydroxyl addition, if it occurs, is a very minor reaction. Identification of a molecule that could only have been formed via hydroxyl addition, e.g. non-3-enal (figure 3.36) would help to confirm and quantify this route.

Within the hydroperoxide and epoxidation mechanisms, there is also a degree of selectivity. The *trans*- epoxides were all favoured over the *cis*- epoxides at all measured temperatures, conforming to standard epoxide/alkene selection rules of *trans*- isomers being favoured due to reduced steric hindrance. Within the *cis*-/*trans*- isomers, the epoxides seemed to form on the 9-10 double bond preferentially as well; a similar trend was noted with the hydroperoxides. The main products noted in the GC spectra were the ones formed from the A and C alkoxyl radicals (the radical being on the 13- and 9-position on the carbon chain respectively) as this allowed rearrangement of the double bonds to achieve a conjugated structure. Figures 3.43 – 3.46 show the total concentration of the scission products formed via each of the different alkoxyl radicals (reproduced in figure 3.42; structures D and F are not represented as no products were detected from these).

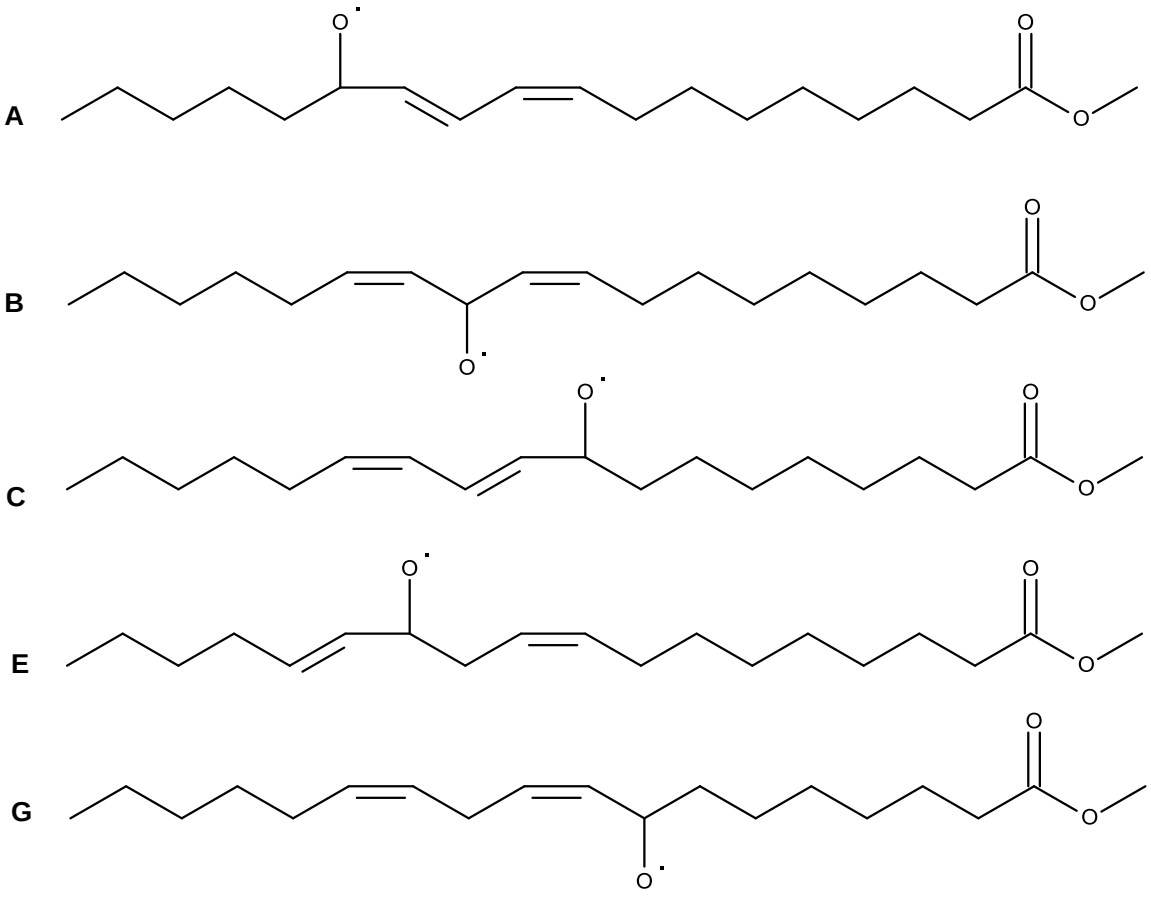

Figure 3.42 – The alkoxyl radical structures from which the observed products were formed.

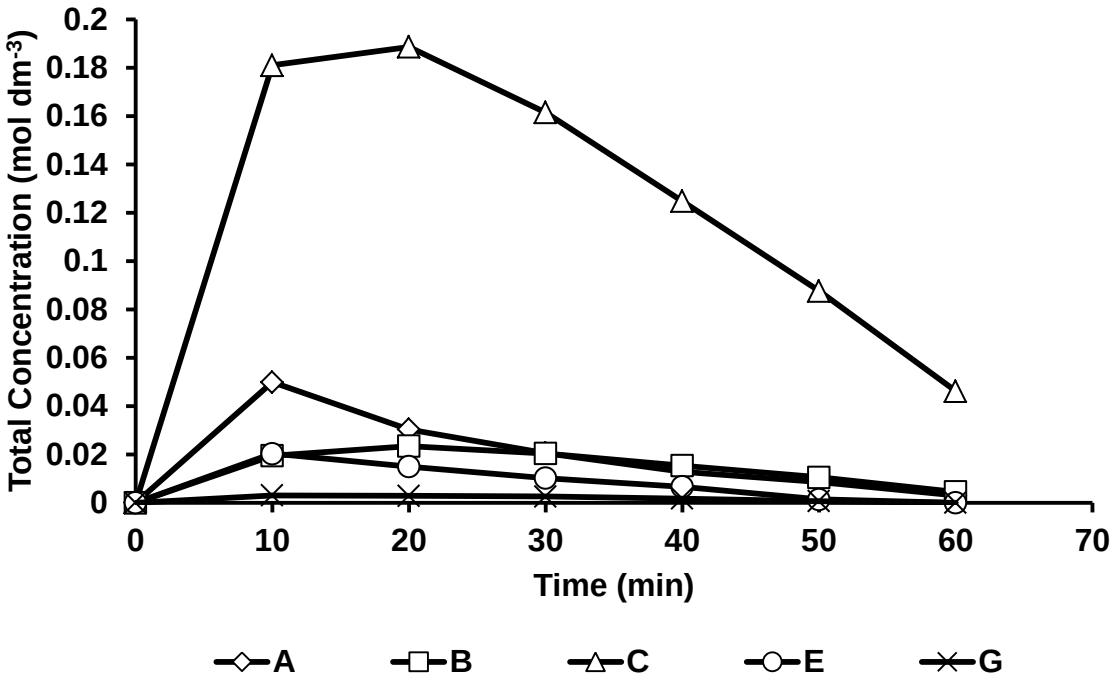

Figure 3.43 – The total concentrations on scission products formed via the different alkoxyl radicals at 170 ^{o}C.

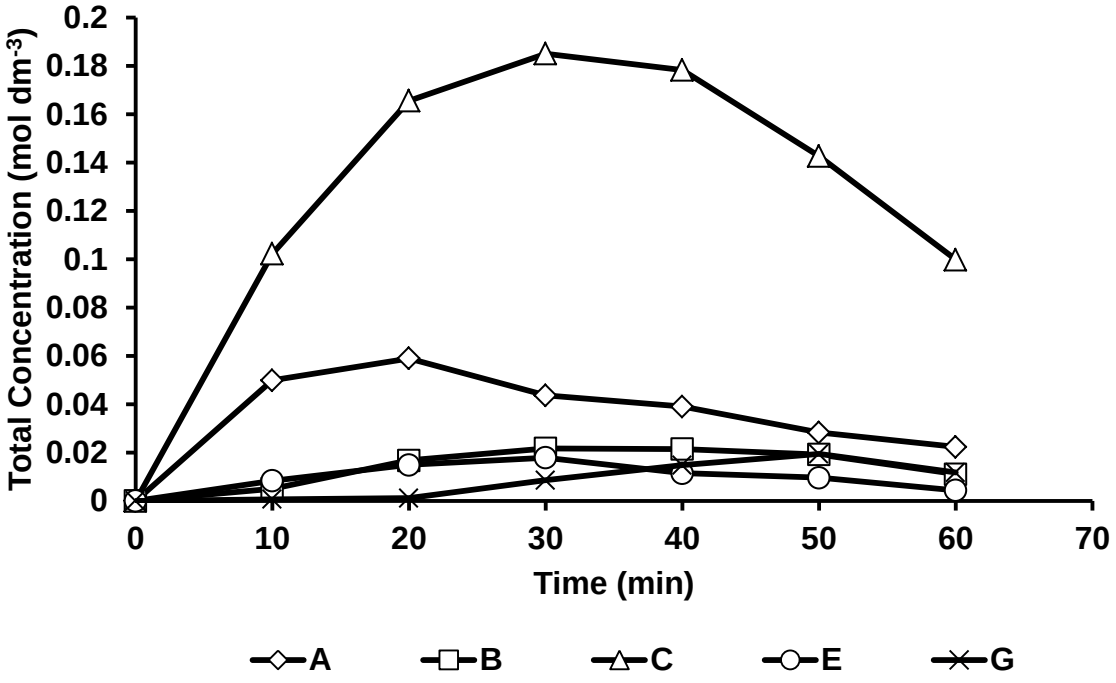

Figure 3.44 – The total concentrations on scission products formed via the different alkoxyl radicals at 150 ^{o}C.

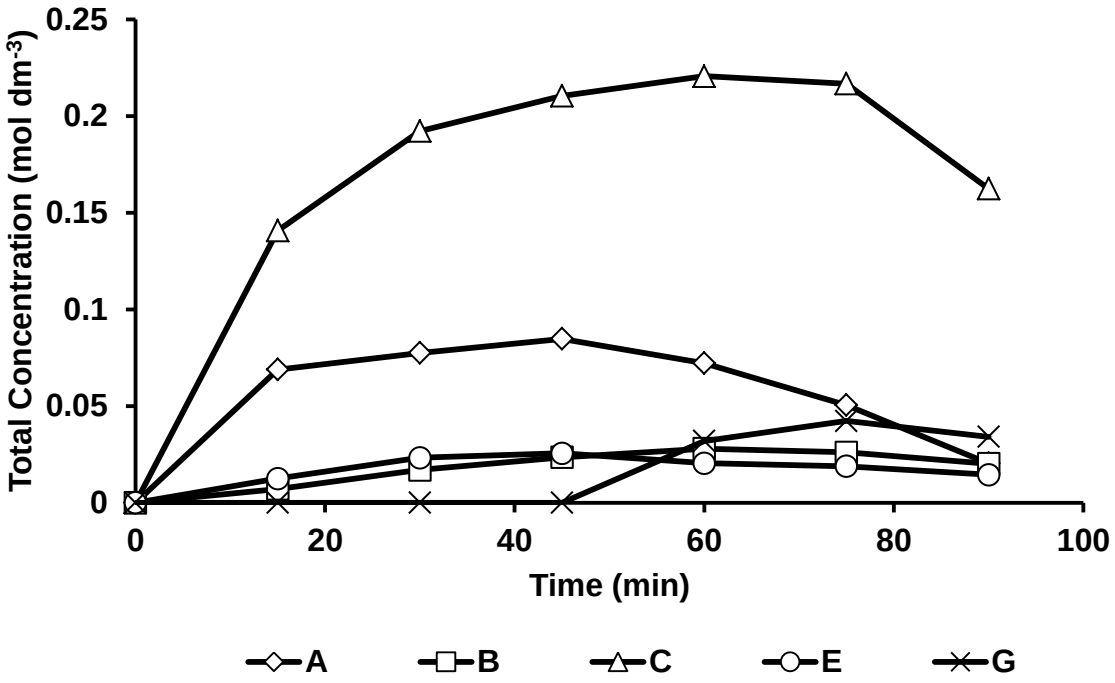

Figure 3.45 – The total concentrations on scission products formed via the different alkoxyl radicals at 130 ^{o}C.

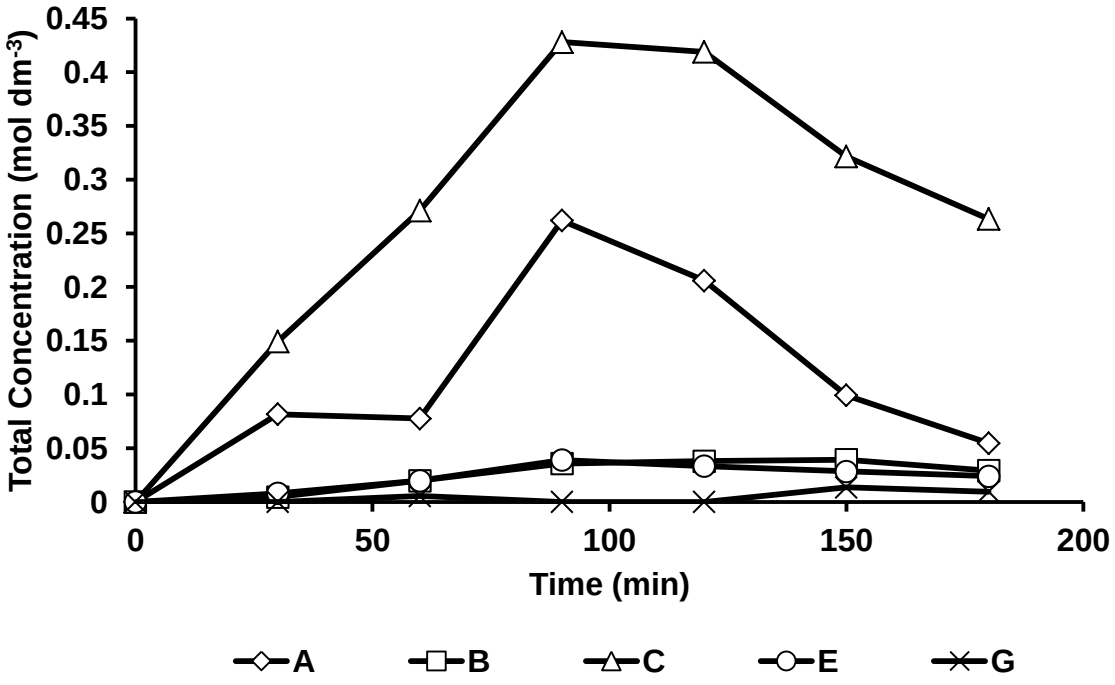

Figure 3.46 – The total concentrations on scission products formed via the different alkoxyl radicals at 100 ^{o}C.

By taking the concentration of one of the alkoxyl structures as a percentage of the total concentration and extrapolating the line of best fit (as with figure 3.40) back to the start point, a ratio of the selectivity for each of the structures can be calculated. The graphs for these are shown in figures 3.47-3.50 with the calculated data presented in table 5.4 from which it can be seen that even within the conjugated system there is a much greater selectivity for hydroperoxides and hence alkoxl radicals to form at the 9- position on the carbon chain, mirroring the trend seen with the epoxides. This can most likely be attributed to greater stabilisation of the radical in the centre of the chain from increased inductive effects of the alkyl chains.

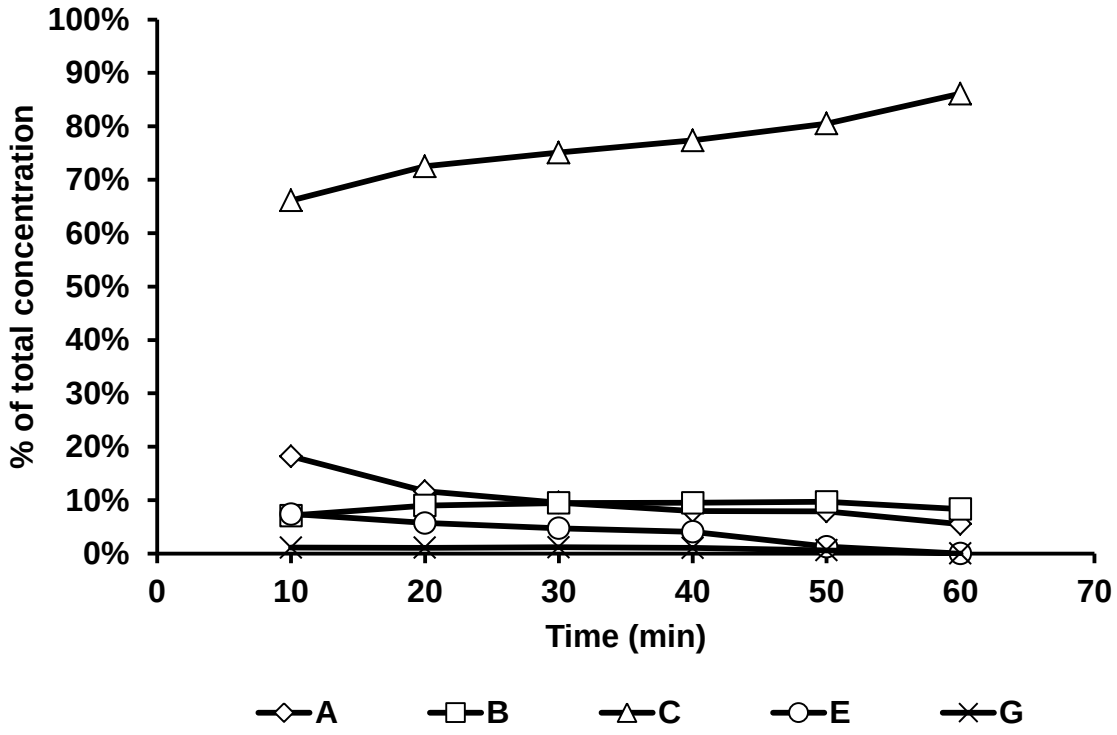

Figure 3.47 – The percentage of each alkoxyl radical structure in the overall concentration at 170 ^{o}C.

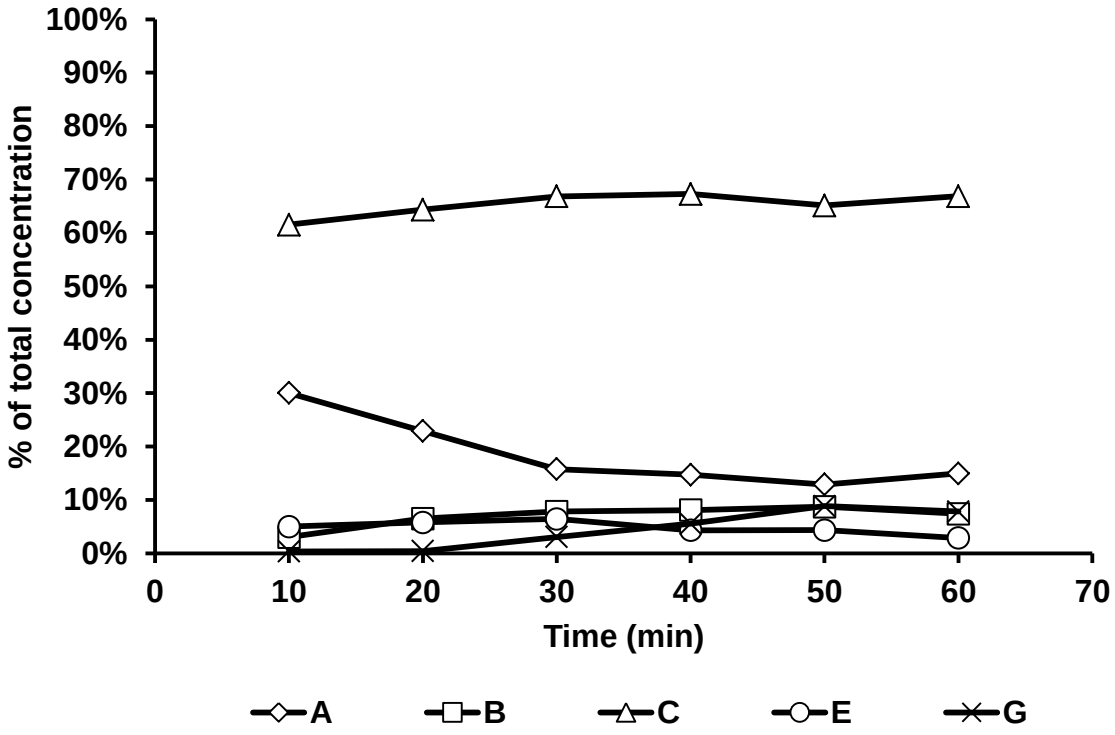

Figure 3.48 – The percentage of each alkoxyl radical structure in the overall concentration at 150 ^{o}C.

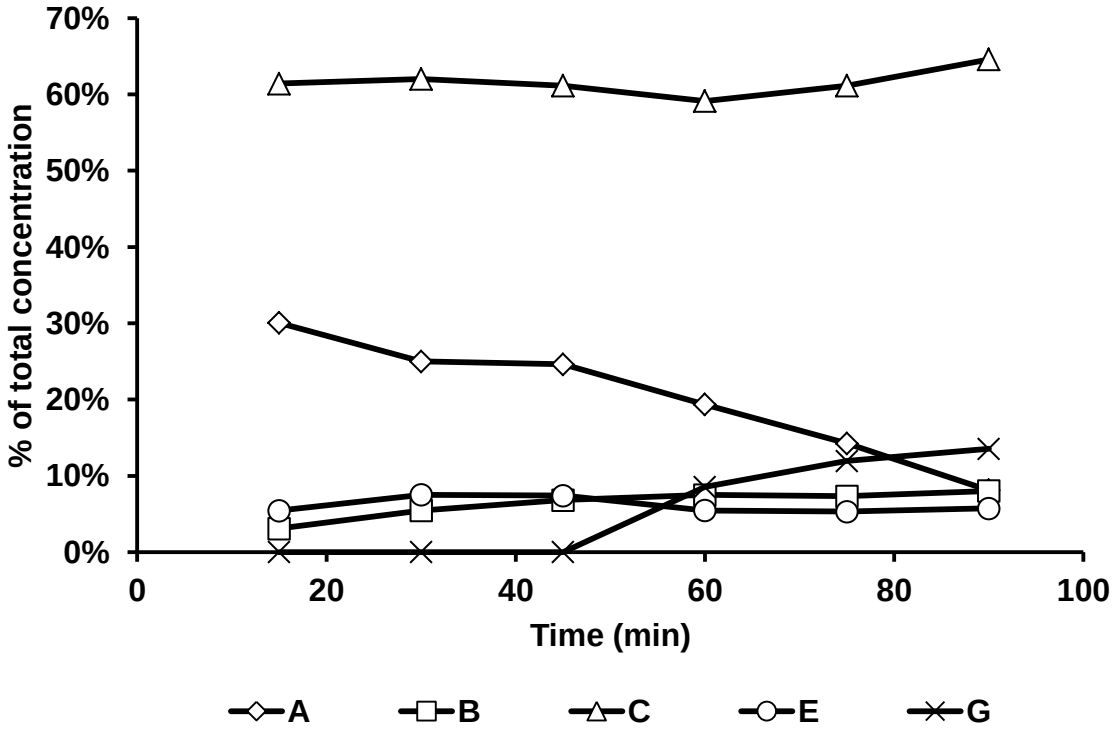

Figure 3.49 – The percentage of each alkoxyl radical structure in the overall concentration at 130 ^{o}C.

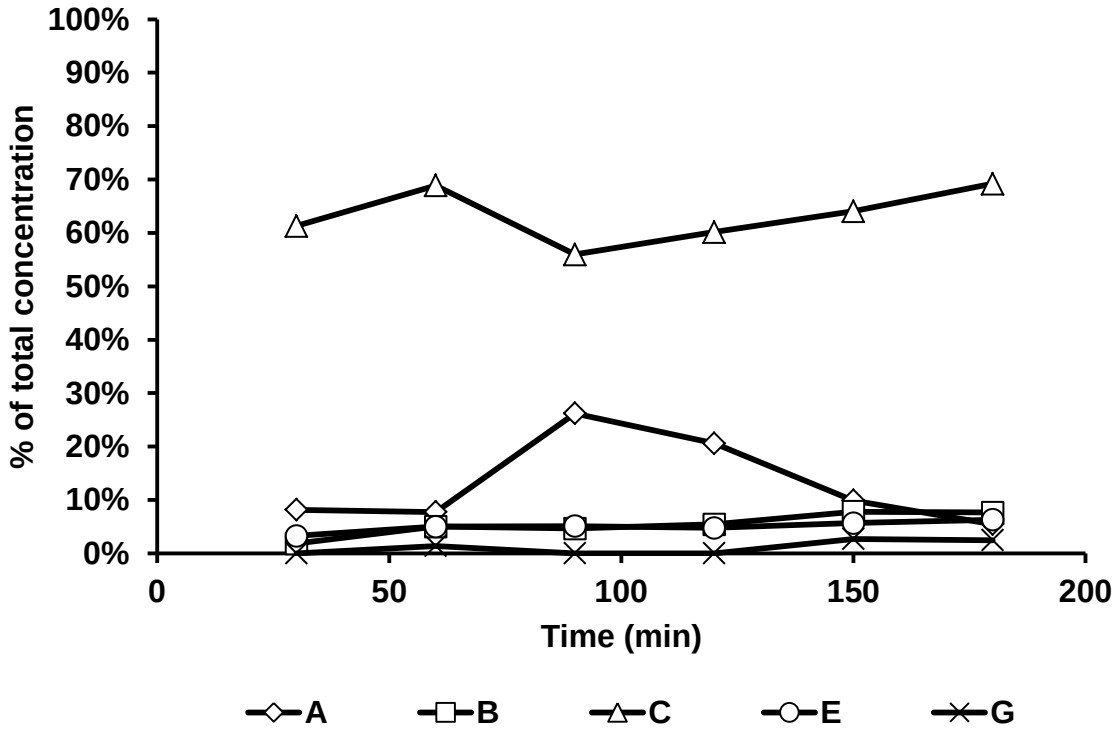

Figure 3.50 – The percentage of each alkoxyl radical structure in the overall concentration at 100 ^{o}C.

Table 3.2 – The % selectivity of each of the alkoxyl radical structures at each temperature.

	Temp (^{o}C)			
	100	130	150	170
A	14.3 ± 6.7	40.4 ± 1.6	40.3 ± 3.5	32.5 ± 1.8
B	1.6 ± 0.9	0.4 ± 0.8	4.0 ± 1.4	5.2 ± 0.9
C	69.5 ± 5.1	64.8 ± 1.7	58.4 ± 1.6	63.7 ± 1.2
E	3.4 ± 0.5	0 ± 0.5	4.2 ± 0.9	8.1 ± 0.5
G	0.5 ± 1.0	0 ± 1.0	0 ± 1.2	0.7 ± 0.3

The final products identified in this study were the dehydrodimers from ML•-ML• termination reactions. Although none of the individual isomers were identified, the confirmation of the formation of such products also has the potential to be highly significant in identifying the reasons for the detrimental effects noted in engines with biodiesel usage as if the fuel has the ability to dimerise, it most likely has the ability to polymerise further. The viscosity of molecules increases exponentially with chain length (Krisnangkura 2006) and hence polymerisation of the unburned fuel has the ability to

thicken, potentially leading to the deposits around the fuel injectors and piston assembly. As hydrogen abstraction is a necessary step for this process, this would also explain why the formation of these deposits appears to be aggravated by the use of unsaturated biodiesel – if the molecule can undergo hydrogen abstraction easier due to a weaker doubly allylic C-H bond (from resonance stabilisation), then theoretically it should be able to polymerise more easily as a result.

This study has identified the major products from the autoxidation of methyl oleate and methyl linoleate, the mechanisms responsible for autoxidation, as well as their selectivity, and identified a temperature dependent effect on the two main ones. Chapter 4 will aim to continue the chemical modelling of biodiesel by investigation its effect on the engine lubricant base fluid drawing in, and building on, the knowledge of the mechanisms identified in this chapter.

3.4 Summary

The rate of autoxidation of methyl linoleate was measured at four temperatures between 100 and 170 ^{o}C, with the breakdown products being identified via GC-MS and their concentrations measured at each temperature by GC-FID. Upon identification of the products, mechanisms for their formation were proposed based upon the known chemistry of oxygen-centred radicals and unsaturated hydrocarbon autoxidation. One of the main species commonly accepted as responsible for hydrocarbon oxidation is the peroxyl, RO_2•, radical which can attack organic compounds either by abstracting a hydrogen atom from a C-H bond, resulting in the formation of hydroperoxides on the carbon chain, or by addition to a C=C bond to form epoxides; with the literature relating to lipid, fatty acid and biodiesel chemistry all indicating the former as the major route to decomposition.

The majority of the research in the literature studied however was carried out at cool to ambient temperatures, well below those found in the engine. Upon investigating methyl linoleate autoxidation at higher temperatures, this study found that this did no longer appear to be the case. Specifically, that as the temperature increased, the ratio of products formed via radical addition to those from hydrogen abstraction was changing in favour of the addition products. By measuring these ratios at different temperature an approximate switchover temperature of 176.5 ± 10.2 ^{o}C was calculated as the temperature at which the rate of radical abstraction was equal to the rate of radical addition. Consequently this study suggests that the current model of alkene autoxidation is not valid above this temperature and hence does not accurately represent unsaturated biodiesel

behaviour in the engine and that the model needs to be altered to take into account radical addition as the new dominant degradation mechanism.

The next main finding in this study was identifying the dehydrodimer of methyl linoleate indicating the ability of the fuel to dimerise and therefore, most likely, polymerise further. The polymerisation of the fuel can likely help to account for the increased deposits found in engines fuelled with biodiesel, especially when these fuels contain multiple double bonds as these can undergo the necessary hydrogen abstraction step easier due to the weakened doubly allylic C-H bond.

The other noted observations in this work came from the selectivity of these mechanisms. The radical addition mechanism to form epoxides conformed to the standard epoxide selection rules of *trans*-epoxides being favoured over *cis*-epoxides due the reduction of steric hindrance. Both radical abstraction and radical addition seemed to favour attacking the reactive sites nearest the centre of the carbon chain, most likely due to the increased inductive stabilisation of the resulting radical coming from both sides of the carbon chain. Finally, upon fragmentation of the carbon chain it was noted that whilst C-C bond scission from autoxidation yields an aldehyde one side and an alkyl chain on the other, this did not happen if the resulting hydrocarbon product would be a terminal alkene. In these cases, the double bonds were believed to rearrange and react further with oxygen-based radicals to form a more thermodynamically favoured aldehyde product conjugated with the double bond.

3.5 References

Balat, M. Balat, H. Progress in Biodiesel Processing, *Applied Energy,* 2010, **87(6),** 1815-1835.

Blanksby, S.J. Ellison, G.B. Bond Dissociation Energies of Organic Molecules, *Acc. Chem. Res.* 2003, **36,** 255-263.

Bors, W. Erben-Russ, M. Saran, M. Fatty acid peroxyl radicals: Their generation and reactivities, *Bioelectrochemistry and Bioenergenetics,* 1987, **18**, 37-49.

Boult, P.J. Fisher, Q.J. Clinch, S.R. Lovibond, J R. Cockshell, C.C. Geomechanical, microstructural, and petrophysical evolution in experimentally reactivated cataclasites: Discussion, *AAPG Bulletin*. 2003, **87**, 1681-1683.

Bush, G.P. Fox, M.F. Picken, D.J. Butcher, L.F. Composition of Lubricating Oil in the Upper Ring Zone of an Internal Combustion Engine, *Tribology International,* 1991, **24(4),** 231-233.

Clark, K.B. Culshaw, P.N. Griller, D. Lossing, F.P. Martinho Simões, J.A. Walton, J.C. Studies of the Formation and Stability of Pentadienyl and 3-Substituted Pentadienyl Radicals, *J. Org. Chem.* 1991, **56,** 5535-5539.

Chan, H.W.S. Levett, G. Matthew, J.A. The Mechanism of the Rearrangement of Linoleate Hydroperoxides. *Chemistry and Physics of Lipids,* 1979, **24**, 245-256.

Demirbas, A. Progress and recent trends in biodiesel fuels. *Energy Conversion and Management*, 2009**, 50**, 14-34.

Department for Transport – Towards a UK Strategy for Biofuels – Public Consultation 2005, 2-4, www.dft.gov.uk/consultations/archive/2004/tuksb/, Archived 02/09/2009, 27/4/2011

Du Plessis, L.M. De Villiers, K.B.M. Van Der Walt, W.H. Stability studies on methyl and ethyl fatty acid esters of sunflowerseed oil**,** *JAOCS.* 1985, **62(4)**, 748-752.

Dvorák, R. Frantisek, F. Komers, K. Transesterification of rapeseed oil in a feedback reactor, *Eur. J. Lipid Sci. Technol,* 2001, **103**, 742–745.

Filipova, T.V. Blyumberg, E.A. Mechanism of the Epoxidation of Alkenes by Molecular Oxygen, *Russian Chemical Reviews,* 1982, **51(6)**, 582-591.

Farmer, E.H. Koch, H.P. Sutton, D.A. The Course of Autoxidation Reactions in Polyisoprenes and Allied Compounds. Part VII. Rearrangement of Double Bonds during Autoxidation, *J. Chem. Soc.* 1943, 541-547.

Frankel, E.N. Garwood, R.F. Khambay, B.P.S. Moss, G.P. Weedon, B.C.L. Stereochemistry of Olefin and Fatty Acid Oxidation. Part 3. The Allylic Hydroperoxides from the Autoxidation of Methyl Oleate, *J. Chem. Soc. Perkin Transactions 1*, 1984, 2233-2240.

Frankel, E.N. Chemistry of Free Radical and Singlet Oxidation of Lipids. *Prog. Lipid Res.* 1985, **23**, 197-221.

Gamble, R.J. Priest, M. Taylor, C.M. Detailed Analysis of Oil Transport in the Piston Assembly of a Gasoline Engine, *Tribology Letters,* 2003, **14(2),** 147-156.

Giuffrida, F. Destaillats, F. Robert, F. Skibsted, L.H. Dionisi, F. Formation and Hydrolysis of Triacylglycerol and Sterol Epoxides: Role of Unsaturated Triacylglycerol Peroxyl Radicals, *Free Radical Biology & Medicine.* 2004, **37(1)**, 104-114.

Goering, C.E. Schwab, A.W. Dangherty, M.J. Pryde, E.H. Heakin, A.J. Fuel Properties of Eleven Vegetable Oils, *ASAE* 1982**, 25(6)**, 1472-1477.

Golden, D.M. Benson, S.W. *Chem.Rev* 1969, **69**,125.

Gómez-Carracedo, M.P. Andrade, J.M. Calviño M., Fernández, E. Prada, D. Muniategui, S. Multivariate prediction of eight kerosene properties employing vapour-phase mid-infrared spectrometry, *Fuel*, 2003, **82**, 1211-1218.

Hamberg, M. Gotthammer, B. A New Reaction of Unsaturated Fatty Acid Hydroperoxides: Formation of 1 1-Hydroxy-12,13-epoxy-9-octadecenoic Acid from 13-Hydroperoxy-9,11 -octadecadienoic Acid, *Lipids*, 1973, **8(12)**, 737-744.

Hiroyasu, H. Kadota, T. Models for Combustion and Formation of Nitric Oxide and Soot in Direct Injection Diesel Engines, *Soc. Automotive Eng. Paper No. 760129*, 1976.

Hirsch, R.L. Bezdek, R. Wendling, R. Peaking of World Oil Production: Impacts, Mitigation and Risk Management, 2005, 11-20, www.netl.doe.gov

Kim, J.S. Min, B.S. Lee, D.S. Oh, D.Y. Choi, J.K. Characteristics of Carbon Deposit Formation in Piston Top Ring Groove of Gasoline and Diesel Engine, *1998 SAE International Congress & Exposition; Detroit, MI, USA*, 1998, 147-154.

Korchek, S. Chenier, J.H.B. Howard, J.A. Ingold, K.U. Absolute rate constants for hydrocarbon autoxidation. XXI. Activation energies for propagation and the correlation of propogation rate constant with carbon–hydrogen bond strengths, *Can. J. Chem*, 1972, **50**, 2285–2297.

Knothe, G. "Designer" Biodiesels: Optimizing Fatty Acid Ester Composition to Improve Fuel Properties, *Energy and Fuels*, 2008, **22**, 1358-1364.

Krisnangkura, K. Yimsuwan, T. Pairintra, R. An Empircal Approach in Predicting Biodiesel Viscosity at Various Temperatures, *Fuel*, 2006, **85,** 107-113.

Labeckas, G. Slavinskas, S. Performance of direct-injection off-road diesel engine on rapeseed oil, *Renewable Energy*, 2006, **31**, 849-863.

Lercker, G. Rodriguez-Estrada, T.M. Bonoli M., Analysis of the oxidation products of cis- and trans-octadecenoate methyl esters by capillary gas chromatography–ion-trap mass spectrometry I. Epoxide and dimeric compounds, *Journal of Chromatography*, 2003, **985**, 333-342.

Lightfoot, P.D. Cox, R.A. Crowley, J.N. Destriau, M.Hayman, G.D. Jenkin, M.E. Moortgat, G.K. Zabel, F. Organic Peroxy Radicals: Kinetics, Spectroscopy and Tropospheric Chemistry, *Atmospheric Environment*, 1992, **26A(10),** 1805-961.

Ma, F. Hanna, M.A. Biodiesel Production: A Review, *Bioresource Technology*, 1999, **70,** 1-15.

McMillen, D.F. Golden, D.M. Hydrocarbon Bond Dissociation Energies, *Ann. Rev. Phys. Chem*, 1982, **33,** 493-532.

Monyem, A. Canakci, M. Van Gerpen, J.H. Investigation of Biodiesel Thermal Stability Under Simulated In-Use Conditions, *Applied Engineering in Agriculture,* 2000, **16(4)**, 373-378.

Moritani, H. Nozawa, Y. Oil Degradation in Second-Land Region of Gasoline Engine Pistons. *R&D Review of Toyota CRDL,* 2004, **38(3)**, 36-43.

Pratt, D.A. Mills, J.H. Porter, N.A. Theoretical Calculations of Carbon-Oxygen Bond Dissociation Enthalpies of Peroxyl Radicals Formed in the Autoxidation of Lipids, *J. Am. Chem. Soc.* 2003, **125**, 5801-5810.

Rakopoulos, C.D. Antonopoulos, K.A. Rakopoulos, D.C. Hountalas, D.T. Giakoumis, E.G. Comparative performance and emissions study of a direct injection Diesel engine using blends of Diesel fuel with vegetable oils or bio-diesels of various origins, *Energy Conversion and Management,* 2006, **47**, 3272-3287.

Ross, J.R. Gebhart, A.I. Gerecht, J.F. The Autoxidation of Methyl Oleate, *J. Am. Chem. Soc.* 1949, **71**, 282-286.

Sapaun, S.M. Masjuki, H.H. Azlan, A. The Use of Palm Oil as Diesel Fuel Substitute. *J. Power Energy A.* 1996, **210**, 47–53.

Shahid, E.M. Jamal, Y. A Review of Biodiesel as a Vehicular Fuel, *Renewable and Sustainable Energy Review,* 2008, **12(9),** 2484-2494.

Sonawane, H.R. Nanjundiah, B.S. Kelkar, R.G. Light-Mediated Transformations of Olefins into Alcohols: Reactions of Hydroxyl Radicals With Cycloalkenes, *Tetrahedron,* 1986, **42(24)**, 6673-6682

Srivastava, A. Prasad, R. Triglycerides-based Diesel Fuels, *Renew. Sustain. Energy Rev.* 2000, **4**, 111-133

Taylor, R.I. Evans, P.G. *In-situ* Piston Measurements, *Proc. Instn. Mech. Engrs.* 2004, **218**(J: J. Engineering Tribology), 185-200.

Tormos, B. Novella, R. García, A. Gargar, K. Comprehensive Study of Biodiesel Fuel for HSDI Engines in Convencional and Low Temperature Combustion Conditions, *Renweable Energy,* 2010, **35,** 368-378.

Trenwith, A.B. Dissociation of 3-methyl-1,4-pentadiene and the Resonance Energy of the Pentadienyl Radical *J. Chem. Soc. Faraday Trans. 1*, Physical Chemistry in Condensed Phases, 1982, **78(10),** 3131-3136.

U.S Department of Energy report **2011** http://tonto.eia.doe.gov/oog/info/twip/twip.asp 27/04/2011

Yizhe, L. Guirong, B. Hua, W. Determination of 11 fatty acids and fatty acid methyl esters in biodiesel using ultra performance liquid chromatography, *Chinese Journal of Chromatography,* 2008, **26(4)**, 494-498.

Yuan, W. Hansen, A.C. Zhang, Q. Vapour Pressure and Normal Boiling Point Predictions for Pure Methyl Esters and Biodiesel Fuels, *Fuel,* 2005, **84,** 943-950.

Zhang, Q. Feldman, M. Peterson, C.L. Diesel engine durability when fuelled with methyl ester of winter rapeseed oil. *ASAE Paper No. 88: 1562.* 1988

Chapter 4. The Effect of Methyl Linoleate and Oleate on Squalane Oxidation

4.1 Introduction

The effect of biodiesel on engine lubricants has been studied since their planned entry into the market in the 1980's. Early tests on sunflower and cottonseed oils (Engler 1983) indicated that even when they were put through purification processes such as degumming and dewaxing, the resultant degree of fouling of the lubricating oil through fuel dilution (as described in Introduction) as a result of their usage over a 40 hour test run rendered them useful only on a short-term basis.

A study by Ryan et al (1984) however, showed that this lubricant contamination issue only seemed to be significant in engines utilising direct-injection (where a dosage of fuel is pumped into the combustion chamber) methods – for indirect injection engines (where the fuel is 'drawn' into the chamber via the pressure gradient caused by the piston movement), test run results with refined vegetable oils were largely comparable to those with mineral diesel. It was noted, however that these tests were run only over a matter of days; far below the average working time of an engine and that greater differences may be observed on longer-term trials. It was also noted that injector coking and lubricant oil contamination in direct-injection engines was aggravated by the use of unsaturated vegetable oils and therefore such fuels would have to be modified in order to allow for sufficient working of the engine. From this, it was proposed that two sets of fuel specification were necessary – one for direct- and one for indirect- injection engines; a proposal that has since been rendered obsolete by the European particulate emission legislation (EC Regulation No. 595/2009) which will require the mandatory introduction of direct-injection engines in order to facilitate the use of Diesel Particulate Filters (DPFs). DPFs are devices fitted to the exhaust system of an engine to reduce Particulate Matter (PM) emissions – of particular concern due to their impacts on the environment and human health (Kittelson 1998) – by trapping them via filtration, usually with the aid of catalytic adsorbants, only allowing exhaust gas molecules to pass through and be released to the atmosphere (van Setten 2001, Yang 2008). They are being introduced as a necessary measure to reduce engine PM emissions but must be cleaned to prevent excess soot clogging the filter. This is where DI engines are utilised, as the excess fuel that is injected

can be used to burn off residual soot gathered on the filter (Conrad 2006). The problem with utilising this method is that this excess fuel can end up in the sump, contributing to fuel dilution. Unfortunately, at present, there is no other more efficient way of reducing PM emissions or cleaning the DPF reported.

Whilst the physical properties of vegetable oils were improved upon transesterification to produce Fatty Acid Methyl Esters, FAME, the levels of unsaturation within the fatty acid chains were still shown to prove problematic with regards to lubricant contamination and oxidation compared to saturated FAME and mineral diesel (Sapaun 1996, Sumathi 2008), again, these effects appeared to be more problematic in DI engines (Radu 2009). Monyem (2000) took biodiesel from soya (Soybean Methyl Ester – SME), currently the most common form of biodiesel in the USA (Van Wechel 2002) – and consisting of over 50% doubly unsaturated FAME (see Chapter 1, Section 3) – and investigated its properties under simulated engine conditions. Among the findings was a large increase in kinematic viscosity of the fuel and the lubricant over time when using neat biodiesel compared to diesel and blends of the two. Viscosity of the lubrication systems is crucial to the smooth running of the engine; too low and the oil film will become too thin to provide sufficient protection between the colliding surfaces to overcome friction and prevent excessive wear and temperature increase, too high and the moving parts cannot slide along as effectively, reducing the efficiency of the engine, hence requiring more fuel and increasing carbon dioxide emissions per mile/km. Any contamination of the lubricant by the fuel must therefore have minimal effect on the viscosity, yet biodiesel's lubrication properties have been reported as worse compared to mineral diesel (Hu 2005, Dermibas 2009). Masjuki (1996) noted that adverse wear conditions could be prevented only if levels of biodiesel in the lubricant were kept below 5%; Fazal (2011) attributed these findings to higher corrosion properties of oxidised biodiesel.

Agarwal (2007) documented the use of biodiesel in engines, including the effect on engine lubricant through FTIR studies, tribology and viscosity measurements. FTIR results showed increased amounts of oxidised base fluid in biodiesel fuelled engines, corresponding with increased viscosity after use and hence it was suggested that this could be due to biodiesel increasing the rate of base oil oxidation once they were mixed.

With all the work done on the effects of biodiesel on engine lubricants, it is quite surprising, particularly given the research on the chemistry of fats, lipids and subsequently FAME, that very little work has been done on the chemistry of how biodiesel and

lubricants physically and, crucially, chemically interact with one another. The aim of this section is to present the work done for this project using methyl linoleate and methyl oleate (as biodiesel analogues) on squalane (a lubricant base fluid analogue) and to draw in knowledge of the methyl linoleate and methyl oleate chemistry (Chapter 3) to try and identify (among others) the causes of viscosity increase, sediment formation and piston deposits. Methyl linoleate is the main focus of the research as the doubly unsaturated system is the suspected cause of reactivity.

4.2 Results

4.2.1 Rate of Squalane Decay

In the previous chapter methyl oleate and linoleate were used to chemically model biodiesel behaviour. In order to model the effect on engine lubricants, it was necessary to find a chemical model for the lubricant base fluid. Squalane was used to achieve this as it is readily available and has properties such as chain length, degree of branching and viscosity comparable to engine lubricants (Kaiser 1981) – it has been used in several other studies on engine lubricants (Adamczyk 1984, Gupta 1997, Jabbarzadeh 2002, Stark 2011 – see chapter 1, section 4) – but crucially for this work, it elutes as a single peak in GC work, meaning its rate of decay is easily monitored. Figure 4.1 shows, for example, the decrease in the concentration of squalane (within the ±5.7% error margin of the GC for squalane) over time reacting with a flow of 1 bar of oxygen at 170 ^{o}C.

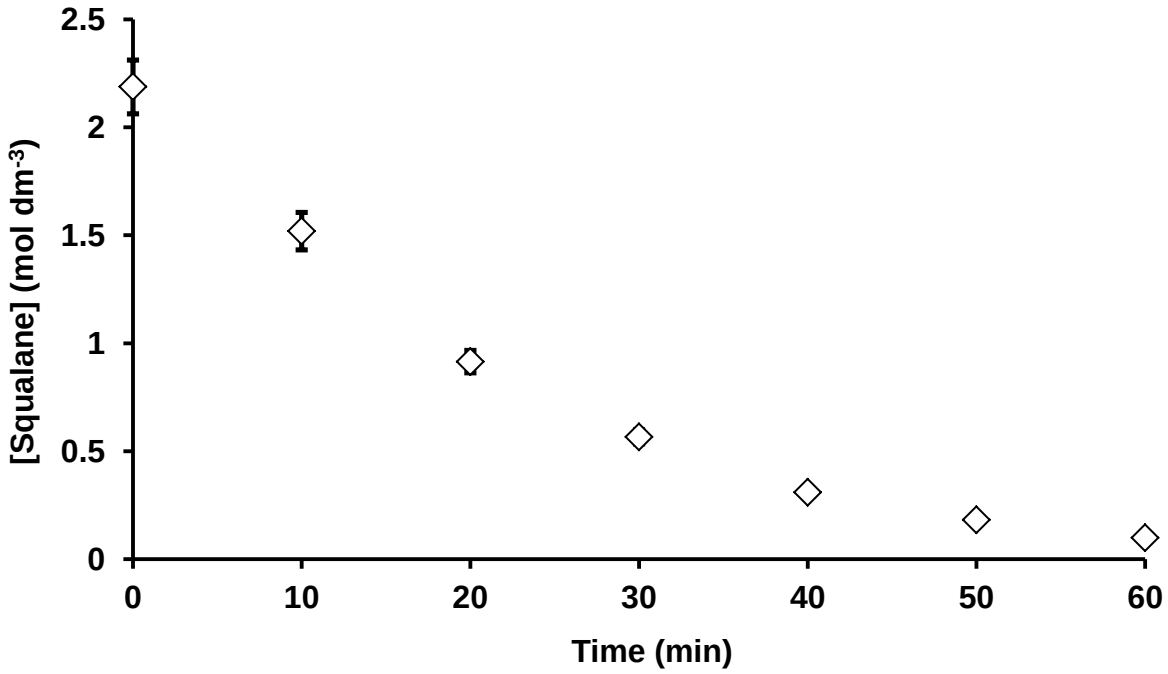

Figure 4.1 – The decay of squalane over time at 170 ^{o}C with a 0.08 dm^{3} min^{-1} flow of oxygen.

Taking the natural logarithms of the concentration of squalane over time in the oxidation reactions yielded a straight-line plot indicating that, as with methyl linoleate oxidation in chapter 3, the reaction is approximately first order with respect to squalane. Figure 4.2 shows the example for 170 ^{o}C.

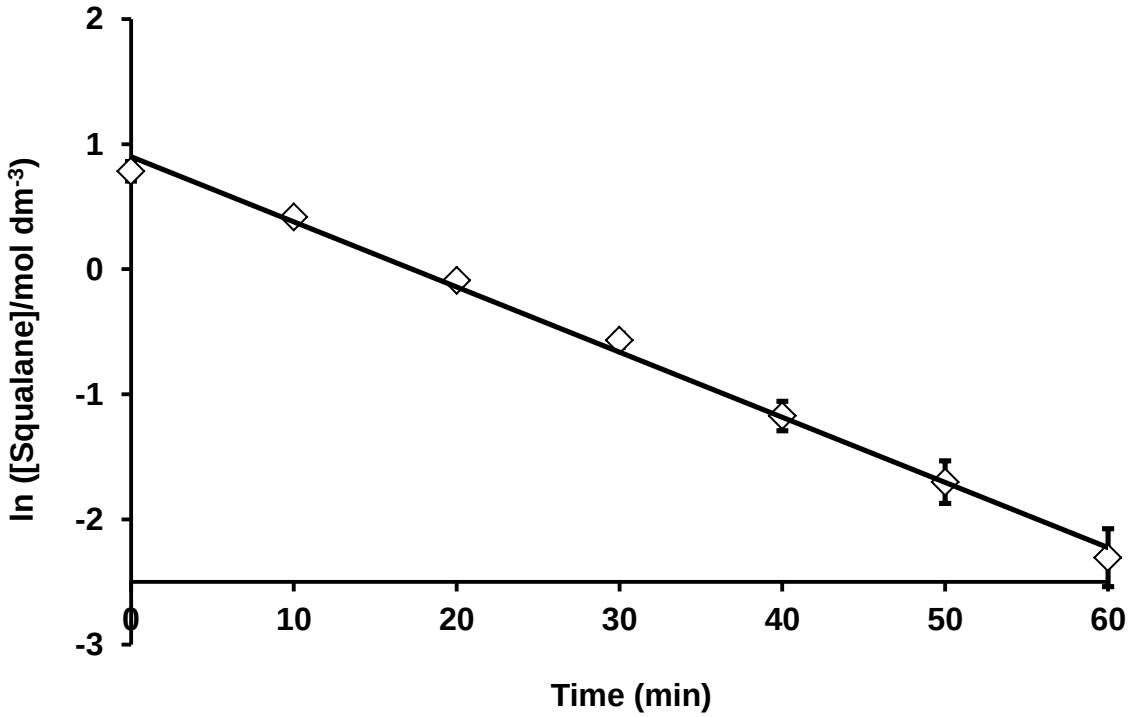

Figure 4.2 – The logarithmic decay of squalane over time at 170 ^{o}C with a 0.08 dm^{3} min^{-1} flow of oxygen.

As the reaction can be assumed to be pseudo 1st order with respect to squalane, it can be represented by Equation 4.1, where $k_{squalane}$ is given by the gradient of the line:

$$\frac{d[Squalane]}{dt} \approx -k_{squalane}[Squalane] \qquad \text{Equation 4.1}$$

This experiment was also repeated at 100, 130, 150 and 160 ^{o}C to give the $k_{squalane}$ value for squalane (see figure 4.3) over a range of temperatures.

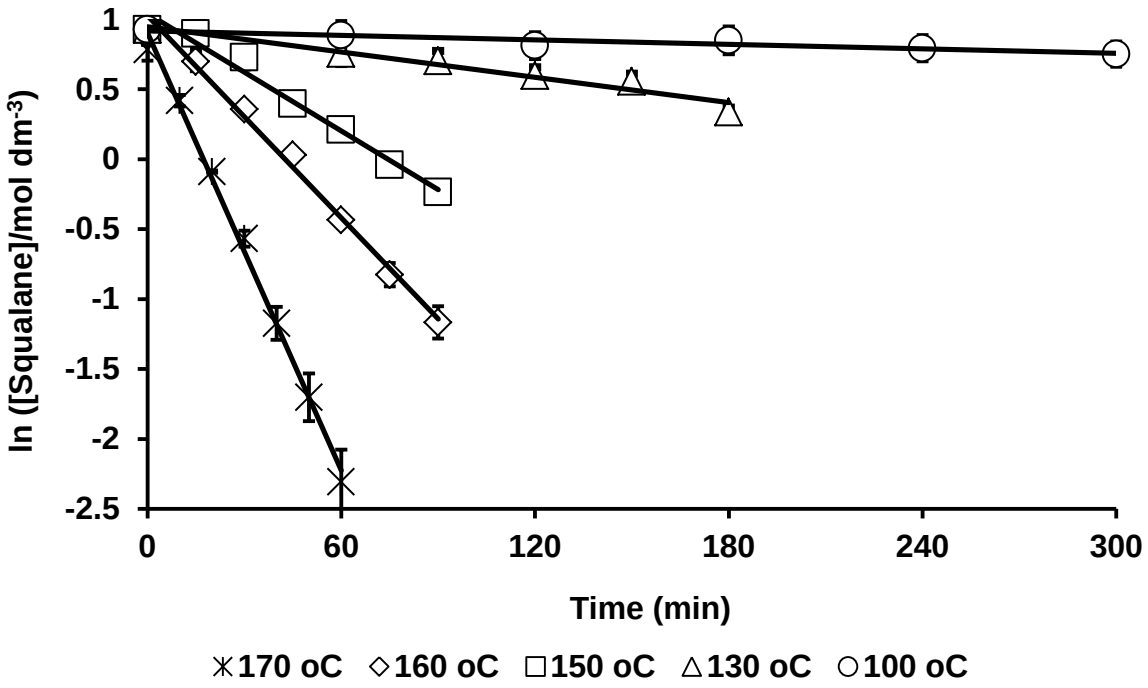

Figure 4.3 – The logarithmic decay of squalane over time between 100 – 170 ^{o}C with a 0.08 dm^{3} min^{-1} flow of oxygen.

The gradients from figure 4.3 are shown in Table 4.1 and figure 4.4 for comparison.

Table 4.1 – The pseudo-first order rate of decay of squalane oxidation between 100 – 170 ^{o}C under a 0.08dm^{3} min^{-1} flow of oxygen.

Temperature (^{o}C)	100	130	150	160	170
$k_{squalane}$ (h^{-1})	0.031±0.008	0.18±0.02	0.84±0.06	1.44±0.05	3.13±0.50

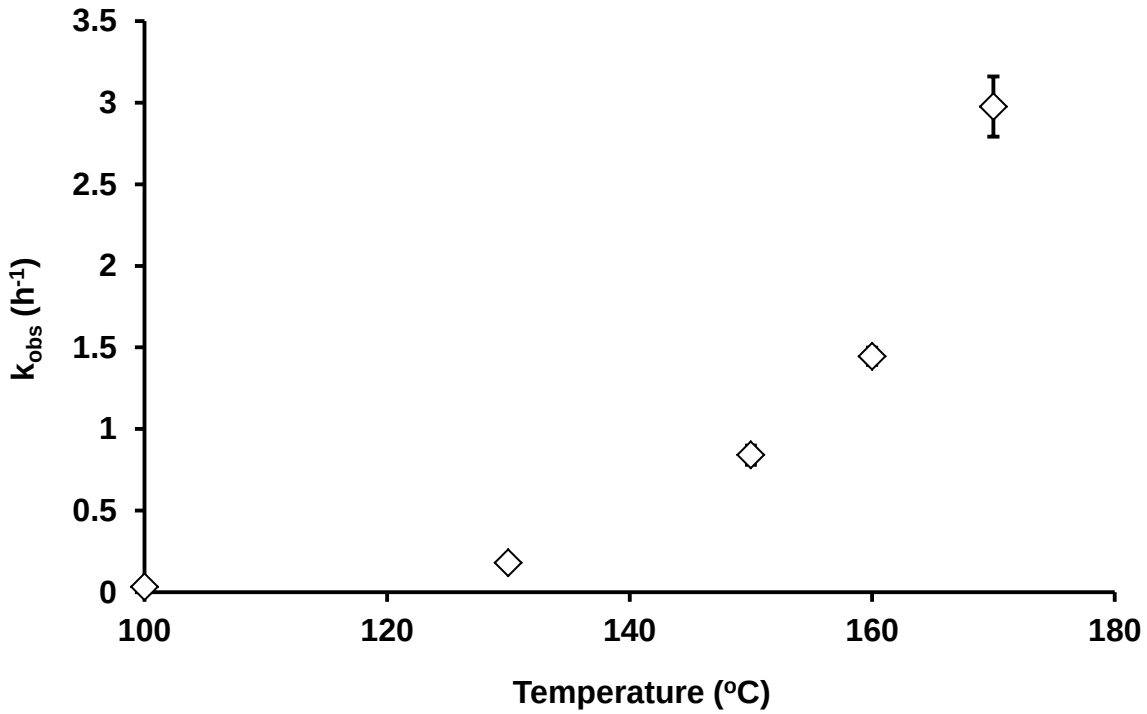

Figure 4.4 – The $k_{squalane}$ for squalane oxidation reaction versus temperature.

An Arrhenius plot yielded a relatively straight line graph (see figure 4.5) with only the value for 100 ^{o}C (0.0026 K^{-1}) looking as though it may be slightly off the axis even with larger error bars, perhaps indicating a mechanism shift as noted for methyl linoleate in chapter 3. Assuming the value for 100 ^{o}C was accurate and following the same reaction mechanism an apparent activation energy of 89.6 ± 0.6 kJ mol^{-1} for squalane autoxidation was calculated. Leaving out the value for 100 ^{o}C, the value was 102.69 ± 3.4 kJ mol^{-1}. The errors associated with the $k_{squalane}$ values in the Arrhenius plot were obtained from the linear regression of the best-fit lines of the logarithmic decay graphs and represent the standard error, i.e. ca. a 95% chance the true value lies within the quoted error limits.

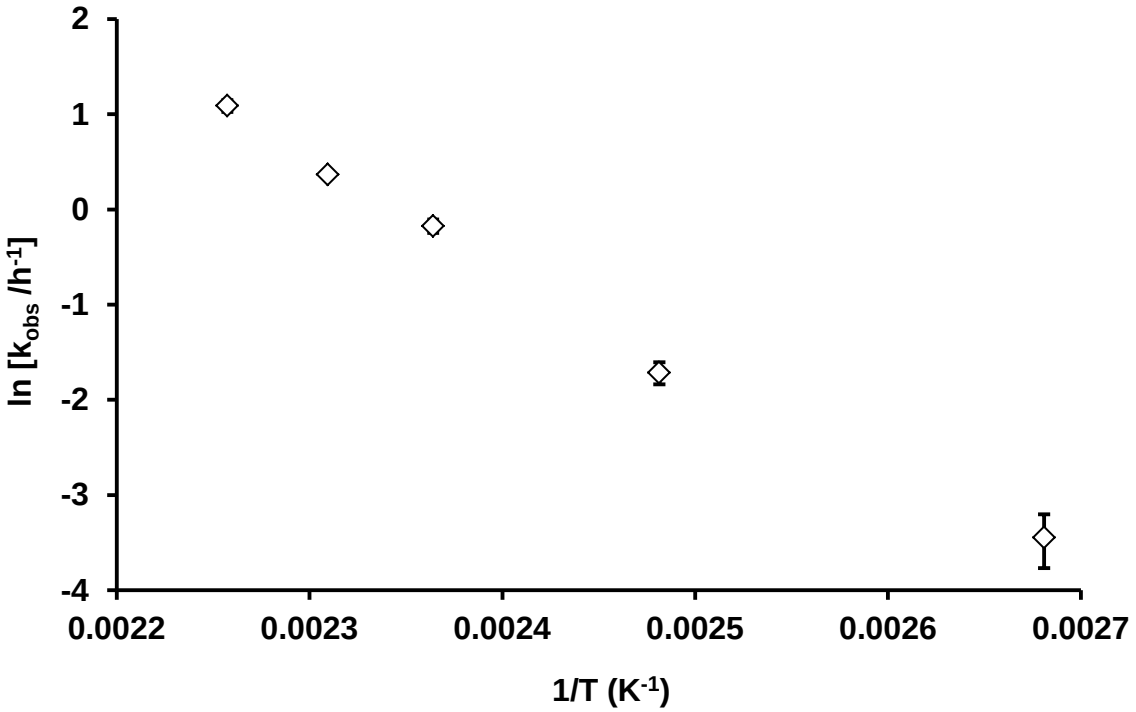

Figure 4.5 – Arrhenius plot for squalane autoxidation.

4.2.2 Effect of Methyl Linoleate on Rate of Decay of Squalane.

Obtaining the pseudo first order $k_{squalane}$ values for squalane oxidation, at various temperatures provided a basis for investigating the effect of adding the biodiesel substrates, methyl linoleate (ML) and methyl oleate (MO). It could be determined how increasing the concentration of each would alter the value of $k_{squalane}$ or whether it would remain the same as it was with no extra methyl ester added.

The addition of methyl linoleate to squalane was investigated between 100 and 170 ^{o}C to represent the various temperatures found in an engine from the sump (lowest) to the piston ring assembly and piston assembly (highest) (Taylor 2004, Moritani 2004) as mentioned in the introduction. Concentrations of methyl linoleate were kept between 0 and 10% to encompass the typical levels of fuel dilution encountered, most notably in the sump where biodiesel accumulates (Shayler 2000) as discussed in the Introduction chapter. From the study of previous literature, particularly the observation that biodiesel with higher levels of unsaturation caused increased fouling of the lubricant (See Chapter 1, Section 4), the hypothesis that was proposed for testing here was that, as polyunsaturated hydrocarbons are more reactive than monounsaturated and saturated ones, methyl linoleate would increase $k_{squalane}$ as it was added, see equation 4.2.

$$k_{squalane^x} > k_{squalane^0}$$ Equation 4.2

Where x = the % of substrate added

Figure 4.6 shows the decay of squalane with different amounts of methyl linoleate at 100 ^{o}C in logarithmic form. The line of best fit was taken for each of these data series with the gradient giving the value of $k_{squalane}^{x}$, plotted in figure 4.7 with the error bars again representing the standard error from the linear regression of the trendline.

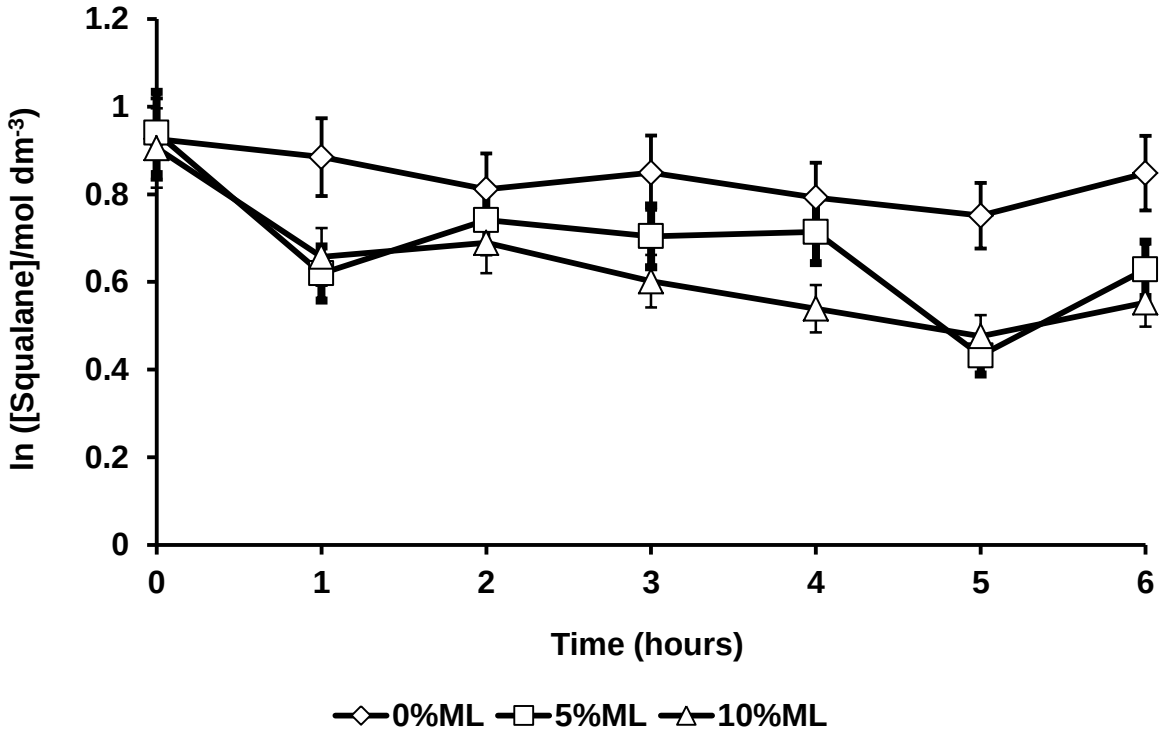

Figure 4.6 – The decay of squalane with varying amounts of methyl linoleate at 100 ^{o}C with a 0.08 dm^3 min^{-1} flow of oxygen.

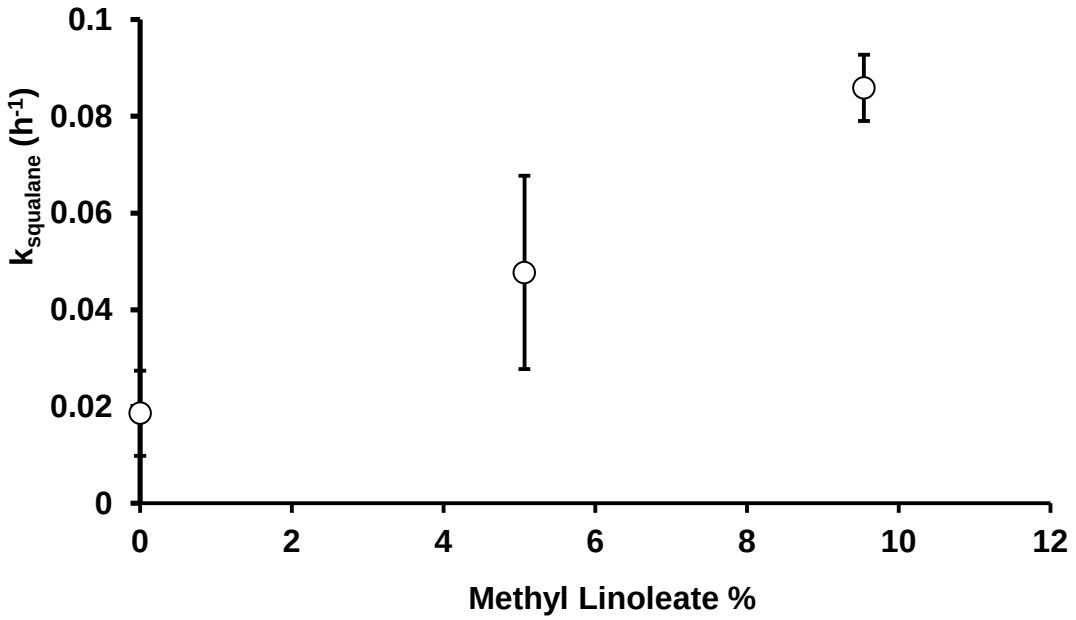

Figure 4.7 – The dependence of the rate of decay of squalane on methyl linoleate at 100 ^{o}C.

Figure 4.8 shows the same data for 130 ^{o}C, correlated in figure 4.9, whilst figure 4.10 shows data for 150 ^{o}C, correlated in figure 4.11. From these graphs it appeared that at these temperatures the hypotheses that adding methyl linoleate would increase $k_{squalane}$ appeared to be true. At 170 ^{o}C (figure 4.12, and figure 4.13), however, the addition of methyl linoleate served to decrease $k_{squalane}$ (figure 4.14 shows all temperatures on one graph).

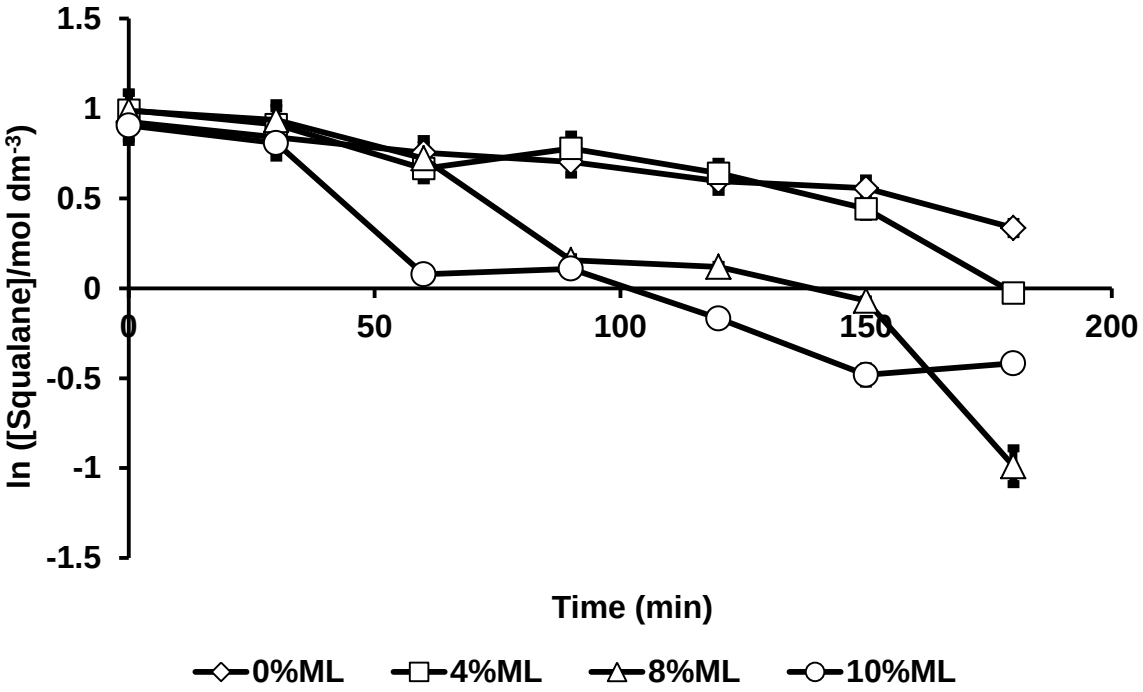

Figure 4.8 – The decay of squalane with varying amounts of methyl linoleate at 130 ^{o}C with a 0.08 dm^{3} min^{-1} flow of oxygen.

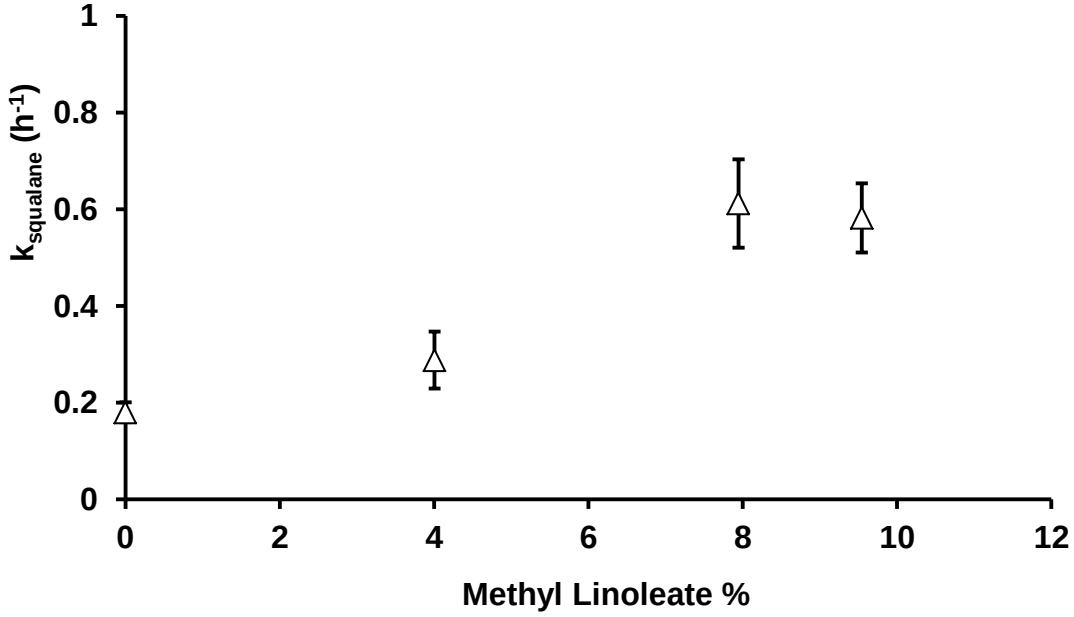

Figure 4.9 – The rate of decay of squalane with methyl linoleate at 130 ^{o}C.

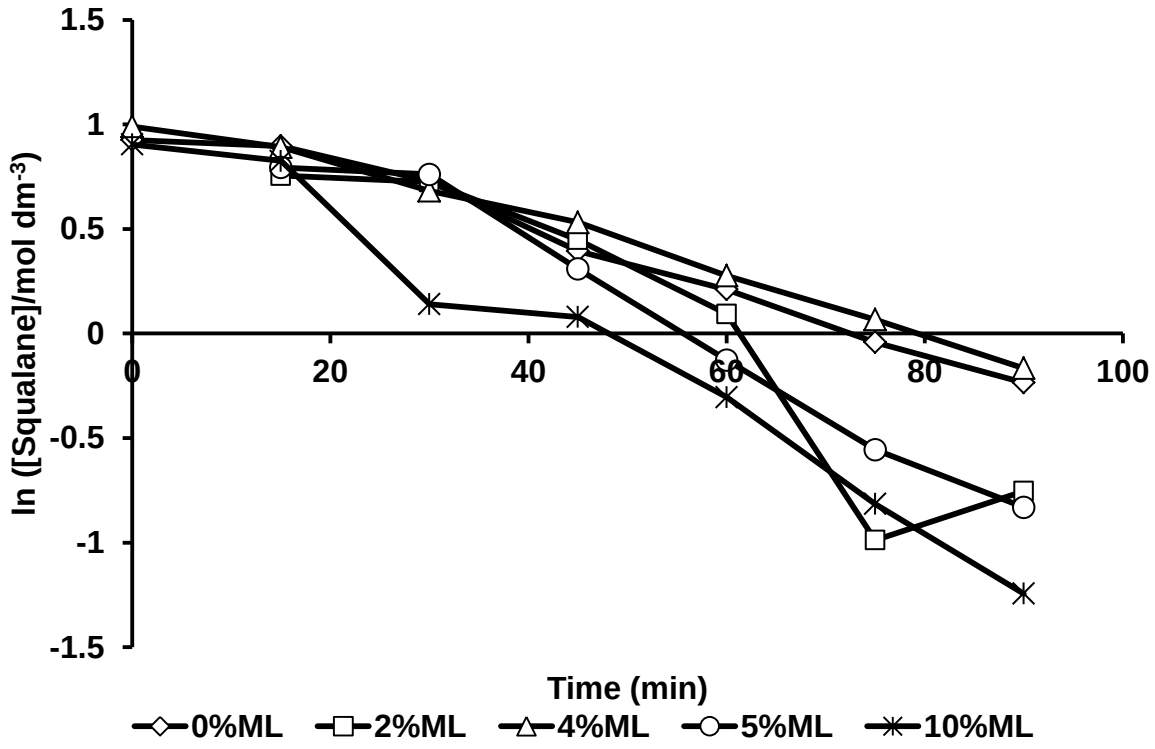

Figure 4.10 – The decay of squalane with varying amounts of methyl linoleate at 150 ^{o}C with a 0.08 dm^{3} min^{-1} flow of oxygen.

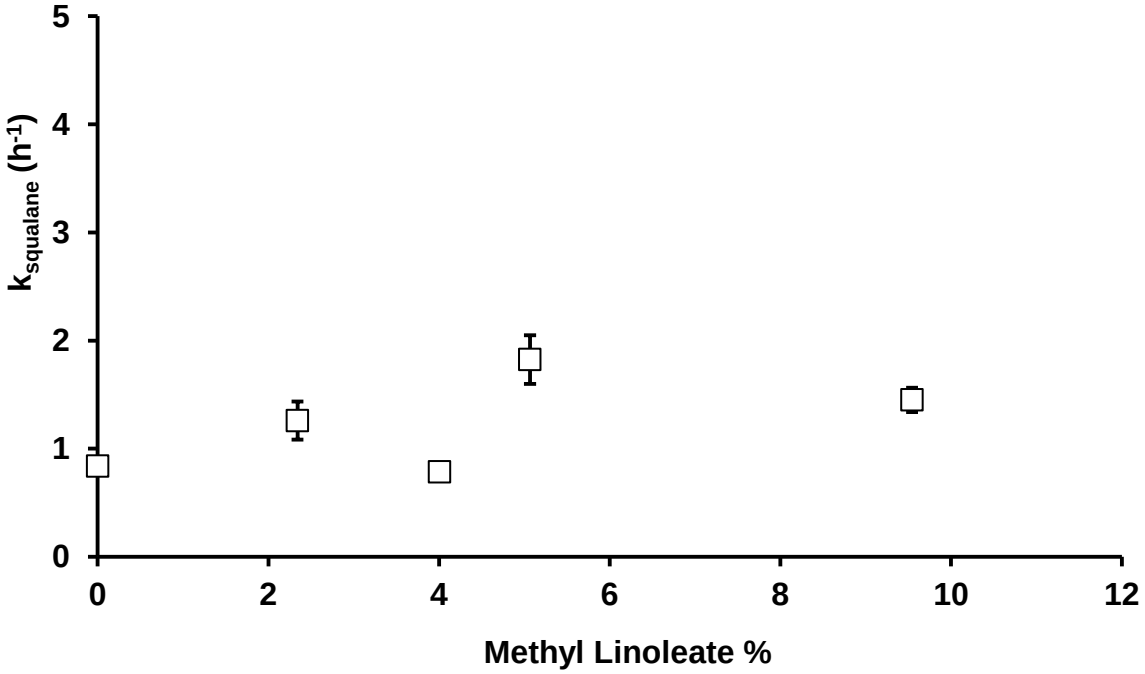

Figure 4.11 – The rate of decay of squalane with methyl linoleate at 150 ^{o}C.

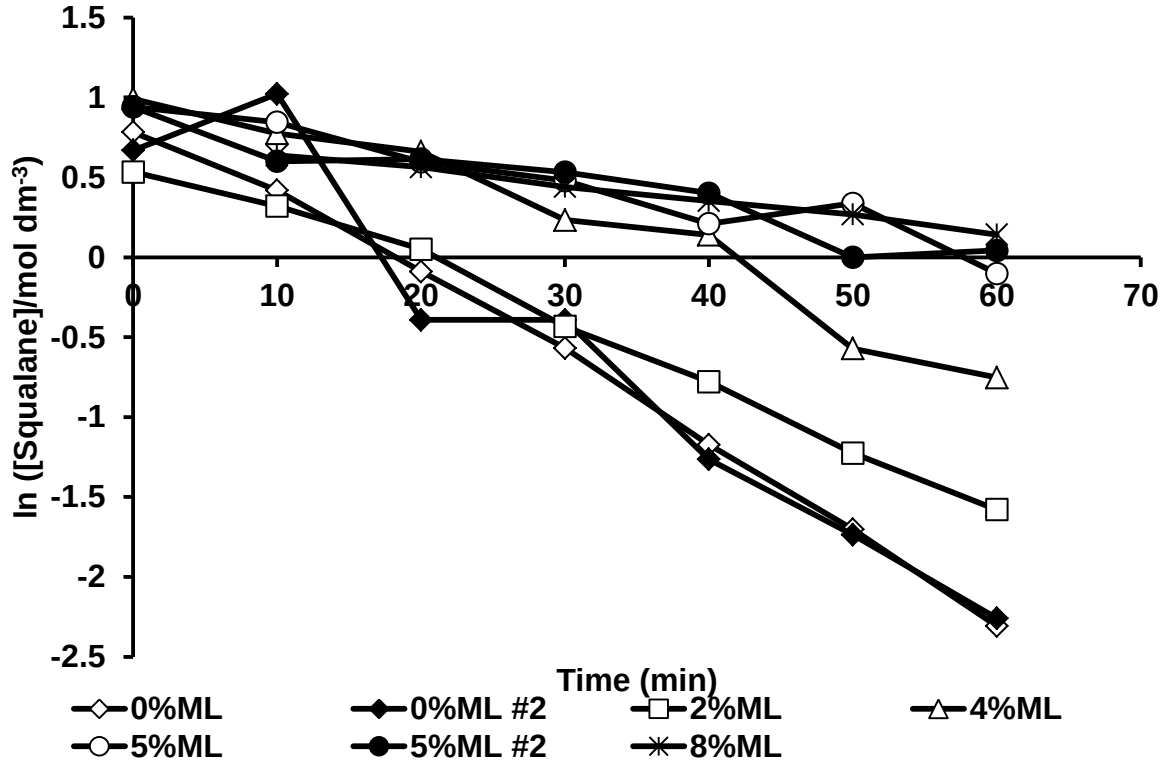

Figure 4.12 – The decay of squalane with varying amounts of methyl linoleate at 170 ^{o}C with a 0.08 dm^{3} min^{-1} flow of oxygen.

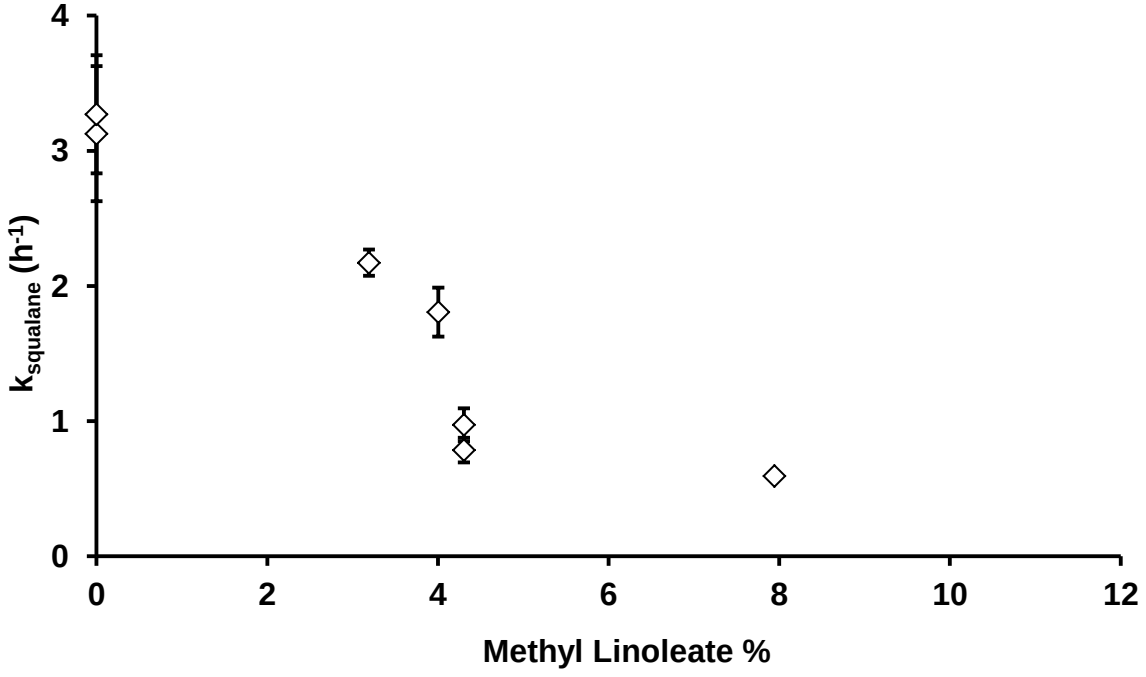

Figure 4.13 – The rate of decay of squalane with methyl linoleate at 170 ^{o}C

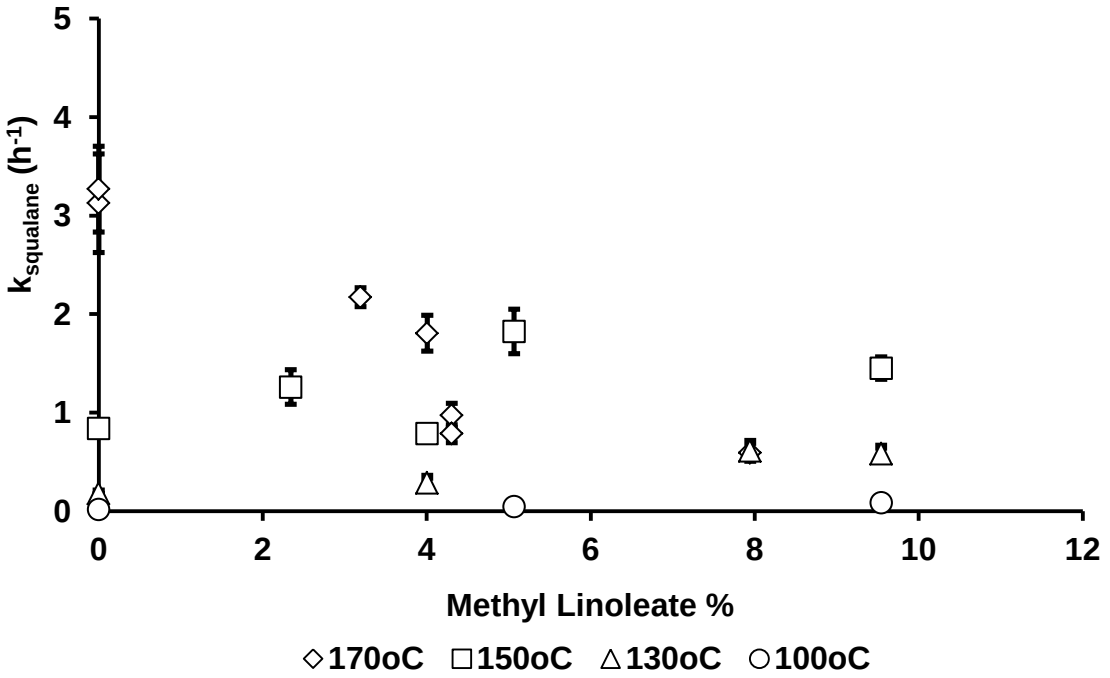

Figure 4.14 – The rate of decay of squalane with methyl linoleate at concentrations of 0 – 10% at 100 – 170 ^{o}C.

The change in rate of methyl linoleate decay (k_{ML}) was also looked at. Unfortunately, this was not as straightforward to analyse as a minor peak started to appear on the GC spectra at the same retention time as methyl linoleate roughly mid-way through the reaction, causing a slight apparent increase in peak area (see Figure 4.15). As there was no other peak in the initial decay spectra of either methyl linoleate or squalane corresponding to this retention time, it was assumed this was a secondary decay product produced from the breakdown of one of the (undetermined) initial decay products. Therefore the observed rate constants were calculated with a greater level of uncertainty due to having fewer data points available. Figure 4.16, 4.17, 4.18 and 4.19 present the decay data for methyl linoleate in squalane at 100, 130, 150 and 170 ^{o}C respectively.

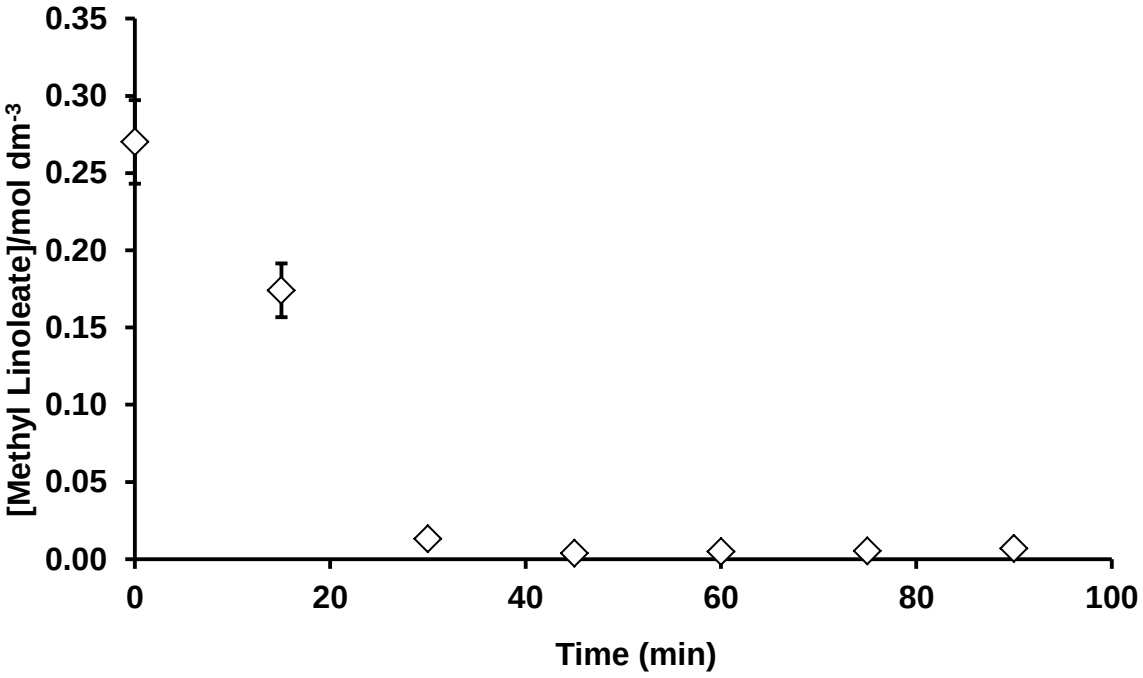

Figure 4.15 – Methyl linoleate concentration versus time at 150 ^{o}C with 8%ML in squalane.

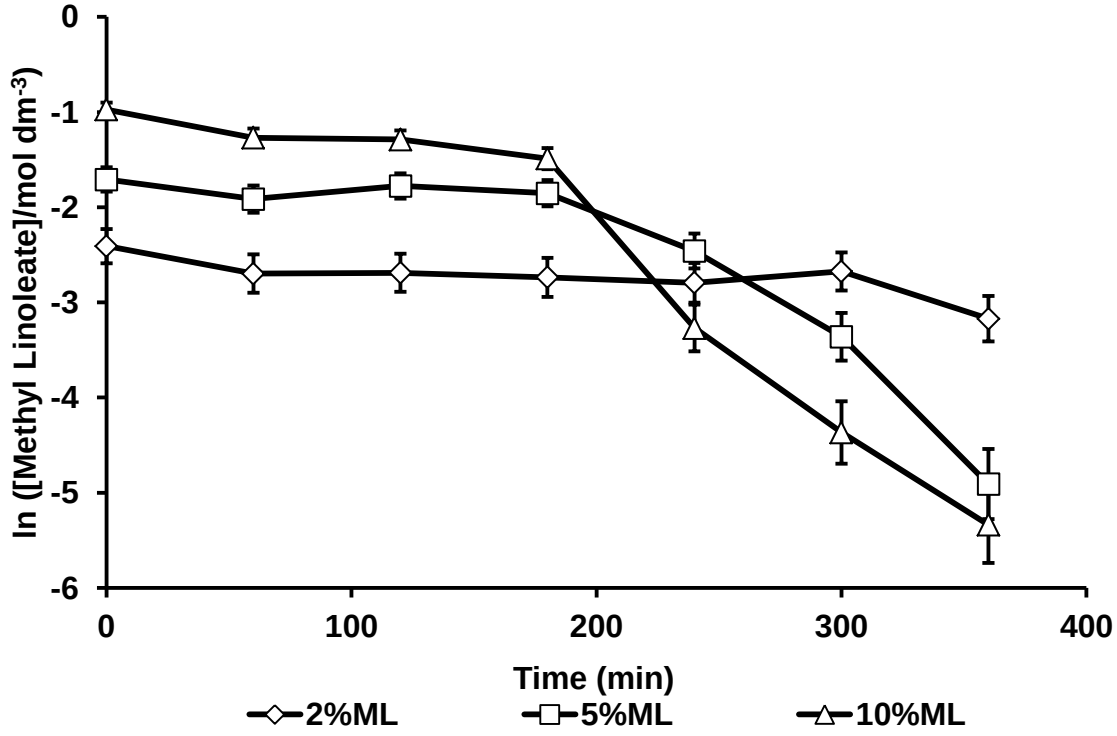

Figure 4.16 – The decay of methyl linoleate in squalane at 100 ^{o}C.

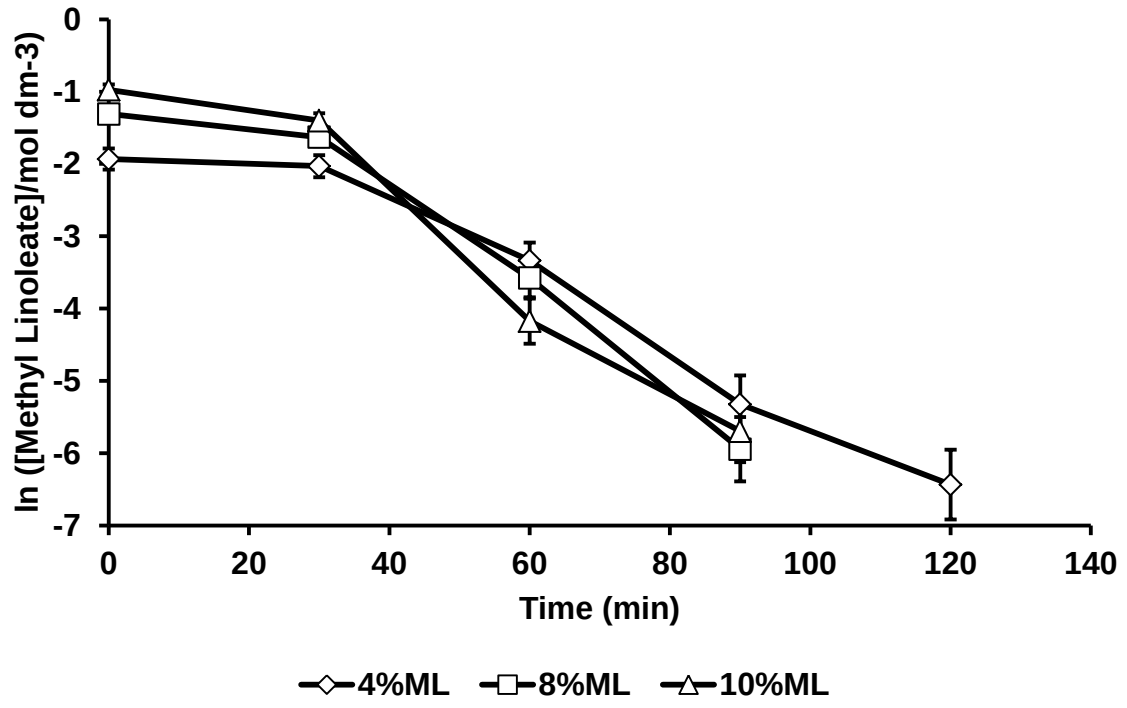

Figure 4.17 – The decay of methyl linoleate in squalane at 130 ^{o}C.

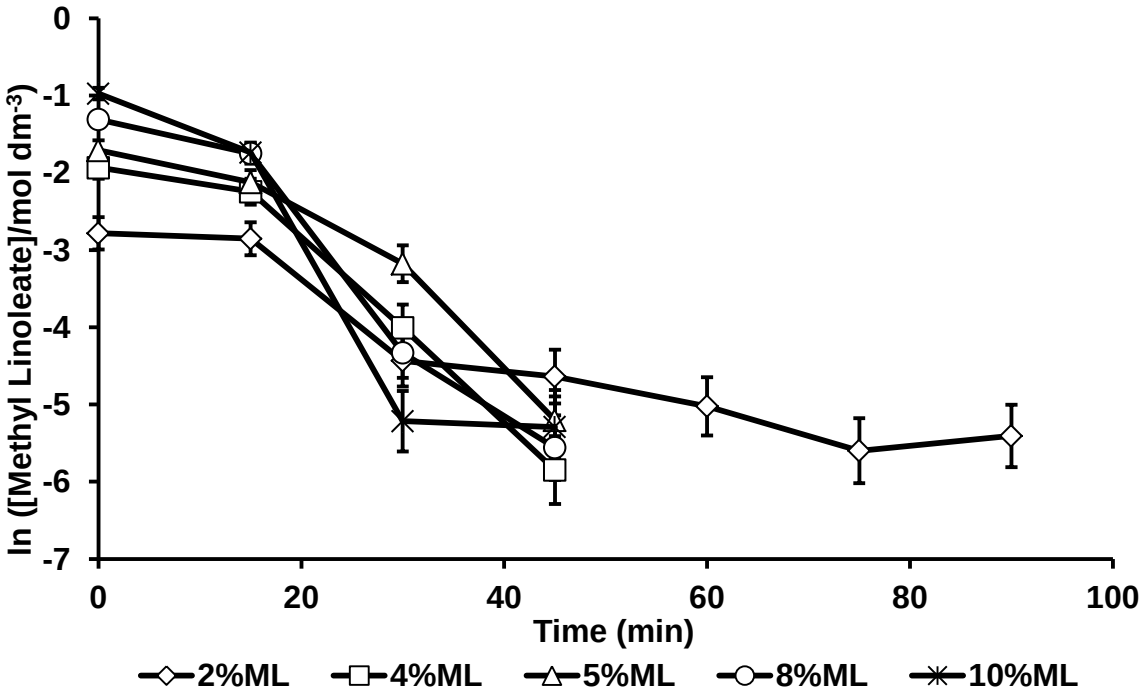

Figure 4.18 – The decay of methyl linoleate in squalane at 150 ^{o}C.

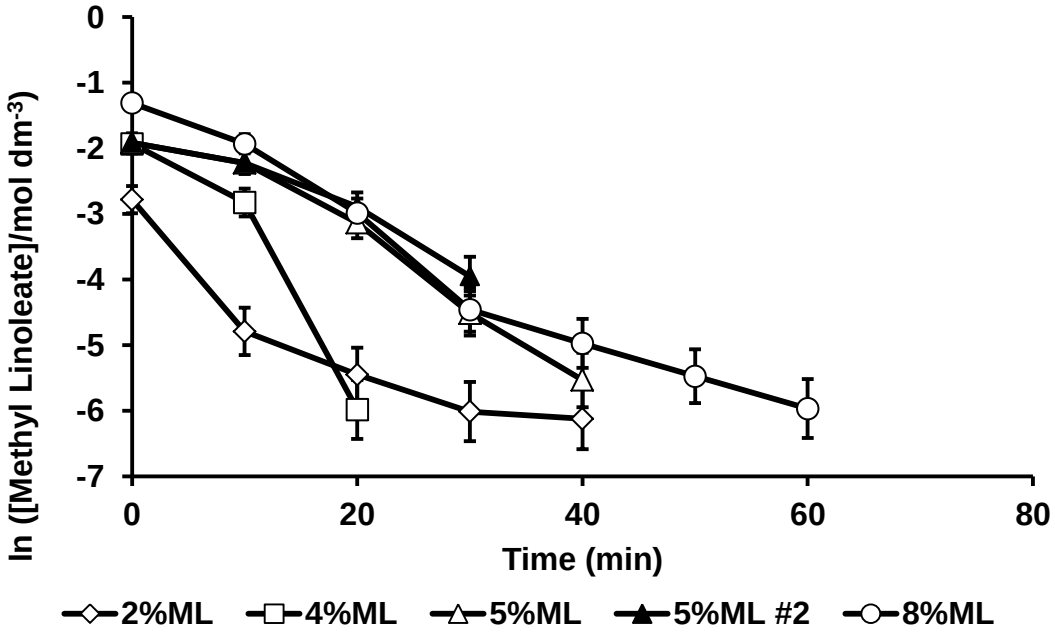

Figure 4.19 – The decay of methyl linoleate in squalane at 170 ^{o}C.

For the 3 data series at 100 ^{o}C (Figure 4.20), methyl linoleate was still in decay after 6 hours with no overlapping peaks for either sample, hence good values for k_{ML} were obtained, showing an apparent increase in k_{ML} with increasing methyl linoleate in solution.

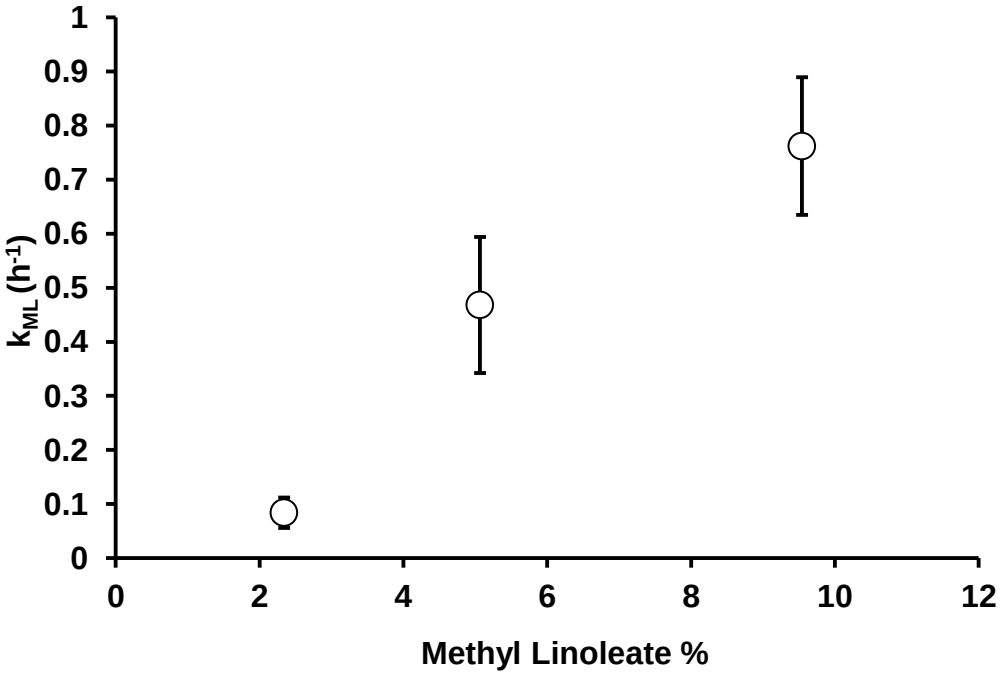

Figure 4.20 – The rate of decay of methyl linoleate in squalane at 100 ^{o}C.

At 130 ^{o}C and 150 ^{o}C (figures 4.21 and 4.22, respectively) the results showed a similar trend of increasing k_{ML} with increasing amounts of methyl linoleate in solution, although as the amount of methyl linoleate increased, so did the rate of peak overlap and hence so did the relative errors. By 170 ^{o}C, due to the relatively rapid rate of both methyl linoleate decay and product formation in some of the samples, there was a much larger degree of uncertainty which made it harder to spot noticeable trends (Figure 4.23).

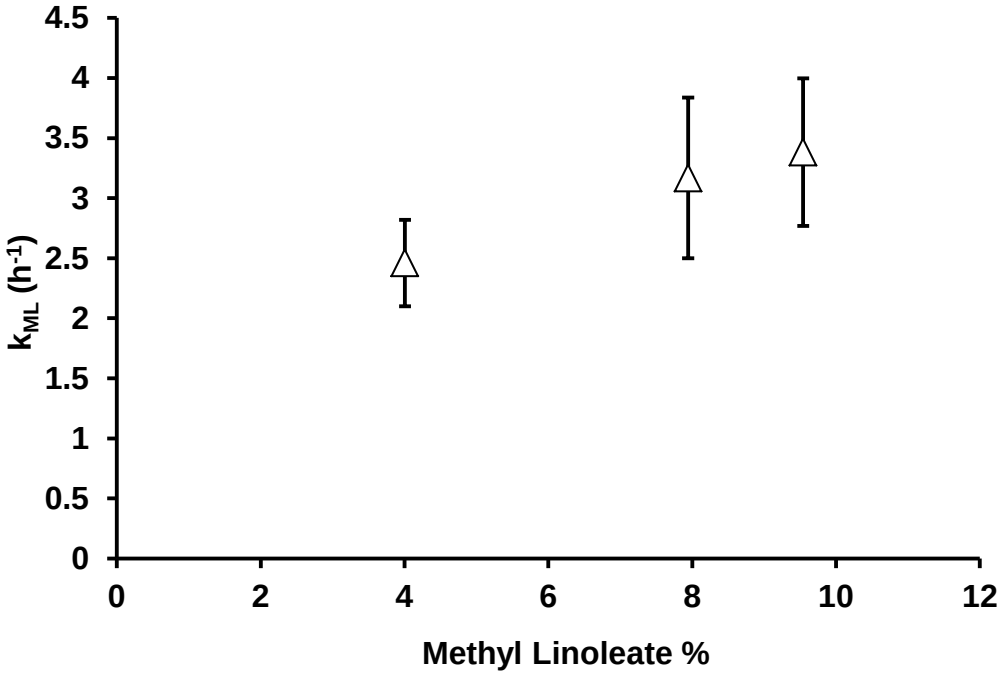

Figure 4.21 – The rate of decay of methyl linoleate in squalane at 130 ^{o}C.

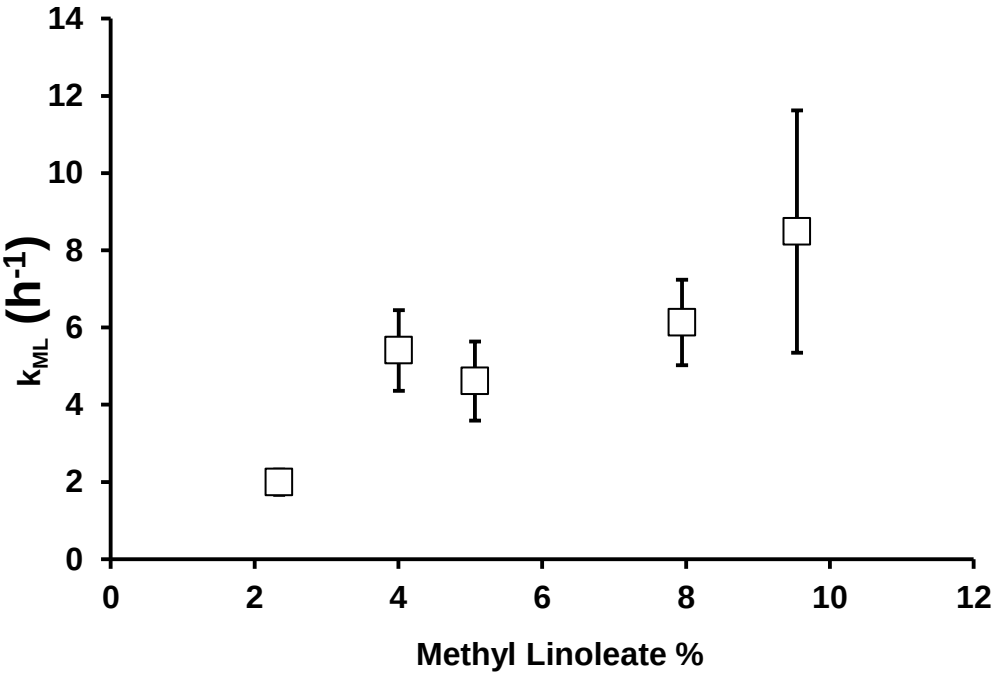

Figure 4.22 – The rate of decay of methyl linoleate in squalane at 150 ^{o}C.

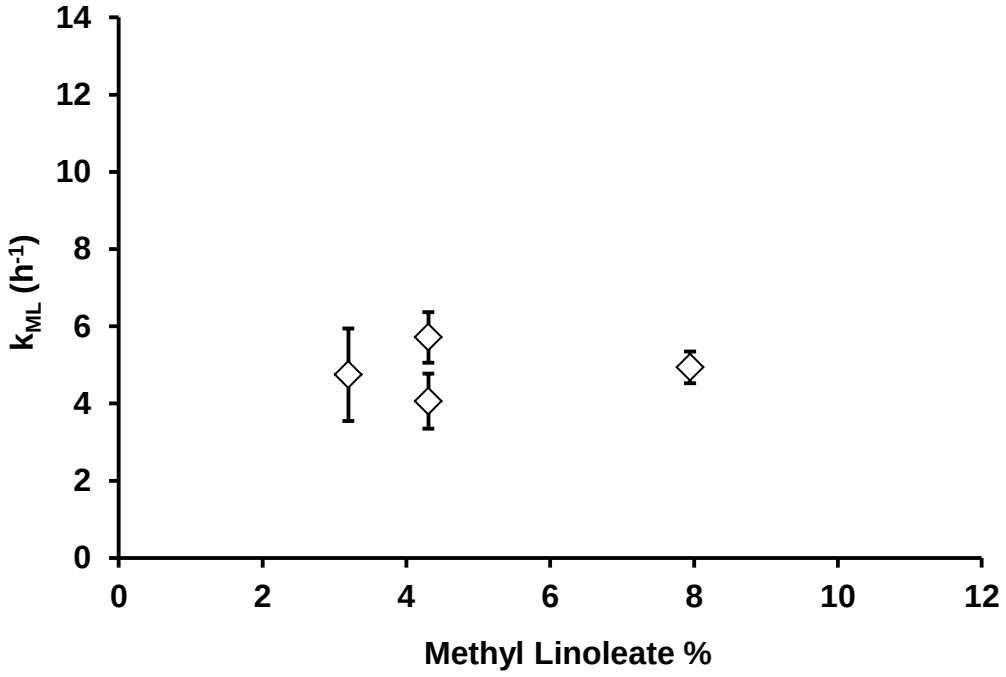

Figure 4.23 – The rate of decay of methyl linoleate in squalane at 170 ^{o}C.

Plotting the rate of change of k_{ML} v temperature (the gradient of figures 4.20 – 4.23), it can be seen that, unlike for squalane, the rate of k_{ML} increase per addition of methyl linoleate increases across all temperatures (Figure 4.24). To summarise, as the concentration of methyl linoleate in squalane/methyl linoleate mixtures increased, the rate

of autoxidation of methyl linoleate also increased at all measured temperatures, as did the rate of squalane autoxidation at 100, 130 and 150 ^{o}C. At 170 ^{o}C, however, the rate of squalane autoxidation decreased with increasing methyl linoleate concentration.

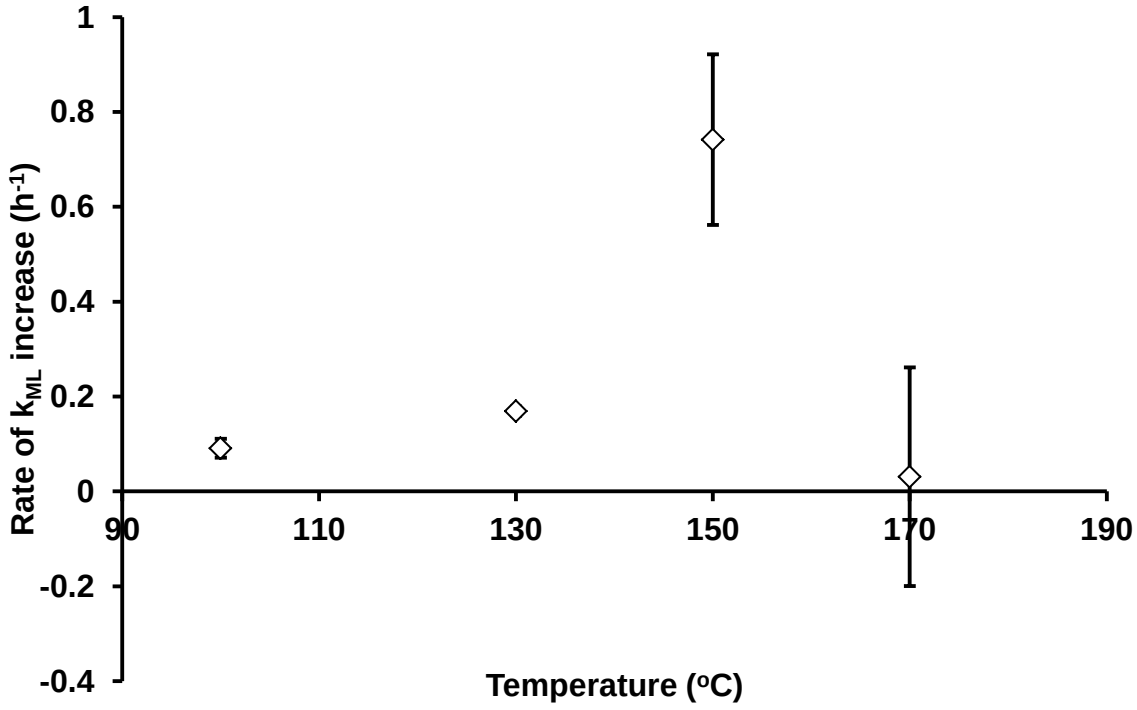

Figure 4.24 – The rate of k_{ML} increase for methyl linoleate versus temperature.

4.2.3 Effect of Methyl Oleate on Rate of Decay of Squalane

To investigate the role of methyl oleate in biodiesel behaviour, flow oxidation reactions were carried out with squalane and varying amounts of methyl oleate in the same manner as the tests with methyl linoleate, as described previously. As before, the value of k_{obs} for squalane oxidation, $k_{squalane}$ was measured to see how it varied with the addition of methyl oleate. The squalane decay results for 170 ^{o}C are shown in figure 4.25 with the $k_{squalane}$ values shown in figure 4.26.

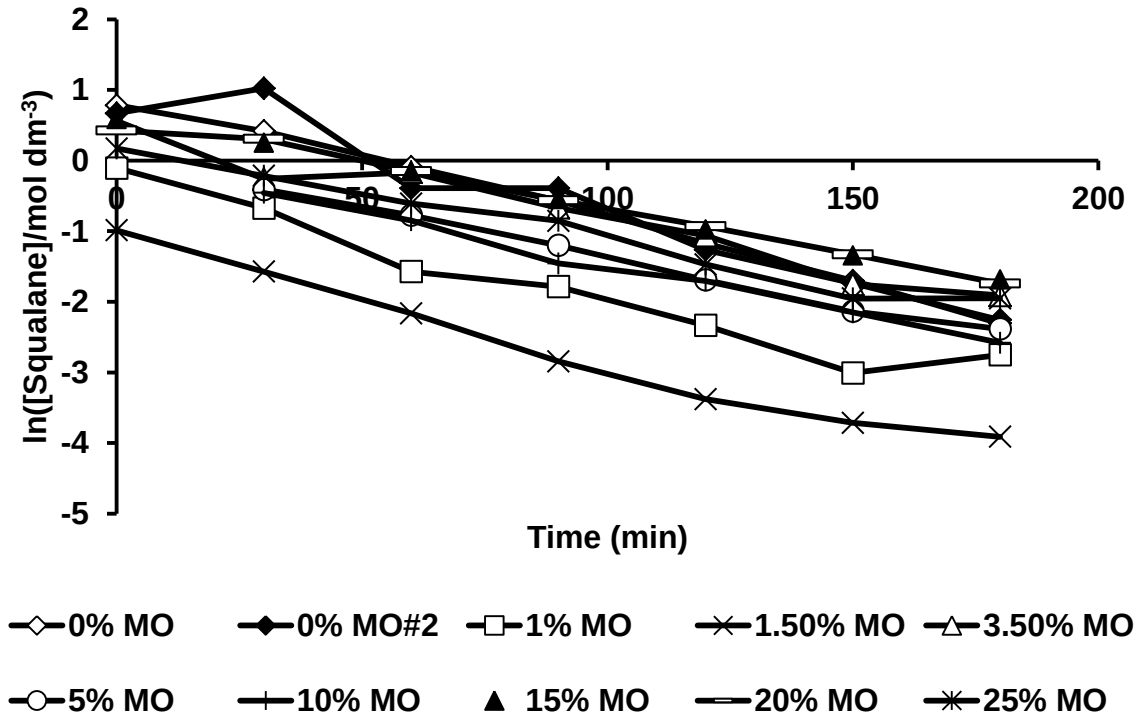

Figure 4.25 – The decay of squalane with varying amounts of methyl oleate at 170 ^{o}C with a 0.08 dm^3 min^{-1} flow of oxygen.

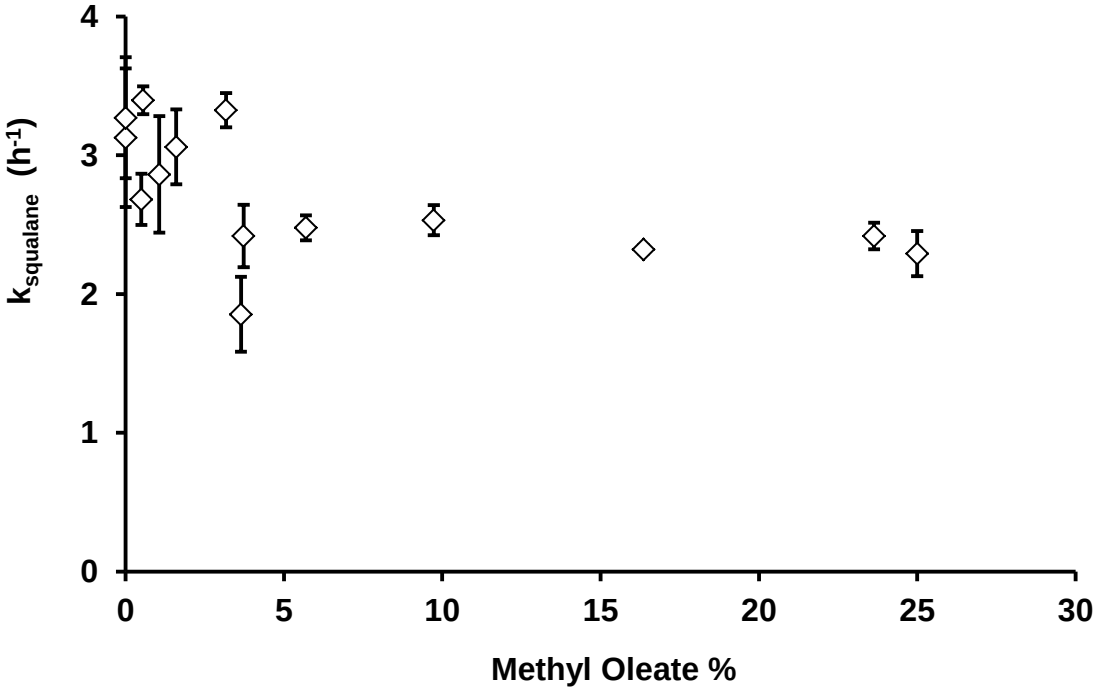

Figure 4.26 – The rate of decay of squalane with methyl oleate at 170 ^{o}C.

Methyl oleate appears to be having a slight inhibiting effect on squalane oxidation, but if so, the effect is much less prominent than for methyl linoleate – an addition of 5% MO reducing the decay rate by ~ 0.5 h^{-1}, compared to a decrease of ~ 2 h^{-1} with the

addition of the same amount of ML. Figure 4.27 shows the squalane decay data at 150 ^{o}C, with the $k_{squalane}$ values shown in figure 4.28. Again, as with ML at 150 ^{o}C, within experimental error, the addition of methyl oleate appears to have negligible effect on the $k_{squalane}$. Finally, figures 4.29 and 4.30 show the results at 130 ^{o}C, unfortunately due to time constraints, there are no results at 100 ^{o}C. Unlike the results for methyl linoleate, which showed that ML would increase $k_{squalane}$ at 130 ^{o}C, methyl oleate appears to have no significant effect at all at this temperature.

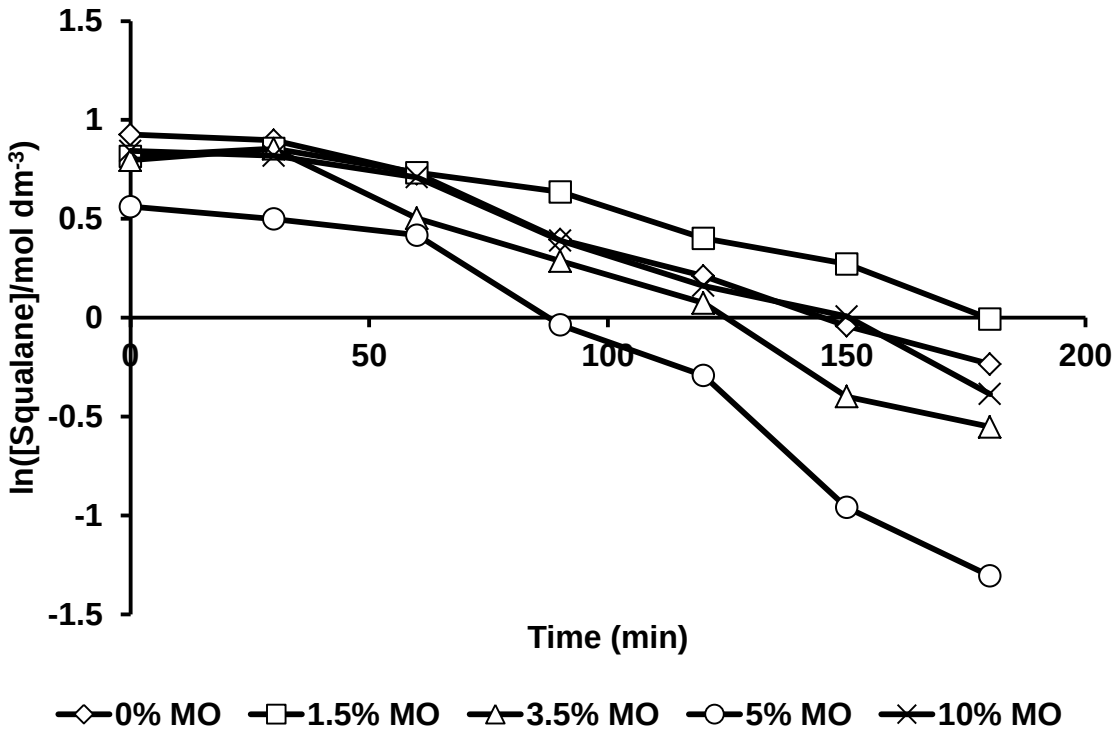

Figure 4.27 – The decay of squalane with varying amounts of methyl oleate at 150 ^{o}C with a 0.08 dm^3 min^{-1} flow of oxygen.

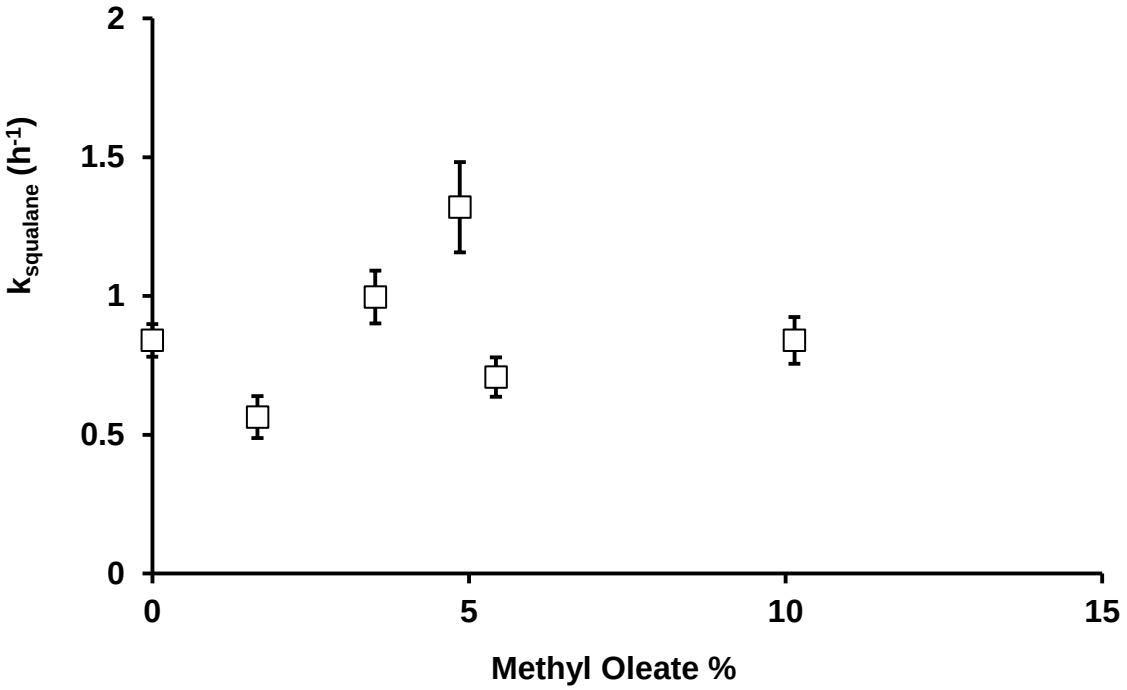

Figure 4.28 – The rate of decay of squalane with methyl oleate at 150 ^{o}C.

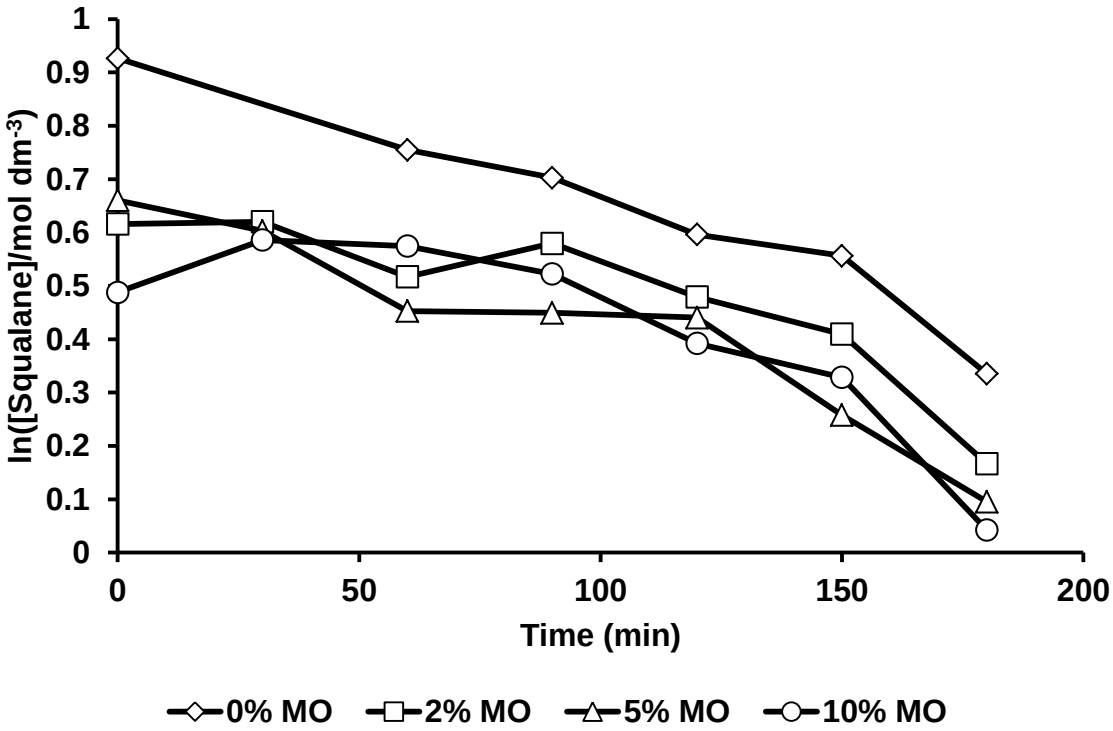

Figure 4.29 – The decay of squalane with varying amounts of methyl oleate at 130 ^{o}C with a 0.08 dm^3 min^{-1} flow of oxygen.

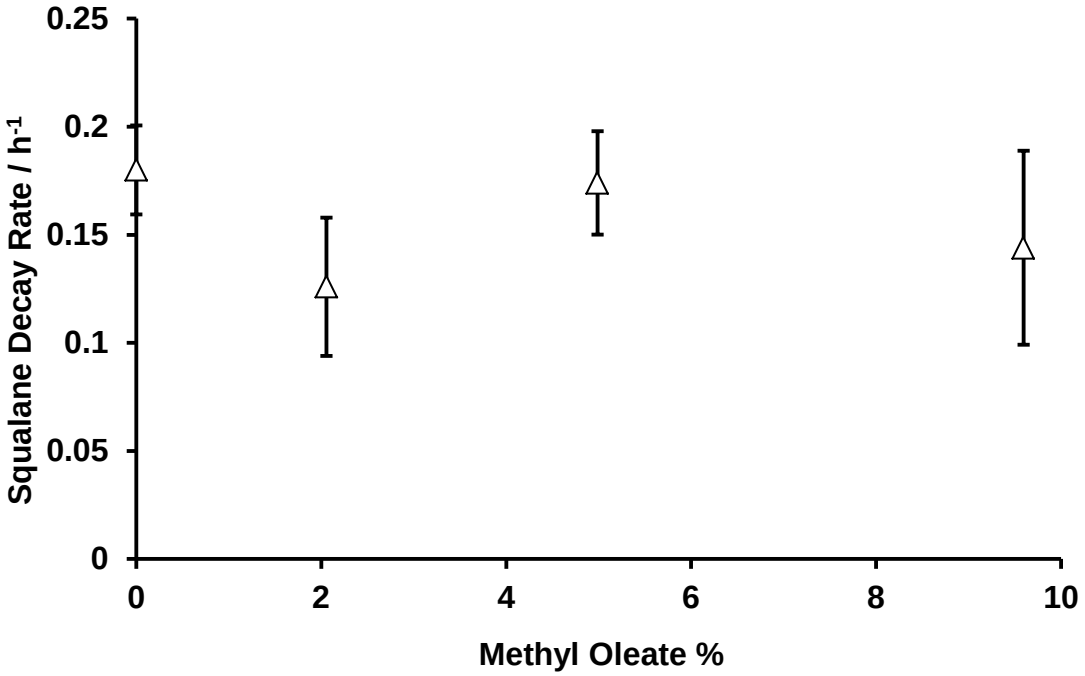

Figure 4.30 – The rate of decay of squalane with methyl oleate at 130 ^{o}C.

As with methyl linoleate, the change in rate of decay of methyl oleate, k_{MO} was also investigated. Unfortunately, the interference on the GC spectra from one of the breakdown products was still present (at 170 and 150 ^{o}C) and hence again, the rate constants were calculated from fewer data points and therefore with less certainty. The decay data is presented in figures 4.31 – 4.33 with the k_{MO} values shown in figures 4.34 – 4.36 where it can be seen that again, as with methyl linoleate, k_{MO} seemed to increase as more methyl oleate was added to the mixture, albeit far more slowly.

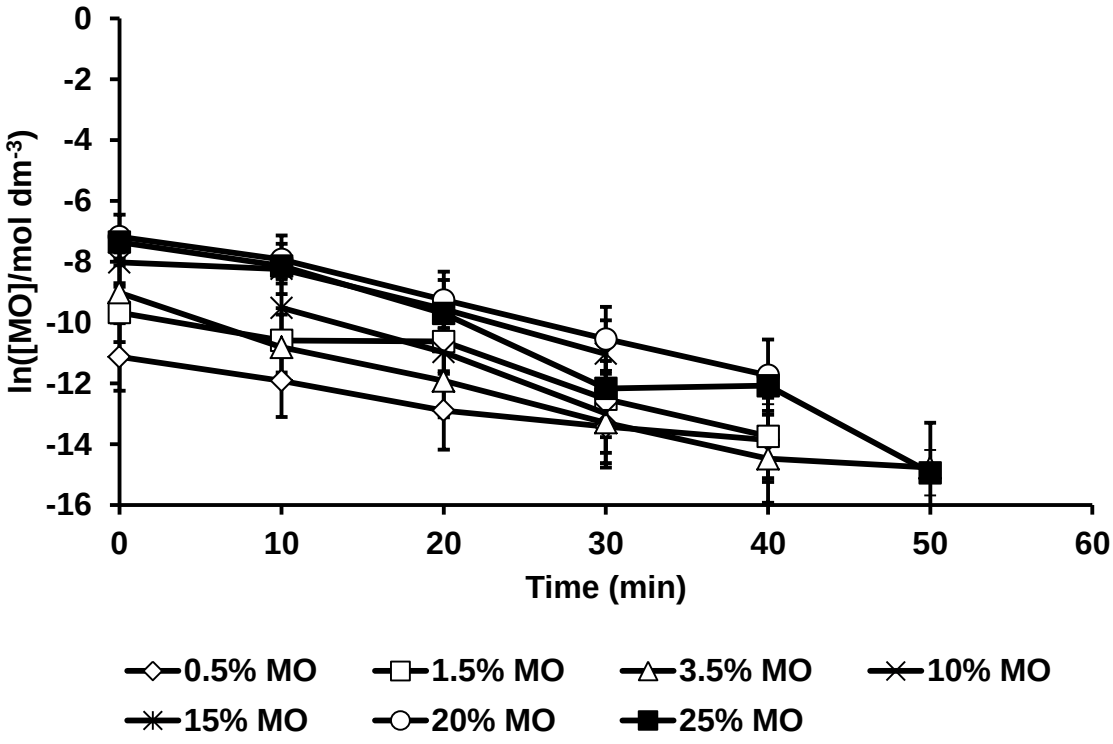

Figure 4.31 – The decay of methyl oleate in squalane at 170 ^{o}C.

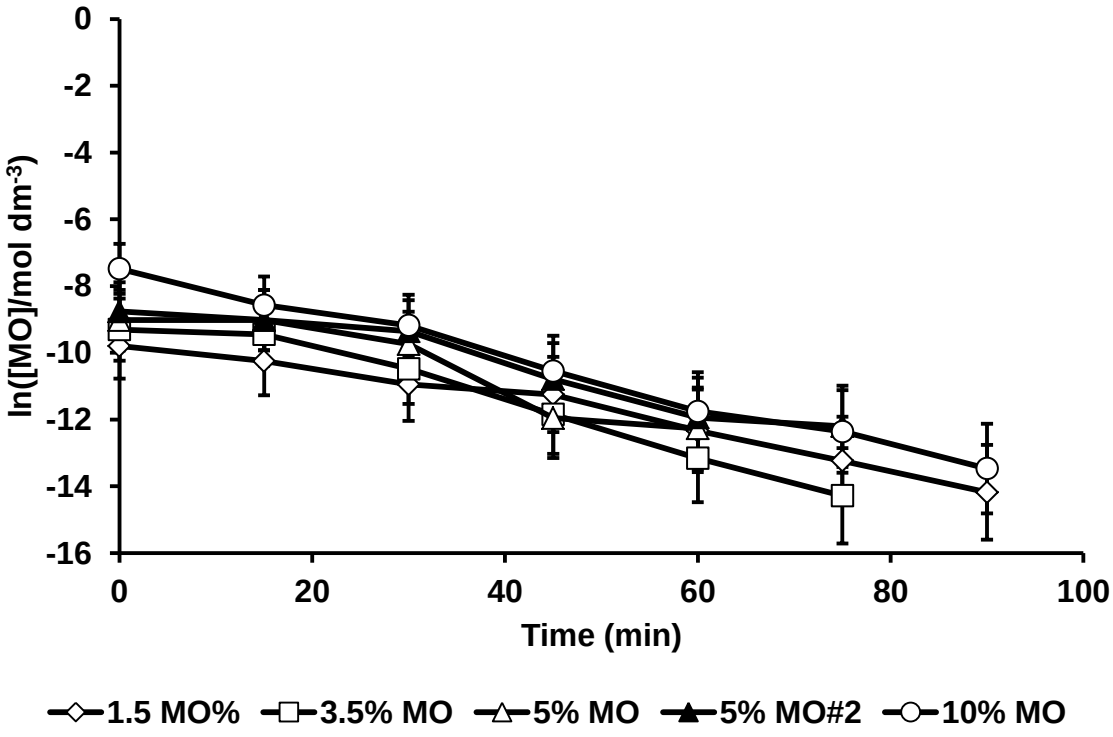

Figure 4.32 – The decay of methyl oleate in squalane at 150 ^{o}C.

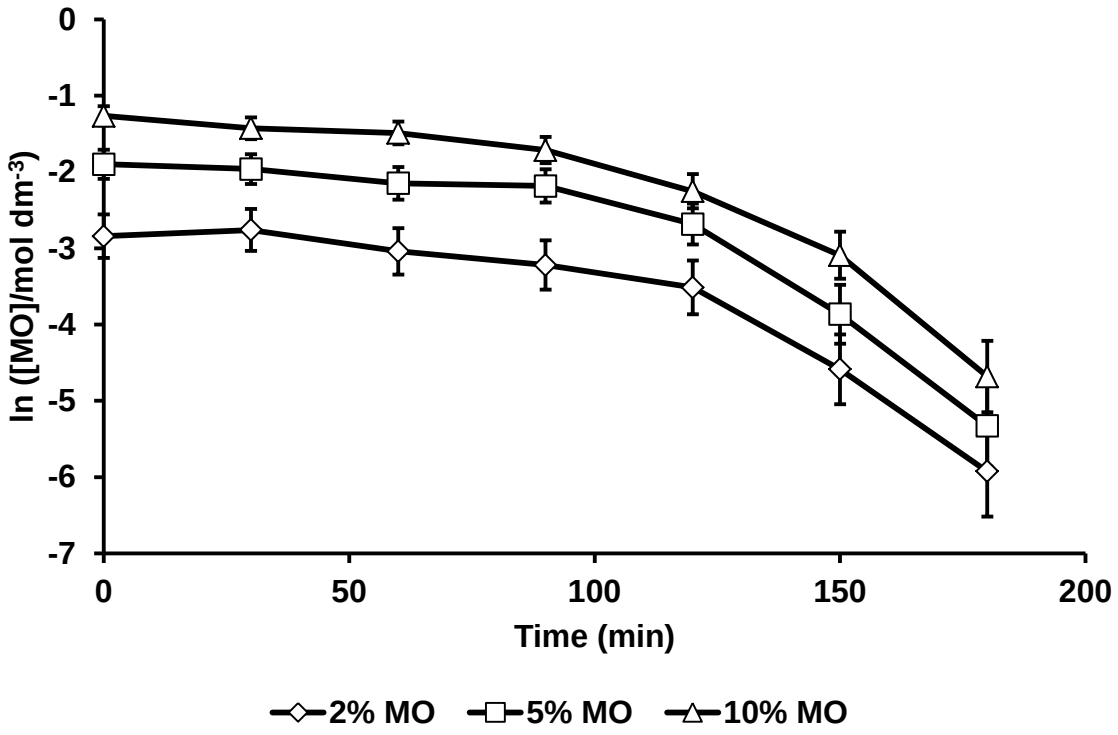

Figure 4.33 – The decay of methyl oleate in squalane at 130 ^{o}C.

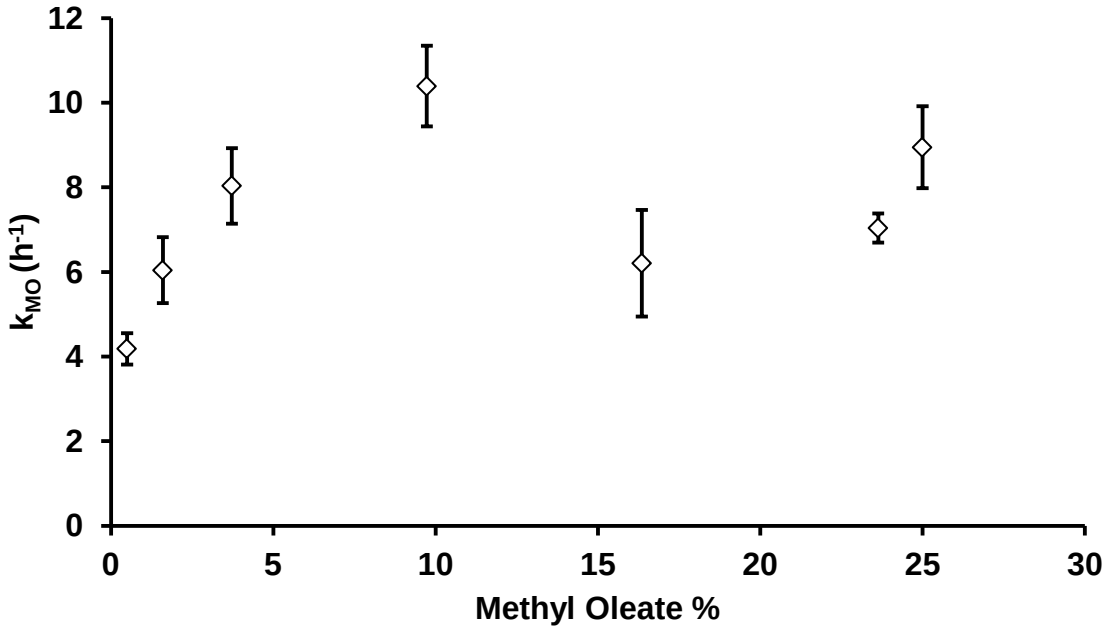

Figure 4.34 – The rate of decay of methyl oleate in squalane at 170 ^{o}C.

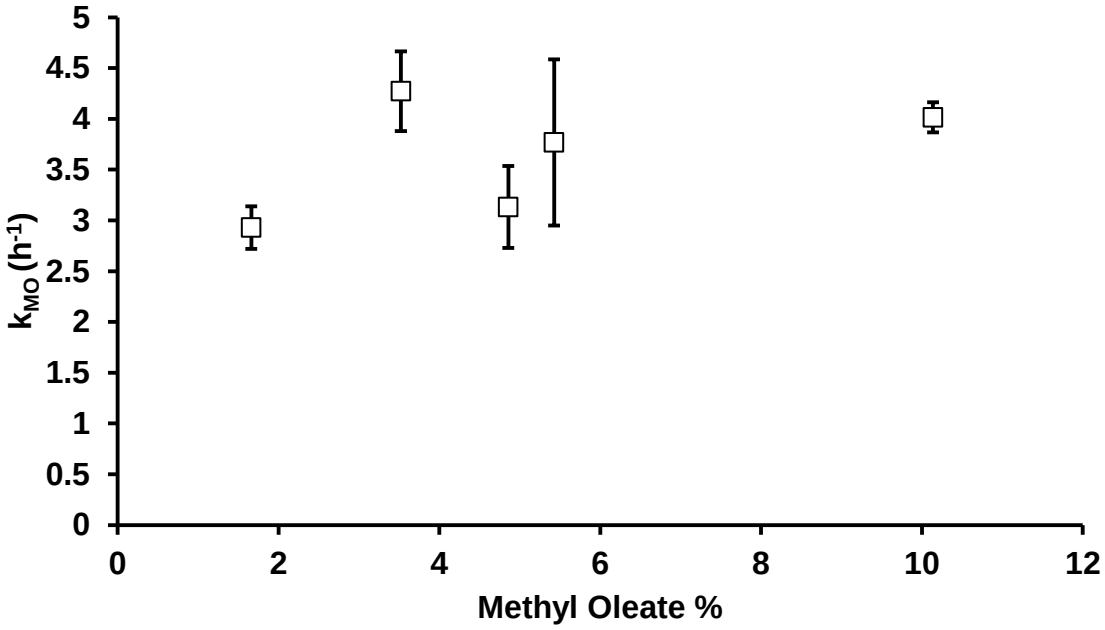

Figure 4.35 – The rate of decay of methyl oleate in squalane at 150 ^{o}C.

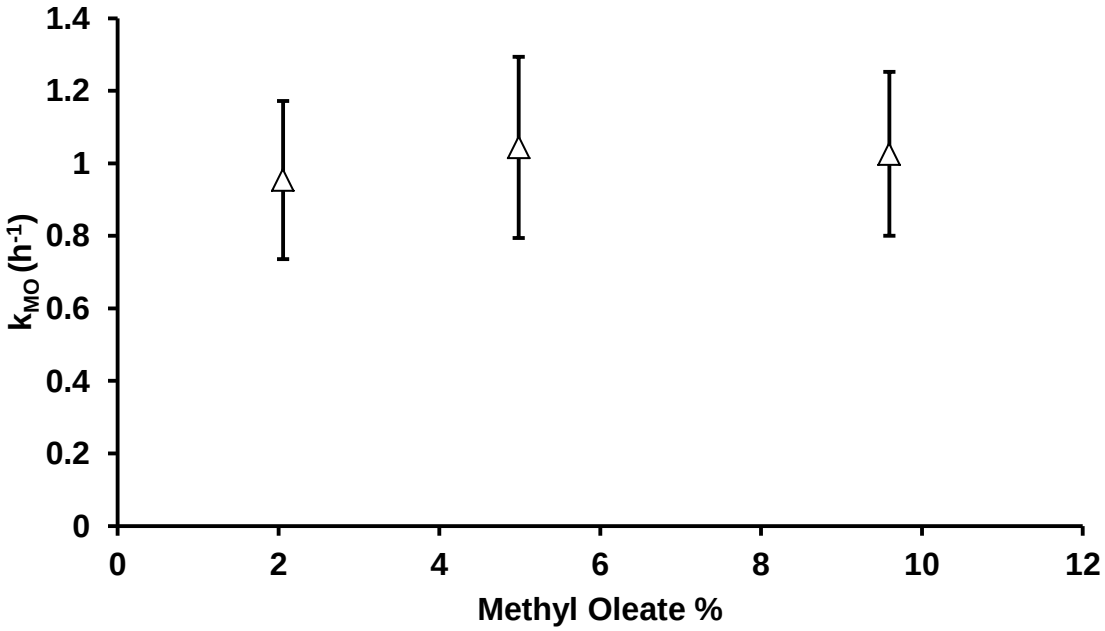

Figure 4.36 – The rate of decay of methyl oleate in squalane at 130 ^{o}C.

4.2.4 Effect of Methyl Linoleate and Oleate on Kinematic Viscosity of Oxidising Squalane.

The viscosity (KV40 – kinematic viscosity at 40 ^{o}C) was also measured for each of samples collected (where possible, i.e. if enough material was collected). For squalane by itself, figure 4.37 shows the change in KV40 over time at 170 ^{o}C, whilst figures 4.38 and

4.39 show the same data for 150 ^{o}C and 130 ^{o}C respectively. The exponential-like curve is typical of those obtained for these reactions reported here, although if the reaction is coming to a close, the curve can start to flatten out leading to a more sigmoid pattern as shown by squalane at 150 ^{o}C (figure 4.38). Part of the reason for this is that the KV40 of the liquid throughout the reaction is also affected by a mixture of dilution from lighter compounds (such as scission products) and thickening from heavier compounds (oxidation products, polymers). This makes getting sufficient data points to get a gradient to measure a rate of change in KV40 for comparison quite problematic. In addition as biodiesel components are less viscous than lubricants (squalane was measured to have KV40 of 19.14 cSt, compared to methyl linoleate at just 3.34 cSt), upon their addition to squalane the overall initial KV40 of the liquid decreases. For these reasons to provide a basis for comparison at a single temperature for all mixtures, the overall change in KV40, i.e. $KV40_{final} - KV40_{initial}$ of the mixtures was measured and to compare between temperatures, the change in KV40 was used after 1 hour as this was the longest time that all experiments ran. At 100 ^{o}C, the change in KV40 after an hour was too negligible to be measured accurately within the confines of the equipment available and as a result these data are not shown.

The trends observed for KV40 upon the addition of methyl linoleate showed good correlation with those for $k_{squalane}$ – the addition of methyl linoleate enhanced KV40 increase at 130 and – to a lesser degree – at 150 ^{o}C, but inhibited it at 170 ^{o}C (see figure 4.40).

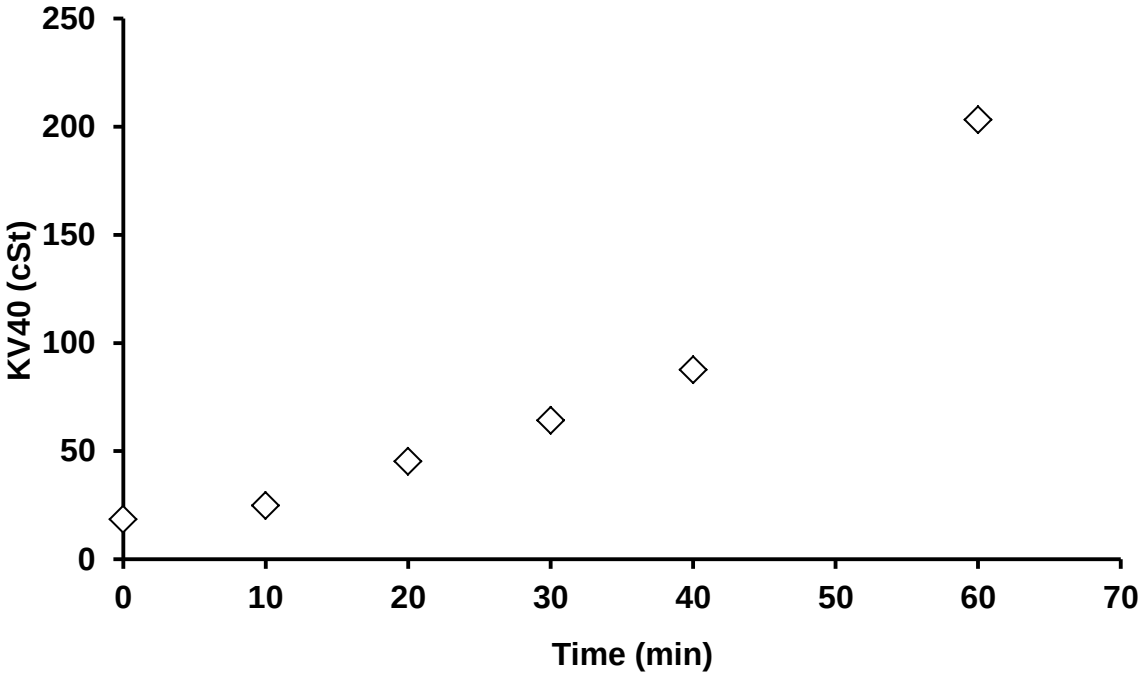

Figure 4.37 – The change in KV40 of squalane over time at 170 ^{o}C with a 0.08 dm^{3} min^{-1} flow of oxygen.

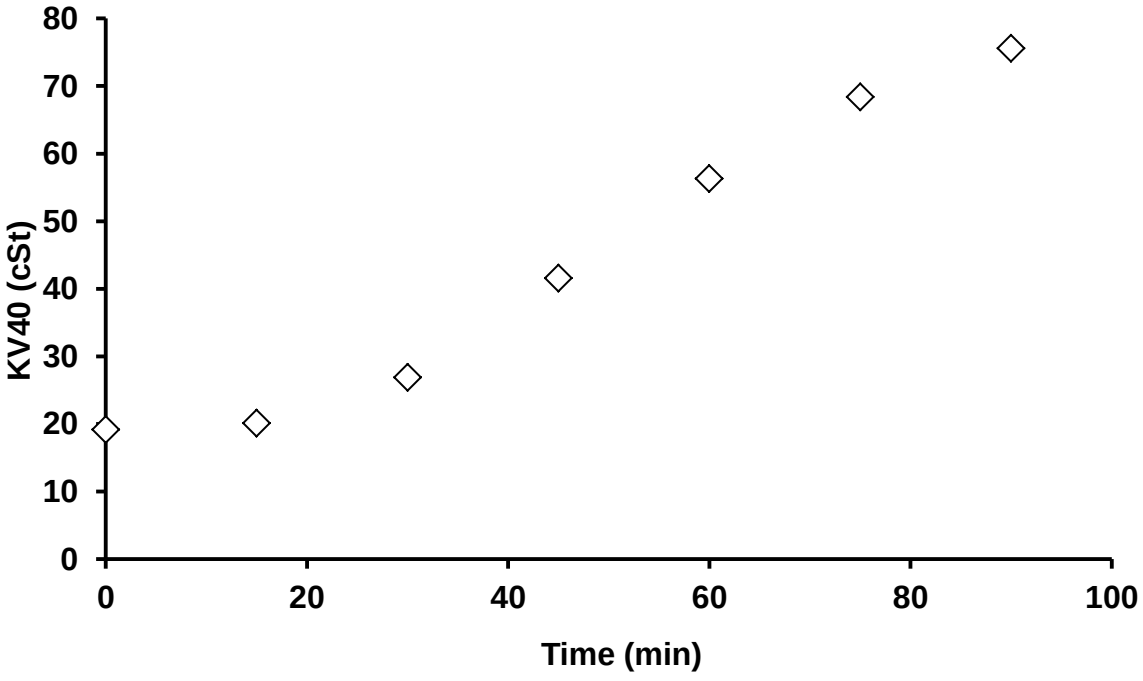

Figure 4.38 – The change in KV40 of squalane over time at 150 ^{o}C with a 0.08 dm^{3} min^{-1} flow of oxygen.

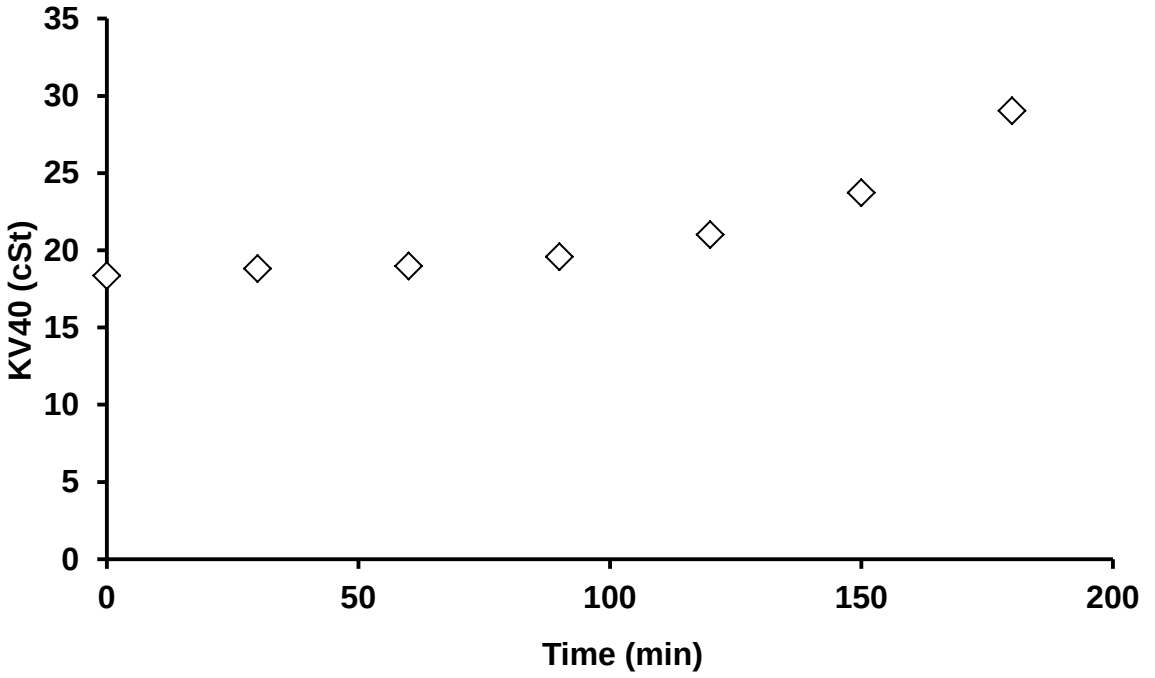

Figure 4.39 – The change in KV40 of squalane over time at 130 ^{o}C with a 0.08 dm^{3} min^{-1} flow of oxygen.

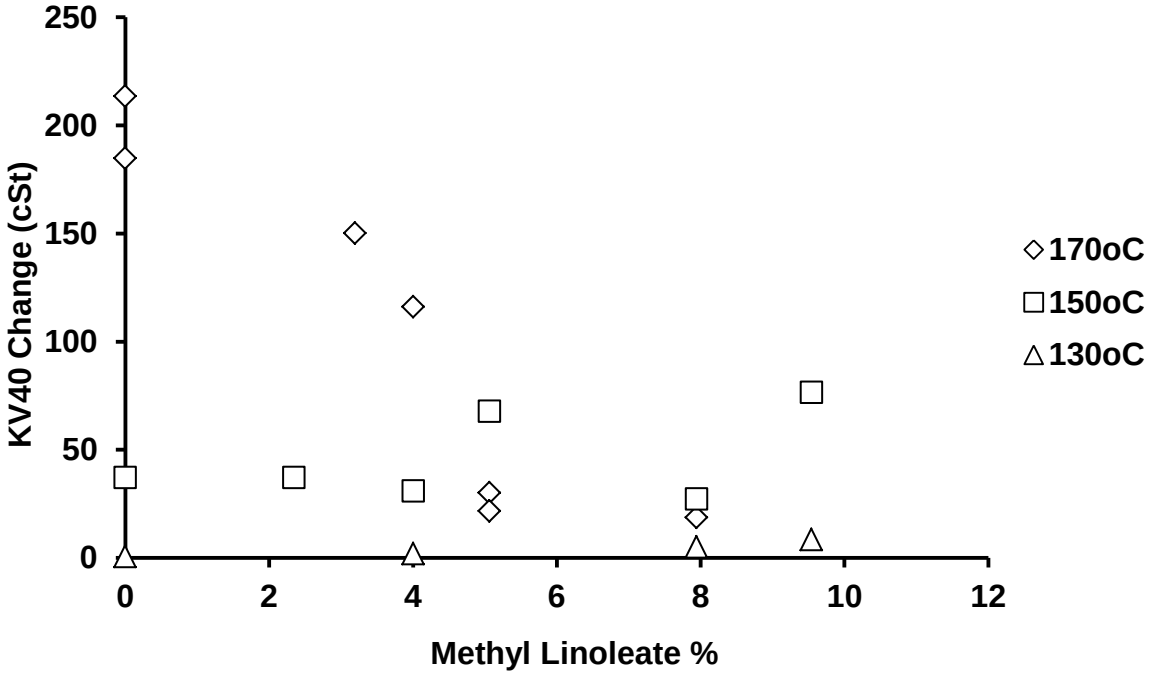

Figure 4.40 – The change in KV40 of squalane/methyl linoleate mixtures at 130 – 170 ^{o}C.

KV40 measurements after an hour were also taken for the samples of methyl oleate and squalane at 170 ^{o}C, 150 ^{o}C and 130 ^{o}C with the results shown in figure 4.41. As

before, changes in KV40 showed good correlation with change in $k_{squalane}$, that decreases in $k_{squalane}$ correspond to decreases in the rate of KV40 increases. However, as with the $k_{squalane}$ results with methyl oleate it is not immediately clear, with the possible exception of 170 ^{o}C, whether or not the addition of methyl oleate is having any noticeable effect on KV40 increase of the mixtures.

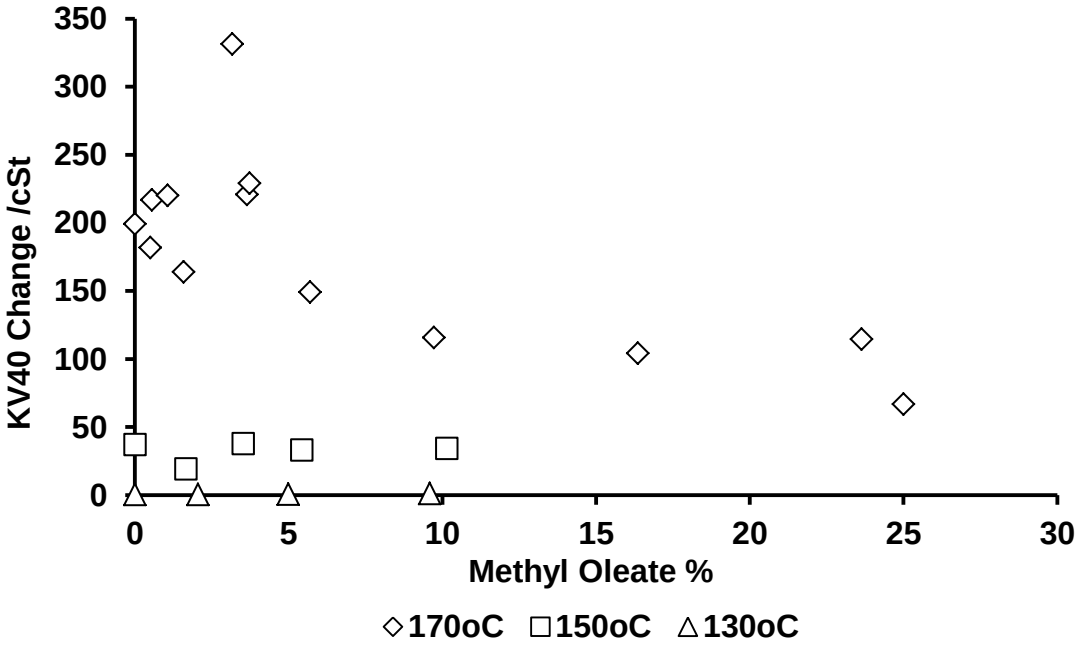

Figure 4.41 – The change in KV40 of squalane/methyl oleate mixtures at 130 – 170 ^{o}C.

4.3 Discussion

The hypothesis proposed for testing initially was that the addition of methyl linoleate to squalane would enhance its rate of decay, $k_{squalane}$. Figures 4.6 – 4.11 showed that this appeared to be the case at 100 – 150 ^{o}C, yet at 170 ^{o}C, the addition of methyl linoleate instead appeared to reduce the value of $k_{squalane}$ as it was added. Whilst this may seem paradoxical at first, it can be better understood if the $k_{squalane}^{x}$ values are standardised against $k_{squalane}^{0}$ to give a ratio of change, $\Delta k_{squalane}$ – see Equation 4.3.

$$\Delta k_{squalane} = \frac{k_{squalane^x}}{k_{squalane^o}} \qquad \text{Equation 4.3}$$

From these calculations it can be seen that even though temperatures 100 – 150 ^{o}C show methyl linoleate increasing $k_{squalane}$, the rate at which it does so decreases with increasing temperature (see table 4.2), hence by the point 170 ^{o}C is reached the ‘rate of

increase' has reduced to less than 1 and hence become a rate of decrease instead. In other words the expected pro-oxidant character of methyl linoleate in fact switches to become antioxidant by 170 ^{o}C.

Table 4.2 – The change in $k_{squalane}$ relative to standard $k_{squalane}^{0}$ at various temperatures.

Temperature (^{o}C)	100	130	150	170
$k_{squalane}^{0}$ (h^{-1})	0.019	0.18	0.84	3.20
$k_{squalane}^{10}$	0.086	0.58	1.45	0.59 (8%ML)
$\Delta k_{squalane}^{10}$ (8 for 170 ^{o}C)	4.6	3.2	1.7	0.2

Figure 4.41 shows the calculated ratios, $\Delta k_{squalane}^{x}$, for all the temperatures to show the proportional effect of methyl linoleate on rate of decay of squalane at each temperature. Ratios of less than 1 are not as easy to see in this graph compared to those greater than 1, therefore figure 4.42 shows the same data plotted in logarithmic form to graphically represent ratios of less than 1 more clearly. From these graphs it is much clearer to see the pro-oxidant character of methyl linoleate decreasing with temperature to the point where it has taken on antioxidant characteristics by 170 ^{o}C. Figures 4.43 and 4.44 show the same data for methyl oleate, however these show no noticeable trends other than to suggest that methyl oleate has no significant effect on the rate of squalane oxidation at the concentrations used.

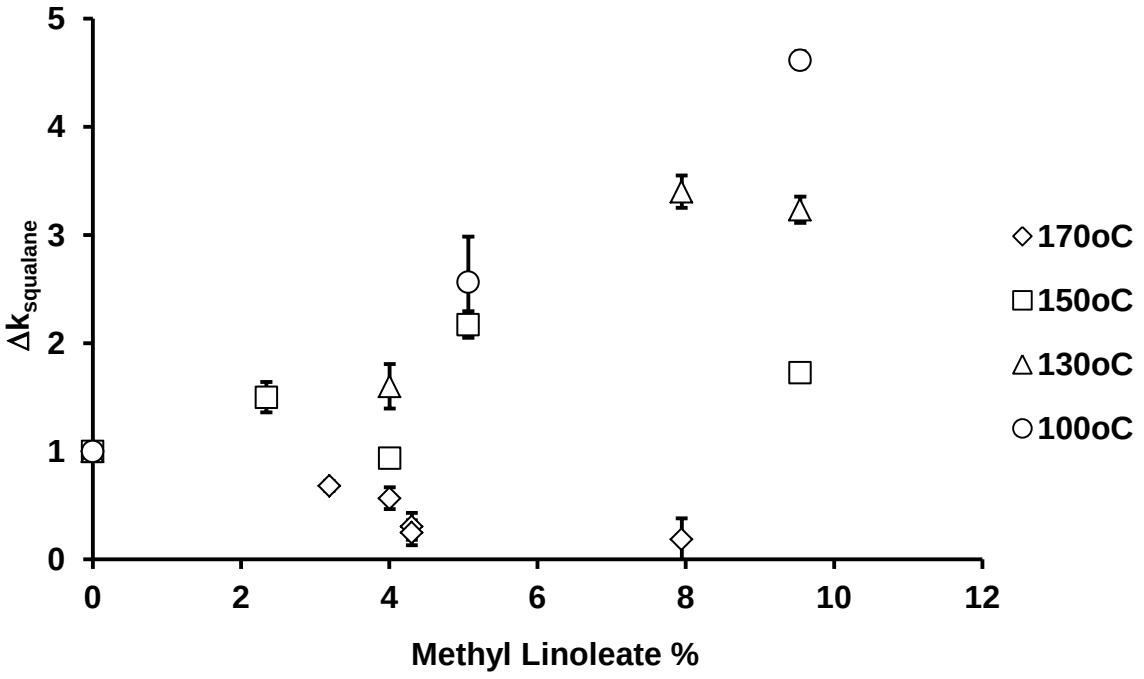

Figure 4.41 – The relative change of squalane decay with added methyl linoleate.

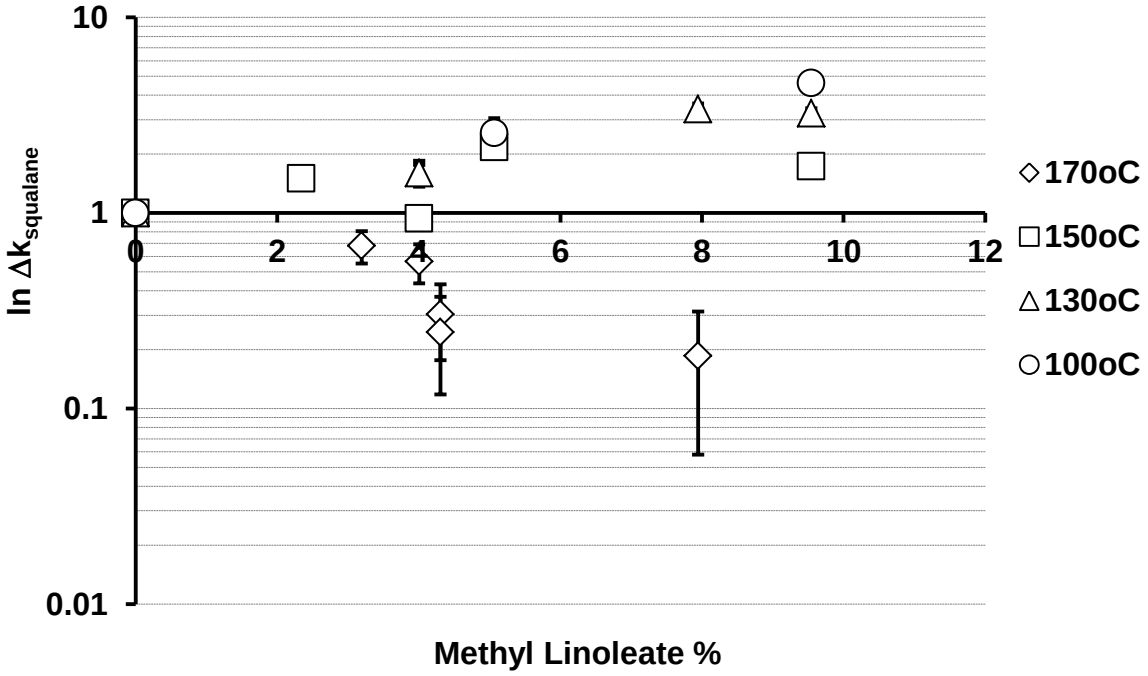

Figure 4.42 – The logarithmic relative change of squalane decay with added methyl linoleate.

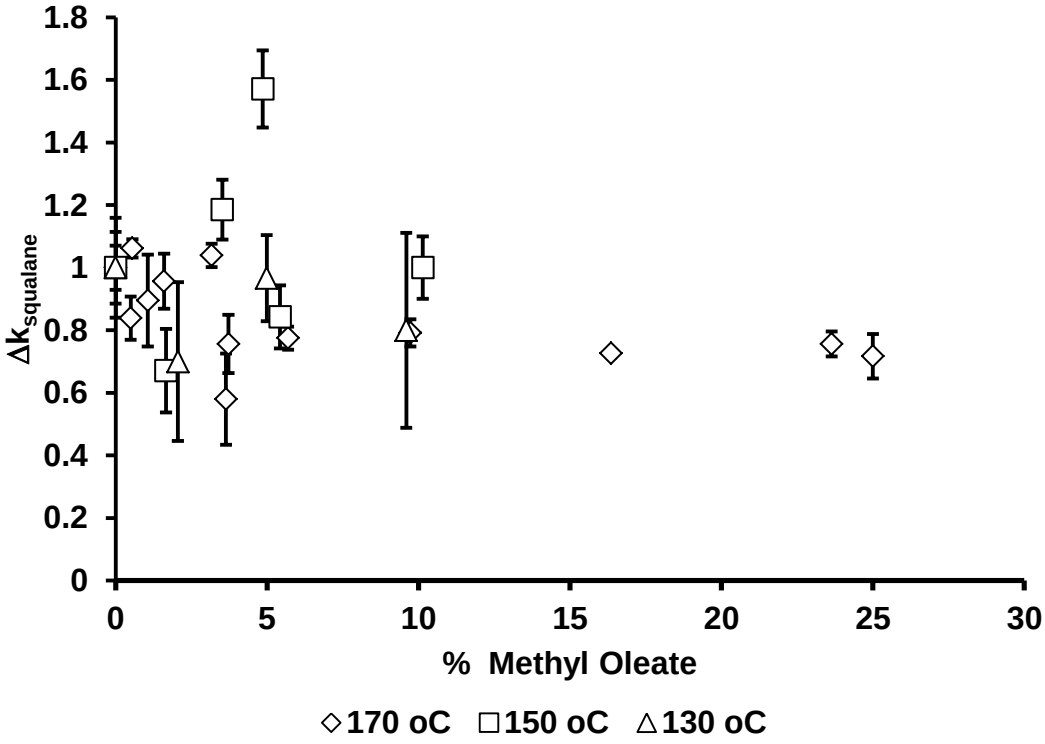

Figure 4.43 – The relative change of squalane decay with added methyl oleate.

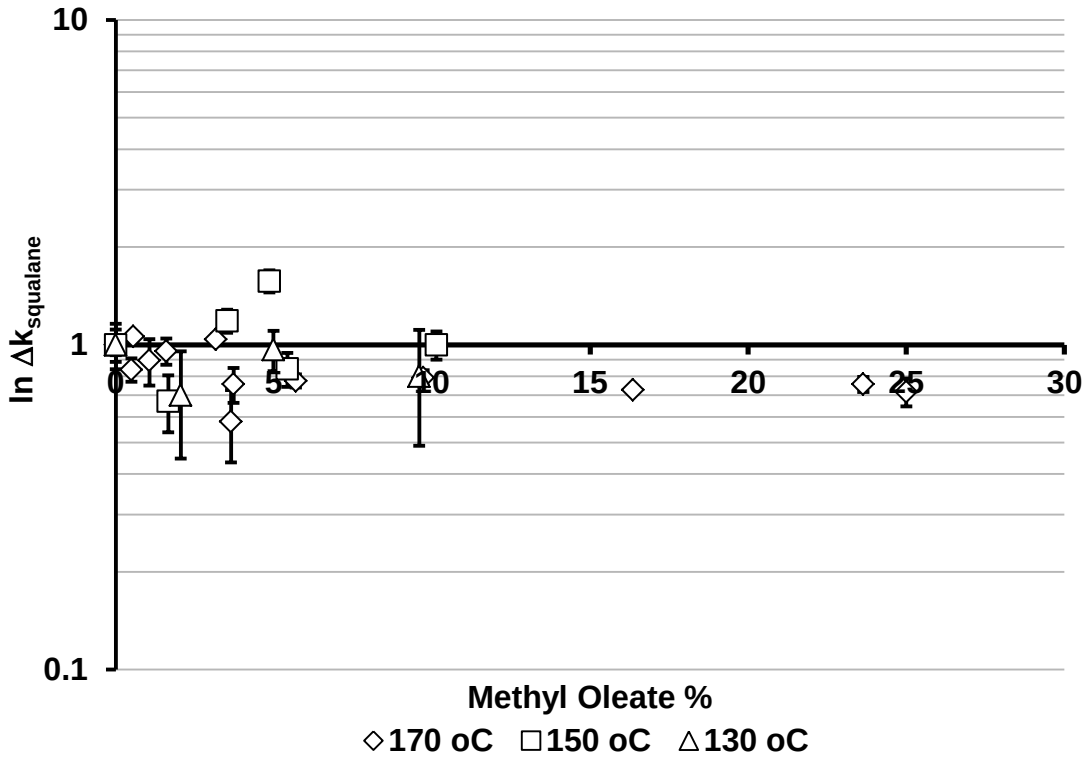

Figure 4.44 – The logarithmic relative change of squalane decay with added methyl oleate.

The trends of KV40 change were noted to show good correlation with the $k_{squalane}$ values; that the addition of methyl linoleate enhanced the rate at which they increased over time at 130 and 150 ^{o}C, yet were slowing down the rate of increase at 170 ^{o}C. This trend is once again easy to see when $KV40^{x}$ values are normalised against $KV40^{0}$ values – see figures 4.45 and 4.46. Unlike with the $k_{squalane}$ results with MO, with KV40 the same trend (increasing the rate of KV40 increase at 130 ^{o}C but reducing it at 170 ^{o}C) appeared to be observed but on a greatly reduced scale – see figures 4.47 and 4.48.

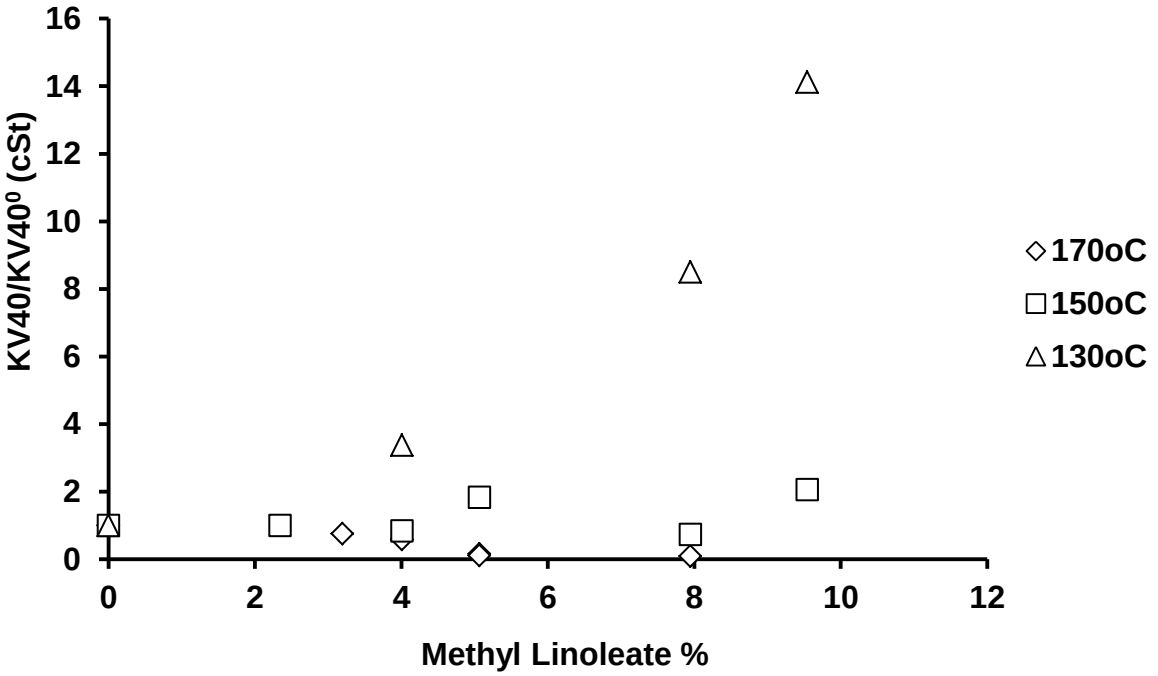

Figure 4.45 – The relative change in KV40 of squalane/methyl linoleate mixtures.

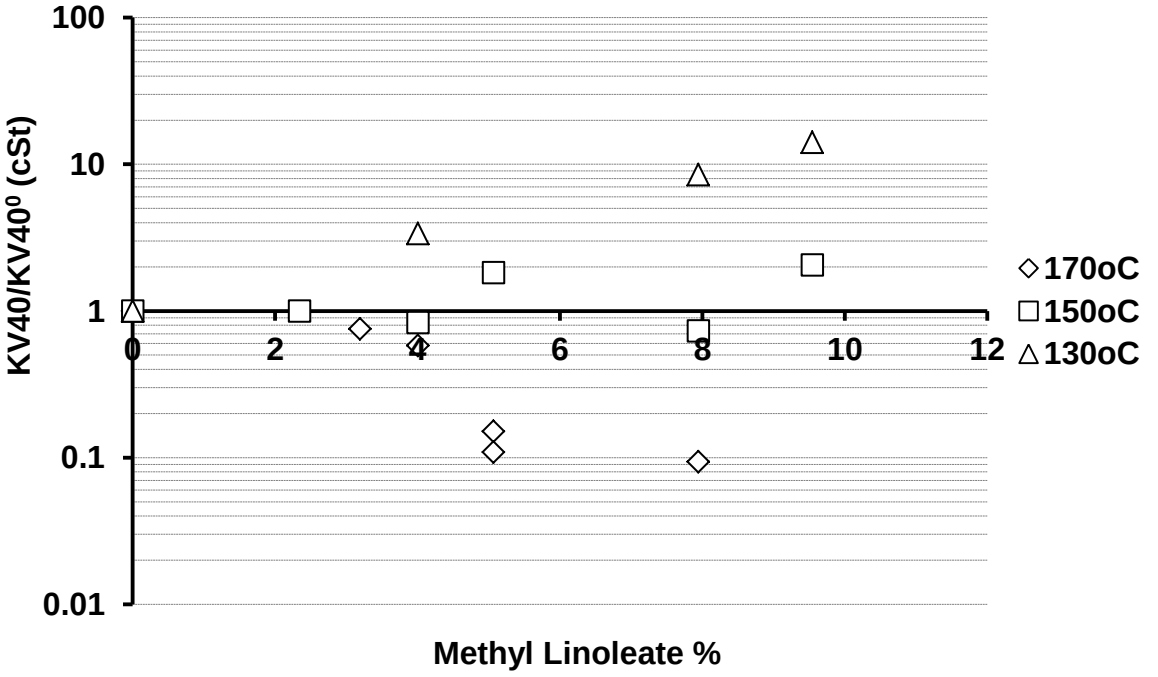

Figure 4.46 – The logarithmic relative change in KV40 of squalane/methyl linoleate mixtures.

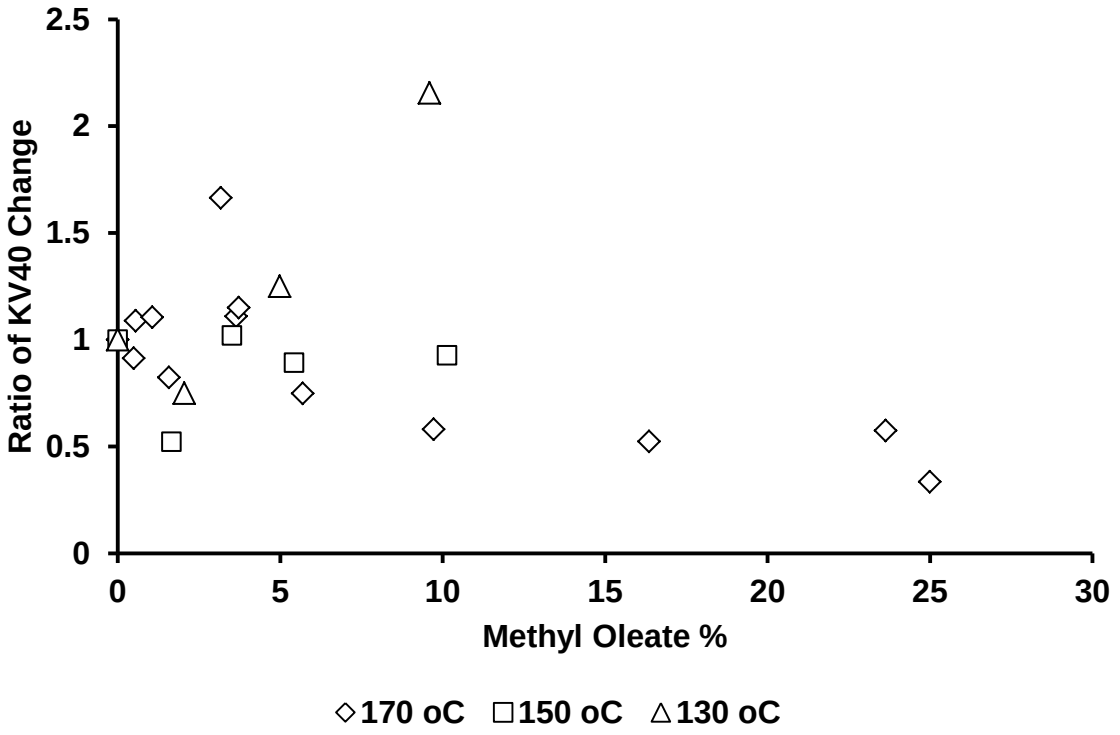

Figure 4.47 – The relative change in KV40 of squalane/methyl oleate mixtures.

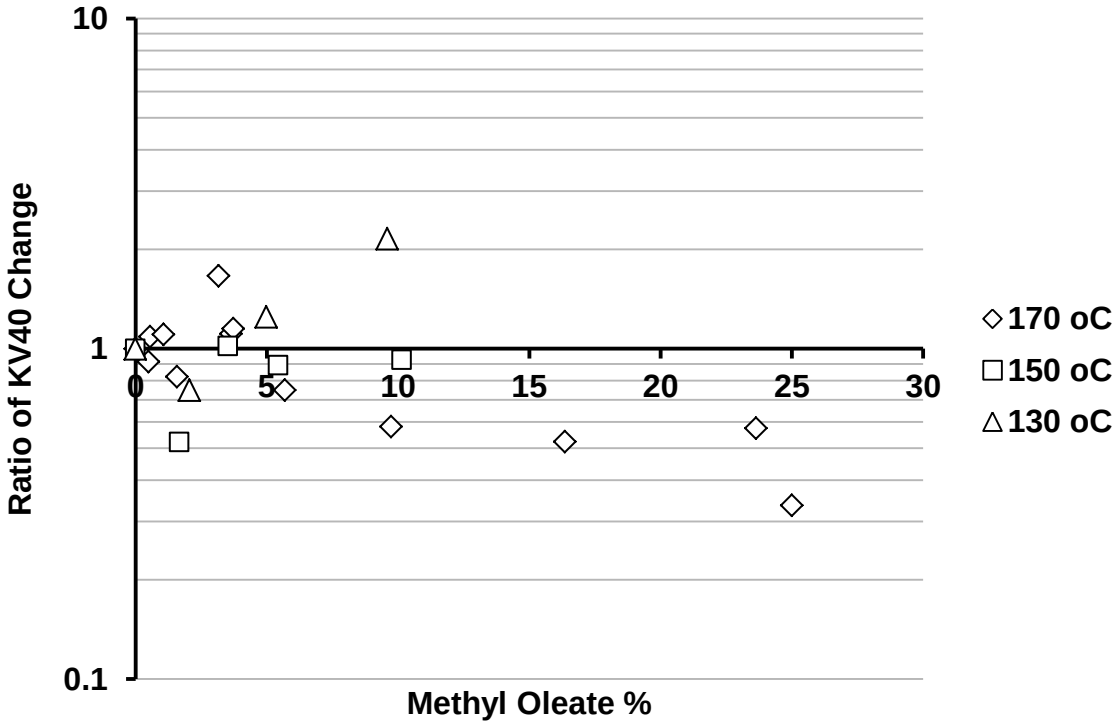

Figure 4.48 – The logarithmic relative change in KV40 of squalane/methyl oleate mixtures.

The gradient of increase or decrease of $k_{squalane}$ with added methyl linoleate or oleate were calculated from figures 4.41 and 4.43 respectively and plotted against

temperature to show in one figure (Figure 4.49) how both temperature and addition of methyl linoleate or oleate affect squalane decay – see Equation 4.4.

$$k_{squalane} change\ by\ \%ML = \frac{d\Delta k_{squalane}}{dML\%} \qquad \text{Equation 4.4}$$

For instance, at 100 ^{o}C, $k_{squalane}$ will increase by ~40% with just 1 percent methyl linoleate added – similarly an addition of 10 percent methyl linoleate will increase the $k_{squalane}$ by a factor of 4. On the other hand, at 170 ^{o}C $k_{squalane}$ will decrease by ~10% per percent methyl linoleate added whilst methyl oleate appears (within experimental error) to have no effect. Figure 4.50 shows the same graph for KV40 against temperature which correlates well with the trends shown in figure 4.49. Figure 4.49 graphically shows that there are two areas of chemistry to investigate – how the addition of methyl linoleate to squalane acts as a pro-oxidant to enhance the rate of reaction ca. below 150 ^{o}C, and why ca. below 150 ^{o}C it switches to become an antioxidant as the temperature increases as well as why methyl oleate has no significant effect whilst figure 4.50 shows a noted physical effect of these observations and hence potential relevance to full biodiesel/lubricant systems and their unwanted side effects.

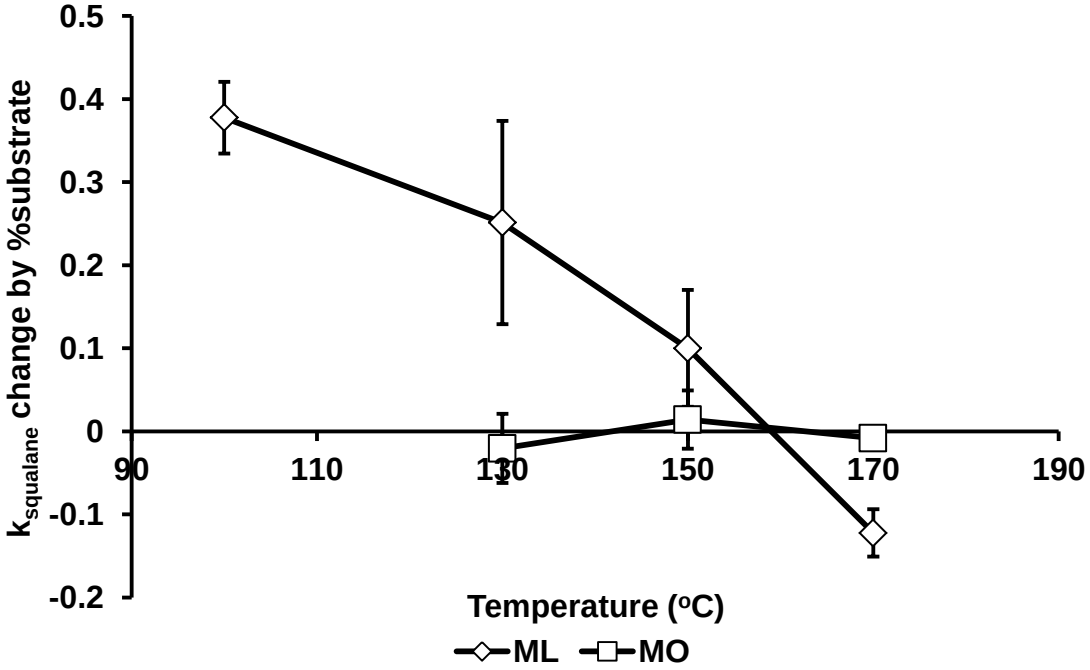

Figure 4.49 – Temperature dependence of the rate of squalane decay to added methyl linoleate/oleate.

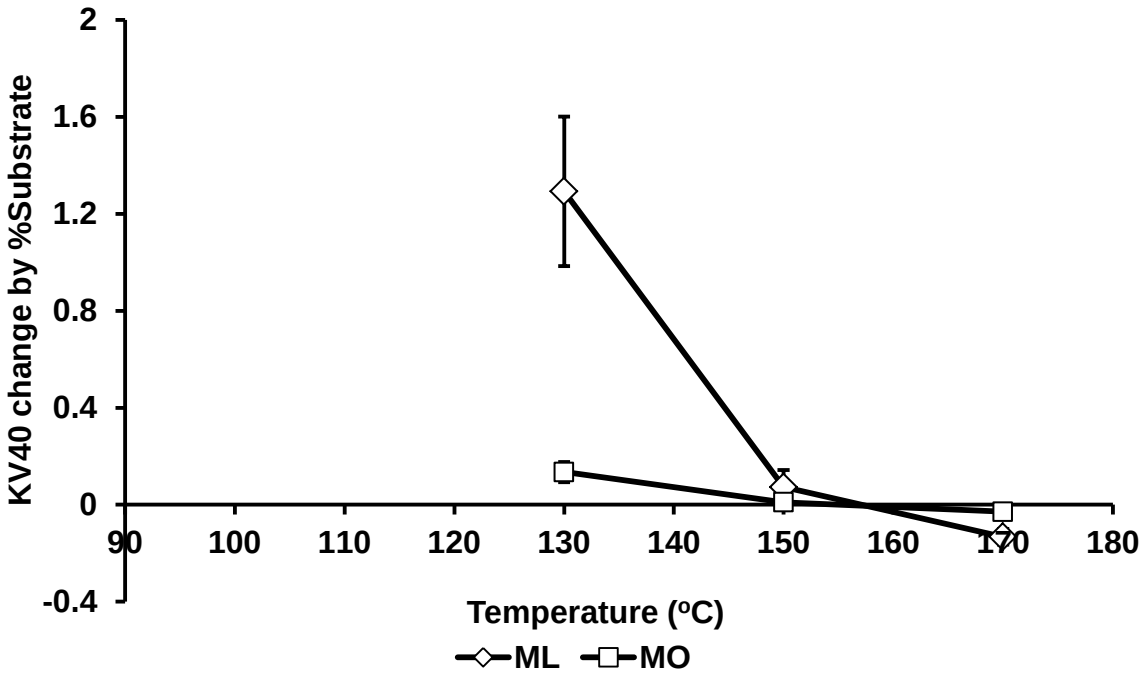

Figure 4.50 – The rate of change in KV40 of squalane per % methyl linoleate/oleate added versus temperature.

4.3.1 Pro-oxidancy of methyl linoleate in squalane at low temperatures

The pro-oxidant effect of methyl linoleate on squalane oxidation at lower temperatures can be understood by considering the mechanism of radical autoxidation as explained in chapter 3 (section 3). The oxidation cycles of both squalane and methyl linoleate are typical of hydrocarbon autoxidation cycles which are initiated by molecular oxygen abstracting a hydrogen atom from the carbon chain to form a carbon-centred radical as detailed in the Introduction (Reaction 4.1) (Frankel 1985, Gardner 1989).

$$RH + O_2 \rightarrow R\bullet + HO_2\bullet \qquad \text{Reaction 4.1}$$

This is usually followed by oxygen addition to the carbon-centred radical (Reaction 4.2) to form a peroxyl radical. The peroxyl radical formed can further attack other species to propagate the radical cycle via a number of different reactions such as abstracting a hydrogen atom from another hydrocarbon to form a carbon-centred radical and hydroperoxide (Reaction 4.3), which can undergo cleavage of the O-O bond to form a hydroxyl and alkoxyl radical (Reaction 4.4). Alkoxyl radicals can also propagate the cycle

by hydrogen atom abstraction to form an alcohol and carbon-centred radical (Reaction 4.5).

$$R\bullet + O_2 \rightarrow RO_2\bullet \qquad \text{Reaction 4.2}$$

$$RO_2\bullet + RH \rightarrow RO_2H + R\bullet \qquad \text{Reaction 4.3}$$

$$RO_2H \rightarrow RO\bullet + \bullet OH \qquad \text{Reaction 4.4}$$

$$RO\bullet + RH \rightarrow ROH + R\bullet \qquad \text{Reaction 4.5}$$

This chain reaction cycle is summarised for squalane in Figure 4.51 and for methyl linoleate in figure 4.52.

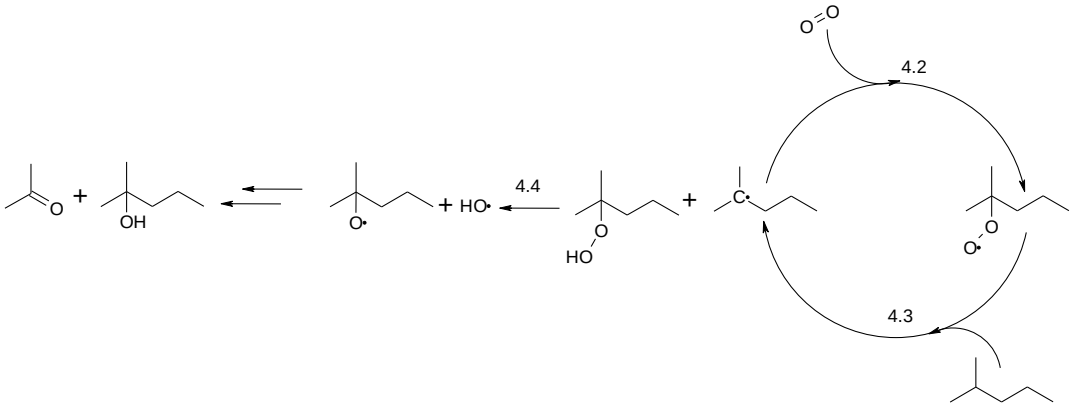

Figure 4.51 – The autoxidation cycle of squalane.

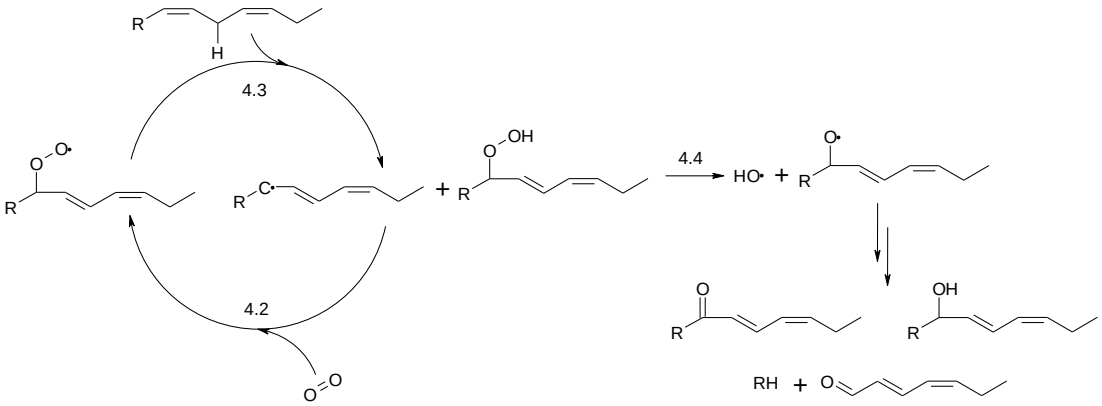

Figure 4.52 – The autoxidation cycle of methyl linoleate.

Despite some uncertainties due to assumptions, under all calulations the apparent activation energy for autoxidation, E_a, has been shown to be smaller for methyl linoleate (26.6 ±7.2 for a single Arrehnius plot or 8.6 and 12.50 for two separate ones kJ mol^{-1}, see chapter 3, section 2), than for squalane (89.6±0.6 or 102.69 ± 3.4 kJ mol^{-1}, section 2), which is consistent with the former having a highly labile, doubly allylic hydrogen atom due to the resulting radical being highly resonance stabilised as described in Chapter 3 – see figure 4.53 (BDE = 318±3 kJ mol^{-1} (McMillen 1982, Trenwith 1983, Clark 1991, Pratt 2003, Blanksby 2003)). The most labile hydrogen atoms on squalane, by comparison, are attached to the tertiary carbon atoms (BDE = 403.8±1.7 kJ mol^{-1} (McMillen 1982, Seetula 1997, Blanksby 2003)).

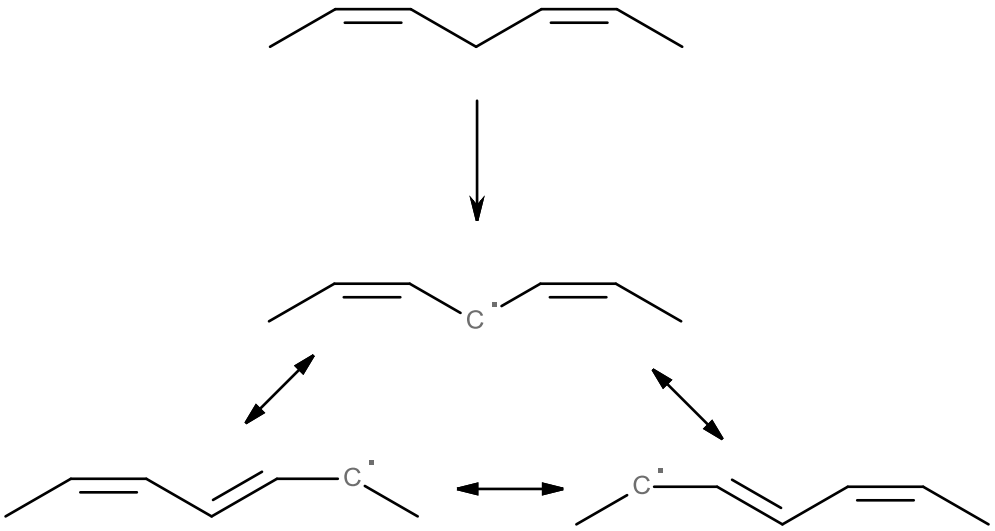

Figure 4.53 – The resonance stabilisation of a doubly allylic system.

As a result, though the basic oxidation reactions are the same for both species, the radical cycle occurs faster in methyl linoleate, also shown by the fact that the k_{ML}^0 values were larger than the $k_{squalane}^0$ at all temperatures (figures 3.4 and 4.4) – $k_{squalane}^0$ ranged from 0.032±0.009 h^{-1}at 100 ^oC to 2.976±0.185 h^{-1} at 170 ^oC, whilst k_{ML} was 2.052±0.233 h^{-1} at 100 ^oC, rising to 6.870±0.300 h^{-1} by 170 ^oC. When the two are in a mixture together, however, only one species is needed to undergo initiation for both species to enter the propagation cycle, for example, by a methyl linoleate peroxy radical ($MLO_2\bullet$) abstracting a hydrogen atom from squalane (SqH) (Reaction 4.6):

$$MLO_2\bullet + SqH \rightarrow MLO_2H + Sq\bullet \qquad \text{Reaction 4.6}$$

As a result, squalane has entered the cycle quicker and there are now more reactive radical species (mainly $RO_2\cdot$ from methyl linoleate) to ensure the propagation stages, especially via reaction 4.3, remain faster than they would be otherwise – methyl linoleate was also shown to react faster the more concentrated it is in squalane; at least at the temperatures where it acts as a pro-oxidant (figures 4.22 – 4.24). Consequently, the more methyl linoleate present in squalane, the faster the radical cycle will be propagated. The interaction between the two species is summarised in figure 4.54.

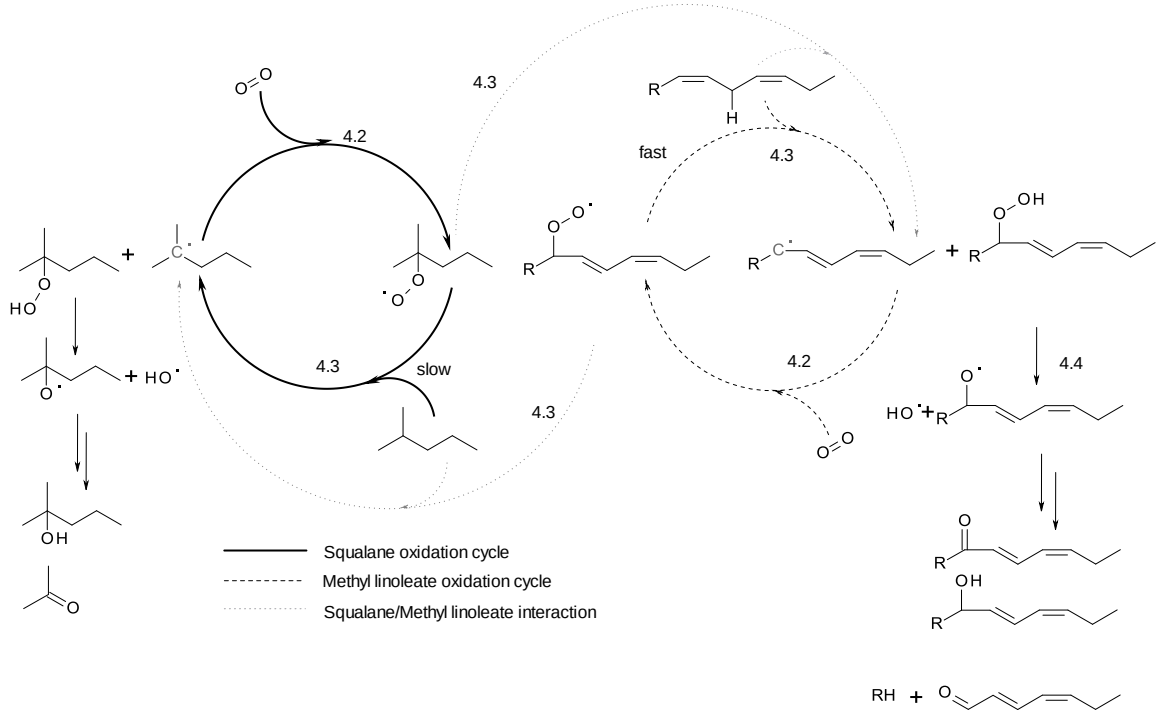

Figure 4.54 – The radical interaction between methyl linoleate and squalane.

Thus by being present alongside squalane, methyl linoleate can produce more peroxyl radicals to attack squalane with the subsequent radicals formed also propagating the cycle and hence increasing the rate of decay as seen at lower temperatures – the larger the amount of methyl linoleate, the faster the reaction of squalane, also shown by the fact that, at these temperatures, methyl linoleate itself, reacts faster the more concentrated it is.

4.3.2 Antioxidant behaviour of methyl linoleate in squalane at elevated temperatures

The observation of this rate enhancement slowing down and eventually becoming rate-inhibiting (Figure 4.49) with increasing temperature is less straightforward to understand, but can be explained by looking at the first step of the propagation cycle:

$$R\bullet + O_2 \rightleftharpoons RO_2\bullet \qquad \text{Reaction 4.2}$$

This step is necessary to form the peroxy radicals that can attack other hydrocarbon species, but crucially this step can also be reversible at a sufficiently high temperature – a process Chan (1979) identified as necessary for the isomerisation of the double bonds in methyl linoleate autoxidation (Chapter 3); in the peroxyl form, the double bond structure was locked and could only rearrange itself upon dissociation of the O_2 group. Under ambient conditions in the study, the forward reaction appeared to be dominant. It is suggested here that, if the back reaction (-4.2) is favoured then this would lead to an increased concentration of R· and hence an increase in termination of the radical cycle which can occur via the combination of two carbon-centred radicals (Reaction 4.6).

$$R\bullet + R\bullet \rightarrow RR \qquad \text{Reaction 4.6}$$

The temperature at which the equilibrium is shifted away from net build up of products over reagents in Reaction 4.2 is known as the 'ceiling temperature' (T_c), first coined by Benson in 1964, it is defined as the temperature at which the equilibrium constant of the reaction is equal to 1. That study suggested that the ceiling temperature would vary according to the stability of the radical; the more stable the radical, the lower the ceiling temperature would be. Lignola (1987) identified the ceiling temperature as the main factor in crossover between slow oxidation, cool flames and hot ignition behaviour in fuel combustion. For the reversible addition of oxygen to a carbon-centred radical (Reaction 4.2), the ceiling temperature is therefore given according to equation 4.5 as the temperature at which the forward and back reaction rates are equal (Benson 1964):

$$T = T_c \ when \ \mathrm{K} = \frac{k_{4.2(T)}}{k_{-4.2(T)}[O_2]} = 1 \qquad \text{Equation 4.5}$$

Where:

T = Temperature

T_c = Ceiling Temperature

$k_{4.2}$ = Rate constant for Reaction 4.2

$k_{-4.2}$ = Rate constant for the reverse of Reaction 4.2

$[O_2]$ = Oxygen concentration

Experimentally, from this work the temperature at which methyl linoleate changes from being a pro-oxidant to an inhibitor can be calculated from the gradient and linear regression of Figure 4.49 to give a temperature of 158±5 ^oC. The point at which this crossover physically alters the KV40 of the system can be similarly calculated from Figure 4.44 as 160 ±7 ^oC. These experiments monitor the entire set of radical reactions however, rather than limiting themselves to the single reaction of oxygen addition. Therefore, the specific ceiling temperature for the reversibility of oxygen binding to the methyl linoleate radical has not been measured from this work, but studies have been done on two similar radicals: the cyclohexadienyl radical (Taylor 2004, reaction 4.7) and the 1-4 pentadienyl radical (Zils 2001, reaction 4.8). These are both similar to ML in the fact that both are doubly unsaturated, but not conjugated molecules, but upon hydrogen abstraction can rearrange to give a highly conjugated, resonance stabilised system and hence rise to two different peroxy radical isomers.

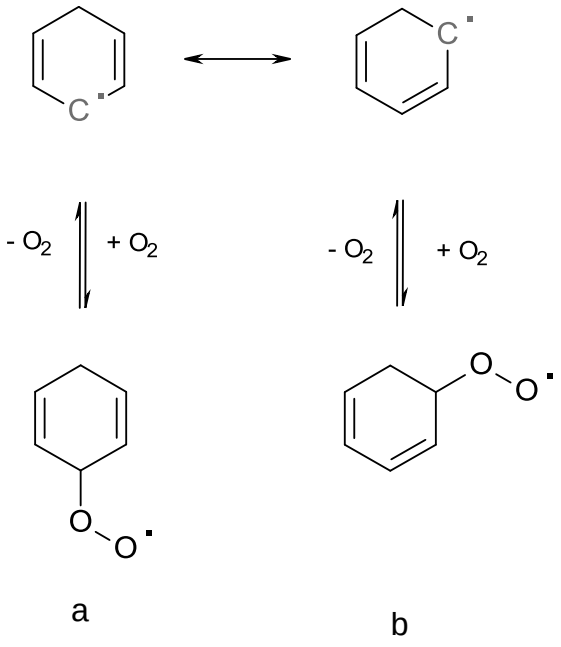

Reaction 4.7

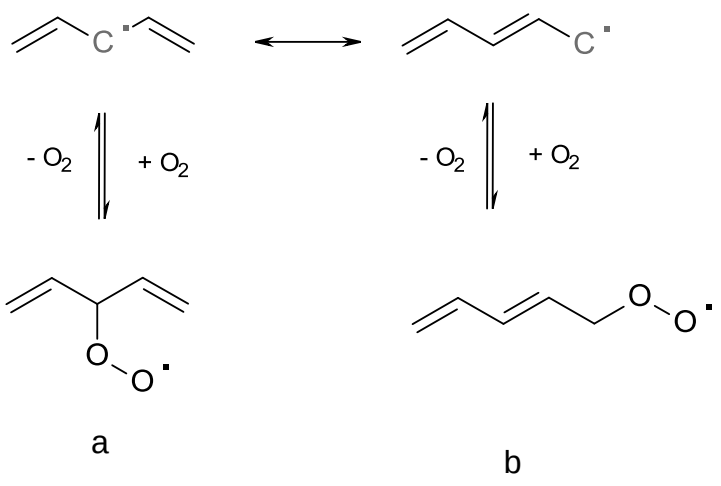

Reaction 4.8

Taylor studied the effects of solvent on the stability of the carbon-centred radicals and noted that at room temperature the right solvent, particularly cyclohexane, could stabilise the radical enough so as to favour the reagents over the products in Reaction 4.7a at low oxygen concentrations but that increasing the oxygen concentration would shift the equilibrium in favour of the products. Zils studied the direct addition of oxygen to pentadienyl radicals in the gas phase in 2001 where the observed rate constant for the addition of oxygen appeared to depend solely on the addition of O_2 at 253K in pressure controlled conditions below 6 mbar, but when the temperature increased to 333K the reverse reaction 'becomes so fast that little net reaction of C_5H_7 with O_2 occurs'. Despite this, at both temperatures, and for temperatures in between, rate constants for both the forward and reverse reactions, as well as an equilibrium constant could be determined.

By plotting the measured equilibrium constants, corrected against heat capacity, against temperature, combined with computational group additivity methods, they then proposed a ΔH_{298} value of -56±5 kJ mol^{-1} and ΔS_{298} parameters of -124 and -132 J mol K^{-1} for reactions 4.8a and 4.8b respectively. Assuming these values are independent of temperature, approximate ceiling temperatures can be calculated at standard pressure from the Gibbs Free Energy rule (Equation 4.6) as 178±4 ^oC for reaction 4.8a and 152±6 ^oC for reaction 4.8b, at standard pressure of 1 bar of oxygen.

$$\Delta G = \Delta H - T\Delta S \qquad \text{Equation 4.6}$$

As the ceiling temperature is defined as when the equilibrium constant is equal to 1 (Equation 4.5), at this temperature ΔG will be 0 (Equation 4.7).

$$\Delta G = -RTlnK \quad \text{Equation 4.7}$$

If ΔG = 0 then Equation 4.6 can be rearranged to give:

$$T_c = \frac{\Delta H}{\Delta S} \quad \text{Equation 4.8}$$

However, in this work the oxygen concentration in the liquid mixture will be noticeably lower than in the reactor headspace, according to Henry's Law – for a typical branched hydrocarbon under standard pressure of oxygen, the mole fraction of oxygen in the liquid is 23.6 kPa at 100 ^{o}C, dropping to 22.0 kPa at 170 ^{o}C and 101.325 kPa partial pressure of oxygen (Batino 1983). To calculate the effect pressure will have on the ceiling temperature it is necessary to define K as the ratio of the forward and reverse rate constants, the forward being dependent on oxygen content from Equation 4.5. Combining Equations 4.6 and 4.7 gives:

$$\Delta H - T\Delta S = -RTlnK \quad \text{Equation 4.9}$$

Substituting Equation 4.5 in:

$$\Delta H - T\Delta S = -RTln\left(\frac{k_{4.2}[O_2]}{k_{-4.2}}\right) \quad \text{Equation 4.10}$$

Dividing both sides by -RT:

$$\frac{\Delta H}{-RT} - \frac{\Delta S}{R} = ln\left(\frac{k_{4.2}[O_2]}{k_{-4.2}}\right) \quad \text{Equation 4.11}$$

At standard pressure $[O_2]$ = 1bar, hence $[O_2]^{\phi}$. Hence from Gibb's free energy law and taking exponentials from both sides:

$$\frac{k_{-4.2}}{k_{4.2}[O2]^{\phi}} = e^{\left(\frac{\Delta H^{\phi}}{RT_c}\right)} e^{\left(\frac{-\Delta S^{\phi}}{R}\right)} \quad \text{Equation 4.12}$$

From equation 4.8, at $T = T_c$,

$$k_{-4.2} = k_{4.2}[O_2] \qquad \text{Equation 4.13}$$

Substituting 4.13 into 4.12:

$$\frac{k_{4.2}[O_2]}{k_{4.2}[O_2]^{\phi}} = e^{\left(\frac{\Delta H^{\phi}}{RT_c}\right)} e^{\left(\frac{\Delta S^{\phi}}{R}\right)} \qquad \text{Equation 4.14}$$

Taking natural logs of both sides and cancelling gives:

$$\ln \frac{[O_2]}{[O_2]^{\phi}} = \frac{\Delta H^{\phi}}{RT_c} - \frac{\Delta S^{\phi}}{R} \qquad \text{Equation 4.15}$$

Rearranging gives:

$$T_c = \frac{\Delta H^{\phi}}{\Delta S^{\phi} + R \ln \frac{[O_2]}{[O_2]^{\phi}}} \qquad \text{Equation 4.16}$$

Using the previous values for ΔH and ΔS and using the calculated value (from Batino's work on Henry's Law constants for O_2 dissolved in branched hydrocarbons) of 22.38 kPa for $[O_2]$ gives ceiling temperatures at these pressures of:

T_c 4.8a = 173 ± 6 ^{o}C

T_c 4.8b = 146 ± 7 ^{o}C

This is in good agreement with the crossover temperature 158 ± 5 ^{o}C measured experimentally in this work, especially as ML oxidation will occur through a mixture of both reactions as shown in Chapter 3. It would appear though, that reaction 4.8b is favoured due to the formation of the conjugated structure – the dominant peaks in the GC traces were the ones with this structure, though the fragments that would be formed via

reaction 4.8a were also detected confirming that oxygen will add to ML radicals via both reaction pathways.

With regard to the chemistry of the squalane/methyl linoleate system, the temperature at which the net production of R• radicals are favoured over the production of RO_2• radicals is the point at which the chemistry of the system changes and the reversibility leads to build-up of R• radicals which then have more chance of combining with each other to terminate the cycle rather than propagate it, especially as the percentage of methyl linoleate, and hence R• radicals in the mixture increases.

As the doubly allylic system is the only functional group not present to both methyl oleate and methyl linoleate, this would suggest that methyl oleate should either have a much reduced effect on squalane oxidation, or no effect at all, with the latter being indicated by the results obtained in this chapter. If there were to a similar (reduced) effect, then the derived equation for ceiling temperature it is possible to calculate a theoretical T_c if ΔH^{ϕ} and ΔS^{ϕ} values exist for the addition of oxygen to the alkyl chain radical. Ruiz (1981) studied this for allyl (C_3H_5) radicals and estimated ΔH to be -71.9 kJ mol^{-1} at 300K and ΔS to be -110.4 J K^{-1} mol^{-1} at 348 Kwhich, using equation 4.15, would give a ceiling temperature of 370 ^{o}C.

4.3.3 Relevance to behaviour of methyl linoleate in engines

The mechanistic switching between pro-oxidant and antioxidant behaviour of methyl linoleate on squalane becomes of considerable interest when the typical engine temperatures are considered. The lowest temperatures that a lubricant experiences are typically in the sump, which is also where the highest amount of fuel dilution occurs as unburned fuel migrates down the cylinder walls (Rakopoulos 2006). Vehicles using post-injection of fuel to burn off soot as it accumulates on the DPFs (see Introduction) are especially prone to this effect. Due to legislation on particulate matter reductions (EC Regulation Nos. 715/2007 and 595/2009), these systems will become commonplace over the next few years as there is (as yet) no other reported technology capable of reducing particulate matter to the levels required by legislation.

With mineral diesel, this was not so much of a problem as during the engine run, a portion of the unburned fuel would evaporate out as the temperature rose. As biodiesel components are typically larger and less volatile (Goodrum 2002, Owczarek 2003 & 2004, Yuan 2005), biodiesel has a greater tendency to accumulate; a typical fuel containing a

blend of 10% biodiesel to mineral diesel (B10) can end up becoming 50% biodiesel (B50) in the sump (Jones 2008) as the mineral diesel evaporates off. In terms of fuel dilution, this can correspond to a B10 fuel being diluted down roughly by a factor of 10 in the sump at 100 ^{o}C (Shayler 2000), i.e. if the lubricant consists of 1% biodiesel, after the mineral diesel fraction of the fuel evaporates off the biodiesel fraction can concentrate to 5% in the lubricant – quite significant as at 100 ^{o}C a 5% addition of methyl linoleate has the ability to double the rate of base fluid autoxidation (figure 4.44). Partial pressure of oxygen would have to be taken into account to determine at what point the ceiling temperature would actually occur in the sump, however, as the headspace above would contain a large amount of nitrogen from the atmosphere, as well as any exhaust gases from the combustion chamber. Using Equation 4.10, the ceiling temperatures have been calculated for a range of oxygen partial pressures below.

Table 4.3 – The ceiling temperature for oxygen addition to ML radicals at different partial pressures of oxygen.

T_c (^{o}C)		Partial pressure of oxygen (bar)			
		1	0.1	0.01	0.001
	Reaction 4.8a	178.5	170.2	162.3	154.5
	Reaction 4.8b	151.1	143.8	136.8	130.0

By contrast, the highest temperatures achieved in the engine are typically in the combustion chamber where the fuel is injected. As the first lubricated area the fuel will encounter is with the piston in the cylinder, the antioxidant effect of methyl linoleate at higher temperatures in the chamber is of relatively little importance as far as the lubricant chemistry is concerned. What is perhaps more significant, however, is the unsaturated fuel's ability to form polymeric compounds (Chapter 3) via radical termination reactions at higher temperatures due to the build up of R• radicals. As the fuel is nearly in its neat form in the combustion chamber, upon oxidation the carbon centred radicals would be in relatively high concentration, further promoting the dimerisation reactions and potentially leading to the piston deposits noted on biodiesel usage.

4.4 Summary

In summary, the addition of methyl linoleate – a model biodiesel compound – to squalane – a model lubricant compound – was investigated at 4 different temperatures from 100 to 170 ^{o}C. The rate of reaction of squalane oxidation increased with temperature as did the rate of KV40 increase of the liquid. At lower temperatures the addition of methyl linoleate increased both these factors as a pro-oxidant. As the temperature increased, however, the role of methyl linoleate switched to become an inhibitor. This behaviour was explained by investigating the role of oxygen binding to a carbon-centred radical to form peroxy radicals – at low temperatures, the production of peroxy radicals was favoured – hence more rapidly producing a reactive species able to attack other molecules. As the temperature rose, the equilibrium continued to shift towards the dissociation of oxygen from the peroxy radicals until the production of carbon-centred radicals became more favoured, which could then terminate the radical cycle more easily rather than propagate it as the peroxy radicals did. The fact that methyl oleate did not exhibit this behaviour suggests that the doubly allylic system is indeed the key functional group responsible for the behaviour shown, as the theoretical ceiling temperature for the reversible binding of oxygen to MO radicals would be 369.6 ^{o}C which is far above the temperatures used for these experiments. As methyl oleate boils at 346 ^{o}C (Krop 1997) experiments to test the effect of methyl oleate on squalane above this ceiling temperature would be difficult and probably impossible on the described experimental setup. As this temperature is also above the typical temperatures in the engine, particularly those in the sump, these would probably be irrelevant to the significance effect of biodiesel on engine lubricants.

4.5 References

Adamczyk, A.A. Kach, R.A. A Combustion Bomb Study of Fuel-Oil Solubility and HC Emissions from Oil Layers, *Twentieth Symposium (International) on Combustion/The Combustion Institute*, 1984, 37-43.

Agarwal, A.K. Das, L.M. Biodiesel Development and Characterization for Use as a Fuel in Compression Ignition Engines. *J. of Eng. For Gas Turbines and Power*, 2001, **123,** 440-447.

Agarwal, A. K. Biofuels (Alcohols and Biodiesel) Applications as Fuels for Internal Combustion Engines, *Progress in Energy and Combustion Science*, 2007, **33**, 233.

Batino, R. Rettich, T.R. Tominaga, T. The Solubility of Oxygen and Ozone in Liquids, *J. Phys. Chem. Ref. Data,* 1983, **12(2),** 163-178.

Benson, S.W. Effect of Resonance and Structure on the Thermochemistry of Organic Peroxy Radicals and the Kinetics of Combustion Reaction, *J. Am. Chem. Soc* 1964, **87(5)**, 972-980.

The British Petroleum Company - Industrial Lubrication. 1966. Published East Grinstead, The British Petroleum Company.

Blanksby, S.J. Ellison, G.B. Bond Dissociation Energies of Organic Molecules, *Acc. Chem. Res.* 2003, **36,** 255-263.

Conrad, B.R. Evaluation of Diesel Particulate Filter Systems at Stobie Mine, *Diesel Emission Evaluation Program,* INCO, 2006, 28-29

Chan, H.W.S. Levett, G. Matthew, J.A. The Mechanism of the Rearrangement of Linoleate Hydroperoxides. *Chemistry and Physics of Lipids,* 1979, **24**, 245-256.

Clark, K.B. Culshaw, P.N. Griller, D. Lossing, F.P. Martinho Simões, J.A. Walton, J.C. Studies of the Formation and Stability of Pentadienyl and 3-Substituted Pentadienyl Radicals, *J. Org. Chem.* 1991, **56,** 5535-5539.

Dermibas, A. Progress and Recent Trends in Biodiesel Fuels, *Energy Conversion and Management,* 2009, **50,** 14-34.

Engler, C. R. J. Johnson, L.A. Effects of Processing and Chemical Characteristics of Plant Oils on Performance of an Indirect-Injection Diesel Engine, *J. Am. Oil Chem. Soc.*, 1983, **60**, 1592–1596.

Fazal, M.A. Haseeb, A.S.M.A. Masjuki, H.H. Biodiesel Feasibility Study: An Evaluation of Material Compatibility; Performance; Emission and Engine Durability, *Renewable and Sustainability Energy Reviews,* 2011, **15(2),** 1314-1324.

Frankel, E.N. Chemistry of Free Radical and Singlet Oxidation of Lipids. *Prog. Lipid Res.* 1985**, 23**,197-221.

Gardner, H.W. Oxygen Radical Chemistry of Polyunsaturated Fatty Acids, *Free Radical Biology & Medicine,* 1989, **7,** 65-86

Golden, D.M. Benson, S.W. *Chem.Rev* 1969, **69**,125.

Goodrum, J.W. Volatility and Boiling Points of Biodiesel from Vegetable Oils and Tallow, *Biomass and Bioenergy,* 2002, **22**, 205–211.

Gupta, S.A. Cochran, H.D. Cummings, P.T. Shear Behaviour of Squalane and Tetracosane under Extreme Confinement. I. Model, Simulation Method and Interfacial Slip, *J. Chem. Phys,* 1997, **107(23),** 10316-10326.

Gupta, S.A. Cochran, H.D. Cummings, P.T. Shear Behaviour of Squalane and Tetracosane under Extreme Confinement. II. Confined Film Structure, *J. Chem. Phys,* 1997, **107(23),** 10327-10334.

Gupta, S.A. Cochran, H.D. Cummings, P.T. Shear Behaviour of Squalane and Tetracosane under Extreme Confinement. III. Effect of Confinement on Viscosity, *J. Chem. Phys,* 1997, **107(23),** 10334-10343.

Hu, J. Du, Z. Li, C. Min, E. Study on the Lubrication Properties of Biodiesel as Fuel Lubricity Enhancers, *Fuel,* 2005, **84,** 1601-1606.

Jabbarzadeh, A. Atkinson, J.D. Tanner, R.I. The effect of Branching on Slip and Rheological Properties of Lubricants in Molecular Dynamics Simulation of Couette Shear Flow, *Tribology International,* 2002, **35(1),** 35-46.

Jones, C. Interactions Between Biofuels and Lubricants and Effects on Engine Oil Durability, *2008 SAE Biofuels: Specifications and Performance Symposium,* Paris, France. July 2008.

Kaiser, E.W. Admczyk, A.A. Lavoie, G.A. The Effect of Oil Layers on the Hydrocarbon Emissions Generated During Closed Vessel Combustion, *Eighteenth Symposium (Inetnational) on Combustion/The Combustion Institute*, 1981, 1881-1890.

Kittelson, D.B. Engines and Nanoparticles: A Review, *J. Aerosol Sci.* 1998, **29(5/6),** 575-588

Krop, H.B. v. Velzen, M.J.M. Parsons, J.R. Govers, H.R.J. Determination of Environmentally Relevant Physical-Chemical Properties of Some Fatty Acid Esters, *JAOCS,* 1997, **74(3),** 309-315

Lightfoot, P.D. Cox, R.A. Crowley, M. Destriau, M. Hayman, G.D. Jenkin, M.E. Moortgat, G.K. Zabel, F. Organic Peroxy Radicals: Kinetics, Spectroscopy and Tropospheric Chemistry, *Atmospheric Environment,* 1992, **26(10)**, 1805–1961.

Lignola, P.G. Reverchon, E. Cool Flames, *Prog. Energy Combust. Sci.* 1987, **13,** 75-96.

Ma, F. Hanna, M.A. Biodiesel Production: A Review, *Bioresource Technology,* 1999, **70,** 1-15.

Masjuki, H.H. Maleque, M.A. The Effect of Palm Oil Diesel Fuel Contaminated Lubricant on Sliding Wear of Cast Irons against Mild Steel, *Wear,* 1996, 198, 293-299.

McMillen, D.F. Golden, D.M. Hydrocarbon Bond Dissociation Energies, *Ann. Rev. Phys. Chem,* 1982, **33,** 493-532.

Monyem, A. Canakci, M. Van Gerpen, J.H. Investigation of Biodiesel Thermal Stability Under Simulated In-Use Conditions, *Am. Soc. of Agricultural Eng,* 2000, **16(4)**, 373-378.

Moritani, H. Nozawa, Y. Oil Degradation in Second-Land Region of Gasoline Engine Pistons. *R&D Review of Toyota CRDL*, 2004, **38(3)**, 36-43.

Owczarek, I. Blazej, K. Recommended Critical Temperatures. Part I. Aliphatic Hydrocarbons. *J. Phys. Chem. Ref. Data* 2003, **32(4)**, 1411-1428.

Owczarek, I. Blazej, K. Recommended Critical Temperatures. Part II. Aromatic and Cyclic Hydrocarbons. *J. Phys. Chem. Ref. Data* 2004, **33(2)**, 541-547.

Pratt, D.A. Mills, J.H. Porter, N.A. Theoretical Calculations of Carbon-Oxygen Bond Dissociation Enthalpies of Peroxyl Radicals Formed in the Autoxidation of Lipids, *J. Am. Chem. Soc.* 2003, **124**, 5801-5810.

Radu, R. Petru, C. Edward, R. Gheroghe, M. Fueling an D.I. Agricultural Diesel Engine with Waste-Oil Biodiesel: Effects Over Injection, Combustion and Engine Characteristics, *Energy Conversion and Management,* 2009, **50,** 2158-2166.

Rakopoulos, C.D. Antonopoulos, K.A. Rakopoulos, D.C. Hountalas, D.T. Giakoumis, E.G. Comparative Performance and Emissions Study of a Direct-injection Diesel Engine Using Blends of Diesel fuel with Vegetable Oils or Bio-diesels of Various Origins, *Energy Conversion and Management,* 2006, **47**, 3272-2387.

Ruiz, R.P. Bayes, K.D. Macpherson, M.T. Pilling, M.J. Direct Observation of the Equilibrium between Allyl Radicals, O_2, and Allylperoxy Radicals, *J. Phys. Chem.* 1981, **85**, 1622-1624.

Ryan, T. W. III. Dodge, L.G., Callahan, T.J. The Effects of Vegetable Oil Properties on Injection and Combustion in Two Different Diesel Engines, *J.Am.Oil.Chem.Soc,* 1984, **61**, 1610–1619.

Sapaun, S.M. Masjuki, H.H. Azlan, A. The Use of Palm Oil as Diesel Fuel Substitute. *J. Power Energy A.* 1996, **210**, 47–53.

Seetula J.A. Slagle I.R. Kinetics and thermochemistry of the R+ HBr $\leftrightarrow$ H+ Br (R= *n*-C_3H_7, *iso*-C_3H_7 , *n*-C_4H_9 , *iso*-C_4H_9 , *sec*-C_4H_9 or *tert*-C_4H_9) equilibrium, *J. Chem. Soc. Faraday Trans.* 1997, **93,** 1709-1719.

Shayler, P.J. Winborn, L.D. Hill, N.J. Eade, D. Fuel Transport to the Crankcase, Oil Dilution and HC Return with Breather Flow During the Cold Operation of a SI Engine, *SAE 2000 World Congress,* 2000, Paper No. 2000-01-1235.

Stark, M.S. Wilkinson, J.J. Lindsay Smith, J.R. Alfadhl, A. Pochopien, B.A. Autoxidation of Branched Alkanes in the Liquid Phase, *Ind, Eng. Chem. Res.* 2011, **50,** 817-823

Sumathi, S. Chai, S.P. Mohamed, A.R. Utilization of Palm Oil as a Source of Renewable Energy in Malaysia, *Renewable and Sustainable Energy Reviews,* 2008, **12**, 2404–2421.

Taylor, J.W. Ehlker, G. Carstensen, H.H. Ruslen, L. Field, R.W. Green, W.H. Direct Measurement of the Fast, Reversible Addition of Oxygen to Cyclohexadienyl Radicals in Nonpolar Solvents, *J. Phys. Chem. A.* 2004, **108,** 7193-7203.

Taylor, R.I. Evans, P.G. *In-situ* Piston Measurements, *Proc. Instn. Mech. Engrs.* 2004, **218**(J: J. Engineering Tribology), 185-200.

Trenwith, A.B. Dissociation of 3-methyl-1,4-pentadiene and the Resonance Energy of the Pentadienyl Radical *J. Chem. Soc. Faraday Trans. 1, Physical Chemistry in Condensed Phases,* 1982, **78(10),** 3131-3136.

Van Setten, B.A.A.L. Makkee, M. Moulijn, J.A. Science and Technology of Catalytic Diesel Particulate Filters, *Catalysis Reviews,* 2001, **43(4),** 489-564.

Van Wechel, T. Gustafson, G.R. Leistritz, F.L. Economic Feasibility of Biodiesel Production in North Dakota, *Agribusiness and Applied Economics Report* 2002, **505.**

Yang, J. Stewart, M. Maupin, G. Herling, D. Zelenyuk, A. Single Wall Diesel Particulate Filter (DPF) Filtration Efficiency Studies Using Laboratory Generated Particles, *Chemical Engineering Science,* 2008, **64(8),** 1625-1634.

Yuan, W. Hansen, A.C. Zhang, Q. Vapor Pressure and Normal Boiling Point Predictions for Pure Methyl Esters and Biodiesel Fuels. *Fuel,* 2005, **84**, 943-950.

Zils, R. Inomata, S. Imamura, T. Miyoshi, A. Washida, N. Determination of the Equilibrium Constant and Thermodynamic Parameters for the Reaction of Pentadienyl Radicals with O_2, *J. Phys. Chem. A.* 2003, **105,** 1277-1282.

Chapter 5. The Effect of Additives on Methyl Linoleate and Squalane

5.1 Introduction

As with many products, neither lubricants nor fuels are supplied as single chemicals, or even sole combinations of their major components. They are instead treated, generally at less than 5% composition, with chemicals known as additives which serve to enhance the product in various ways by altering in a positive manner various properties such as hardness, elasticity or (crucially for lubricant chemistry) viscosity and resistance to degradation, to keep the product suitable for the task, either whilst in storage, or to increase the working lifetime and/or performance of the product during this period.

Perhaps the most important group of additives in the fuel and lubricant industry are the antioxidants – chemicals added to prevent oxidation of the product (Mahoney 1969). Antioxidants are not confined to lubricant chemistry but are found in a vast range of systems, both biological and non-biological. As molecular oxygen is both a powerful oxidising agent and present at 21% of the atmosphere, it is inevitable that any system exposed to air will be vulnerable to oxidation. In fuel and lubricant systems, oxidation can lead to detrimental products and processes such as polymerisation, previously outlined in greater detail in chapters 1, 3 and 4. In biological systems oxidation can lead to cell and DNA damage (Hochstein 1988, Hu 1995, Gedik 2002) and hence many plants produce antioxidant chemicals to protect themselves; ascorbic acid (Vitamin C – figure 5.1) is an example of a natural antioxidant (Cort 1982, Yen 2002).

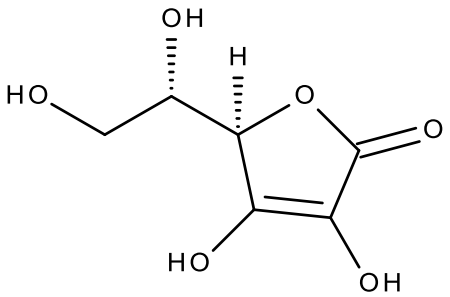

Figure 5.1 – The chemical structure of ascorbic acid (Vitamin C).

Whilst nature already provides a large range of antioxidants to work with, as these compounds are produced in plants and animals evolved to survive at ambient temperatures, they are not necessarily as well suited to the elevated temperatures and other harsh conditions found inside the engine. Fortunately, as the mechanisms of these compounds

have been studied and understood, it has been possible to develop synthetic antioxidants drawing on these principles. The most common types are developed around a benzene ring and are of two types; phenolic and aminic antioxidants.

Other important additives in lubricant chemistry include: anti-wear additives, corrosion inhibitors, detergents, dispersants, viscosity modifiers and antifoaming agents. Overall, as a package, the additives typically make up around 5% of the lubricant (Stachowiak 2006).

5.1.1 Phenolic Antioxidant Mechanism

The mechanism for phenolic antioxidants centres around the fact that after hydrogen abstraction, the resulting radical can be resonance stabilised around the delocalised aromatic ring (reaction 5.1), in a similar manner to the allylic radicals in methyl oleate and linoleate.

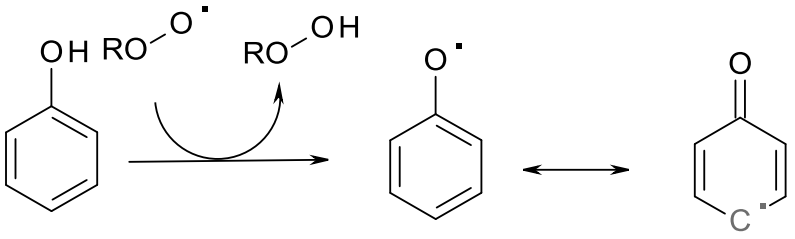

Reaction 5.1 – The hydrogen abstraction from a phenolic ring.

The O-H bond dissociation energy can be lowered further by introducing stabilising groups onto the ring. The most commonly used group is the t-butyl group on both the ortho- positions. An alkyl, or alkyl ester R group at the para- position can also help stabilise the radical, see figure 5.2

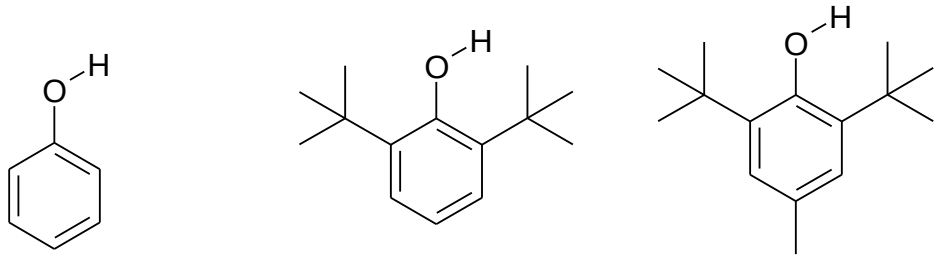

361.9 ± 8.0 346.4 ± 0.9 339.0

Figure 5.2 – Bond dissociation energies (kJ mol^{-1}) of the O-H bond in 3 phenolic species. (Denisov 2005, McMillen 1982, Wright 2001)

In addition to lowering the bond dissociation energy of the O-H bond, the R group can also change the antioxidant properties in other ways. Firstly, a long alkyl chain can increase the boiling point of the molecule – a point frequently utilized in lubricant chemistry to ensure the antioxidant does not evaporate out of the base fluid during the harsh temperatures experienced in engines. However, an alkyl chain attached to the aromatic ring can, if sufficiently stable as a radical, become a leaving group when substituted by peroxy radicals. This is achieved when peroxy radicals add to the phenoxyl radical formed in a reaction (usually at the para- position) to form a peroxide. The peroxide bond then generally cleaves to give two alkoxyl radicals; the phenolic alkoxyl one then loses the alkyl chain to form a stable quinone molecule, reaction 5.2 (Mahoney 1975).

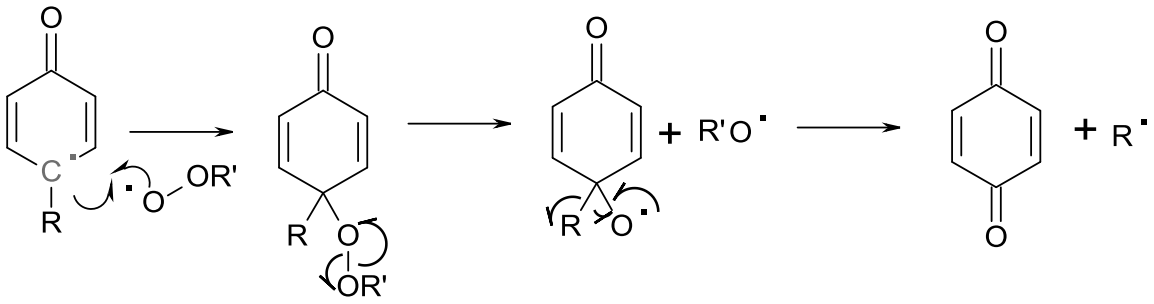

Reaction 5.2 – The formation of 1, 4- Benzoquinone from a phenolic antioxidant intermediate.

The overall aim of the synthesis of these antioxidants is that they will produce more stable radicals and hence be targeted preferentially by peroxy radicals as opposed to the fuel/lubricant molecules they are meant to be protecting. In terms of efficiency, in reactions 5.1 and 5.2, two peroxy radicals are consumed, however one carbon centred radical is produced, which will be susceptible to reaction with oxygen to generate a peroxy radical meaning in practice, the net consumption of peroxy radicals is only one. This overall count of radicals consumed is termed the stoichiometric number and is commonly used to evaluate the efficiency of an antioxidant.

5.1.2 Aminic Antioxidant Mechanism

As with phenolic antioxidants, aminic antioxidants work through stabilisation of the radical intermediate through an aromatic ring. Unlike phenolic antioxidants though, the

aminic group is generally attached to two benzene rings, hence providing an additional resonance structure for stabilisation – reaction 5.3.

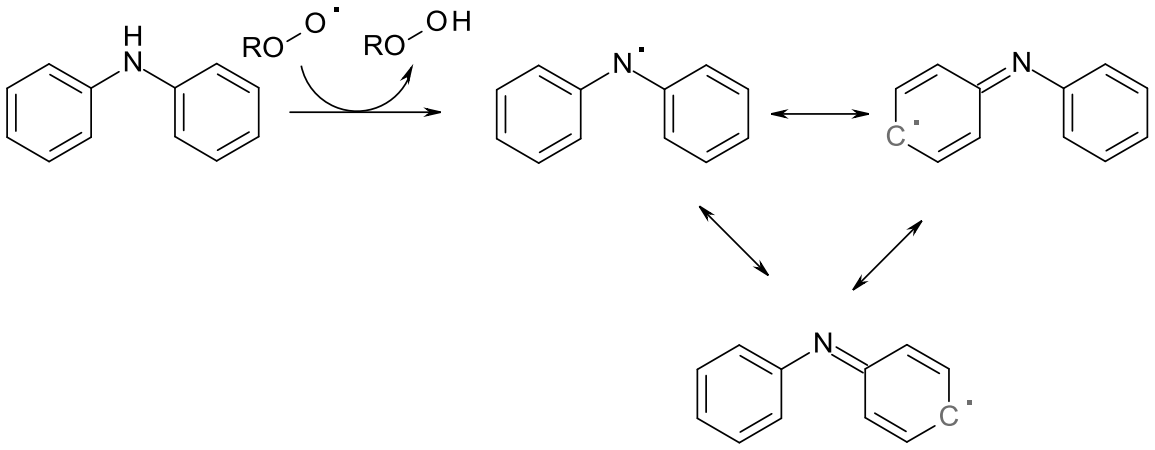

Reaction 5.3 – The hydrogen abstraction from an aminic antioxidant.

Despite being attached to two benzene rings, the bond dissociation energy of the N-H bond is only 364.7 kJ mol^{-1} which is close to the phenolic O-H bond of 361.9 ± 8 kJ mol^{-1} (Denisov 2005). Again, these energies can be lowered (and raising the boiling point) by introducing alkyl groups onto the benzene ring, but the lowest recorded value by Denisov is still 358.8 kJ mol^{-1} when introducing t-butyl groups onto the para- position of both aromatic rings (see figure 5.3), which is still higher than for the phenolic antioxidants mentioned previously at 339.0 kJ mol^{-1}.

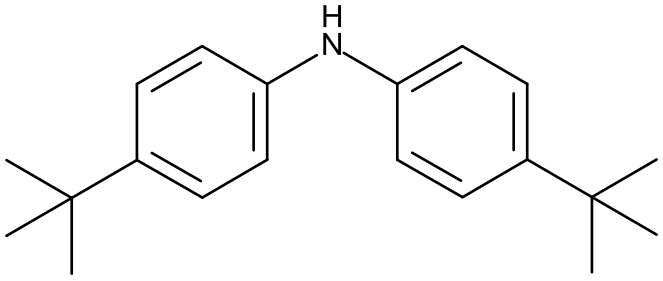

Figure 5.3 – An aminic antioxidant stabilised by t-butyl groups on the para positions of the aromatic ring.

The advantages that aminic antioxidants have over their phenolic counterparts however is their potential to achieve much higher stoichiometric numbers due to the role of the nitroxy radical formed through the reaction of peroxy radicals, reaction 5.4

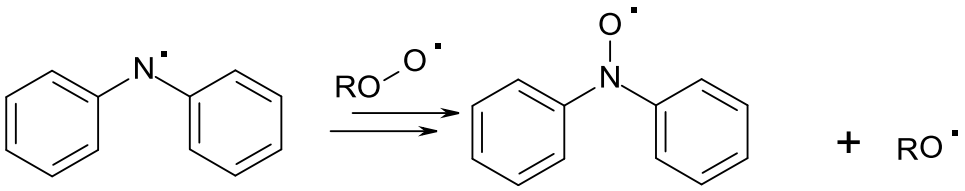

Reaction 5.4 – The formation of the nitroxyl radical

These radicals are heavily resonance stabilised through both the aromatic rings and the fact that both nitrogen and oxygen can support charge easier then carbon can in organic molecules (see figure 5.4) meaning they are formed more easily than their phenolic counterparts and as a result, at a sufficiently high temperature (varies according to substituents on the aromatic rings) are capable of being regenerated during radical cycles (Figure 5.5 – Denisov 1989, Rudnick 2009). This chain reaction is known as the 'Denisov Cycle' and as a result of the regeneration of radical scavenging agents, stoichiometric numbers as high as 40 have been reported, again depending on the substituents on the aromatic rings (Jensen 1995).

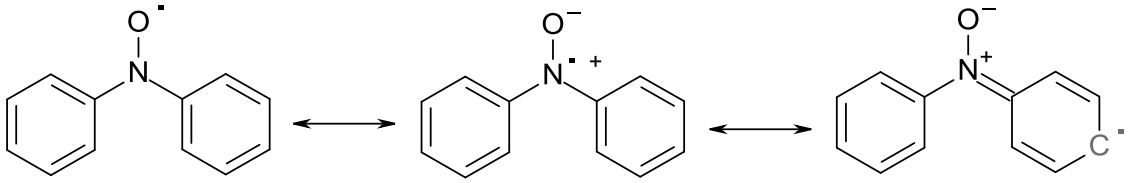

Figure 5.4 – The resonance stabilisation if the nitroxyl radical.

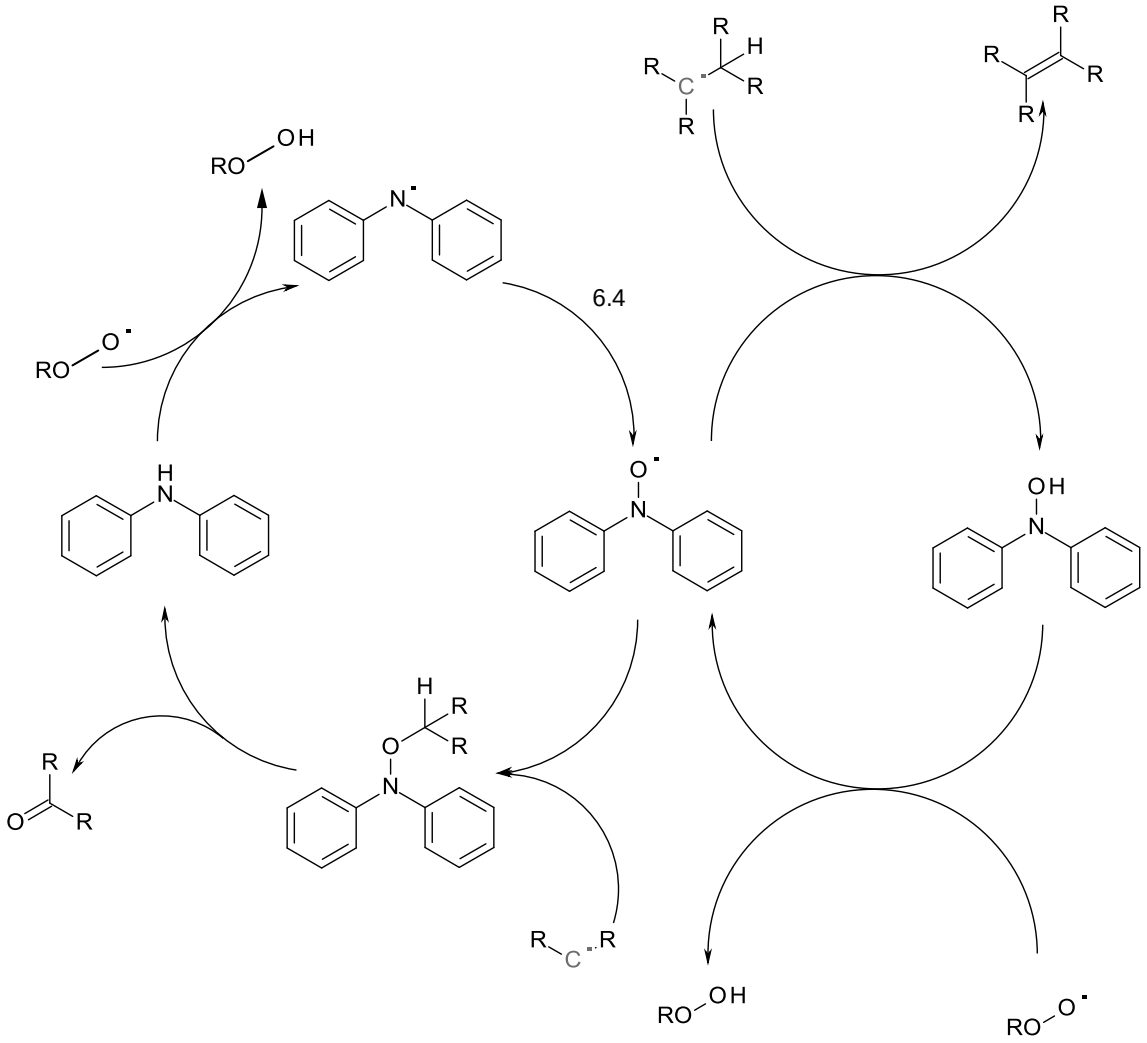

Figure 5.5 – The Denisov cycle. – From Denisov 2005

5.2 Results

5.2.1 The Effect of Additives on Squalane

5.2.1.1 Phenolic Antioxidants

The first additive investigated was a phenolic antioxidant Octadecyl 3-(3,5 di-tertbutyl, 4-hydroxyphenyl propanoate) (Irganox L107 – see Figure 5.6). This was chosen as it is a commercially available antioxidant from BASF, and its structure, chemical formula and mass were known, allowing accurate concentration values to be calculated. Also, it eluted as a single peak in GC work making it relatively straightforward to monitor.

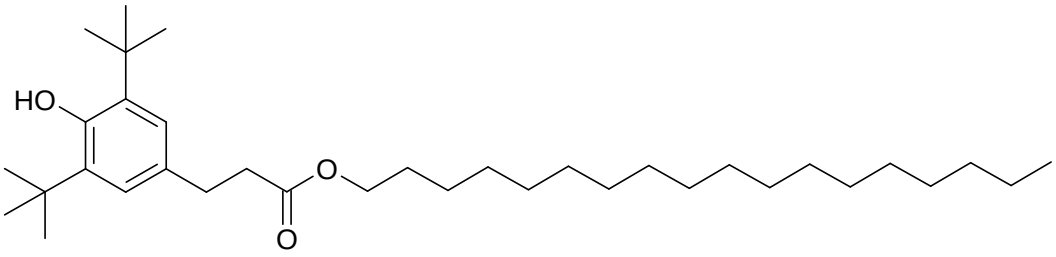

Figure 5.6 – The structure of Irganox L107.

The first reactions were done using the static oxidation method explained in Chapter 2 to measure the induction time of the reactions. Figure 5.7 below shows two sample pressure traces.

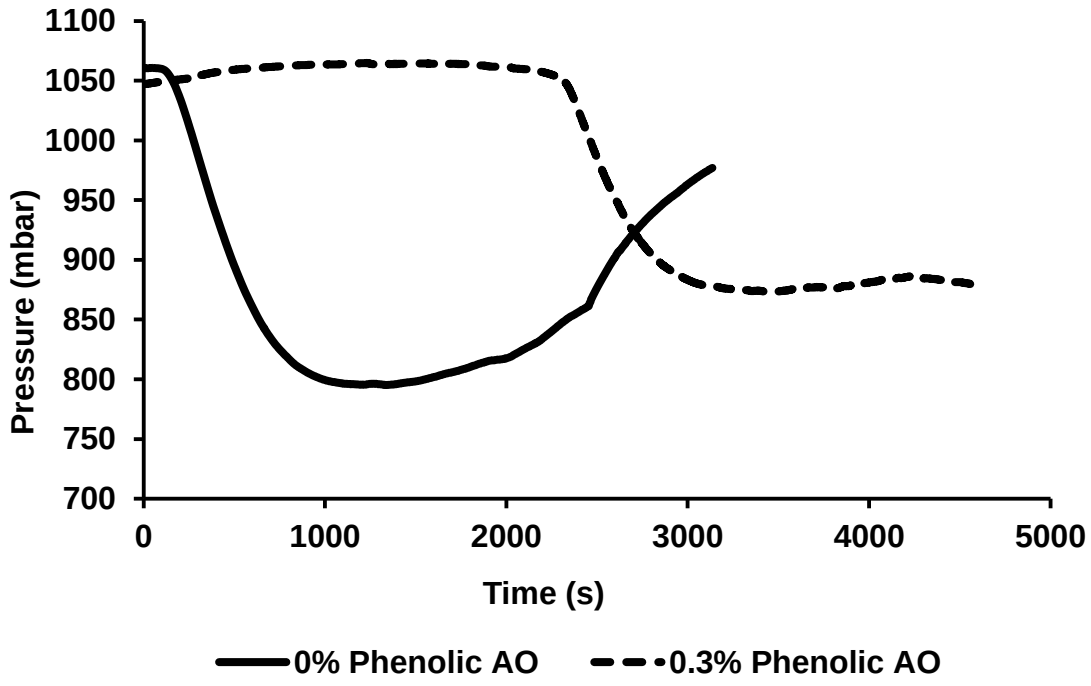

Figure 5.7 – The pressure traces of squalane by itself and with 0.3% Irganox L107 at 170 ^{o}C under 1 bar of oxygen.

These traces show that the antioxidant greatly extended the induction period, but that once the reaction started the rates of pressure drop and hence, oxygen consumed were very similar to one another, suggesting that the antioxidant was delaying the onset of the reaction, but having little effect once started. The induction period was measured at several different concentrations at 170 ^{o}C where it was seen that only trace amounts of antioxidant

were needed to increase the induction period, but that this effect seemed to plateau out at approximately 0.5% addition of L107. At 130 ^{o}C, the rates of reaction were much slower, the timescale being measured in hours rather than seconds, but the overall trend was similar to that at 170 ^{o}C (see figures 5.8 and 5.9).

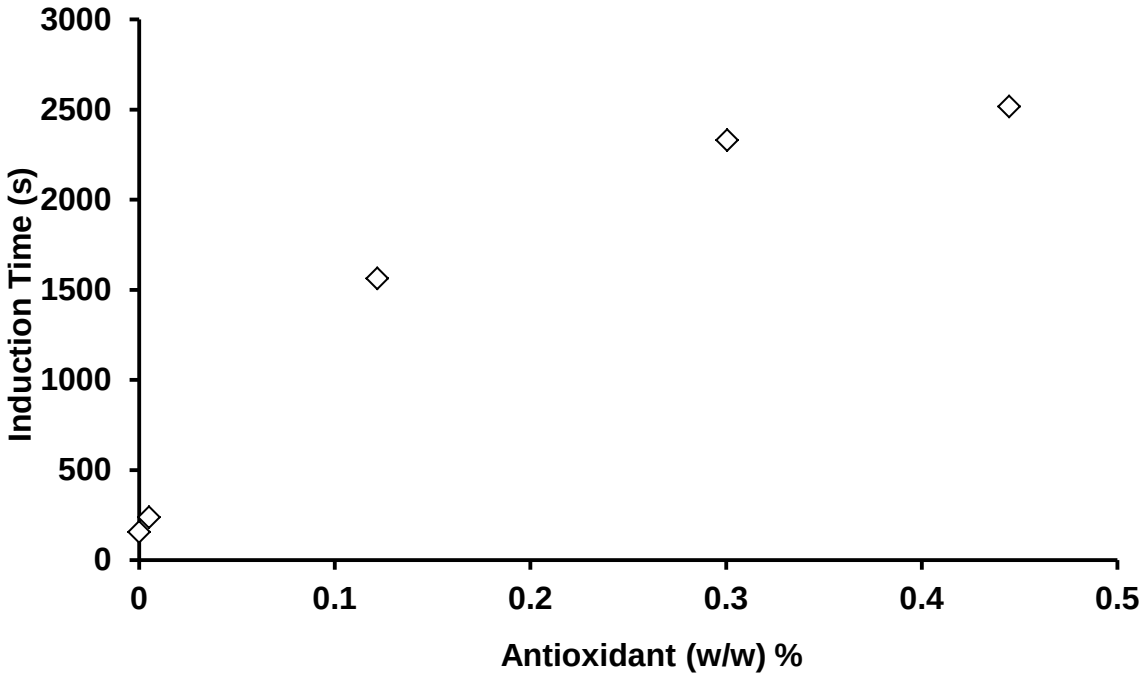

Figure 5.8 – The induction time of squalane with varying amounts of Irganox L107 at 170 ^{o}C.

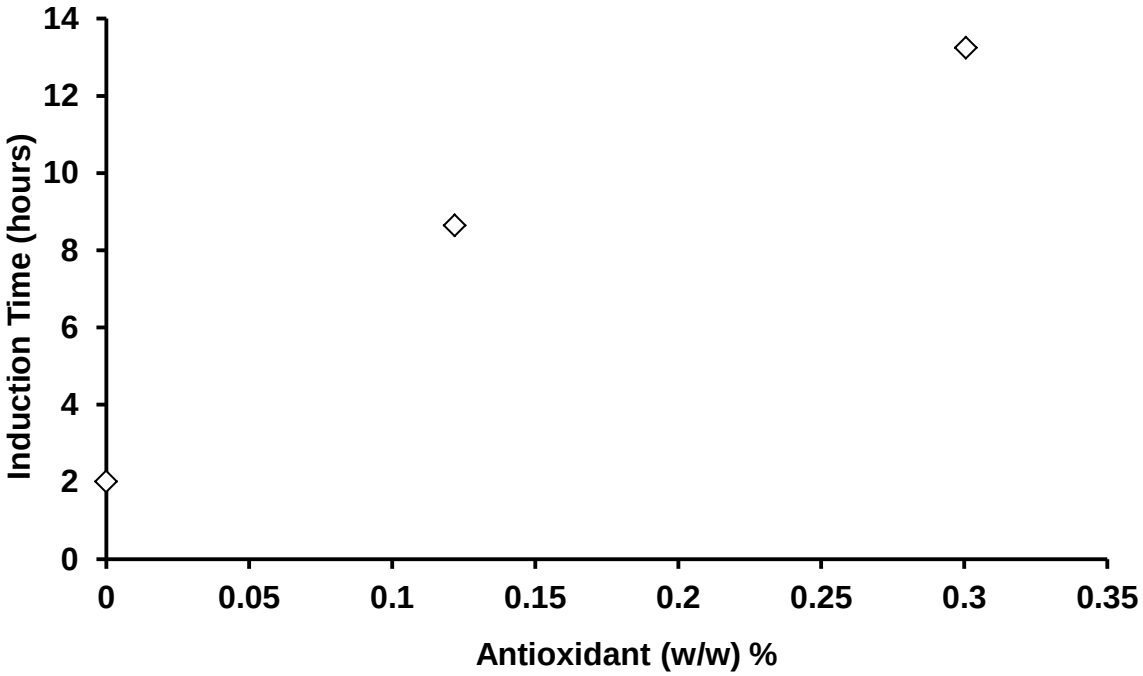

Figure 5.9 – The induction time of squalane with varying amounts of Irganox L107 at 130 ^{o}C.

5.2.1.2 Aminic Antioxidants

The second additive to be tested was an aminic sourced antioxidant from Lubrizol. This is an in-house additive, not currently commercially available and hence is identified only by its product code, OS146100 and the generic chemical structure shown below, where the R group is a range of branched alkyl chains (see Figure 5.10).

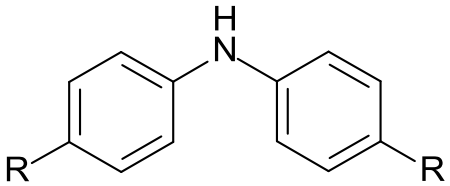

Figure 5.10 – The generic chemical structure of aminic antioxidant OS146100.

The initial experiments done were identical to the ones for Irganox L107 and the trends in the results were also very similar – addition of antioxidant would initially increase the induction time, but would then plateau out. At 170 ^{o}C, OS146100 was initially a stronger antioxidant than L107 at low concentrations, but appeared to reach its threshold

at a lower concentration (see Figure 5.11), whilst at 130 °C, OS146100 was a stronger antioxidant at all measured concentrations (see Figure 5.12).

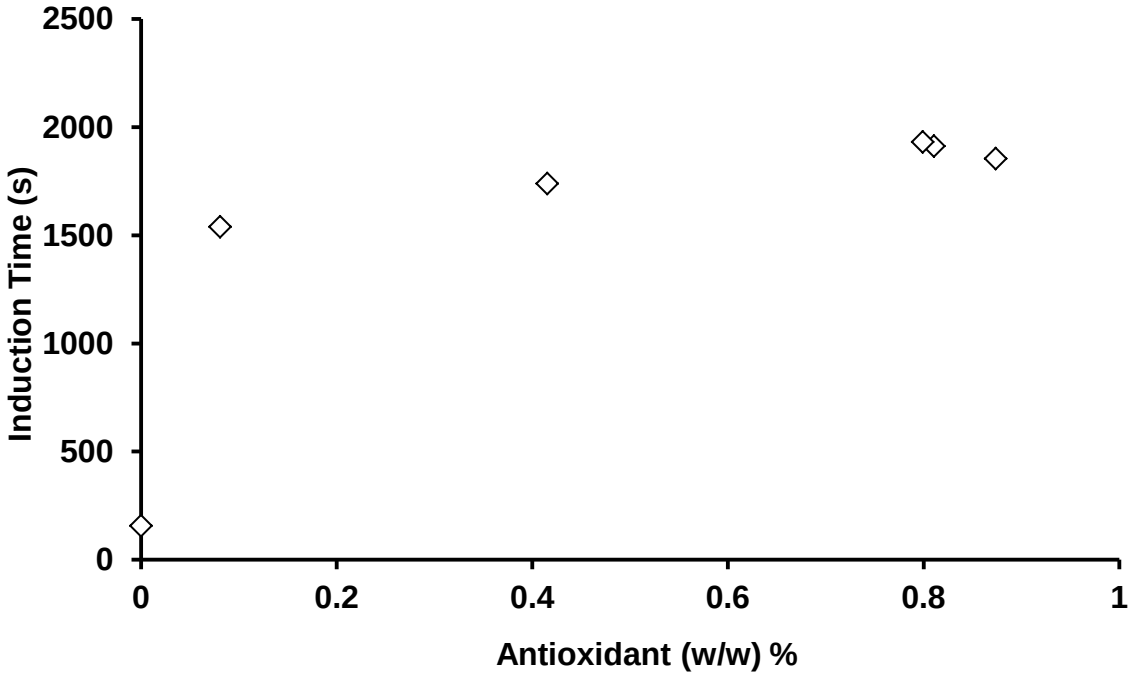

Figure 5.11 – The induction time of squalane with varying amounts of aminic antioxidant OS146100 at 170 °C.

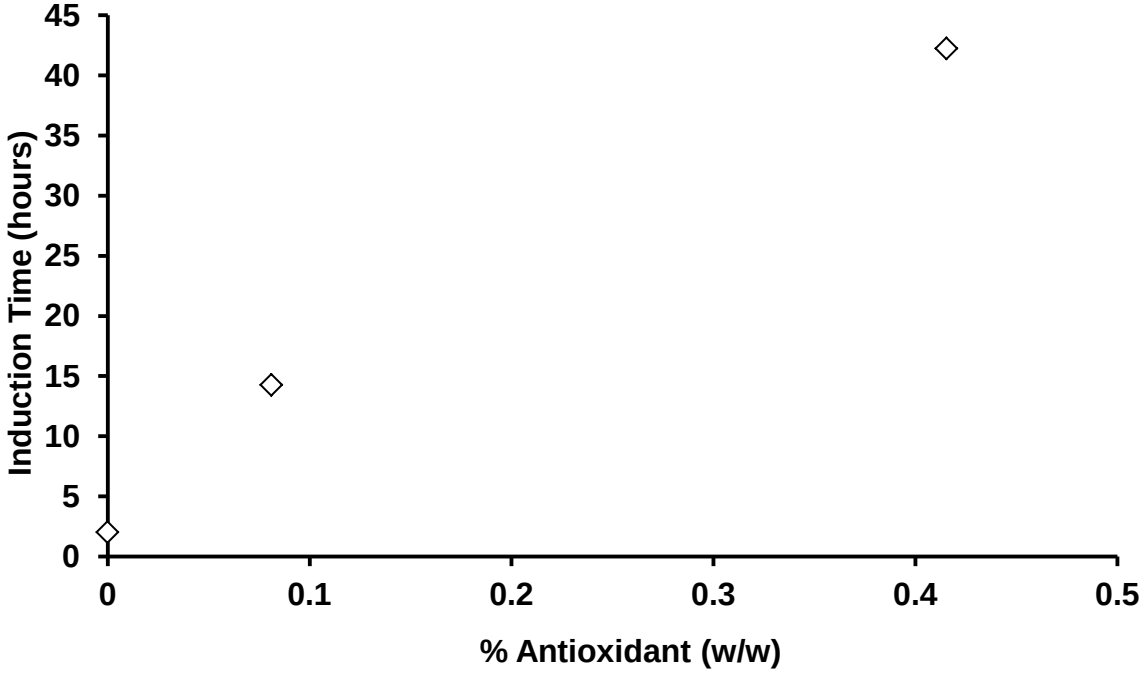

Figure 5.12 – The induction time of squalane with varying amounts of aminic antioxidant OS146100 at 130 °C.

5.2.1.3 Detergent

The final additive to be investigated was another Lubrizol in-house additive; an overbased sodium sulphonate detergent with the generic chemical structure $RC_6H_4SO_3Na/Na_2CO_3$ (see figure 5.13) is available, with the R group being unknown and identified by its product code OS102880.

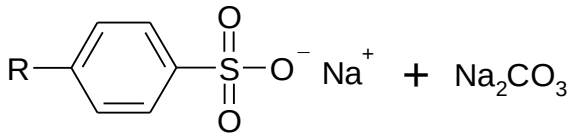

Figure 5.13 – The generic chemical structure for detergent OS102880.

Initially static oxidation runs were carried out to see if the detergent mechanism was comparable, or could be measured in the same way antioxidants. However this did not appear to be the case; at both 170 and 130 ^{o}C, the addition of OS102880 initially served to reduce the induction period, in one case at 170 ^{o}C eliminating it altogether, although at higher concentrations the induction period then started to decrease – see figures 5.14 and 5.15.

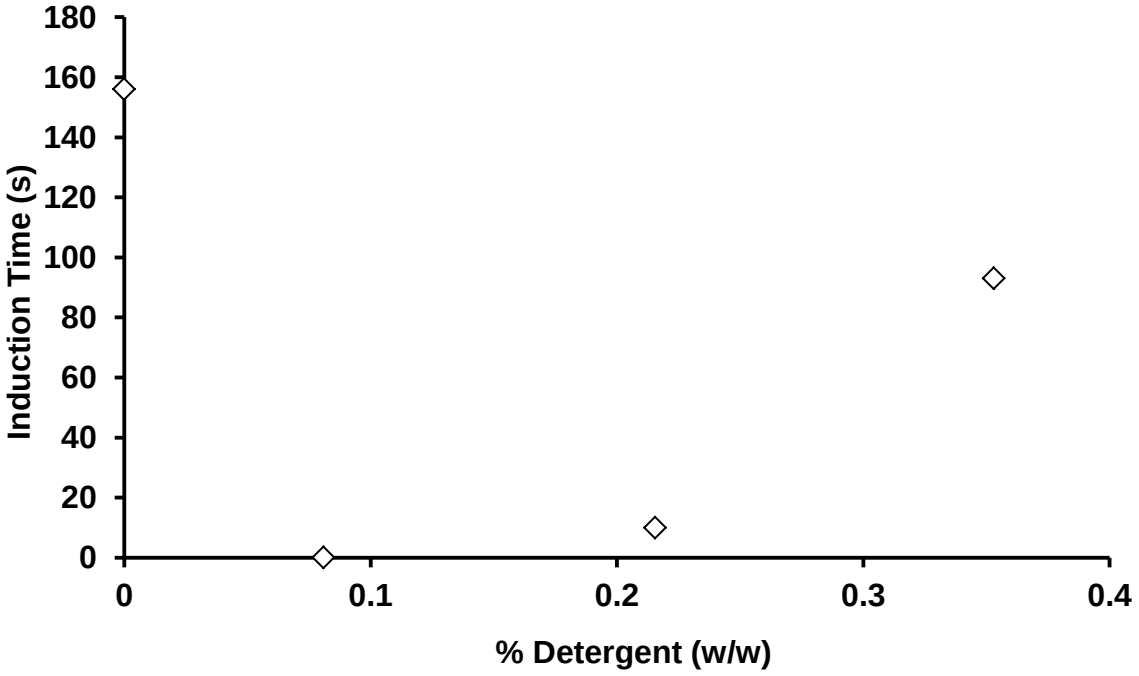

Figure 5.14 – The induction time of squalane with varying amounts of detergent OS102880 at 170 ^{o}C.

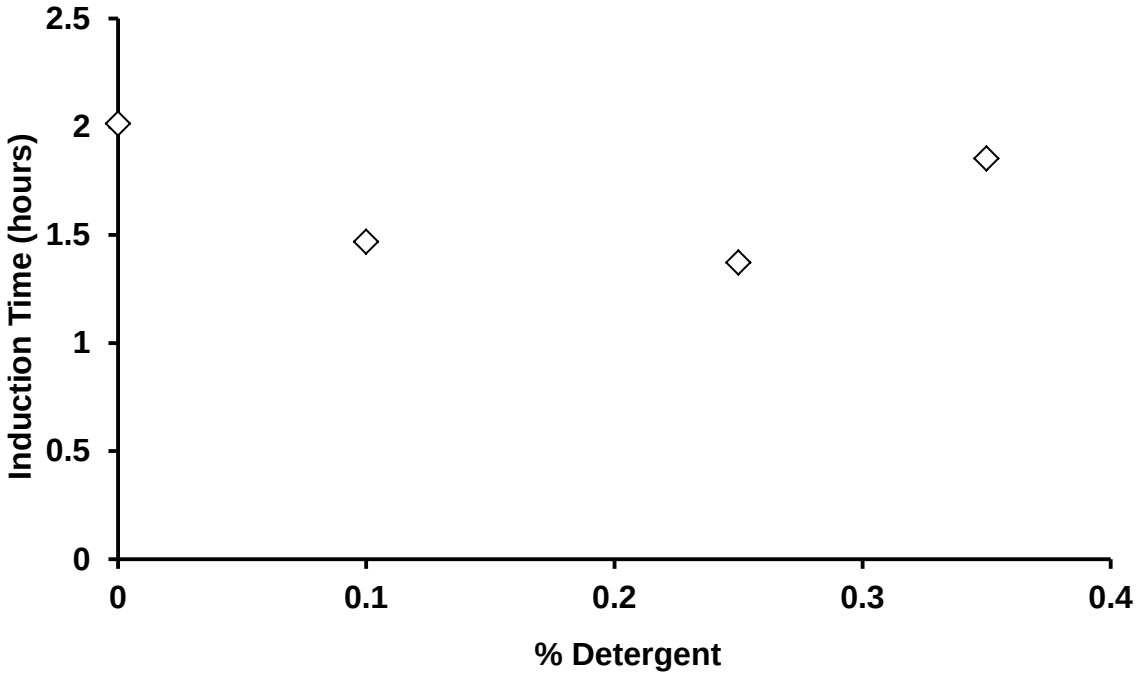

Figure 5.15 – The induction time of squalane with varying amounts of detergent OS102880 at 130 ^{o}C.

5.2.2 The Effect of Additives on Squalane with Methyl Linoleate

Following the initial static oxidation reactions, methyl linoleate was added to the systems to see what effect it would have on the induction period. Due to the fact that the antioxidants appear to reach a threshold concentration above which there is no noticeable change in induction period, coupled with the fact that antioxidants are only used in concentrations of 0.5%, it was decided to go no higher than this and to use concentrations of ~0.1 and 0.25% antioxidant with methyl linoleate (as identified as the primary reactive biodiesel component in chapter 4) concentrations of 2, 5 and 10% to represent various levels of fuel dilution in the sump. See Tables 5.1 – 5.3.

Table 5.1 – The exact amounts of methyl linoleate and phenolic antioxidant in the squalane, ML and phenolic AO mixtures.

	%AO (w/w)	%ML (w/w)	%ML (v/v)
2%ML 0.1%AO	0.102	3.62	3.30
5%ML, 0.1%AO	0.096	7.21	6.61
10%ML 0.1%AO	0.093	11.93	10.98
2%ML 0.25%AO	0.266	2.45	2.24
5%ML 0.25%AO	0.253	5.75	5.27
10%ML 0.25%AO	0.254	11.68	10.77

Table 5.2 – The exact amounts of methyl linoleate and aminic antioxidant in the squalane, ML and Aminic AO mixtures.

	%AO (w/w)	%ML (w/w)	%ML (v/v)
2%ML 0.08%AO	0.133	4.07	3.72
5%ML, 0.08%AO	0.117	7.64	7.00
10%ML 0.08%AO	0.069	12.73	11.72
2%ML 0.4%AO	0.447	3.97	3.63
5%ML 0.4%AO	0.386	7.30	6.69
10%ML 0.4%AO	0.441	12.43	11.45

Table 5.3 – The exact amounts of methyl linoleate and detergent in the squalane, ML and detergent mixtures.

	%Det (w/w)	%ML (w/w)	%ML (v/v)
2%ML 0.1%Det	0.105	2.62	2.40
5%ML, 0.1%Det	0.093	5.87	5.38
10%ML 0.1%Det	0.136	10.58	9.73
2%ML 0.22%Det	0.205	3.08	2.81
5%ML 0.22%Det	0.197	5.83	5.34
10%ML 0.22%Det	0.295	8.95	8.22

As expected, the addition of methyl linoleate served to reduce the induction time of all squalane/antioxidant mixtures, but appeared to be levelling out at around 10%. The effect appeared to be more noticeable with the aminic antioxidant than for Irganox L107, and at 130 ^{o}C rather than 170 ^{o}C – see figures 5.16 – 5.19.

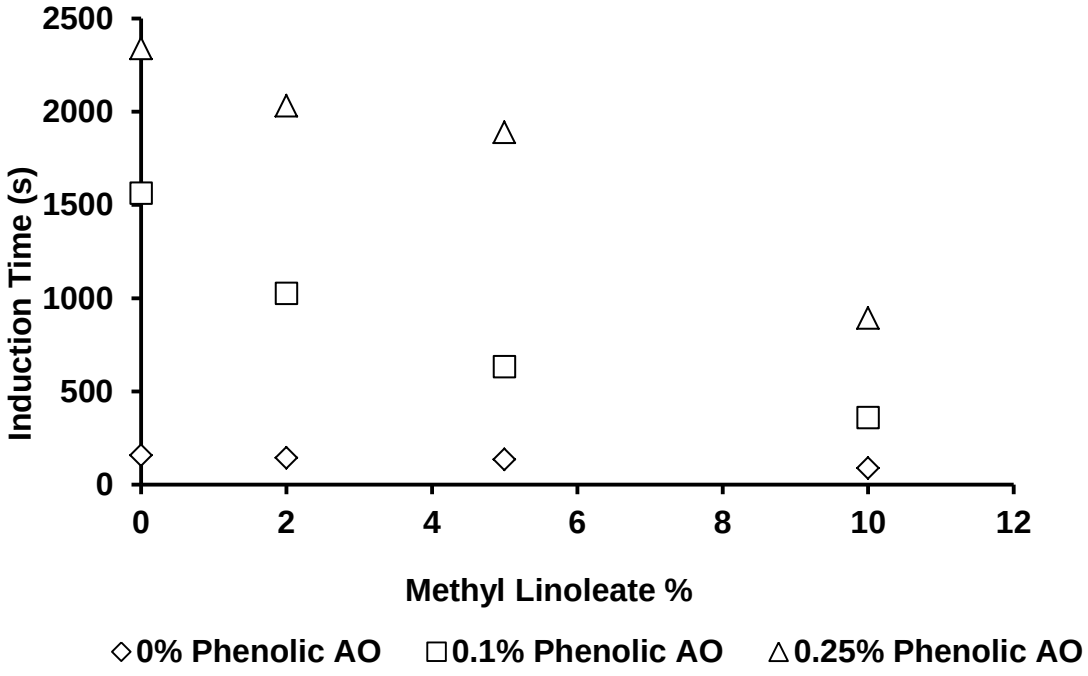

Figure 5.16 – The induction time of squalane with varying amounts of phenolic antioxidant and methyl linoleate at 170 ^{o}C.

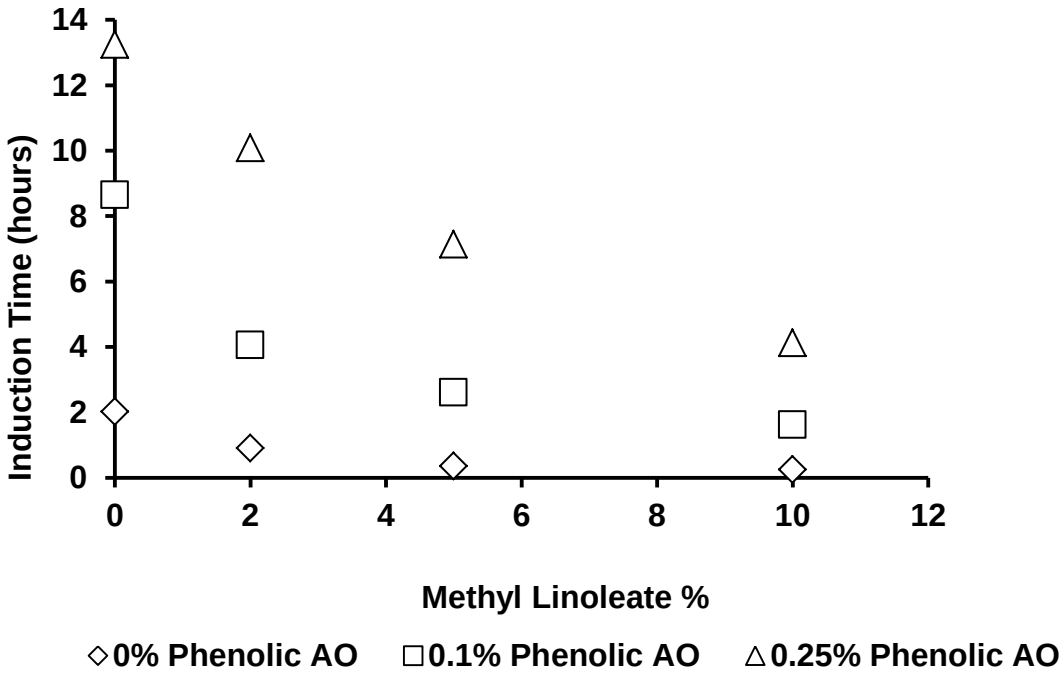

Figure 5.17 – The induction time of squalane with varying amounts of phenolic antioxidant and methyl linoleate at 130 ^{o}C.

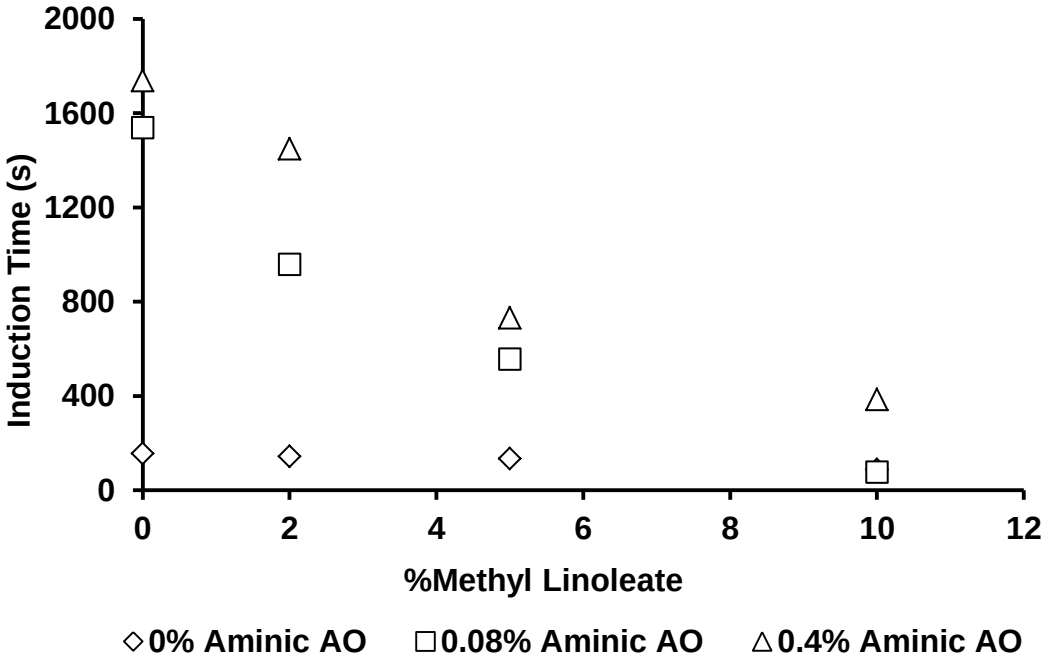

Figure 5.18 – The induction time of squalane with varying amounts of aminic antioxidant and methyl linoleate and 170 ^{o}C.

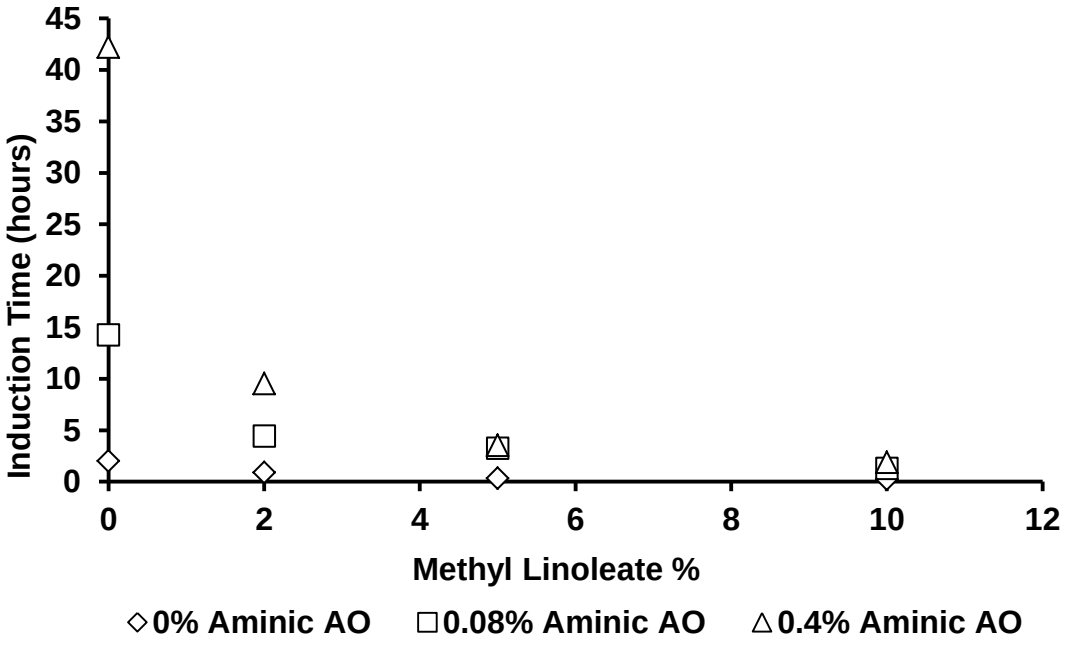

Figure 5.19 – The induction time of squalane with varying amounts of aminic antioxidant and methyl linoleate at 130 ^{o}C.

The trend was similar with the detergent at 130 ^{o}C (figure 5.21) however any noticeable trends were hard to spot at 170 ^{o}C (figure 5.20).

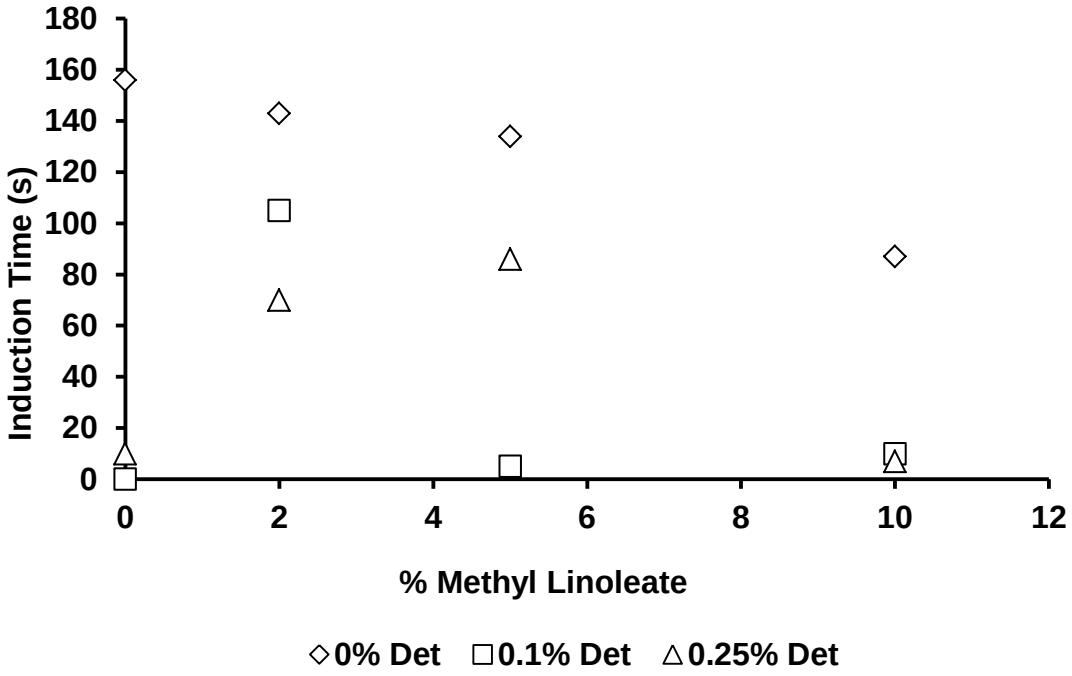

Figure 5.20 – The induction time of squalane with varying amounts of detergent and methyl linoleate at 170 ^{o}C.

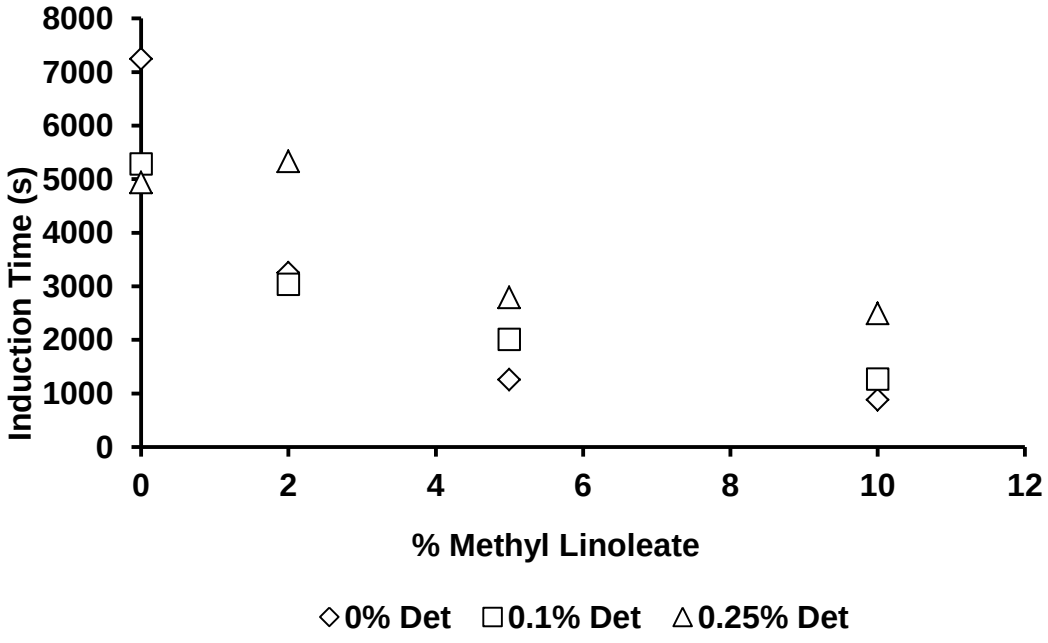

Figure 5.21 – The induction time of squalane with varying amounts of detergent and methyl linoleate at 130 ^{o}C.

After the static oxidation reactions were carried out, flow oxidation reactions were then carried out to try and understand the mechanism of how methyl linoleate served to

reduce the induction periods of autoxidation. Without the need for KV40 testing, smaller and therefore more samples were able to be taken as only trace amounts of sample were needed for GC analysis. As a result it was possible to observe the decay of products before and after the induction period of the reactions. Unfortunately due to time constraints, it was not possible to run reactions for each mixture due to the variety of induction periods and reaction times. Reactions which had an induction period of less than 10 minutes were ruled out as it would have been problematic to gather enough samples before and during the reaction, whilst reactions with induction periods over 4 hours (reactions were run for twice as long as the induction period) were also ruled out as they would not be able to be carried out during a single working day – unlike the static reactions, due to sampling, flow reactions were unable to be left unattended. In all flow reactions the decays of the three main components; squalane, methyl linoleate and the additive were measured and compared to the pressure trace obtained from the static oxidation reaction. For clarity, the three products are shown as a percentage of the initial concentration rather than absolute concentration; as methyl linoleate and the additives were present in less than 10% and 1% respectively.

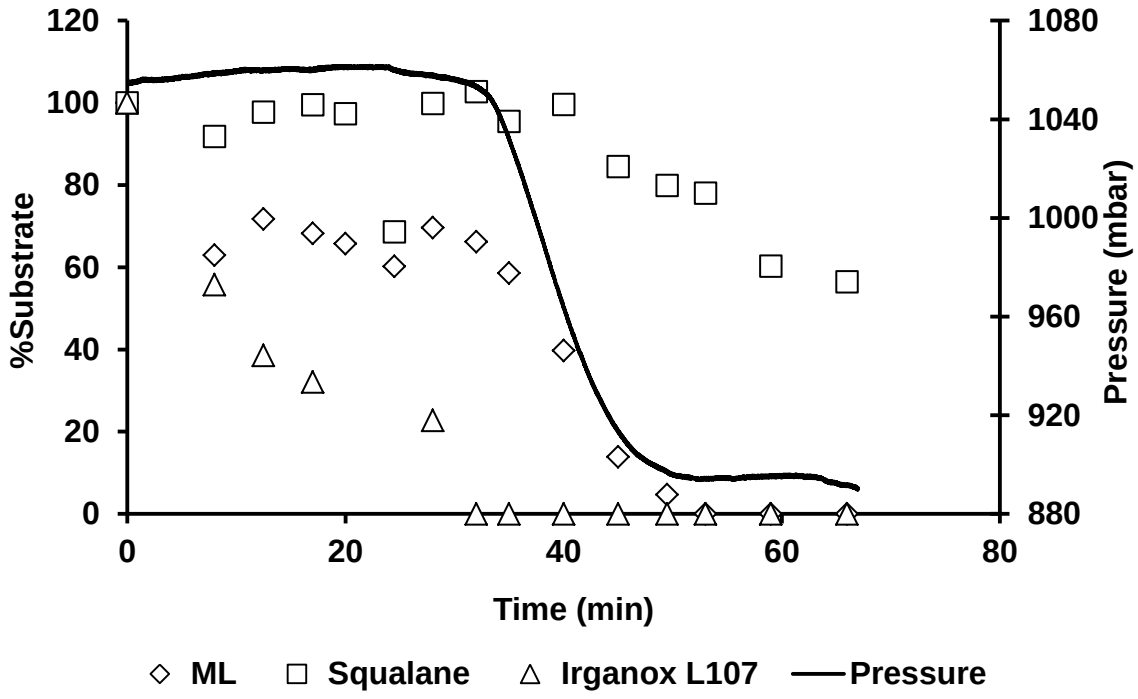

Figure 5.22 – The concentrations of the starting materials of squalane with 2% methyl linoleate and 0.25% Irganox L107 over time at 170 ^{o}C.

Figure 5.22 shows the results for squalane with 2% methyl linoleate and 0.25% Irganox L107. From the graph it shows that a small amount of methyl linoleate is initially consumed, but neither it, nor squalane start decaying significantly until the antioxidant has been consumed. Also, the graph shows that the start of the reaction appears to correlate well with the consumption of all the antioxidant both in terms of the product decay and the static oxidation pressure trace. Figure 5.23 shows the same graph for squalane with 10% methyl linoleate and 0.25% Irganox L107 but at 130 ^{o}C. The pressure trace does not match as neatly with the decay of methyl linoleate, but the same trend is exhibited in terms of squalane and methyl linoleate decaying only when the antioxidant is all used up.

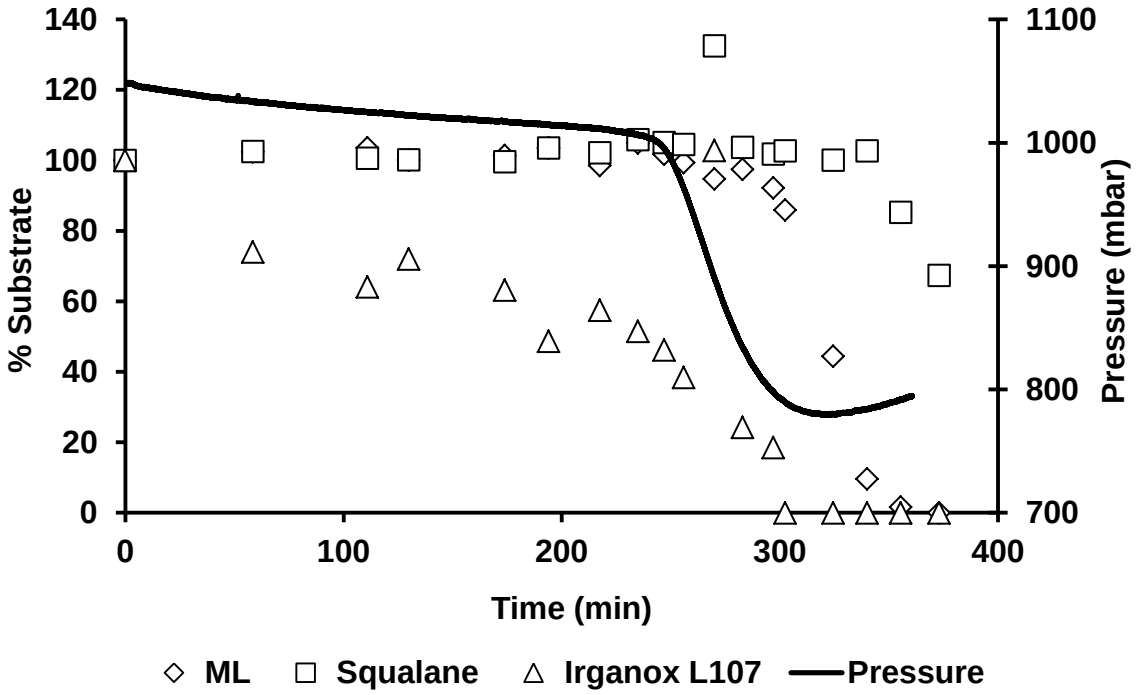

Figure 5.23 – The concentrations of the starting materials of squalane with 10% methyl linoleate and 0.25% Irganox L107 over time at 130 ^{o}C.

5.3 Discussion

5.3.1 *Antioxidant Effect on Autoxidation*

In Chapter 4 the decay of squalane was measured with and without the presence of methyl linoleate to determine the effect of biodiesel on lubricant degradation. From these results, it was shown that methyl linoleate would act as a pro-oxidant on squalane below 158 ± 5 ^{o}C, above which it switched over to have an inhibiting effect instead. In these studies though, figures 5.16 – 5.19 showed methyl linoleate seemingly having a pro-oxidant effect with both the phenolic and aminic antioxidants both below (130 ^{o}C) and

above (170 ^{o}C) the calculated ceiling temperature of 158 ± 5 ^{o}C for addition of O_2 to doubly allylic radicals as described in chapter 4. Figure 5.21 showed ML acting as a pro-oxidant at 130 ^{o}C in the presence of the detergent as well, but no noticeable trends could be observed in figure 5.20 for 170 ^{o}C.

However, the shapes of the pressure decay curves from squalane static oxidation in figure 5.7, after the induction time had ended once the pressure started to drop, were similar regardless of the amount of antioxidant added. From these results, it suggested that once the induction period was over, the reaction proceeded as usual as if no antioxidant were present and that there was the possibility that methyl linoleate was merely shortening the induction time.

To compare this, $k_{squalane}$ were measured from the GC traces from each of the flow reactions and compared to those obtained in chapter 4 (from figures 4.9 and 4.13 for 130 and 170 ^{o}C respectively). Figure 5.24 shows these new $k_{squalane}$ with antioxidant values plotted alongside the ones without antioxidant from chapter 4 at 170 oC. The values from both sets of reactions correlate well with each other, all seeming to fit along a similar line of best fit. Figure 5.25 shows the same at 130 ^{o}C. Only one $k_{squalane}$ value was obtained at this temperature due to lack of data points in the reaction periods, but again, it correlates well with the values obtained without antioxidant. Both graphs suggest that the assumption that the reactions proceeded as usual (as described in chapter 4) once started was a valid one. They also suggest that whilst the antioxidants could delay the onset of the oxidation reactions, they had no effect on them once they were initiated. Similarly that, after the induction period was over, methyl linoleate behaved as described previously, as a pro-oxidant below 158 ± 5 ^{o}C and as an inhibitor above it.

In summary, this indicated that the only phase of the squalane/methyl linoleate reactions affected by the addition of antioxidants was the time it took for the reaction to start; the induction time. The rate of reaction, $k_{squalane}$, was unaffected hence so too was the ability of methyl linoleate to act as either a pro-oxidant or an inhibitor (depending on temperature – see chapter 4) on squalane autoxidation.

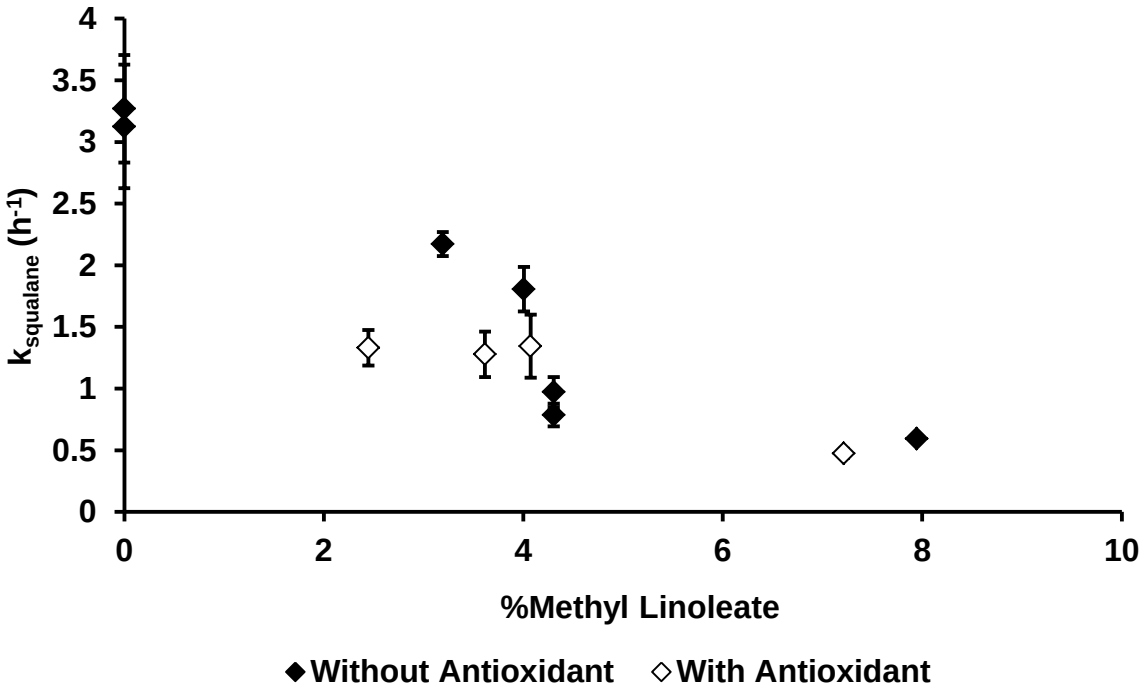

Figure 5.24 – The $k_{squalane}$ values both with and without antioxidants at 170 ^{o}C.

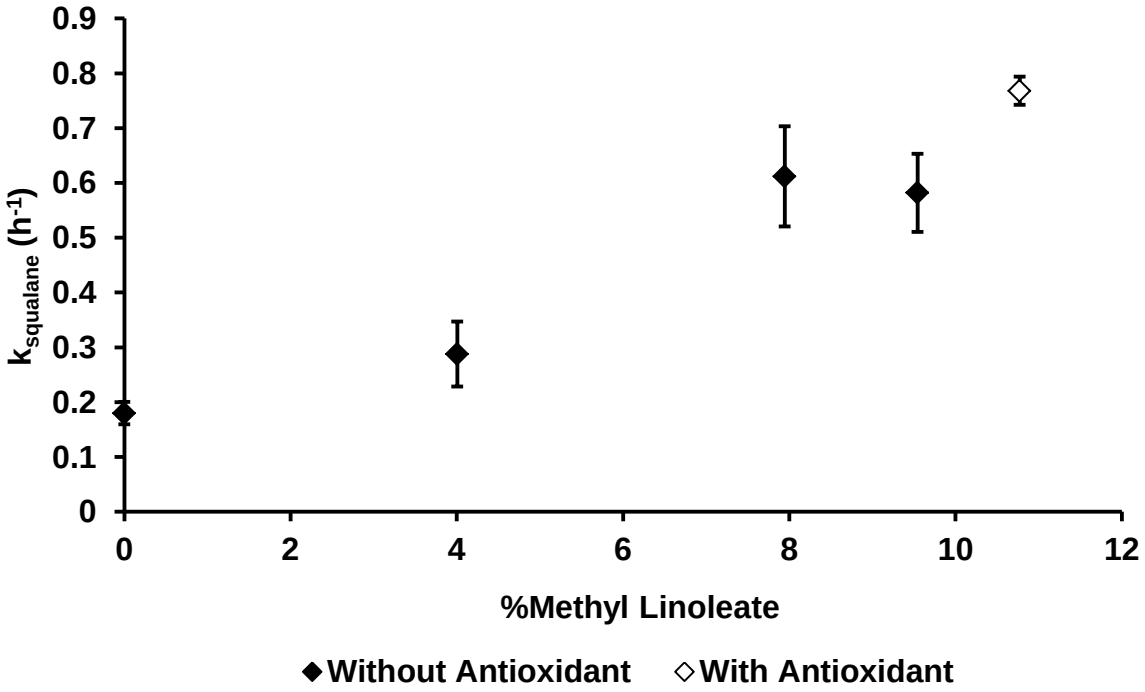

Figure 5.25 – The $k_{squalane}$ values both with and without antioxidants at 130 ^{o}C.

5.3.2 Antioxidant Effect on Induction Period

This still raises two questions however. Firstly as to why methyl linoleate shortens the induction time of the reactions, seemingly as a pro-oxidant at both temperatures, but

also why it seems to have a much more profound effect at reducing the induction times of the aminic antioxidant compared to the phenolic. To answer this it is important to look not only as to whether and how methyl linoleate affects the squalane/antioxidant systems – as shown in figures 5.16 – 5.19, but also how and if the antioxidants affect the squalane/MLsystems. For this reason figures 5.26 – 5.29 show the same data as those in 5.16 – 5.19, but this time with the induction time plotted against antioxidant concentration instead of methyl linoleate concentration.

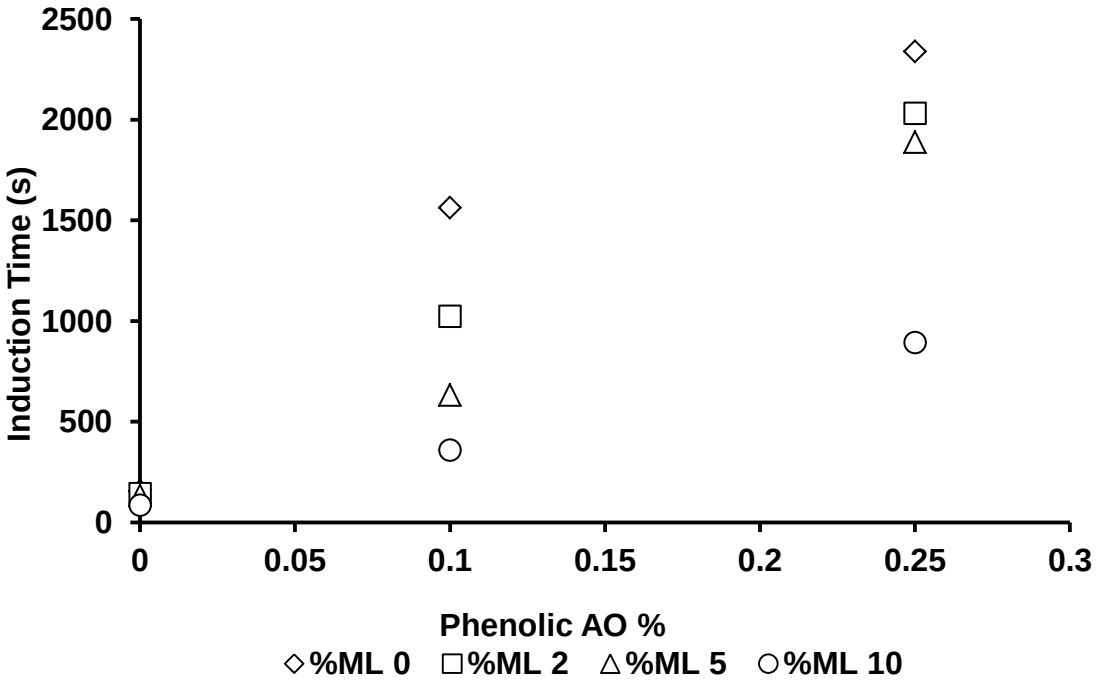

Figure 5.26 – The induction time of squalane with varying amounts of methyl linoleate and phenolic antioxidant at 170 ^{o}C.

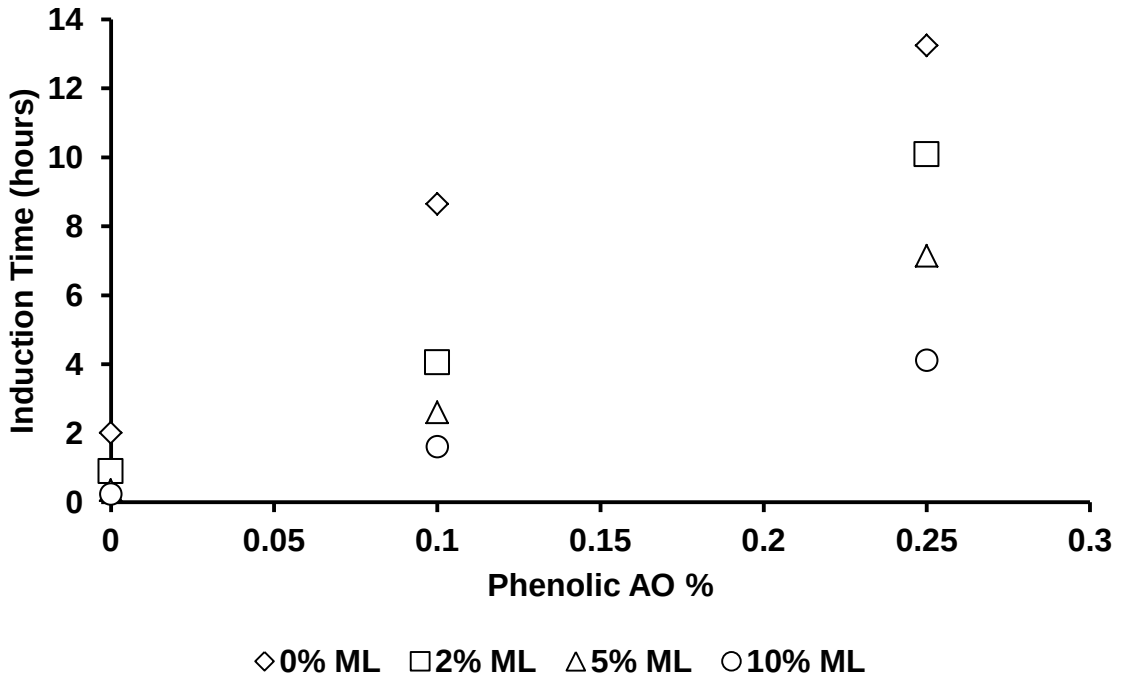

Figure 5.27 – The induction time of squalane with varying amounts of methyl linoleate and phenolic antioxidant at 130 ^{o}C.

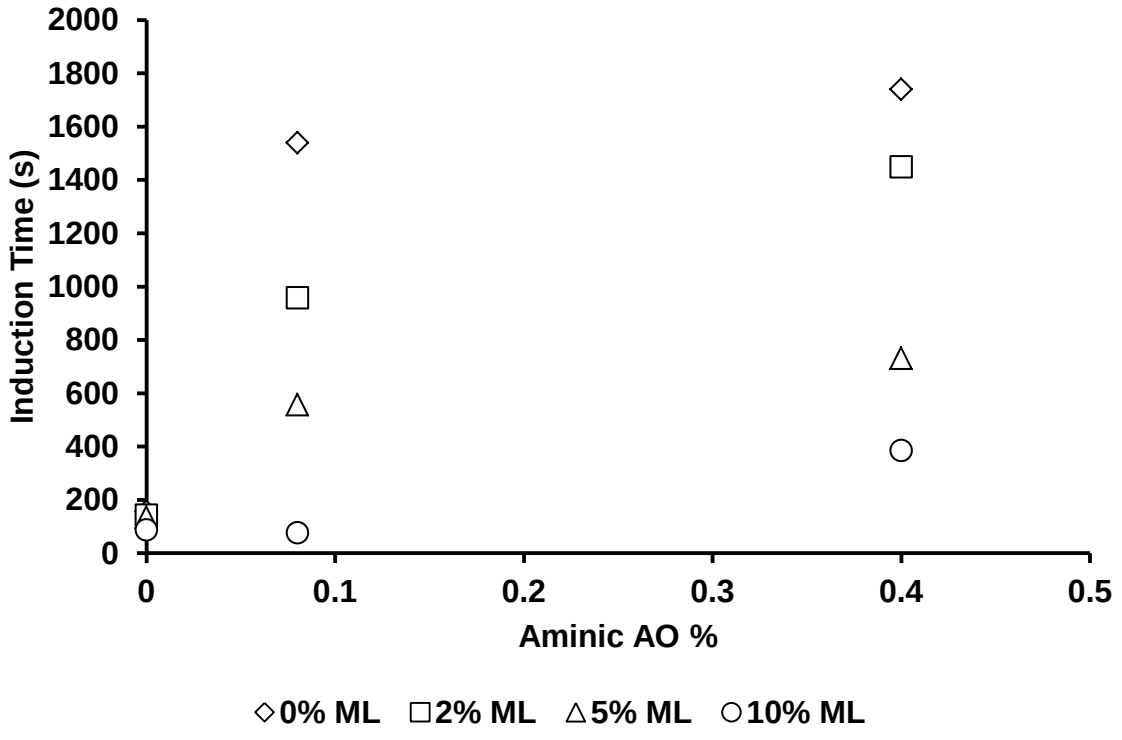

Figure 5.28 – The induction time of squalane with varying amounts of methyl linoleate and aminic antioxidant at 170 ^{o}C.

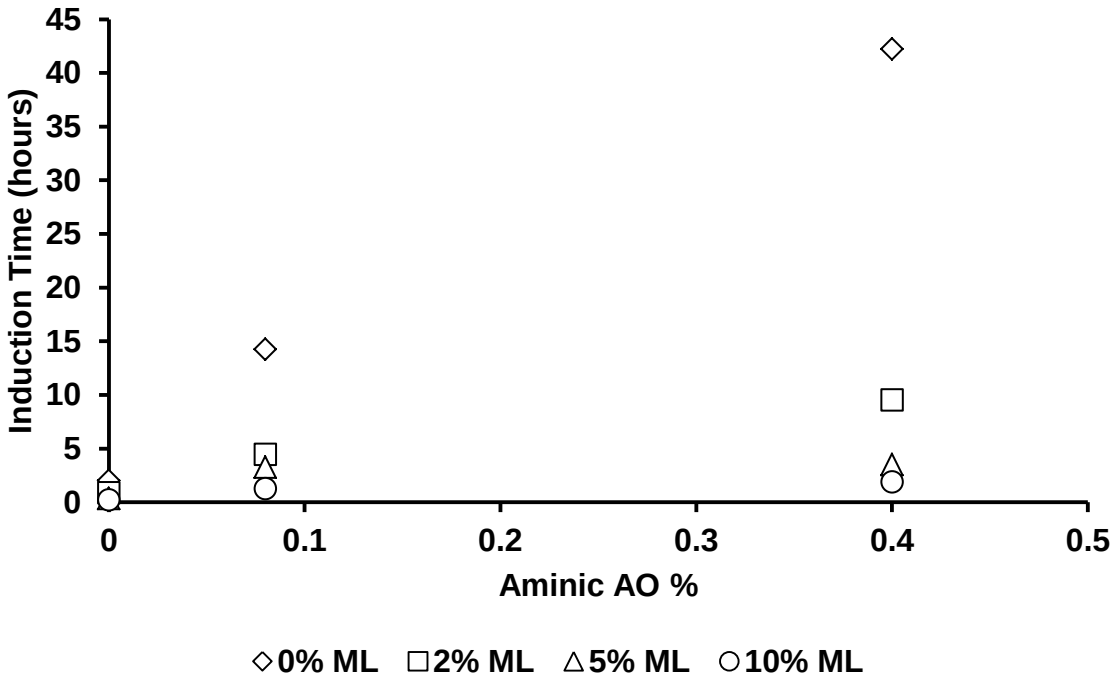

Figure 5.29 – The induction time of squalane with varying amounts of methyl linoleate and aminic antioxidant at 130 ^{o}C.

These graphs show that a) for a fixed antioxidant concentration, the addition of methyl linoleate will serve to reduce the induction time and b) at a fixed concentration of methyl linoleate the addition of antioxidant will still serve to reduce the induction time at both measured temperatures. The patterns also show, however, that methyl linoleate will reduce the induction time of squalane/AO mixtures to a much greater extent at 130 ^{o}C than at 170 ^{o}C.

One possible explanation for these trends is that the antioxidant 'donates' the labile hydrogen atom to the peroxyl radicals to generate hydroperoxides (see figure 5.30 – phenolic structure representing both classes of antioxidant), as is typical of scavenging mechanisms observed in antioxidants. Specifically with regards to the squalane/methyl linoleate mechanisms, this would prevent the radical cycle described in chapter 4 (figure 4.50) being propagated, thus preventing the formation of RO_2· radicals which would attack squalane, or to prevent the subsequent build-up of R· radicals to terminate the cycle above the ceiling temperatures. Peroxyl radicals would still have to form initially however, before the antioxidant could start to act and methyl linoleate's BDE of 318 ± 3 kJ mol^{-1} is still lower than any of the cited values for the antioxidants which explains the initial slight drop

in ML concentration in figures 5.22 and 5.23 before it falls more dramatically upon consumption of the antioxidant. More work would be needed to confirm this however.

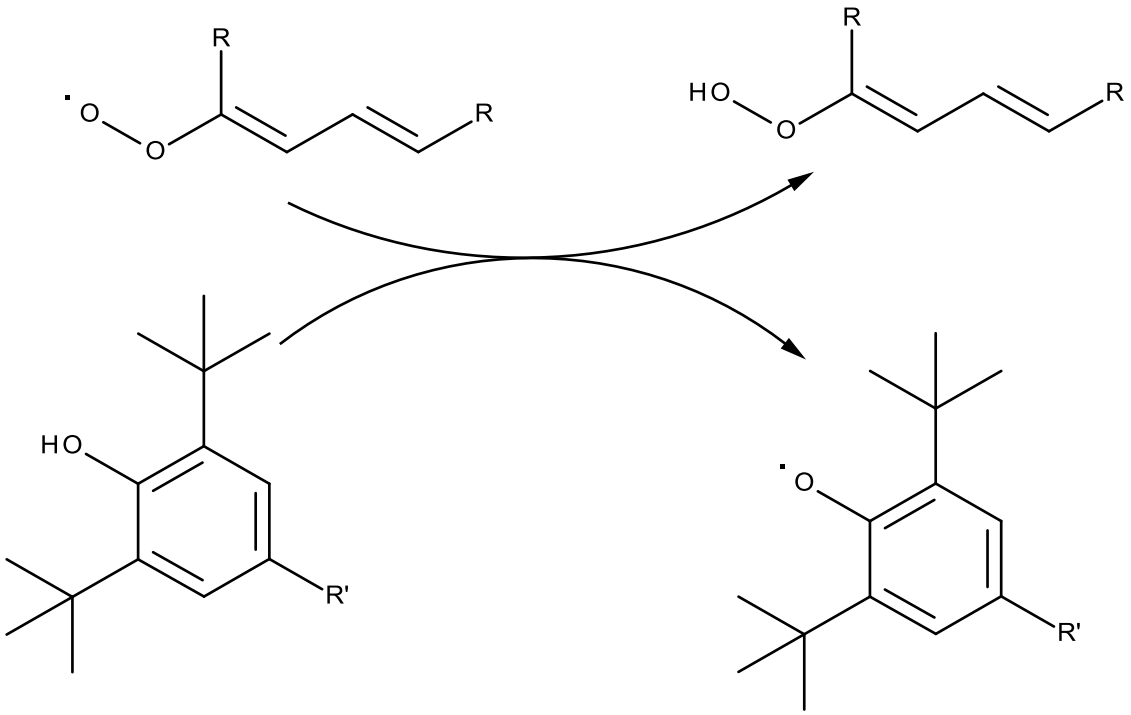

Figure 5.30 – The 'donation' of a hydrogen atom to ML peroxy radicals to inhibit the propagation cycle.

According to this model and the data shown in figures 5.22 and 5.23, it would appear that the induction time is related to the lifetime of the antioxidant, which itself is related to the ML-AO reactions upon which methyl linoleate was observed to have pro-oxidant characteristics in both temperature, despite being observed to switch over to have inhibiting properties as the temperature rose in the squalane/ML systems. The key point to notice here is that in the squalane/AO systems; ML was still having a more significant pro-oxidant effect at the lower temperature (130 ^{o}C) compared to the higher (170 ^{o}C). In Chapter 4, the ceiling temperature as defined by Benson (1964) for the addition of oxygen to ML radicals to form peroxyl radicals (reaction 5.5), was calculated at 158 ± 5 ^{o}C.

$$R\bullet + O_2 \rightleftharpoons RO_2\bullet \qquad \text{Reaction 5.5}$$

Below this temperature, in this case at 130 ^{o}C, the equilibrium will be to the right and hence favour a build-up of peroxyl radicals, which will be subsequently scavenged by the antioxidant, hence accelerating its rate of decay as observed. Above this temperature the equilibrium shifts to the left away from the build-up of peroxyl radicals however, crucially, not completely elimating the forward reaction that produces them and therefore, whilst at a comparatively lower concentration, peroxyl radicals will still be formed above the ceiling temperature – as shown in Chapter 3 where the breakdown products formed via peroxyl radicals were seen at all temperatures – and therefore will still be scavenged by the antioxidant and hence reducing the induction period of the overall reaction. The ceiling temperature for the reaction between ML (or another doubly allylic species) will still be the same, but for the case of the induction period, the main mechanism responsible is slightly different. In this case, any hypothetical switchover in behaviour – e.g. ML starting to increase the induction period – would occur at the temperature where the reverse reaction would become so fast as to either essentially eliminate the production of peroxyl radicals or to make them dissociate faster than antioxidants could scavenge them. This switchover mechanism could theoretically be investigated, by determining the temperature at which this occurred with various different antioxidants. If the former mechanism (elimination of the production of peroxyl radicals), the temperature should be consistent whichever antioxidant was used, if the latter, it should vary according to the AO's speed and efficiency at scavenging peroxyl radicals. In practice, this would be very difficult to achieve (probably impossible on the described experimental setup) due to the extremely high speeds that induction periods would be likely to occur at; another problem would occur if that theoretical temperature occurred higher than ML's boiling point of 346 ^{o}C (at 1atm – Krop 1997), although a different doubly allylic species could be substituted for this purpose. From this work, it would initially suggest that the latter is the case as ML had a more noticeable effect on the aminic antioxidant compared to the phenolic, perhaps due to some interference with the Denisov cycle (Figure 5.5) preventing regeneration of the nitroxyl radical and hence reducing the overall longevity of the antioxidant. Again, this would require further work to confirm/disprove.

A second possible explanation is that the rate of squalane autoxidation, described in chapter 4, is dependent on the propagation reaction of oxygen addition to the doubly allylic radicals (reaction 5.5) which is reversible above the ceiling temperature, whereas the induction period is dependent upon the initiation reaction of methyl linoleate oxidation,

whereby hydrogen is abstracted to give doubly allylic and hydroperoxyl radicals (reaction 5.6).

$$R + O_2 \rightarrow R\bullet + HO_2\bullet \qquad \text{Reaction 5.6}$$

As described already, due to bond strengths, this is much faster than the initiation rate for squalane, but critically no studies (as of yet) have reported this reaction as being reversible meaning it would get faster as temperature increased and hence reduce the induction period at all measured temperatures. The fact that the proportional effect is lower at 170 ^{o}C than at 130 ^{o}C can also be explained via this mechanism by considering the bond strengths. As the two ML + O_2 reactions (from chapter 3) occur more readily than squalane + O_2 due to the difference in bond strengths, it naturally follows that the activation energy for the these two are lower and hence the rate constants faster which seems to be the case considering the observed rate constants for overall autoxidation where all larger for k_{ML} (both reactions) than $k_{squalane}$ at all measured temperatures (as shown in chapters 3 and 4 respectively). As the temperature increases the gap between the k_{ML} and $k_{squalane}$ values should decrease, again as shown in the observed rate constants for both reactions (see figure 5.31), meaning that the proportional effect of linoleate would also decrease as observed.

In summary, as the temperature increases, the difference between the k_{ML} and $k_{squalane}$ values decrease, hence so too does the proportional effect of methyl linoleate reducing the induction time of squalane/methyl linoleate/antioxidant systems.

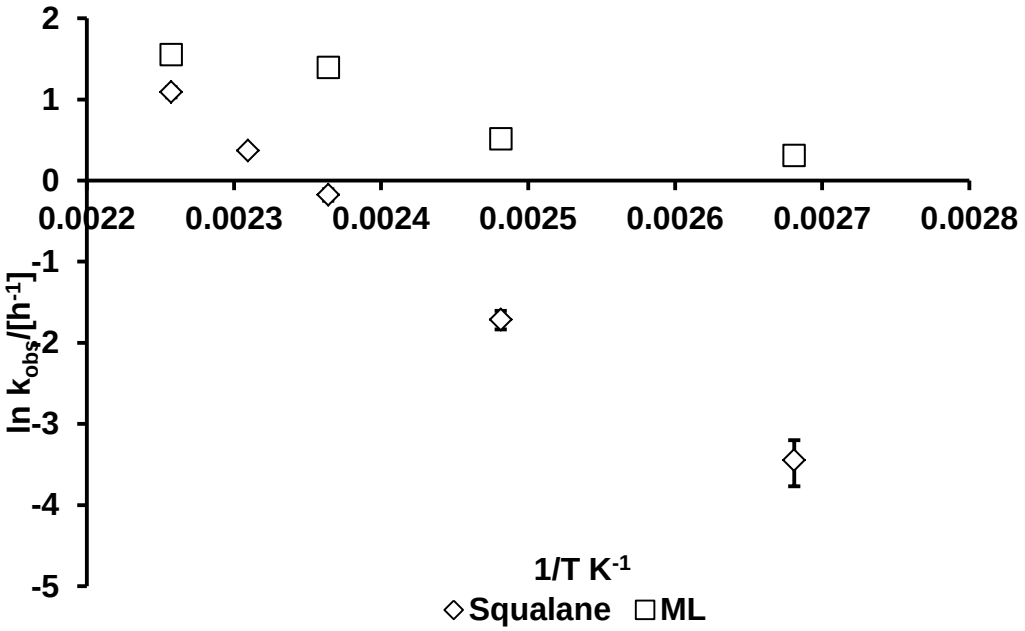

Figure 5.31 – Arrhenius plots for squalane and both methyl linoleate autoxidation reactions.

5.3.3 Relevance to Behaviour in Engines

As before, these results have potential significance when the temperatures in engines are considered. Antioxidants are employed to increase the overall longevity of the engine lubricant and hence any reduction in their effectiveness will impact on the overall efficiency of the engine. In Chapter 4, it was shown that the lubricant base fluid was most susceptible to enhanced degradation rates from doubly unsaturated biodiesel components at lower (100 – 130 ^{o}C) temperatures, typical of those found in the sump. It is therefore important that antioxidants can function effectively at these temperatures in order to protect the engine efficiently. The results from this chapter show that, unfortunately, methyl linoleate can both reduce the lifetime of the antioxidant and still go on to attack the lubricant base fluid upon consumption of the antioxidant at these temperatures. Furthermore, as with the ceiling temperature effect shown in Chapter 4, its relative effectiveness at this increases as temperature decreases, meaning that the area in which the lubricant and fuel come into contact the most (in the sump) is the area where the antioxidant is required to work more efficiently, yet is also the area where its performance is most likely to be hindered.

More positively, however, both phenolic and aminic antioxidants were shown to delay the onset of autoxidation reactions at very low (<1%) concentrations, even if that delay could be shortened by methyl linoleate. It was also shown that the aminic AO was more effective than the phenolic, indicating the possibility of developing antioxidants that could have greater efficiency at increasing these induction periods; though these combined results still suggest that doubly unsaturated compounds in the fuel should ideally be kept at low concentrations.

Of further interest here would be investigating the effect of the phenolic and aminic antioxidants together in solution as previous work on the two has shown the ability of phenolic antioxidants to help regenerate aminic antioxidants in a process known as synergism, described by Bishov for phenolic antioxidants in food chemistry (1975 and 1977) and reported for synthetic antioxidants (aminic and phenolic) by Denisov (2005) and Alfadhl (2008). It would therefore be beneficial to see whether these could prolong induction periods further, or, more crucially, whether methyl linoleate would have the ability to inhibit synergistic effects significantly.

5.3.4 Detergent

Trends with the detergent were much harder to determine however, mainly due to error margins. The errors associated with the static oxidation come from two sources, experimental error from variability in the method itself (though figure 6.10 does show good reproducibility where the antioxidant concentrations are similar) and human error in reading the induction time off the pressure trace. Unfortunately, the exact error margin of both is unknown, but by examining the two closest cases of OS146100 in squalane where concentrations of 0.80% and 0.81% w/w had induction times of 1932 and 1912 seconds respectively, and from them assuming a rough estimate of ±10s for the error, it can be seen that on the timescales of less than 100s (as is the case for the detergent below 170 ^{o}C) the experimental setup is not precise enough to obtain accurate results within a good error margin. All the other experiments had timescales over 100s where the approximate error is therefore less than 10% of the value obtained.

As the trends shown with detergent and squalane in the absence of methyl linoleate in figures 5.14 and 5.15 are very different to those shown with antioxidants, it also suggests that any effect detergent has on biodiesel/lubricant system are sufficiently

different mechanistically as to perhaps require a different method to the ones described here in any case.

5.4 Summary

Following on from the work on methyl linoleate and squalane in Chapter 4, the effects of 3 different additives were tested on these mixtures; a phenolic antioxidant (Irganox L107), an aminic antioxidant (OS146100) and an overbased sodium sulphonate detergent (OS102880). The antioxidants both appeared to delay the onset of the main squalane/ML reactions but then did not affect them once depleted. The most likely cause was attributed to the antioxidants converting the reactive peroxyl radicals into hydroperoxides. The detergents did not show as many noticeable trends due to the reactions being too fast to measure within the error margins on the current equipment setup, but did suggest that the radical scavenging model did not apply to these compounds.

Overall, these results would require more work in order to properly support the models proposed. The antioxidants could perhaps be tested for the breakdown products or the presence methyl linoleate hydroperoxides, though the former would require a very sensitive GC technique due to the trace concentrations in which antioxidants are used – perhaps a column with a lower affinity for aromatics. Also of interest would be to test the two models proposed for the effect of linoleate switching between pro-oxidant and inhibitor in squalane with increasing temperature, whilst reducing the induction period at all temperatures in antioxidant reactions. One potential study could be to measure equilibrium constants of the initiation reaction of methyl linoleate + O_2, specifically to see if any degree of reversibility can be detected as the second model requires the reaction to be irreversible. Another (though more expensive) test for the first model could be to isotopically label the labile hydrogen on the antioxidants with deuterium and look for deuteriated ML hydroperoxides via GC-MS to see if the antioxidant is indeed donating the hydrogen atom to the peroxyl radicals and hence preventing the propagation cycle.
The detergent work would most likely have to be carried out at lower temperatures – though this would raise questions about how valid any models would be at higher temperatures; particularly at those higher than the ceiling temperatures of any of the reagents. Alternatively a different experimental setup would be required – perhaps one with a greater degree of automation – that would be more sensitive to the short reaction times at high temperatures.

5.5 References

Alfadhl, A. The Behaviour of Antioxidants in Lubricant Base Fluids at High Gasoline Engine Temperatures. *PhD Thesis, University of York*, **2008**.

Benson, S.W. Effect of Resonance and Structure on the Thermochemistry of Organic Peroxy Radicals and the Kinetics of Combustion Reaction, *J. Am. Chem. Soc* 1964, **87(5)**, 972-980.

Bishov, S.J. Henick, A.S. Antioxidant Effect of Protein Hydrolyzates in Freeze-Dried Model Systems; Synergistic Action with a Series of Phenolic Antioxidants, *Journal of Food Science,* 1975, **40(2),** 345-348

Bishov, S.J. Masuoka, Y. Kapsalis, J.G. Antioxidant Effect of Spices, Herbs and Protein Hydrolyzates in Freeze-Dried Model Systems: Synergistic Action with Synthetic Phenolic Antioxidants, *Journal of Food Processing and Preservation,* 1977, **1(2),** 153-166

The British Petroleum Company - Industrial Lubrication. 1966. Published East Grinstead, The British Petroleum Company.

Cort, W.M. Antioxidant Properties of Ascorbic Acid in Foods, *Advances in Chemistry,* 1982, **200(22),** 533-550.

Denisov, E.T. Mechanism of Regeneration of Hindered Nitroxyl and Aromatic Amines, *Polymer Degradation and Stability*, 1989, **25,** 209-215.

Denisov, E.T. Afanas'ev, I.B. Oxidation and Antioxidants in Organic Chemistry and Biology, *CRC Press* 2005, ISBN 0-8247-5356-9.

Gedik, C.M. Boyle, S.P. Wood, S.G. Vaughan, S.J. Collins, A.R. Oxidative Stress in Humans: Validation of Biomarkers of DNA Damage, *Carcinogenesis,* 2002, **23(9),** 1441-1446.

Hochstein, P. Atallah, A.S. The Nature of Oxidants and Antioxidant Systems in the Inhibition of Mutation and Cancer, *Mutation Research,* 1988, **202,** 363-375.

Hu, J.J. Dubin, N. Kurland, D. Ma, B. Roush, G. The Effects of Hydrogen Peroxide on DNA Repair Activities, *Mutation Research,* 1995, **336,** 193-201.

Jensen, R.K. Korcek, S. Zinbo, M. Gerlock, J.L. Regeneration of Amine in Catalytic Inhibition of Oxidation, *J. Org. Chem.* 1995, **60,** 5396-5400.

Krop, H.B. v. Velzen, M.J.M. Parsons, J.R. Govers, H.R.J. Determination of Environmentally Relevant Physical-Chemical Properties of Some Fatty Acid Esters, *JAOCS,* 1997, **74(3),** 309-315

Mahoney, L.R.Antioxidants, *Angew. Chem. Int. Ed.* 1969, **8(8),** 547-555.

Mahoney, L.R. DaRooge, M.A. The Kinetic Behavior and Thermochemical Properties of Phenoxy Radicals. *J. Am. Chem. Soc.* 1975, **97(16)**, 4722-4731.

McMillen, D.F. Golden, D.M. Hydrocarbon Bond Dissociation Energies, *Ann. Rev. Phys. Chem*, 1982, **33,** 493-532.

Rudnick, L.R. Lubricant Additives, Chemistry and Applications, 2nd Ed. *CRC Press* 2009, ISBN 1-4200-5964-9.

Stachokiak, G.W. Batchelor, A.W. Engineering Tribology, Chapter 3, Lubricants and their Composition, 2006.

Wright, J.S. Johnson, E.R. DiLabio, G.A. Predicting the Activity of Phenolic Antioxidants: Theoretical Method, Analysis of Substituent Effects, and Application to Major Families of Antioxidants, *J. Am. Chem. Soc*, 2001, **123,** 1173-1183.

Yen, G. Duh, P. Tsai, H. Antioxidant and Pro-oxidant Properties of Ascorbic Acid and Gallic Acid, *Food Chemistry*, 2002, **79,** 307-313.

6. Conclusions and Future Work

6.1 Overview of Results

Prior to this study, it was known that increasing the length of the alkyl chain of FAME biodiesel would increase the cetane number (CN) as well as the pour point and kinematic viscosity, whilst introducing unsaturated sites onto the chain would reduce all three. However, it also appeared that biodiesel with higher levels of unsaturation exacerbated detrimental effects of the engine over time, such as injector clogging, piston ring sticking and sludge and soot formation. The general consensus was that there was a tradeoff – unsaturates would bring viscosities and freezing/pour points into specification at the expense of enhancing engine degradation. Consequently in the UK biodiesel is currently only allowed to be blended with mineral diesel in levels up to 7% - any higher and the fuel must be labelled as such.

From this work, however it appears that only polyunsaturated compounds enhance the rate of lubricant degradation or have chemical influence on other engine components. In the model systems at least, with methyl oleate (the monounsaturated analogue) present squalane (the lubricant analogue) behaved exactly the same as it did with none present. Only methyl linoleate (the polyunsaturated analogue) had any effect on oxidation rates; below 158 ± 5 ^{o}C methyl linoleate acted as a pro-oxidant, switching to an inhibitor above this temperature. This was attributed to the reversible binding of oxygen radicals to the doubly allylic radical formed by hydrogen abstraction in chapter 4. In chapter 3, whilst examining the autoxidation of methyl linoleate by itself, it was noted that the decomposition of methyl linoleate by formation of hydroperoxides after hydrogen abstraction – currently the accepted main mechanism of autoxidation – became less significant as the temperature increased with epoxidation, formed instead by addition of peroxyl radicals to double bonds, started to become the dominant mechanism. A rough cross-over temperature of 176.5 ± 10.2 ^{o}C was calculated which, despite some assumptions, correlates relatively well with the ceiling temperature of 158 ± 5 ^{o}C calculated in chapter 4 indicating that there is perhaps some connection between the reversibility of oxygen binding to allylic radicals to form peroxyl radicals and the main mechanisms (hydrogen abstraction or addition to double bonds) by which peroxyl radicals attack species.

In chapter 5 antioxidants were also added to the methyl linoleate and squalane mixtures from which it was shown that antioxidants could delay the induction period of reactions whilst methyl linoleate could accelerate them. Interestingly the latter point appeared true at all temperatures; there was no crossover to methyl linoleate becoming an inhibitor as there had been with squalane. More detailed analysis revealed however, that when the antioxidant was consumed the reactions between squalane and methyl linoleate proceeded the same as if no antioxidant were present. From this it was deduced that antioxidants could only prevent the onset of a reaction, not alter the rate of it once started.

Two possible mechanisms were suggested as to why methyl linoleate served to accelerate the onset of a reaction at all temperatures contrary to what was observed with squalane. The first was that methyl linoleate radicals, both in allylic and peroxyl form, were scavenged by the antioxidant. As the concentration of methyl linoleate increased, more radicals were produced hence the antioxidant was consumed faster. The second was that the crossover temperature was based around radical propagation reactions, crucially the reversible binding of oxygen to doubly allylic radicals whilst the induction period is based on radical initiation reactions, mainly hydrogen abstraction by molecular oxygen which is irreversible and hence faster at all temperatures.

6.2 Future Work on Autoxidation

As the temperature calculated in chapter 3 is based on some large assumptions due to availability of data, one useful future study would be to gather further data by carrying out flow reactions of methyl linoleate but taking samples earlier to try and obtain rate constants for both the hydrogen abstraction via peroxyl radicals and addition of peroxyl radicals to double bonds. This work would also hopefully identify a formation and decay trend for the dehydrodimer which would help clarify some of the trends seen in chapter 4 – if the hydroperoxide route is less favoured above the ceiling temperature, yet hydrogen abstraction is still occurring then dimeric compounds should be being formed as well as epoxides. If dimeric compounds are short lived, then polymerisation would be expected which would explain why, even though ML is inhibiting squalane degradation, KV40 continues to increase. Other methods such as GPC may have to be investigated if these compounds cannot be detected via GC.

It would also be highly beneficial to continue with the study of methyl oleate to the same level; as well as cataloguing the products measuring the rates of their formation and calculating the selectivity of radical attack sites in the same way as was done for methyl

linoleate. This completed study would be of benefit both industrially and academically; the former by examining how similar monounsaturated compounds behaved compared to polyunsaturated ones in storage and combustion. If methyl oleate also has the same crossover between degradation mechanisms (peroxyl radical hydrogen abstraction v addition) then the temperature at which this did or did not occur would help to tell whether the similarity between two crossover temperatures observed with methyl linoleate ($158 \pm 5\ ^{o}C$ for reversible addition of oxygen to doubly allylic radicals and $176.5 \pm 10.2\ ^{o}C$ for the hydrogen abstraction/addition degradation mechanism) indicates a connection between the mechanisms or is purely coincidental. Either way would help to further the knowledge of autoxidation mechanisms of not only biodiesel, but unsaturated molecules in general.

6.3 Future Work on Chemically Modelling Biodiesel

Monounsaturated compounds appeared to behave the same as saturated ones assuming the current model, that saturated FAME compounds are chemically inert with respect to their fuel properties, is correct. Another beneficial future study therefore would be to study the effect of saturated FAME compounds such as methyl palmitate or methyl stearate (16 and 18 carbon chain respectively) to test whether, like methyl oleate, they would have no effect on squalane oxidation rates. The study of these compounds would also be highly relevant to the effect of biodiesel on lubricants as they are also very common biodiesel components and studies of these would not only mean all three different FAME classes had been covered, but also all of the four major biodiesel compounds – methyl stearate, palmitate, oleate and linoleate.

Another piece of potential future work could be to investigate the role of FAME with 3 or 4 double bonds such as methyl linolenate (18 carbons, 3 double bonds) or methyl arachidonate (20 carbons, 4 double bonds) on squalane oxidation. As they are polyunsaturated, the basic chemistry principles of doubly allylic systems should be the same as for methyl linoleate, although with more double bonds to act on, the molecule as a whole may be more reactive. For instance, methyl arachidonate may cause squalane to degrade much faster than methyl linoleate (due to producing peroxyl radicals faster) whilst having a much greater inhibiting effect above it. As they are still based around doubly allylic chemistry, however, the ceiling temperature should be the same as for doubly allylic systems. A study of this nature may not be of as great an interest as far as relevance to

engines goes, depending on the outcome of the results (linolenate and arachidonate are much rarer than oleate and linoleate as FFA), but it would certainly test the validity of using methyl linoleate to represent all polyunsaturated compounds as well as the theory that polyunsaturated compounds all behave the same as diunsaturated ones as is the currently accepted model.

6.4 Future Work on Antioxidants

As the development of more powerful and efficient antioxidants is a continually ongoing process, this area possibly has the most potentially interesting future work for industry; most notably as to why the aminic antioxidant had a far greater potential to extend the induction period of methyl oleate/squalane autoxidation compared to the phenolic, yet was more dramatically effected by increasing methyl linoleate concentration. This could be tested by using different antioxidants (both phenolic and aminic) with different, known substituents. Of particular interest would be which substituents increased the induction periods and which also increased the lifetime of the antioxidant.

Such a study would also help to determine which (if either) of the two mechanisms for methyl linoleate reducing the induction proposed in Chapter 5 are most likely to be correct (in addition to those mentioned in the Discussion) – if it is due to the scavenging ability of the antioxidants, then the induction time should depend heavily on the efficiency of the antioxidant.

Overall as this field impacts on biodiesel behaviour in engines as well as being dependant on the mechanisms of oxidation, further work in this area potentially has a lot more to offer both industrially and academically.

Appendix A: Mass Spectrometry Data

Table A.1 – The GC EI-MS data for methyl linoleate oxidation at 170 ^{o}C, including NIST library matches and subsequent product identification.

Peak no.	Product Identification	EI Mass Spectra	NIST Library Spectra
1	Pentane	39(17), 41(60), 43(100), 57(20), 72(12)	39(13), 41(50),43(100), 57(21), 72(17)
2	hexanal	39(29), 41(92), 43(71), 43(68), 44(100), 56(88), 57(64),100(2)	39(21), 41(71), 43(75), 44(100), 56(83), 57(38), 100(2)
3	2-heptenal (*cis* and *trans*)	41(100), 55(88), 70(48) 83(100), 97(12), 112(4)	41(100), 55(83), 70(33), 83(54), 97(4), 112(8)
4	Methyl Heptanoate	43(35), 55(21), 74(100), 87(40), 101(14.5), 113(16)	43(50), 55(15), 74(100), 87(25), 101(13), 113(10), 144(2)
5	2-Octenal	51(17), 55(86), 57(61), 69(100), 70(48), 83(97), 97(9), 126(2)	29(74), 39(42) ,41(99), 55(85), 70(71), 83(62), 126(10)
6	Methyl Octanoate	39(13), 41(41), 43(54), 55(41), 57(38), 59(31), 69(17), 74(100), 87(44), 101(19), 115(23), 127(33), 158(2)	39(10), 41(31), 43(46), 55(17), 57(17), 59(13), 69(6), 74(100), 87(38), 101(6), 115(6), 127(8), 158(2)
7	2,4 decadienal (Z,Z)	41(30), 55(19), 67(35), 81(100), 95(17), 123(7), 152(7), 325(1), 341(4), 429(1)	41(19), 55(11), 67(13), 81(100), 95(9), 123(4), 152(9)
8	2,4 decadienal (E,Z)	41(30), 55(17), 67(22), 81(100), 95(15), 109(4), 123(4), 152(9)	41(19), 55(11), 67(13), 81(100), 95(9), 123(4), 152(9)
9	8-oxo Methyl -octanoate	41(44), 55(52), 74(100), 87(94), 97(44), 112(7) 129(46), 141(33), 154(1)	41(67), 55(48), 74(100), 87(94), 97(44), 112(7), 129(63), 141(33), 154(2), 172(1)
10	8-hydroxy Methyl Octanoate	31(4), 41(48), 43(28), 55(61), 74(100), 87(54), 96(30), 124(13), 144(11)	31(19), 41(33), 43(50), 55(50), 74(100), 87(46), 96(11), 124(11), 144(13), 174(1)
11	9-oxo Methyl Nonanoate	32(2), 41(54), 55(81), 59(41), 69(37), 74(100), 87(96), 98(17), 111(61), 143(48), 155(33)	32(4), 41(43), 55(59), 59(28), 69(28), 74(100), 87(61), 98(9), 111(35), 143(30), 155(17), 171(2), 185(1)
12	10-oxo Methyl decanoate	41(39), 55(76), 74(100), 87(72), 97(35), 108(7), 125(52), 157(26), 169(15)	41(39), 55(54), 74(100), 87(70), 97(31), 125(65), 157(63), 169(50), 200(2)
13	Methyl Nonandioic acid	41(39), 43(31), 55(85), 60(15), 74(100), 83(48), 97(22), 98(19), 111(35), 124(33), 152(81), 171(30)	41(30), 43(35), 55(43), 60(13), 74(100), 83(30), 97(13), 98(19), 111(30), 124(15), 152(91), 171(26)
14	10-oxo Methyl dec-8-enoate	41(81), 55(100), 59(56), 69(83), 74(76), 83(61), 98(54), 110(), 121(24), 138(57), 148(7), 166(11)	41(100), 55(69), 69(48), 74(44), 83(30), 98(22), 110(7), 121(4), 138(13), 166(4), 198(2)
15	11-oxo Methyl undec-9-enoate	41(67), 55(100), 74(59), 83(72), 98(59), 109(20), 135(19), 152(17), 162(6), 181(7)	41(100), 55(69), 74(37), 83(28), 98(24), 109(7), 135(4), 152(4), 181(4)
16	12-oxo Methyl dodec-9-enoate	41(59), 55(100), 67(48), 74(87), 87(59), 95(31), 98(24), 109(15), 151(65), 166(11), 195(6)	41(85), 55(100), 67(37), 74(65), 95(22), 98(61), 109(15), 151(4), 166(6), 195(6), 226(4)
17	13-oxo Methyl tridec-9,11-dienoate	41(42), 55(38), 59(19), 67(40), 74(13), 81(100), 95(38), 109(19), 121(9), 135(6), 149(6), 160(2), 178(9), 188(6), 194(2), 206(11), 220(6), 238(4)	41(70), 55(85), 67(95), 74(24), 81(100), 95(69), 109(33), 121(20), 135(17), 149(11), 152(20), 178(17), 194(6), 206(1), 210(9), 220(2)
18	Methyl Linoleate	41(32), 55(45), 67(95), 74(14). 81(100), 95(64), 109(32), 123(19), 135(15), 150(18), 164(16), 178(12), 220(8), 263(29), 294(60)	41(46), 55(65), 67(100), 81(96), 95(72), 109(38), 123(20), 135(15), 150(16), 165(10),

			178(6), 220(4), 163(12), 294(18)
19	Methyl *trans*-9-epoxy octadec-12-enoate	41(89), 55(100), 67(94), 81(89), 95(61), 99(33), 109(22), 121(26), 136(20), 149(13), 164(19), 178(6), 207(4), 235(4), 249(2), 263(2), 279(4), 292(15), 310(1)	
20	Methyl *trans*-12-epoxy octadec-9-enoate	41(78), 55(100), 67(82), 74(19), 81(74), 95(48), 109(27), 121(19), 135(12), 150(16), 155(23), 168(7), 185(9), 199(5), 207(3), 235(2), 279(3), 292(8), 310(1)	Peaks 19 – 22: No NIST database matches – Identified from Lercker 2003 as described in text
21	Methyl *cis*-9-epoxy octadec-12-enoate	41(81), 55(100), 67(86), 74(17), 81(86), 95(59), 109(19), 121(23), 136(19), 149(12), 164(19), 167(12), 179(6), 189(3), 207(4), 236(4), 279(5), 292(8), 310(1)	
22	Methyl *cis*-12-epoxy octadec-9-enoate	41(74), 55(100), 67(82), 74(17), 81(73), 95(49), 109(27), 121(17), 135(12), 155(19), 168(6), 185(9), 199(9), 207(5), 221(3), 235(2), 279(4), 292(5), 310(1)	
23	Methyl Linoleate alcohol – positional isomer unknown	51(5), 53(14), 54(12), 55(71), 57(15), 59(16), 65(12), 66(11), 67(80), 68(19), 69(53), 71(20), 74(10), 77(53), 78(23), 79(100), 80(56), 81(54), 82(16), 83(17), 87(16), 91(86), 92(16), 93(92), 94(35), 95(37), 96(17), 97(12), 105(32), 106(12), 107(37), 108(17), 108(16), 109(18), 119(19), 121(28), 131(28), 135(18), 136(16), 149(10), 157(3), 161(8), 163(10), 171(11), 175(4), 176(3), 185(10), 189(7), 207(10), 219(36), 235(2), 261(3), 238(10), 292(50), 293(9), 294(1), 310(1)	
24	Methyl Linoleate alcohol – positional isomer unknown	53(11), 54(15), 55(55), 57(11), 59(13), 67(60), 68(17), 69(100), 71(35), 74(14), 77(19), 79(64), 80(21), 81(47), 82(12), 83(15), 91(38), 93(41), 94(15), 95(39), 96(16), 97(13), 99(48), 100(10), 105(20), 107(31), 108(19), 109(15), 110(10), 119(11), 121(20), 125(16), 131(63), 135(12), 136(5), 137(6), 143(4), 147(7), 151(13), 153(5), 161(6), 163(4), 164(5), 169(8), 185(14), 194(4), 207(13), 219(65), 235(2), 264(19), 292(9), 293(2), 294(1), 310(1)	15-hydroxy methyl linoleate: 55(100), 67(70), 68(55), 73(22), 74(14), 79(56), 80(40), 81(77), 82(42), 93(38), 94(33), 95(52), 96(30), 107(23), 108(24), 109(32), 110(17), 121(27), 122(27), 135(25), 136(21), 149(18), 150(24), 163(11), 164(21), 177(7), 198(4), 199(2), 206(19), 217(2), 238(21), 239(4), 249(2), 279(4), 292(15), 293(4), 310(1)
25	Methyl Linoleate alcohol – positional isomer unknown	53(12), 55(63), 57(16), 59(18), 65(12), 67(83), 68(17), 69(32), 71(19), 74(9), 77(41), 79(100), 80(55), 81(59), 82(18), 83(19), 87(11), 91(78), 93(90), 94(31), 95(37), 96(15), 97(15), 99(25), 105(25), 107(37), 108(17), 109(17), 119(16), 121(24), 122(11), 125(13), 131(14), 133(10), 135(22), 136(18), 147(8), 149(13), 150(14), 153(15), 163(7), 175(5), 185(12), 189(5), 191(3), 207(6), 219(19), 221(4), 235(2), 249(2), 261(5), 264(5), 278(2), 292(45), 293(10), 294(3), 310(1)	
26	Methyl Linoleate alcohol – positional isomer unknown	51(4). 55(36), 57(14), 67(39), 69(100), 77(11), 79(30), 81(26), 83(10), 91(22), 93(18), 95(21), 100(12), 105(10), 109(7), 119(8), 121(8), 125(7), 131(58), 135(10), 141(3), 147(4), 149(3), 150(5), 151(7), 166(4), 180(5), 185(3), 193(4), 207(18), 219(68), 264(18), 281(5), 292(2), 310(1)	
27	9-oxo methyl linoleate	53(16), 55(65), 59(18), 67(52), 69(70), 71(17), 74(12), 79(39), 81(100), 91(23), 95(38), 99(25), 105(10), 111(10), 123(15), 131(42), 138(28), 151(32), 165(5), 177(12), 193(13), 207(17), 219(51), 225(5), 237(5), 264(13), 281(3), 293(9), 308(2)	17-oxo methyl linoleate: 54(25), 65(12), 67(100), 68(22), 69(13), 71(14), 80(50), 81(64), 82(11), 83(14), 87(14), 91(43), 92(15), 93(39), 94(30), 95(31), 105(11), 106(11), 107(18), 108(14), 109(14), 121(12), 125(5), 135(6), 142(1), 149(2), 163(4), 164(3), 177(2), 218(2), 250(11), 260(1), 276(4), 277(6), 290(2), 291(1), 293(1), 308(3)
28	13-oxo methyl linoleate	41(21), 55(45), 67(58), 74(7), 79(100), 93(96), 107(39), 121(47), 135(47), 149(19), 163(11), 185(11), 207(6), 221(4), 235(4), 237(66), 249(4), 261(7), 279(1), 292(83), 308(1)	
29	Impurity – suspected squalane		
30	Methyl linoleate dehydrodimer	55(17), 67(16), 69(26), 73(17), 74(6), 78(11), 79(11), 81(15), 83(7), 91(14), 93(10), 95(12), 105(10), 107(5), 109(6), 117(6), 119(6), 131(16),	Not available – assignment described in text

	133(10), 135(5), 149(3), 161(5), 163(3), 165(2), 175(3), 177(6), 191(14), 193(9), 195(3), 207(100), 208(17), 209(14), 219(17), 221(2), 233(2), 249(5), 253(14), 253(3), 254(3), 264(6), 265(8), 267(8), 268(2), 269(4), 281(41), 282(11), 283(6), 293(2), 313(2), 315(2), 319(3), 320(3), 327(7), 329(3), 331(4), 341(4), 345(2), 355(6), 356(2), 357(1), 373(1), 389(7), 397(4), 403(6), 405(3), 415(2), 429(10), 430(4), 443(2), 451(2), 469(1), 475(6), 476(2), 483(2), 489(2), 501(1), 515(10), 516(4), 555(4), 586(4), 588(2)

Table A.2 – The GC FI-MS data for methyl linoleate oxidation at 170 ^{o}C and subsequent product identification.

Peak no.	**Product Identification**	**FI Mass Spectra**
1	Pentane	Not obtained
2	Hexanal	82(25) (M-18),100(50) (M), 101(100) (M+1)
3	2-heptenal (*cis* and *trans*)	111(5) (M-1), 112(68) (M), 113(100) (M+1)
4	Methyl Heptanoate	112(8) (M-32), 144(100) (M), 145(70) (M+1)
5	2-Octenal	Not obtained
6	Methyl Octanoate	158(100) (M), 159(25) (M+1)
7	2,4 decadienal (Z,Z)	152(100) (M), 153(17) (M+1)
8	2,4 decadienal (E,Z)	152(100) (M), 153(17) (M+1)
9	8-oxo Methyl -octanoate	171(40) (M-1), 172(30) (M), 173(100) (M+1), 174(8) (M+2)
10	8-hydroxy Methyl Octanoate	129(5) (M-45), 173(6) (M-1), 174(12) (M), 175(100) (M+1), 176(8) (M+2)
11	9-oxo Methyl Nonanoate	185(20) (M-1), 187(100) (M+1), 188(10) (M+2)
12	10-oxo Methyl decanoate	168(14) (M-32), 185(7) (M-15), 200(76) (M), 201(100) (M+1), 202(14) (M+2)
13	Methyl Nonandioic acid	182(7) (M-20), 199(17) (M-3), 200(14) (M-2), 201(100) (M-1), 202(14) (M)
14	10-oxo Methyl dec-8-enoate	197(10) (M-1), 198(32) (M), 199(100) (M+1), 200(12) (M+2)
15	11-oxo Methyl undec-9-enoate	211(10) (M-1), 212(38) (M), 213(100) (M+1), 214(14) (M+2)
16	12-oxo Methyl dodec-9-enoate	226(24) (M), 227(100) (M+1), 228(10) (M+2)
17	13-oxo Methyl tridec-9,11-dienoate	206(17) (M-32), 238(100) (M), 239(79) (M+1), 240(10) (M+2)

18	Methyl Linoleate	294(100) (M), 295(25) (M+1)
19	Methyl *trans*-9-epoxy octadec-12-enoate	Not Obtained
20	Methyl *trans*-12-epoxy octadec-9-enoate	Not Obtained
21	Methyl *cis*-9-epoxy octadec-12-enoate	Not Obtained
22	Methyl *cis*-12-epoxy octadec-9-enoate	Not Obtained
23	Methyl Linoleate alcohol – positional isomer unknown	310(100) (M), 311(54) (M+1), 312(8) (M+2)
24	Methyl Linoleate alcohol – positional isomer unknown	310(100) (M), 311(54) (M+1), 312(8) (M+2)
25	Methyl Linoleate alcohol – positional isomer unknown	Not Obtained
26	Methyl Linoleate alcohol – positional isomer unknown	Not Obtained
27	9-oxo methyl linoleate	308(100) (M), 309(62) (M+1), 310(10) (M+2)
28	13-oxo methyl linoleate	308(100) (M), 309(62) (M+1), 310(10) (M+2)
29	Impurity – suspected squalane	Not Obtained
30	Methyl linoleate dehydrodimer	Not Obtained

Table A.3 – The GC EI-MS data for methyl oleate oxidation at 170 ^{o}C including NIST library matches and subsequent product identification.

Peak no.	Product Identification	EI Mass Spectra	NIST Library Spectra
1	Heptane	41(45), 43(100), 56(25), 57(53), 70(15), 71(52), 100(15)	41(56), 43(100), 56 (27), 57(47), 70 (18), 71(45), 100(13)
2	Octane	41(35), 43(100), 56(20), 57(40), 71(25), 85(34), 114(25)	41(44), 43(100), 56(18), 57(33), 71(20), 85(26), 114(6)
3	Heptanal	41(70), 42(60), 43(70), 44(100), 55(65), 57(35), 70(100), 81(20), 96(70)	41(90), 42(51), 43(84), 44(88), 55(78), 57(63), 70(100), 81(31), 96(16), 114(1)
4	Octanal	41(75), 42(40), 43(100), 44(70), 55(55),56(65), 57(75), 69(30), 84(50), 95(35), 100(50), 110(35)	41(67), 42(40), 43(100), 44(81), 55(51), 56(66), 57(51), 69(28), 84(55), 95(7), 100(10), 110(8), 128(1)
5	Methyl heptanoate	43(50), 55(20), 59(20), 74(100), 87(35), 101(55), 113(70), 115(15), 144(1)	43(50), 55(15), 74(100), 87(25), 101(13), 113(10), 144(2)
6	Nonanal	41(70), 43(67), 44(50), 55(45), 56(55), 57(100), 69(35), 70(38), 81(15), 82(20), 98(30), 114(20), 124(10), 142(1)	41(90), 43(88), 44(72), 55(59), 56(80), 57(100), 69(39), 70(42), 81(23), 82(29), 98(41), 114(8), 124(5), 142(1)
7	Methyl octanoate	43(32), 55(20), 57(20), 59(18), 74(100), 87(40), 115(25), 127(35), 158(1)	39(10), 41(31), 43(46), 55(17), 57(17), 59(13), 69(6), 74(100), 87(38), 101(6), 115(6), 127(8), 158(2)
8	7-oxo methyl heptanoate	55(14), 57(15), 69(21), 74(100), 87(48), 101(8), 115(8), 127(13), 131(13), 158(1)	
9	2-decenal (*trans* and *cis*)	55(40), 57(55), 60(100), 61(12), 69(77), 70(10),	27(50), 29(67), 41(88), 43(100), 47(46),

		73(95), 83(7), 87(15), 91(9), 98(11), 119(10), 121(1),	55(70), 70(70), 83(51), 98(22), 110(15), 121(5), 136(1), 154(1)
10	8-oxo methyl octanoate	55(25), 59(14), 67(11), 69(100), 74(54), 87(51), 91(13), 95(18), 97(28), 100(12), 101(13), 112(2), 119(14), 129(19), 131(63), 141(12),	41(67), 55(48), 74(100), 87(94), 97(44), 112(7), 129(63), 141(33), 154(2), 172(1)
11	2-undecenal (*trans* and *cis*)	55(44), 57(23), 69(100), 70(43), 81(12), 83(29), 97(12), 111(4), 119(11), 121(6), 131(50), 135(1), 150(2)	27(39), 29(72), 39(31), 41(94), 43(82), 55(80), 57(89), 70(100), 83(57), 97(18), 111(12), 121(10), 135(2), 150(3), 168(1)
12	9-oxo methyl nonanoate	53(7), 55(55), 57(14), 59(26), 67(22), 69(100), 74(86), 81(10), 83(37), 87(60), 98(9), 100(13), 111(40), 115(13), 119(11), 131(70), 143(28), 155(17),	32(4), 41(43), 55(59), 59(28), 69(28), 74(100), 87(61), 98(9), 111(35), 143(30), 155(17), 171(2), 185(1)
13	10-oxo methyl dec-8-enoate (*trans* and *cis*)	55(45), 59(29), 67(20), 69(100), 74(40),79(17), 83(22), 87(13), 91(11), 94(14), 95(12), 97(14), 98(24), 110(9), 119(13), 121(10), 131(61), 138(27), 166(2),	41(100), 55(69), 69(48), 74(44), 83(30), 98(22), 110(7), 121(4), 138(13), 166(4), 198(2)
14	11-oxo methyl undec-9-enoate (*trans* and *cis*)	55(37), 59(13), 67(17), 69(100), 74(21), 81(13), 83(18), 87(14), 98(21), 109(4), 119(10), 131(57), 135(5), 152(3), 181(1)	41(100), 55(69), 74(37), 83(28), 98(24), 109(7), 135(4), 152(4), 181(4)
15	Methyl sterate (impurity)	55(23), 57(14), 69(29), 74(100), 87(70), 97(4), 101(7), 111(2), 115(2), 129(8), 131(18), 143(19), 157(1), 171(5), 185(6), 199(5), 207(2), 213(3), 219(23), 227(17), 241(2), 264(6),	43(34), 55(3), 69(17), 74(100), 87(74), 97(9), 111(4), 129(9), 143(24), 157(4), 171(2), 184(5), 199(10), 213(4), 227(1), 241(3), 255(11), 267(6), 298(14)
16	Methyl oleate	55(100), 59(14), 69(75), 74(59), 83(55), 87(38), 97(29), 98(30), 109(16), 111(15), 123(13), 131(28), 137(10), 141(6), 152(7), 166(5), 180(10), 193(1), 207(5), 194(33), 219(33), 222(16), 235(3), 246(2), 264(28), 265(17), 296(2)	29(9), 41(46), 55(100), 59 (21), 69(66), 74(54), 83(52), 87(42), 97(51), 111(24), 123(16), 137(10), 152(9), 166(7), 180(13), 193(2), 207(2), 222(16), 235(3), 246(2), 264(29), 278(1), 296(6)
17	*trans*-methyl oleate epoxide	53(6), 54(15), 55(87), 56(21), 57(22), 59(17), 67(64), 68(28), 69(78), 70(16), 71(11), 74(89), 75(3), 79(13), 81(44), 82(25), 83(41), 87(44), 93(11), 94(18), 95(39), 96(19), 97(32), 98(4), 101(7), 109(41), 110(6), 111(7), 121(14), 125(8), 127(18), 136(8), 139(25), 153(14), 155(100), 156(7), 167(9), 171(15), 181(2), 187(2), 199(10), 219(2), 245(2), 263(2), 294(3)312(1)	27(13), 28(13), 29(29), 39(12), 41(72), 42(23), 43(70), 54(16), 55(100), 56(33), 57(58), 59(24), 67(42), 68(31), 69(74), 70(25), 71(35), 74(93), 75(11), 81(33), 82(27), 83(48), 84(18), 85(18), 87(52), 94(20), 95(33), 96(29), 97(44), 98(14), 109(24), 110(13), 111(13), 124(11), 125(13), 127(18), 138(10), 139(17), 153(13), 155(81), 156(12), 171(15), 199(12), 214(1), 263(1), 281(2), 294(2), 312(1)
18	*cis*-methyl oleate epoxide	53(7), 54(14), 55(96), 56(26), 57(25), 59(17), 67(57), 68(27), 69(80), 70(17), 71(17), 74(94), 75(4), 79(12), 81(41), 82(23), 83(43), 85(10), 87(44), 93(10), 94(18), 95(38), 96(20), 97(35), 101(7), 107(6), 109(41), 110(5), 111(9), 121(14), 125(10), 127(18), 137(8), 139(26), 141(7), 149(3), 153(17), 155(100), 156(8), 157(3), 171(17), 181(2), 185(6), 187(2), 199(10), 219(4), 245(1), 263(1), 294(2), 312(1)	Stereochemistry undefined. Assigned from Lercker as described in text
19	Hydroxymethyl oleates	54(19), 55(68), 57(41), 59(15), 67(100), 68(26), 69(45), 71(11), 74(14), 79(43), 80(22), 81(89), 82(32), 83(28), 87(29), 91(10), 93(25), 94(17), 95(69), 96(30), 97(17), 98(13), 101(10), 107(17), 109(30), 110(16), 111(15), 115(5), 121(30), 123(10), 125(14), 131(16), 135(26), 136(6), 137(7), 138(5), 139(16), 149(10), 150(10), 151(6), 155(12), 163(8), 164(7), 167(30), 169(10), 178(5), 181(29), 182(4), 185(4), 195(3), 199(9), 200(3), 207(3), 209(3), 213(7), 214(2), 219(17), 220(5), 221(2), 223(2), 245(3), 262(5), 263(5), 264(5), 294(20), 295(3), 312(1)	12-hydroxy methyl oleate: 29(14), 41(32), 43(32), 54(15), 55(99), 67(24), 68(21), 69(44), 74(53), 81(25), 82(39), 83(31), 84(60), 87(33), 94(10), 95(18), 96(52), 97(42), 98(57), 109(10), 110(16), 111(17), 115(10), 119(10), 123(20), 124(46), 125(18), 137(18), 148(24), 166(100), 167(14), 180(2), 195(5), 198(35), 199(6), 221(1), 227(2), 245(1), 263(3), 269(1), 294(5), 295(2), 312(1)
20	Ketomethyl oleates	53(17), 55(100), 57(36), 59(21), 67(54), 68(17), 69(58), 70(18), 71(16), 74(9), 79(20), 81(40), 82(14), 83(30), 84(17), 85(13), 91(10), 93(21), 94(19), 95(52), 97(64), 98(13), 99(4), 107(17), 108(17), 109(48), 110(34), 111(19), 119(14), 123(14), 125(14), 131(10), 133(26), 134(5), 135(8), 137(74), 138(14), 139(10), 141(9), 151(59), 152(35), 153(95), 154(13), 165(10), 166(11),	12-oxo methyl oleate: 55(25), 57(2), 59(8), 67(9), 68(4), 69(6), 74(6), 81(8), 83(4), 85(38), 95(8), 113(100), 114(8), 123(2), 139(2), 147(2), 150(5), 165(3), 166(2), 167(2), 193(2), 222(3), 279(7), 310(3)

		167(47), 168(19), 169(22), 179(11), 183(14), 193(4), 194(7), 195(6), 197(6), 207(5), 211(20), 212(11), 219(11), 221(3), 226(5), 235(3), 251(6), 264(4), 279(9), 310(2)	
21	Methyl oleate dehydrodimers	55(10), 57(5), 67(8), 69(39), 73(13), 74(3), 78(12), 81(10), 83(8), 91(5), 95(7), 97(6), 100(5), 109(4), 111(2), 119(7), 121(2), 131(23), 133(8), 135(4), 147(4), 163(3), 177(5), 179(2), 191(13), 193(8), 207(100), 269(3), 281(43), 282(11), 294(7), 295(3), 315(2), 327(7), 331(3), 341(4), 343(2), 355(5), 356(2), 357(1), 389(1), 405(3), 414(2), 429(2), 502(2), 590(1)	Not available – assignment described in text

Table A.4 – The GC CI-MS data for methyl oleate oxidation at 170 ^{o}C and subsequent product identification.

Peak no.	Product Identification	CI Mass Spectra
1	Heptane	not obtained
2	Octane	not obtained
3	Heptanal	not obtained
4	Octanal	not obtained
5	Methyl heptanoate	145(6) (M+1), 162(100) (M+18), 163(6) (M+19)
6	Nonanal	142(100) (M), 157(29) (M+15), 160(25) (M+18), 176(14) (M+34)
7	Methyl octanoate	145(6) (M-13), 159(7) (M+1), 162(40) (M+4), 176(100) (M+18), 177(7) (M+19)
8	Methyl 7-oxoheptanoate	159(8) (M+1), 173(11) (M+15), 176(100) (M+18), 177(12) (M+19)
9	2-decenal (*trans* and *cis*)	154(14) (M), 172(100) (M+18), 173(10) (M+19)
10	Methyl-8-oxooctanoate	173(7) (M+1), 187(14) (M+15), 190(100) (M+18), 191(11) (M+19)
11	2-undecenal (*trans* and *cis*)	168(19) (M), 186(100) (M+18), 187(14) (M+19)
12	Methyl-9-oxononanoate	187(10) (M+1), 201(14) (M+15), 204(100) (M+18), 205(13) (M+19)
13	Methyl-10-oxodec-8-enoate (*trans* and *cis*)	199(16) (M+1), 216(100) (M+18), 217(100) (M+19)
14	Methyl-11-oxoundec-9-enoate (*trans* and *cis*)	213(29) (M), 230(100) (M+18), 231(13) (M+19)
15	Methylsterate (impurity)	270(9) (M), 271(7) (M+1), 288(100) (M+18), 289(26) (M+19)
16	Methyl oleate	
17	*trans*-methyl oleate epoxide	295(35) (M-17), 313(33) (M+1), 314(33) (M+2), 330(100) (M+18), 331(19) (M+19)
18	*cis*-methyl oleate epoxide	295(44) (M-17), 313(49) (M+1), 314(50) (M+2), 330(100) (M+18), 331(24) (M+19)
19	Hydroxymethyl oleates	313(33) (M+1), 330(100) (M+18), 331(23) (M+19)
20	Ketomethyl oleates	311(100) (M+1), 312(23) (M+2), 328(61) (M+18), 329(13) (M+19)
21	Methyl oleate dehydrodimers	not obtained

List of Abbreviations.

AO	Antioxidant
B.D.E.	Bond Dissociation Energy
BXX	Diesel blend consisting of XX% biodiesel
CN	Cetane Number
Det	Detergent
DI	Direct Injection
DPF	Diesel Particulate Filter
EC	European Commission
EI	Electron Impact
ESI	Electron Spray Ionisation
EU	European Union
FAME	Fatty Acid Methyl Ester
FFA	Free Fatty Acid
FI	Field Ionisation
FID	Flame Ionisation Detector
HPLC	High Performance Liquid Chromatography
Irganox L107	Octadecyl 3-(3,5 di-tertbutyl, 4-hydroxyphenyl propanoate)
GC	Gas Chromatography
IPCC	International Panel for Climate Change
KVx	Kinematic Viscosity at x ^{o}C
ML	Methyl Linoleate (Methyl *cis*-*cis*-octadec-9,11-dienoate)
MO	Methyl Oleate (Methyl *cis*-octadec-9-enoate)
MS	Mass Spectrometry
p.a.	Per Annum
PM	Particulate Matter

PME	Palm Methyl Ester
RME	Rapeseed Methyl Ester
SME	Soybean Methyl Ester
UCO	Used Cooking Oil
VOCs	Volatile Organic Compounds

List of References

Adamczyk, A.A. Kach, R.A. A Combustion Bomb Study of Fuel-Oil Solubility and HC Emissions From Oil Layers, *Twentieth Symposium (International) on Combustion/The Combustion Institute*, 1984, 37-43.

Affleck, W.S. Fish, A. Two-stage Ignition under Engine Conditions Parallels that at Low Pressures, *Eleventh Symposium (International) on Combustion/The Combustion Institute,* 1967, 1003-1013.

Agarwal, A.K. Das, L.M. Biodiesel Development and Characterization for Use as a Fuel in Compression Ignition Engines. *J. of Eng. For Gas Turbines and Power,* 2001, **123,** 440-447.

Agarwal, A. K. Biofuels (Alcohols and Biodiesel) Applications as Fuels for Internal Combustion Engines, *Progress in Energy and Combustion Science*, 2007, **33**, 233.

Alfadhl, A. The Behaviour of Antioxidants in Lubricant Base Fluids at High Gasoline Engine Temperatures. *PhD Thesis, University of York*, **2008**.

Alexiadas, A. Global Warming and Human Activity: A Model for Studying the Potential Instability of the Carbon Dioxide/Temperature Feedback Mechanism, *Ecological Modelling,* 2007, **203(3-4),** 243-256.

Ali, Y. Hanna, M.A. Cuppett, S.L. Fuel Properties of Tallow and Soybean Oil Esters. *J. Am. Oil Chem. Soc.* 1995, **72(12)**, 1557-1564.

Aske, N. Kallevik, H. Sjöblom, J. Determination of Saturate, Aromatic, Resin and Asphaltenic (SARA) Components in Crude Oils by Means of Infrared and Near-Infrared Spectroscopy, *Energy and Fuels,* 2001, **15,** 1304-1312.

Attiwill, P.M. Atmospheric Carbon Dioxide and the Biosphere, *Environmental Pollution,* 1971, **(1),** 249-261.

Balat, M. Balat, H. Progress in Biodiesel Processing, *Applied Energy*, 2010, **87(6),** 1815-1835.

Barsky, R. Kilian, L. Oil and the Macroeconomy since the 1970's, *National Bureau of Economic Research,* Working Paper 10855, October 2004.

Batino, R. Rettich, T.R. Tominaga, T. The Solubility of Oxygen and Ozone in Liquids, *J. Phys. Chem. Ref. Data,* 1983, **12(2),** 163-178.

Batt L, Reactions of Alkoxy and Alkyl Peroxy Radicals, *International Reviews in Physical Chemistry,* 1987, **6(1),** 53-90.

Benson, S.W. Combustion, A Chemical and Kinetic View, *Twenty-First Symposium (International) on Combustion/The Combustion Institute,* 1986, 703-711.

Berchmans, H.J. Hirata, S. Biodiesel Production from Crude *Jatropha Curcas* L. Seed Oil with a High Content of Free Fatty Acids, *Bioresource Technology,* 2008, **99(6),** 1716-1721.

Bishov, S.J. Henick, A.S. Antioxidant Effect of Protein Hydrolyzates in Freeze-Dried Model Systems; Synergistic Action with a Series of Phenolic Antioxidants, *Journal of Food Science,* 1975, **40(2),** 345-348

Bishov, S.J. Masuoka, Y. Kapsalis, J.G. Antioxidant Effect of Spices, Herbs and Protein Hydrolyzates in Freeze-Dried Model Systems: Synergistic Action with Synthetic Phenolic Antioxidants, *Journal of Food Processing and Preservation,* 1977, **1(2),** 153-166

Blanksby, S.J. Ellison, G.B. Bond Dissociation Energies of Organic Molecules, *Acc. Chem. Res.* 2003, **36,** 255-263.

Bockey, D. Situation and Development Potential for the Production of Biodiesel – An International Report, 2002.

Bondioli, P. Gasparoli, A. Della Bella, L. Tagliabue, S. Toso, G. Biodiesel Stability under Comercial Storage Conditions over One Year, *Eur. J. Lipid Sci. Technol.* 2003, **105,** 735-741.

Borg-Warner Turbo and Emission Systems - http://www.3k-warner.de/products/turbochargerPrinciples.aspx - accessed 12/08/11

Bors, W. Erben-Russ, M. Saran, M. Fatty acid peroxyl radicals: Their generation and reactivities, *Bioelectrochemistry and Bioenergenetics,* 1987, **18**, 37-49.

Bouaid, A. Martinez, M. Aracil, J. Long Storage Stability of Biodiesel from Vegetable and Used Frying Oils, *Fuel,* 2007, **86,** 2596-2602.

Boult, P.J. Fisher, Q.J. Clinch, S.R. Lovibond, J R. Cockshell, C.C. Geomechanical, microstructural, and petrophysical evolution in experimentally reactivated cataclasites: Discussion, *AAPG Bulletin*. 2003, **87**, 1681-1683.

Bowman, C.T. Kinetics of Pollutant Formation and Destruction in Combustion, *Prog. Energy Combust. Sci.* 1975, **1,** 33-45.

The British Petroleum Company - Industrial Lubrication. 1966. Published East Grinstead, The British Petroleum Company.

Bush, G.P. Fox, M.F. Picken, D.J. Butcher, L.F. Composition of Lubricating Oil in the Upper Ring Zone of an Internal Combustion Engine, *Tribology International,* 1991, **24(4),** 231-233.

Bryant, L. The Development of the Diesel Engine, *Technology and Culture,* 1976, **17(3),** 432-446.

Cadle, R.D. Formation and Chemical Reactions of Atmospheric Particles, *Journal of Colloid and Interface Science,* 1972, **39(1),** 25-31.

Campbell, C.J. The End of Cheap Oil, *Scientific American,* March 1998.

Cao, M. Woodward, F. I. Dynamic Responses of Terrestrial Ecosystem Carbon Cycling to Global Climate Change, *Nature,* 1998, **393,** 249-252.

Carlton, A.C. James Watt (1736 – 1819), *Journal of the Franklin Institute,* 1953, **256(4),** 375-376.

Chan, H.W.S. Levett, G. Matthew, J.A. The Mechanism of the Rearrangement of Linoleate Hydroperoxides. *Chemistry and Physics of Lipids,* 1979, **24**, 245-256.

Chauhan, R.D. Sharma, M.P. Saini, R.P. Singal, S.K. Biodiesel from *Jatropha* as Transport Fuel – A Case Study of UP State, India, *Journal of Scientific and Industrial Research,* 2006, **66(5),** 394-398.

Conrad, B.R. Evaluation of Diesel Particulate Filter Systems at Stobie Mine, *Diesel Emission Evaluation Program,* INCO, 2006, 28-29

Cort, W.M. Antioxidant Properties of Ascorbic Acid in Foods, *Advances in Chemistry,* 1982, **200(22),** 533-550.

Cox, P.M, Betts, R.A. Jones, C.D. Spall, S.A. Totterdell, I.J. Acceleration of Global Warming due to Carbon-Cycle Feedbacks in a Coupled Climate Model, *Nature,*2000, **408,** 184-187.

Clark, K.B. Culshaw, P.N. Griller, D. Lossing, F.P. Martinho Simões, J.A. Walton, J.C. Studies of the Formation and Stability of Pentadienyl and 3-Substituted Pentadienyl Radicals, *J. Org. Chem.* 1991, **56,** 5535-5539.

Deegan, R.D. Leheny, R.L. Menon, N. Nagel, S.R. Dynamic Shear Modulus of Tricresyl Phosphate and Squalane, *J. Phys. Chem. B,* 1999, **103,** 4066-4070.

Demirbas, A. Biodiesel from Vegetable Oils via Transesterification in Supercritical Methanol, *Energy Conversion and Management,* 2002, **43,** 2349-2356.

Dermibas, A. The Importance of Biodiesel as Transportation Fuel, *Energy Policy,* 2007, **35,** 4661-4670.

Demirbas, A. Progress and recent trends in biodiesel fuels. *Energy Conversion and Management,* 2009**, 50**, 14-34.

Denisov, E.T. Mechanism of Regeneration of Hindered Nitroxyl and Aromatic Amines, *Polymer Degradation and Stability*, 1989, **25,** 209-215.

Denisov, E.T. Afanas'ev, I.B. Oxidation and Antioxidants in Organic Chemistry and Biology, *CRC Press* 2005, ISBN 0-8247-5356-9.

Department for Transport – Towards a UK Strategy for Biofuels – Public Consultation 2005, 2-4, www.dft.gov.uk/consultations/archive/2004/tuksb/, Archived 02/09/2009, 27/4/2011

Dickinson, H.W. A Short History of the Steam Engine, *Cambridge University Press,* 1939 (Online 2010).

Du Plessis, L.M. De Villiers, J.B.M. Van Der Walt, W.H. Stability Studies on Methyl and Ethyl Fatty Acid Esters of Sunflowerseed Oil, *J. Am. Oil Chem. Soc.* 1985, **62(4),** 748-752.

Dvorák, A. Skopal, F. Komers, K. Transesterification of Rapeseed Oil in a Feedback Reactor, *Eur. J. Lipid Sci. Technol.* 2001, **103,** 742-745.

European Commission Paper COM(2006) 105 – A European Strategy for Sustainable, Competitive and Secure Energy, 8/3/2006.

European Commission Regulation No. 715/2007 – Euro 5

European Commission Regulation No. 28/2009

European Commission Regulation No. 595/2009 – Euro 6

El-Fadel, M. Massoud, M. Particulate Matter in Urban Areas: Health-based Economic Assessment, *Science of the Total Environment,* 2000, **257(2-3),** 133-146.

Encinar, J.M. González, J.F. Sabio, E. Ramiro, M.J. Preparation and Properties of Biodiesel from *Cynara cardunculus* L. Oil, *Ind. Eng. Chem. Res.* 1999, **38,** 2927-2931

Encinar, J.M. González, J.F.Rodríguez-Reinares. Biodiesel from Used Frying Oil. Variables Affecting the Yields and Characteristics of the Biodiesel, *Ind. Eng. Chem. Res.* 2005, **44,** 5491-5499.

Engler, C. R. J. Johnson, L.A. Effects of Processing and Chemical Characteristics of Plant Oils on Performance of an Indirect-Injection Diesel Engine, *J. Am. Oil Chem. Soc.*, 1983, **60**, 1592–1596.

Enweremadu, C.C. Mbarawa, M.M. Technical Aspects of Production and Analysis of Biodiesel from Used Cooking Oil – A Review, *Renewable and Sustainable Energy Reviews,* 2009, **13(9),** 2205-2224.

Farmer, E.H. Koch, H.P. Sutton, D.A. The Course of Autoxidation Reactions in Polyisoprenes and Allied Compounds. Part VII. Rearrangement of Double Bonds during Autoxidation, *J. Chem. Soc.* 1943, 541-547.

Fazal, M.A. Haseeb, A.S.M.A. Masjuki, H.H. Biodiesel Feasibility Study: An Evaluation of Material Compatibility; Performance; Emission and Engine Durability, *Renewable and Sustainability Energy Reviews,* 2011, **15(2),** 1314-1324.

Ferguson, C.R. Internal Combustion Engines, *John Wiley, New York,* 1986.

Florides, G.A. Christodoulides, P. Global Warming and Carbon Dioxide Through Sciences, *Environment International,* 2009, **35**, 390-401.

Filipova, T.V. Blyumberg, E.A. Mechanism of the Epoxidation of Alkenes by Molecular Oxygen, *Russian Chemical Reviews,* 1982, **51(6)**, 582-591.

Frankel, E.N. Garwood, R.F. Khambay, B.P.S. Moss, G.P. Weedon, B.C.L. Stereochemistry of Olefin and Fatty Acid Oxidation. Part 3. The Allylic Hydroperoxides from the Autoxidation of Methyl Oleate, *J. Chem. Soc. Perkin Transactions 1*, 1984, 2233-2240.

Frankel, E.N. Chemistry of Free Radical and Singlet Oxidation of Lipids. *Prog. Lipid Res.* 1985, **23**, 197-221.

Gamble, R.J. Priest, M. Taylor, C.M. Detailed Analysis of Oil Transport in the Piston Assembly of a Gasoline Engine, *Tribology Letters,* 2003, **14(2),** 147-156.

Ganguly, J. Studies on the Mechanism of Fatty Acid Synthesis: VII. Biosynthesis of Fatty Acids from Malonyl CoA, *Biochim. Biophys. Acta,* 1960, **40,** 110-118.

Gardner, H.W. Oxygen Radical Chemistry of Polyunsaturated Fatty Acids, *Free Radical Biology & Medicine,* 1989, **7,** 65-86.

Gedik, C.M. Boyle, S.P. Wood, S.G. Vaughan, S.J. Collins, A.R. Oxidative Stress in Humans: Validation of Biomarkers of DNA Damage, *Carcinogenesis,* 2002, **23(9),** 1441-1446.

German Patent (DRP) No. 37435 – Karl Benz, gasoline fuelled car

Giuffrida, F. Destaillats, F. Robert, F. Skibsted, L.H. Dionisi, F. Formation and Hydrolysis of Triacylglycerol and Sterol Epoxides: Role of Unsaturated Triacylglycerol Peroxyl Radicals, *Free Radical Biology & Medicine.* 2004, **37(1)**, 104-114.

Ghadge, S.V. Raheman, H. Biodiesel Production from Mahua (*Madhuca Indica*) Oil having Free Fatty Acids, *Biomass and Bioenergy*, 2005, **28(6),** 601-605.

Goering, C.E. Schwab, A.W. Dangherty, M.J. Pryde, E.H. Heakin, A.J. Fuel Properties of Eleven Vegetable Oils. *ASAE* 1982, **25(6)**, 1472-1477.

Golden, D.M. Benson, S.W. *Chem.Rev* 1969, **69**,125.

Gómez-Carracedo, M.P. Andrade, J.M. Calviño M., Fernández, E. Prada, D. Muniategui, S. Multivariate prediction of eight kerosene properties employing vapour-phase mid-infrared spectrometry, *Fuel*, 2003, **82**, 1211-1218.

Goodrum, J.W. Volatility and Boiling Points of Biodiesel from Vegetable Oils and Tallow, *Biomass and Bioenergy*, 2002, **22**, 205–211.

Graboski, M.S. McCormick, R.L. Combustion of Fat and Vegetable Oil Derived Fuels in Diesel Engines, *Prog. Energy Combust. Sci.* 1998, **24,** 125-164.

Griffin Shay, E. Diesel Fuel from Vegetable Oils: Status and Oppurtunities, *Biomass and Bioenergy*, 1993, **4(4),** 247-242.

Gruntman, M. Blazing the Trail: The Early History of Spacecraft and Rocketry, *American Institute of Aeronautics and Astronautics*, 2004.

Gupta, S.A. Cochran, H.D. Cummings, P.T. Shear Behaviour of Squalane and Tetracosane under Extreme Confinement. I. Model, Simulation Method and Interfacial Slip. *J. Chem. Phys*, 1997, **107(23),** 10316-10326.

Gupta, S.A. Cochran, H.D. Cummings, P.T. Shear Behaviour of Squalane and Tetracosane under Extreme Confinement. II. Confined Film Structure, *J. Chem. Phys*, 1997, **107(23),** 10327-10334.

Gupta, S.A. Cochran, H.D. Cummings, P.T. Shear Behaviour of Squalane and Tetracosane under Extreme Confinement. III. Effect of Confinement on Viscosity, *J. Chem. Phys*, 1997, **107(23),** 10334-10343.

Haas, M.J. McAloon, A.J. Yee, W.C. Foglia, T.A. A Process Model to Estimate Biodiesel Production Costs, *Bioresource Technology*, 2006, **97(4),** 671-678.

Hamberg, M. Gotthammer, B. A New Reaction of Unsaturated Fatty Acid Hydroperoxides: Formation of 1 1-Hydroxy-12,13-epoxy-9-octadecenoic Acid from 13-Hydroperoxy-9,11 -octadecadienoic Acid, *Lipids*, 1973, **8(12)**, 737-744.

Hamrock, B.J. Fundamentals of Fluid Film Lubrication, 1994, *McGraw-Hill Publishing*.

Harwood, H.J. Oleochemicals as a Fuel: Mechanical and Economic Feasability, *J. Am. Oil Chem. Soc.*, 1984, **61(2)**, 315-324.

Hayes, T.K. White, R.A. Peters, J.E. Combustion Chamber Temperature and Instantaneous Local Heat Flux Measurements in a Spark Ignition Engine, *SAE Technical Paper 930217*, 1993.

Hele, P. Biosynthesis of Fatty Acids, *Brit. Med. Bull.* 1958, **14(3),** 201-206

Heywood, J.B. – Internal Combustion Engine Fundamentals, International Edition, *McGraw-Hill Book Company*, 1988.

Hill, J. Nelson, E. Tilman, D. Polasky, S. Tiffany, D. Environmental, Economic and Energetic Costs and Benefits of Biodiesel and Ethanol Biofuels, *PNAS*, 2006, **103(30),** 11206-11210.

Hill, K. Fats and Oils as Oleochemical Raw Materials, *Pure Appl. Chem.* 2000, **72(7),** 1255-1264.

Hills, R.L. Power from Steam: A History of the Stationary Steam Engine, *Cambridge University Press*, 1993.

Hiroyasu, H. Kadota, T. Models for Combustion and Formation of Nitric Oxide and Soot in Direct Injection Diesel Engines, *Soc. Automotive Eng. Paper No. 760129*, 1976.

Hirsch, R.L. Bezdek, R. Wendling, R. Peaking of World Oil Production: Impacts, Mitigation and Risk Management, 2005, 11-20, www.netl.doe.gov

Hochstein, P. Atallah, A.S. The Nature of Oxidants and Antioxidant Systems in the Inhibition of Mutation and Cancer, *Mutation Research*, 1988, **202,** 363-375.

Hsu, S.M. Nano-lubrication: Concept and Design, *Tribology International*, 2004, **37(7),** 537-545.

Hu, J. Du, Z. Li, C. Min, E. Study on the Lubrication Properties of Biodiesel as Fuel Lubricity Enhancers, *Fuel*, 2005, **84,** 1601-1606.

Hu, J.J. Dubin, N. Kurland, D. Ma, B. Roush, G. The Effects of Hydrogen Peroxide on DNA Repair Activities, *Mutation Research*, 1995, **336,** 193-201.

Jabbarzadeh, A. Atkinson, J.D. Tanner, R.I. The effect of Branching on Slip and Rheological Properties of Lubricants in Molecular Dynamics Simulation of Couette Shear Flow, *Tribology International*, 2002, **35(1),** 35-46.

Jain, S. Sharma, M.P. *Prospects* of Biodiesel from Jatropha in India: A Review, *Renewable and Sustainable Energy Reviews*, 2010, **14,** 763-771.

Jensen, R.K. Korcek, S. Zinbo, M. Gerlock, J.L. Regeneration of Amine in Catalytic Inhibition of Oxidation, *J. Org. Chem.* 1995, **60,** 5396-5400.

Johnson, F.S. The Balance of Atmospheric Oxygen and Carbon Dioxide, *Biological Conservation*, 1970, **2(2),** 83-89.

Jones, C. Interactions Between Biofuels and Lubricants and Effects on Engine Oil Durability, *2008 SAE Biofuels: Specifications and Performance Symposium*, Paris, France. July 2008.

Jones, E. Combustion of Methane, *Nature,* 1956, **178,** 1112.

Kaiser, E.W. Admczyk, A.A. Lavoie, G.A. The Effect of Oil Layers on the Hydrocarbon Emissions Generated During Closed Vessel Combustion, *Eighteenth Symposium (Inetnational) on Combustion/The Combustion Institute*, 1981, 1881-1890.

Kearns, D.R. Physical and Chemical Properties of Singlet Molecular Oxygen, *Chemical Reviews,* 1971, **71(4),** 395-427.

Kim, J.S. Min, B.S. Lee, D.S. Oh, D.Y. Choi, J.K. Characteristics of Carbon Deposit Formation in Piston Top Ring Groove of Gasoline and Diesel Engine, *1998 SAE International Congress & Exposition; Detroit, MI, USA,* 1998, 147-154.

Kimura, Y. Okabe, H. An Introduction to Tribology, *Youkandou Press,* 1982, 69-82

Kittelson, D.B. Engines and Nanoparticles: A Review, *J. Aerosol Sci.* 1998, **29(5/6),** 575-588

Knothe, G. Bagby, M.O. Ryan, T.W. *Soc. Automotive Eng. Technical Paper No. 971681* 1997.

Knothe, G. Bagby, M.O. Ryan, T.W. III. Precombustion of Fatty Acid and Esters of Biodiesel. A Possibile Explanation for Differing Cetane Numbers. *J.Am. Oil Chem. Soc.* 1998, **75(8),** 1007-1013.

Knothe, G. Dependence of Biodiesel Fuel Properties on the Structure of Fatty Acid Alkyl Esters, *Fuel Processing Technology,* 2005, **86,** 1059-1070.

Körbitz, W. Biodiesel Production in Europe and North America, an Encouraging Prospect, *Renewable Energy,* 1999, **16,** 1078-1083.

Korchek, S. Chenier, J.H.B. Howard, J.A. Ingold, K.U. Absolute rate constants for hydrocarbon autoxidation. XXI. Activation energies for propagation and the correlation of propogation rate constant with carbon–hydrogen bond strengths, *Can. J. Chem*, 1972, **50**, 2285–2297.

Krisnangkura, K. Yimsuwan, T. Pairintra, R. An Empircal Approach in Predicting Biodiesel Viscosity at Various Temperatures, *Fuel,* 2006, **85,** 107-113.

Krop, H.B. v. Velzen, M.J.M. Parsons, J.R. Govers, H.R.J. Determination of Environmentally Relevant Physical-Chemical Properties of Some Fatty Acid Esters, *JAOCS,* 1997, **74(3),** 309-315

Kumagi, A. Takahashi, S. Viscosity and Density of Liquid Mixtures of n-Alkanes with Squalane, *International Journal of Thermophysics*, 1995, **16(3),** 773-779.

Kyoto Protocol, http://kyotoprotocol.com.

Labeckas, G. Slavinskas, S. Performance of direct-injection off-road diesel engine on rapeseed oil, *Renewable Energy*, 2006, **31**, 849-863.

Lansdown, A.R. Lubrication and Lubricant Selection, A Practical Guide, 3rd Edition, *Tribology in Practice Series*, *Professional Engineering Publishing*, 2004.

Lapuerta, M. Rodríguez-Fernández, J. Agudelo, J.R. Diesel Particulate Emissions from Used Cooking Oil Biodiesel, *Bioresource Technology,* 2008, **99,** 731-740.

Lapuerta, M. Armos, A. Rodríguez-Fernández, J. Effect of Biodiesel Fuels on Diesel Engine Emissions, *Progress in Energy and Combustion Science,* 2008, **34(2),** 198-223.

Lazaroiu, G. Modeling and Simulation Combustion and Generation of NO_x, *Fuel Processing Technology,* 2007, **88,** 771-777.

Lercker, G. Rodriguez-Estrada, T.M. Bonoli M., Analysis of the oxidation products of cis- and trans-octadecenoate methyl esters by capillary gas chromatography–ion-trap mass spectrometry I. Epoxide and dimeric compounds, *Journal of Chromatography*, 2003, **985**, 333-342.

Leung, D.Y.C. Luo, Y. Chan, T.L. Optimization of Exhaust Emissions of a Diesel Engine Fuelled with Biodiesel, *Energy & Fuels*, 2006, **20(3),** 1015-1023.

Levy II, H. Photochemistry of the Lower Troposphere, *Planetary and Space Science*, 1972, **20,** 919-935.

Lightfoot, P.D. Cox, R.A. Crowley, J.N. Destriau, M.Hayman, G.D. Jenkin, M.E. Moortgat, G.K. Zabel, F. Organic Peroxy Radicals: Kinetics, Spectroscopy and Tropospheric Chemistry, *Atmospheric Environment*, 1992, **26A(10),** 1805-961.

Lignola, P.G. Reverchon, E. Cool Flames, *Prog. Energy Combust. Sci.* 1987, **13,** 75-96.

Ma, F. Hanna, M.A. Biodiesel Production: A Review, *Bioresource Technology*, 1999, **70,** 1-15.

Mahoney, L.R.Antioxidants, *Angew. Chem. Int. Ed.* 1969, **8(8),** 547-555.

Mahoney, L.R. DaRooge, M.A. The Kinetic Behavior and Thermochemical Properties of Phenoxy Radicals. *J. Am. Chem. Soc.* 1975, **97(16)**, 4722-4731.

Manabe, S. Wetherald, R.T. The Effects of Doubling CO_2 Concentration on the Climate of a General Circulation Model, *J. of the Atmos. Sci.* 1975, **32(1),** 3-15.

Manabe, S. Stouffer, R.J. Century-scale Effects of Increased Atmospheric CO2 on the Ocean-atmosphere System, *Nature,* 1993, **364,** 215-218.

Mantashyan, A.A. Khachatryan, L.A. Niazyan, O.M. Arsentyev, S.D. On the Reactions of Peroxy Radicals in the Slow Combustion of Methane and Ethylene, *Combustion and Flame*, 1981, **43,** 221-227.

Marshall, W. Schumacher, L.G. Howell, S. Engine Exhaust Emissions: Evaluation of a Cummins L10E when Fuelled with a Biodiesel Blend. *SAE paper 952363*, 1995.

Masjuki, H.H. Maleque, M.A. The Effect of Palm Oil Diesel Fuel Contaminated Lubricant on Sliding Wear of Cast Irons against Mild Steel, *Wear,* 1996, 198, 293-299.

McMillen, D.F. Golden, D.M. Hydrocarbon Bond Dissociation Energies, *Ann. Rev. Phys. Chem*, 1982, **33,** 493-532.

Monyem, A. Canakci, M. Van Gerpen, J.H. Investigation of Biodiesel Thermal Stability Under Simulated In-Use Conditions, *Applied Engineering in Agriculture*, 2000, **16(4)**, 373-378.

Moritani, H. Nozawa, Y. Oil Degradation in Second-Land Region of Gasoline Engine Pistons, *R&D Rev. Toyota CRDL,* 2003, **38,** 36-43.

Mulliken, R.S. The Interpretation of Band Spectra Part III. Electron Quantum Numbers and States of Molecules and Their Atoms, *Rev. Mod. Phys.* 1932, **4(1),** 1-86.

Naik, S.N. Goud, V.V. Rout, P.K. Dalai, A.K. Production of First and Second Generation Biofuels: A Comprehensive Review, *Renewable and Sustainable Energy Reviews,* 2010, **14(2),** 578-597.

Nebel, B.A. Mittelbach, M. Biodiesel from Extracted Fat out of Meat and Bone Meal, *Eur. J. Lipid Sc. Technol.* 2006, **108,** 398-403.

Nicolet, M. Aeronomic Chemistry of the Stratosphere, *Planetary and Space Science,* 1972, **20,** 1671-1702.

NIST database, www.nist.gov, 21/2/2011

Nitschke, W.R. Wilson, C.M. Rudolph Diesel, Pioneer of the Age of Power, *The University of Oklahoma Press*, Norman, OK 1965.

Owczarek, I. Blazej, K. Recommended Critical Temperatures. Part I. Aliphatic Hydrocarbons. *J. Phys. Chem. Ref. Data* 2003, **32(4)**, 1411-1428.

Owczarek, I. Blazej, K. Recommended Critical Temperatures. Part II. Aromatic and Cyclic Hydrocarbons. *J. Phys. Chem. Ref. Data* 2004, **33(2)**, 541-547.

Oxford English Dictionary, *Oxford University Press,* 1996.

Pousa, G.P.A.G. Santos, A.L.F. Suarez, P.A.Z. History and Policy of Biodiesel in Brazil, *Energy Policy*, 2007, **35(11),** 5393-5398.

Pratt, D.A. Mills, J.H. Porter, N.A. Theoretical Calculations of Carbon-Oxygen Bond Dissociation Enthalpies of Peroxyl Radicals Formed in the Autoxidation of Lipids, *J. Am. Chem. Soc.* 2003, **124**, 5801-5810.

Priest, M. Dowson, D. Taylor, C.M. Predictive Wear Modelling of Lubricated Piston Rings in a Diesel Engine, *Wear*, 1999, **231,** 89-101.

Radich, A. Biodiesel Performance, Costs and Use, *Energy Information Administration,* 2004.

Radu, R. Petru, C. Edward, R. Gheroghe, M. Fueling an D.I. Agricultural Diesel Engine with Waste-Oil Biodiesel: Effects Over Injection, Combustion and Engine Characteristics, *Energy Conversion and Management,* 2009, **50,** 2158-2166.

Rakopoulos, C.D. Antonopoulos, K.A. Rakopoulos, D.C. Hountalas, D.T. Giakoumis, E.G. Comparative Performance and Emissions Study of a Direct-injection Diesel Engine Using Blends of Diesel fuel with Vegetable Oils or Bio-diesels of Various Origins, *Energy Conversion and Management,* 2006, **47**, 3272-2387.

Ranz, A. Maier, E. Lankwayr, E. Determination of Fatty Acid Derivatives in Fuel and Diesel Oil, *Fuel*, 2010, **89(8),** 2133-2139.

Ross, J.R. Gebhart, A.I. Gerecht, J.F. The Autoxidation of Methyl Oleate. *J. Am. Chem. Soc.* 1949, **71**, 282-286.

Rudnick, L.R. Lubricant Additives, Chemistry and Applications, 2nd Ed. *CRC Press* 2009, ISBN 1-4200-5964-9.

Ruiz, R.P. Bayes, K.D. Macpherson, M.T. Pilling, M.J. Direct Observation of the Equilibrium between Allyl Radicals, O_2, and Allylperoxy Radicals, *J. Phys. Chem.* 1981, **85**, 1622-1624.

Ryan, T. W. III. Dodge, L.G., Callahan, T.J. The Effects of Vegetable Oil Properties on Injection and Combustion in Two Different Diesel Engines, *J.Am.Oil Chem.Soc*, 1984, **61**, 1610–1619.

Sapaun, S.M. Masjuki, H.H. Azlan, A. The Use of Palm Oil as Diesel Fuel Substitute. *J. Power Energy A.* 1996, **210**, 47–53.

Sarin, R. Sharma, M. Sinharay, S. Malhorta, R.K. Jatropha – Palm Biodiesel Blends: An Optimum Mix for Asia. *Fuel*, 2007, **86,** 1365-1371.

Sarmiento, J.L. Hughes, T.M.C. Stouffer, R.J. Manabe, S. Simulated Response of the Ocean Carbon Cycle to Anthropogenic Climate Warning, *Nature¸*1998, **393,** 245-249.

Scanlon, J.T. Willis, D.E. Calculation of Flame Ionization Detector Relative Response Factors Using the Effective Carbon Number Concept, *Journal of Chromatographic Science,* 1985, **23(8),** 333-340.

Seetula J.A. Slagle I.R. Kinetics and thermochemistry of the R+ HBr ↔ H+ Br (R= *n*-C_3H_7, *iso*-C_3H_7 , *n*-C_4H_9 , *iso*-C_4H_9 , *sec*-C_4H_9 or *tert*-C_4H_9) equilibrium, *J. Chem. Soc. Faraday Trans.* 1997, **93,** 1709-1719.

Shahid, E.M. Jamal, Y. A Review of Biodiesel as a Vehicular Fuel, *Renewable and Sustainable Energy Review,* 2008, **12(9),** 2484-2494.

Sharma, Y.C. Singh, B. Development of Biodiesel: Current Scenario, *Renewable and Sustainable Energy Reviews,* 2009, **13(6-7),** 1646-1651.

Shayler, P.J. Winborn, L.D. Hill, N.J. Eade, D. Fuel Transport to the Crankcase, Oil Dilution and HC Return with Breather Flow During the Cold Operation of a SI Engine, *SAE 2000 World Congress,* 2000, Paper No. 2000-01-1235.

Siegbahn, P.E.M. Multireference CCI Calculations on the Bond Dissociation Energies of Methane, *Chemical Physics Letters,* 1985, **119(6),** 515-522.

Smeets, E. Junginger, M. Faaij, A. Walter, A. Dolzan, P. Turkenburg, W. The Sustainability of Brazilian Ethanol—An Assessment of the Possibilities of Certified Production, *Biomass and Bioenergy,* 2008, **32(8),** 781-813.

Sonawane, H.R. Nanjundiah, B.S. Kelkar, R.G. Light-Mediated Transformations of Olefins into Alcohols: Reactions of Hydroxyl Radicals With Cycloalkenes, *Tetrahedron,* 1986, **42(24)**, 6673-6682

Spear, B. James Watt: The Steam Engine and Commercialization of Patents, *World Patent Information,* 2008, **30,** 53-58.

Srinisavan, S. The Food v Fuel Debate: A Nuanced View of Incentive Structures, *Renewable Energy,* 2009, **34(4),** 950-954.

Srivastava, A. Prasad, R. Triglycerides-based Diesel Fuels, *Renewable and Sustainable Energy Reviews,* 2000, **4,** 111-133.

Stachowiak, G.W. Batchelor, A.W. Lubricants and their Composition, *Engineering Tribology,* 2005, **Ch. 3**, 51-101.

Stark, M.S. Wilkinson, J.J. Lindsay Smith, J.R. Alfadhl, A. Pochopien, B.A. Autoxidation of Branched Alkanes in the Liquid Phase, *Ind, Eng. Chem. Res.* 2011, **50,** 817-823

Sumathi, S. Chai, S.P. Mohamed, A.R. Utilization of Palm Oil as a Source of Renewable Energy in Malaysia, *Renewable and Sustainable Energy Reviews,* 2008, **12**, 2404–2421.

Szulcyk, K.R. McCarl, B.A. Market Penetration of Biodiesel, *Renewable and Sustainable Energy Reviews,* 2010, **14(8),** 2426-2433.

Tan, Y.C. Ripin, Z.M. Frictional Behaviour of Piston Rings of Small Utility Two-Stroke Engine Under Secondary Motion of Piston, *Tribology International*, 2010, **44,** 592-602.

Taylor, J.W. Ehlker, G. Carstensen, H.H. Ruslen, L. Field, R.W. Green, W.H. Direct Measurement of the Fast, Reversible Addition of Oxygen to Cyclohexadienyl Radicals in Nonpolar Solvents, *J. Phys. Chem. A.* 2004, **108,** 7193-7203.

Taylor, R.I. Evans, P.G. *In-situ* Piston Measurements, *Proc. Instn. Mech. Engrs.* 2004, **218**(J: J. Engineering Tribology), 185-200.

Thoenes, P. Biofuels and Commodities Market – Palm Oil Focus, FAO, Commodities and Trades Division.

Thornton, M.J. Alleman, T.L. Luecke, J. McCormick, R.L. Impacts of Biodiesel Fuel Blends, Oil Dilution on Light-Duty Diesel Engine Operation, *National Renewable Energy Laboratory*, Conference Paper NREL/CP-549-44833, August 2009.

Tiwari, A.K. Kumar, A. Raheman, H. Biodiesel Production from Jatropha Oil *(Jatropha Curcas*) with High Free Fatty Acids: An Optimised Process, *Bioresource Technology*, 2007, **31(8),** 569-575.

Tormos, B. Novella, R. García, A. Gargar, K. Comprehensive Study of Biodiesel Fuel for HSDI Engines in Convencional and Low Temperature Combustion Conditions, *Renweable Energy*, 2010, **35,** 368-378.

Trenwith, A.B. Dissociation of 3-methyl-1,4-pentadiene and the Resonance Energy of the Pentadienyl Radical *J. Chem. Soc. Faraday Trans. 1*, Physical Chemistry in Condensed Phases, 1982, **78(10),** 3131-3136.

Tutorvista.com http://www.tutorvista.com/content/chemistry/chemistry-iv/atomic-structure/oxygen-molecule.php Accessed 04/08/2011

U.S Department of Energy report **2011** http://tonto.eia.doe.gov/oog/info/twip/twip.asp 27/04/2011

U.S. Patent 388,372, 08/1888 – Nikolaus Otto, Otto Cycle Engine.

Van Setten, B.A.A.L. Makkee, M. Moulijn, J.A. Science and Technology of Catalytic Diesel Particulate Filters, *Catalysis Reviews*, 2001, **43(4),** 489-564.

Van Wechel, T. Gustafson, G.R. Leistritz, F.L. Economic Feasibility of Biodiesel Production in North Dakota, *Agribusiness and Applied Economics Report* 2002, **505.**

Wainwright, M.S. Haken, J.K. Effective Carbon Number of Methane in Gas Chromatography, *Journal of Chromatography*, 1983, **256,** 193-199.

Wakuri, Y. Hamatake, T. Soejima, M. Kitahara, T. Piston Ring Friction in Internal Combustion Engines, *Tribology International*, 1992, **25(5),** 299-308.

Walker, K. Biodiesel from Rapeseed, *J. R. Agric. Soc. Engl.* 1994, **155,** 43–47.

Wayne, R.P. Chemistry of Atmospheres, 3rd Edition, *Oxford University Press*, 2000, 50-60.

Wilkinson, J.J. The Autoxidation of Branched Hydrocarbons in the Liquid Phase as Models for Understanding Lubricant Degradation. *PhD Thesis, University of York*, **2006**. 231-233

Williams, D.H. Fleming, I. Spectroscopic Methods in Organic Chemistry, 1989, 4th Edition

Woodwell, G.M, MacDonald, G.J. Revelle, R, Kelling, C.D. The Carbon Dioxide Problem: Implications for Policy in the Management of Energy and Other Resources, *Report to the Council on Environmental Quality*, 1979, Reprinted 2008.

Wright, J.S. Johnson, E.R. DiLabio, G.A. Predicting the Activity of Phenolic Antioxidants: Theoretical Method, Analysis of Substituent Effects, and Application to Major Families of Antioxidants, *J. Am. Chem. Soc*, 2001, **123,** 1173-1183.

Yizhe, L. Guirong, B. Hua, W. Determination of 11 fatty acids and fatty acid methyl esters in biodiesel using ultra performance liquid chromatography, *Chinese Journal of Chromatography*, 2008, **26(4)**, 494-498.

Xue, J. Grift, T.E. Hansen, A.C. Effect of Biodiesel on Engine Performances and Emissions, *Renewable and Sustainable Energy Reviews*, 2011, **15(2),** 1098-1116.

Yang, J. Stewart, M. Maupin, G. Herling, D. Zelenyuk, A. Single Wall Diesel Particulate Filter (DPF) Filtration Efficiency Studies Using Laboratory Generated Particles, *Chemical Engineering Science*, 2008, **64(8),** 1625-1634.

Yen, G. Duh, P. Tsai, H. Antioxidant and Pro-oxidant Properties of Ascorbic Acid and Gallic Acid, *Food Chemistry*, 2002, **79,** 307-313.

Yuan, W. Hansen, A.C. Zhang, Q. Vapour Pressure and Normal Boiling Point Predictions for Pure Methyl Esters and Biodiesel Fuels, *Fuel*, 2005, **84,** 943-950.

Zhang, F.L. Niu, B. Wang, Y.C. Chen, F. Wang, S.H. Xu, Y. Jiang, L.D. Gao, S. Wu, J. Tang, L. Jia, Y.J. A Novel Betain Aldehyde dehydrogenase gene from *Jatropha Curcas*, encoding an enzyme implicated in adaptation to environmental stress, *Plant Science*, 2008, **174,** 510-518.

Zhang, H. Machutta, C.A. Tonge, P.J. Fatty Acid Biosynthesis and Oxidation, *Comprehensive Natural Products II*, 2010, **8.07**, 231-275.

Zhang, Y. Dubé, M.A. McLean, D.D. Kates, M. Biodiesel Production from Waste Cooking Oil: 1. Process Design and Technological Assessment, *Bioresource Technology*, 2003, **89(1),** 1-16.

Zils, R. Inomata, S. Imamura, T. Miyoshi, A. Washida, N. Determination of the Equilibrium Constant and Thermodynamic Parameters for the Reaction of Pentadienyl Radicals with O_2, *J. Phys. Chem. A.* 2003, **105,** 1277-1282.